UNIVERSITÉ DU LUXEMBOURG

PhD-FSTM-2023-052

The Faculty of Science, Technology and Medicine

DISSERTATION

Defense held on 04/07/2023 in Luxembourg

to obtain the degree of

DOCTEUR DE L'UNIVERSITÉ DU LUXEMBOURG

EN PHYSIQUE

by

Mohammad Sadeq Salehi Kadijani

Born on 3rd April 1994 in Tehran-Iran

Heat currents, work statistics and fluctuations in quantum systems

Dissertation defense committee

Dr. Thomas SCHMIDT, Dissertation supervisor

Professor, UNIVERSITÉ DU LUXEMBOURG

Dr. Ludger WIRTZ, Chairman

Professor, UNIVERSITÉ DU LUXEMBOURG

Dr. Massimiliano ESPOSITO, Member

Professor, UNIVERSITÉ DU LUXEMBOURG

Dr. Benjamin HUARD, Member

Professor, ECOLE NORMALE SUPERIEURE DE LYON

Dr. Patrik RECHER, Member

Professor, TECHNISCHE UNIVERSITÄT BRAUNSCHWEIG

Abstract

We study the concept of heat and work in quantum thermodynamics. Our analysis focuses on overdamped quantum systems, specifically investigating the currents in two magnetically coupled quantum RLC circuits. We derive an analytical expression for the heat current between two damped quantum oscillators, which are in contact with local thermal baths at different temperatures. By exploiting the time scale separation inherent in the overdamped regime, our analysis separates the total heat current into classical and quantum contributions, without relying on conventional weak coupling and Markovian approximations. Interestingly, our study reveals the persistence of non-trivial quantum corrections even when the temperatures greatly exceed the frequency scale relevant to the system's overdamped dynamics.

Building upon this, we extend our investigation to non-linear quantum circuits involving superconducting qubits. We provide a detailed description of how the Josephson junction can be manipulated to function as a qubit. Subsequently, we discuss the interaction between these qubits and demonstrate that, in the regime of strong coupling, Feynman path integral techniques are necessary when connecting the qubits to the environment.

In the context of quantum electronic circuits, we examine the dynamical Casimir effect, which involves cavities interrupted by a superconducting quantum interference device (SQUID). By quantizing the degrees of freedom of the SQUID, we obtain a three-body interaction Hamiltonian. We show that this interaction can be reduced to a quantum autonomous refrigerator.

Furthermore, we explore the statistics of work in closed quantum systems. By introducing a modified version of the Keldysh contour, we construct a consistent perturbation expansion of the moment generating function (MGF) for work that satisfies fluctuation theorems (FT) at all orders of the expansion. Additionally, we extend standard diagrammatic techniques to compute work MGFs and demonstrate that these contributions can be combined to obtain a general expression for work statistics, represented as a sum of independent rescaled Poisson processes. In this context, the FT can be understood as a detailed balance condition that connects each Feynman diagram with its time-reversed counterpart. In the second part

of our study, we investigate path integral approaches for calculating the MGF and explore the influence of the choice of contour on the final form of the path integral action. Our analysis reveals that using a symmetrized contour allows for a straightforward generalization of the Keldysh rotation, enabling a semiclassical expansion of the work MGF. Finally, we leverage our findings to discuss a generalization of the detailed balance conditions at the level of quantum trajectories.

Acknowledgements

I would like to express my deepest gratitude to my supervisor, Prof. Thomas Schmidt, for his unwavering support, immense knowledge, and guidance throughout my PhD journey. His availability for scientific discussions has been invaluable over the course of these four years, and I am truly grateful for his mentorship.

Furthermore, I would like to thank Nahuel Freitas with whom I did my very first project. It is very difficult to teach him something that he does not already know, however, I learnt from him more than a bunch that I did not already know.

I would also thank Vasco Cavina for all those very extensive discussions on a lot of different things. I learnt a lot from him during the projects that we did together. He has been a great roommate and colleague for me.

Moreover, I would like to express my gratitude to Belen Farias, with whom I am currently engaged in my third project. It has been an absolute pleasure to engage in discussions with her, and I am truly thankful for the opportunity to continue our collaboration beyond my PhD.

I extend my thanks to Prof. Massimiliano Esposito for the fruitful collaborations and insightful discussions we shared during my PhD journey. I am grateful for his acceptance to be a part of my PhD defense committee. In this regard, I would like to express my gratitude to Prof. Benjamin Huard, Prof. Patrik Recher, and Prof. Ludger Wirtz for agreeing to be a part of my defense committee as well. Their participation is truly appreciated.

Contents

Chapter 1

Introduction

Quantum thermodynamics has been the subject of extensive research for more than two decades. Similar to the thermodynamics of classical systems, the concepts of exchanged work and heat are central parameters that need to be extended to the quantum regime. In fact, *heat* arises from the interaction of the system with its surrounding environment. One immediately realizes that heat can be interpreted as a source of noise in the system. In quantum information processing, one of the most undesirable but unavoidable issues is the presence of environmental noise and dissipation [43]. Therefore, it is essential to understand and control noise in quantum systems.

To analyze heat currents, one needs access to the dynamics of the dissipative system. In classical non-equilibrium systems, this is achieved by using Langevin and Fokker-Planck equations [93], which describe the time evolution of the probability distribution function of a system subject to drag forces or dissipation. However, these equations are not applicable in the quantum regime. Obtaining tractable descriptions for the reduced dynamics of open quantum systems is generally only possible for weak coupling between the system and the environment. This is accomplished by deriving quantum master equations, such as the well-known Gorini-Kossakowski-Sudarshan-Lindblad equation [75].

In most quantum information tasks, the coupling between the system and the environment is weak, making quantum master equations a fruitful tool to describe heat currents in such systems. However, the regime of strong dissipation can still lead to the understanding of interesting emergent processes in the dynamics of the system. Recent efforts in stochastic and quantum thermodynamics have therefore focused on understanding the effects of strong coupling in both equilibrium and non-equilibrium settings [31, 30, 32, 10, 14, 64, 98, 40, 85, 13, 28, 52, 104]. Interestingly, it has been shown that in the overdamped limit, where strong friction induces a time scale separation, with the momentum degree of freedom relaxing much faster than the position degree of freedom, one can obtain the quantum version of the

Smoluchowski equation using path integral techniques [83, 6, 26]. Therefore, analyzing the behavior of heat currents in this regime becomes a compelling task.

Work, on the other hand, is the result of an imposed external drive on the system of interest. This can be translated into explicit time dependence in the Hamiltonian of the system, which drives it out of equilibrium [108, 107]. This can indeed be interpreted as a useful form of energy that can be utilized for specific quantum information tasks. For instance, one can store work in quantum batteries and then use it later to create entanglement among atoms [3, 59, 18]. Therefore, understanding the behavior of work in closed and open quantum systems will be essential for both theoretical and practical reasons.

In this thesis, we analyze both heat and work. We first study the heat currents in the overdamped regime. We explore the overdamped limit of a quantum system in contact with a non-equilibrium environment, where the system simultaneously interacts with two thermal baths at different temperatures. Specifically, the system of interest is an electrical circuit composed of two parallel RLC circuits coupled by a mutual inductance, where the resistors represent the thermal baths into which energy can be dissipated. In this case, the nonequilibrium stationary state reached by the system results in heat flowing from the hot to the cold resistor. The properties of this heat current in the overdamped limit, where dissipation dominates, are of interest and can be achieved. The heat current can be split into classical and quantum contributions, and analytical expressions for both contributions can be obtained for linear systems such as this one [78, 39]. Moreover, we provide a detailed analysis of the behavior of the heat currents in different regimes, taking into account non-Markovian effects. Interestingly, the quantum corrections to the heat current do not necessarily vanish even when both temperatures are high with respect to the slow frequency scale, with the surviving quantum corrections depending logarithmically on the temperatures.

Afterward, we also consider non-linear quantum systems where one needs to rely on path integral techniques to find an analytical solution for the heat currents. We study superconducting qubits in contact with their environments as the non-linear system and outline the approach one might take to analyze the interaction in detail. We comment on the fact that, for a non-equilibrium situation where a single qubit is in contact with two thermal baths at different temperatures, an analytical solution can be obtained. However, as the number of qubits increases, along with internal interactions among them, the calculations become significantly more challenging, and numerical solutions become necessary.

In the next chapter, we expand the analysis of the quantum RLC circuit to study systems of cavities that are connected via a Superconducting Quantum Interference Device (SQID).

This setup is similar to the study of the dynamical Casimir effect in [34, 116] and the usual transmission lines interrupted by SQUIDs. However, in those studies, the degrees of freedom of the SQUIDs are not quantized, and they typically act as an external drive in the system. Nevertheless, we show that by quantizing the SQUID, one can obtain a three-body interaction term within the Hamiltonian of the dynamical Casimir setup. We indicate that such a form of interaction term can indeed be reduced to the Hamiltonian of a quantum *absorption refrigerator* [54, 82, 80].

At the end, we shift our attention to the other main ingredient of quantum thermodynamics, i.e., work. We investigate the work statistics of closed driven quantum systems by calculating the moment generating functions (MGFs). In fact, by introducing a modification of the Keldysh-Schwinger contour [66, 96, 60], we construct a perturbation of the MGF of work that satisfies the fluctuation theorem (FT) [5, 4, 56, 29] at all perturbative orders. Additionally, the contour can be used to generalize the notion of Keldysh rotation [62] to the work counting statistics case, introducing a new procedure to compute the semiclassical limit of MGFs.

Moreover, we investigate the semiclassical limit of the work MGF. We generalize the usual Feynman path integral technique [35] to the modified contour. A generalization of the Keldysh rotation is considered, and it is proven that a convenient way to achieve this is to introduce a symmetrization of the modified contour. After performing such a symmetrization, procedures similar to those in [88, 86, 89, 27] are adapted to obtain a semiclassical expansion of the MGF where we explicitly compute the zeroth (classical) order and the first quantum correction to the work MGF.

Chapter 2

Heat current in quantum RLC circuits

2.1 Introduction

This chapter concerns itself with the work that has been done in the paper *Heat transport in overdamped quantum systems* [61]. In this work, we explored the overdamped limit of a quantum system in contact with a non-equilibrium environment, where the system interacts with two thermal baths at different temperatures. To study the system of interest, we first describe the elements of quantum RLC circuits. Next, we incorporate dissipation by modeling it with the Caldeira-Leggett model of the bath. Using this model, we derive the Heisenberg equations of motion for the system and solve them by employing Green's function techniques. Afterwards, we introduce the overdamped limit and obtain an exact analytical expression for the heat currents, which consist of classical and quantum contributions in the overdamped regime. Finally, we extend our analysis to non-linear quantum systems by investigating superconducting qubits. We demonstrate how qubits can be constructed using Josephson junctions and how they can be made to interact with each other. Subsequently, we analyze heat currents in these systems using Feynman path integral techniques.

2.2 Quantization of LC circuit

The idea of a quantum electric circuit is based on the notion that certain variables of the circuit can capture the collective behavior of its microscopic degrees of freedom. In order to quantize these variables, two specific conditions must be satisfied:

1. The temperature of the system should be much smaller than the natural frequency of the system, i.e., $kT \ll \hbar\omega_0$.

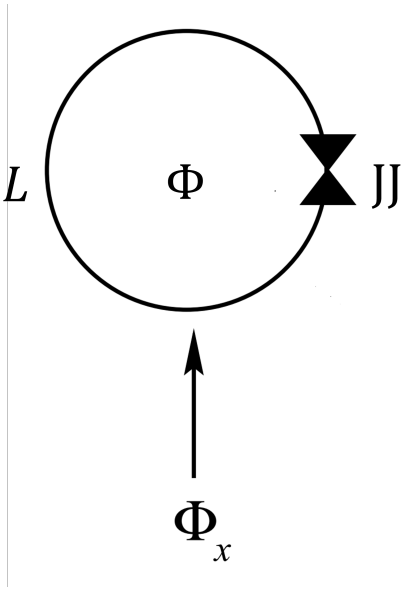

FIGURE 2.1: A SQUID ring consists of a Josephson junction (JJ) and a superconducting ring with inductance L. Φ_x represents the external applied flux to the ring.

2. The width of the energy levels must be smaller than their separations.

One example that satisfies these conditions is a superconducting interference device (SQUID), which consists of a superconducting ring interrupted by a Josephson junction. It has been suggested that using this device, one can observe quantum tunneling from a metastable state to a more stable state [17]. The collective macroscopic degree of freedom that describes the system is the trapped flux Φ in the ring. The potential energy of the SQUID ring represented in Fig 2.1 can be written as

$$U(\Phi) = \frac{(\Phi - \Phi_x)^2}{2L} - I_c \Phi_0 cos(2\pi\Phi/\Phi_0), \tag{2.1}$$

where L represents the self-inductance of the ring, I_c denotes the critical current of the Josephson Junction, Φ_0 represents the flux quantum, and Φ_x corresponds to the external flux passing through the ring, which we have control over. If the parameters satisfy $2\pi L I_C/\Phi \geq 1$, we can adjust Φ_x in a way that allows $U(\Phi)$ to possess at least one metastable state. Therefore, there is a possibility of observing flux tunneling through the barrier at a temperature of $T = 0$. To elaborate, if the system is initially located inside the metastable state ψ_{in} at time t_0, we can observe the system in the state outside the barrier ψ_{out} at a later time t_1. However, due to the strong interaction between the system and the environment, the superposition state $\psi = a\psi_{in} + b\psi_{out}$ may not be observable.

Having motivated our topic, we proceed to quantize a simple LC circuit. We begin by

discussing the Hamiltonian formulation of a classical LC circuit. One approach to justify this Hamiltonian is to utilize the Lagrangian of the system and perform a Legendre transformation to derive the corresponding Hamiltonian. To begin, we consider an LC circuit (shown in Fig. 2.2) comprising an inductance L and a capacitor C. By applying Kirchhoff's circuit laws, which govern voltages and currents, we obtain the following equations:

$$V_L = V_C \tag{2.2}$$

$$i_C + i_L = 0, \tag{2.3}$$

where $V_{L/C}$ represents the voltages across the inductance and capacitance, respectively, while $i_{L/C}$ denotes the currents flowing through these circuit elements. Using the relation between the voltages we can write

$$\frac{q}{C} = \dot{\phi}, \tag{2.4}$$

where ϕ is the flux inside the inductance and q is the charge stored in the capacitor. Above relation between charges and fluxes together with Kirchhoff's current law will result in

$$\ddot{\phi} + \frac{\phi}{LC} = 0, \tag{2.5}$$

which is the equation of motion for the circuit. This can be shown that, the above equation of motion is associated with the Euler-Lagrange equation of motion. In fact, if we use the definition of the Lagrangian of the system we will have

$$\mathcal{L} = T - U = \frac{1}{2}C\dot{\phi}^2 - \frac{\phi^2}{2L}. \tag{2.6}$$

We can see

$$q = \frac{\partial \mathcal{L}}{\partial \dot{\phi}}, \tag{2.7}$$

which plays the role of the conjugate momentum. Now employing Legendre transformation we will have

$$H = q\dot{\phi} - \mathcal{L} = \frac{1}{2}C\dot{\phi}^2 + \frac{\phi^2}{2L}. \tag{2.8}$$

Replacing $q = C\dot{\phi}$ in the above Hamiltonian we have

$$H = \frac{\phi^2}{2L} + \frac{q^2}{2C}. \tag{2.9}$$

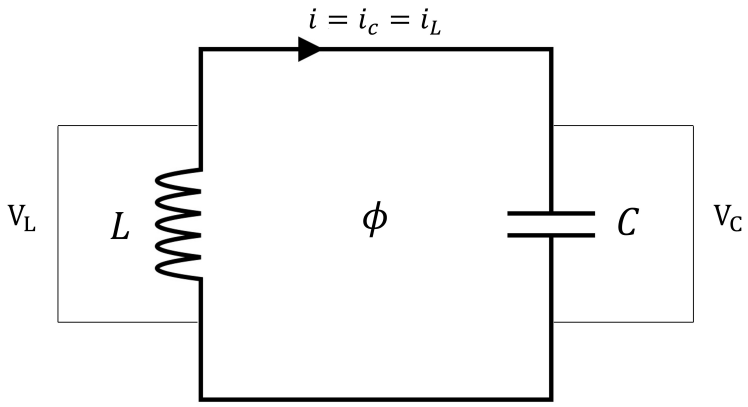

FIGURE 2.2: The LC circuit involves an inductance L, where the flux is denoted by ϕ. The voltage across the inductance and capacitance is represented by V_L and V_C, respectively. The currents passing through the inductance and capacitance are denoted as i_L and i_C.

Using the Hamilton equations of motions we obtain

$$\dot{q} = -\frac{\partial H}{\partial \phi} \tag{2.10}$$

$$\dot{\phi} = \frac{\partial H}{\partial q} \tag{2.11}$$

By solving the above equations, we can derive the equation of motion for the flux in the circuit, which is analogous to that of a harmonic oscillator. To quantize the LC circuit, we must replace the classical variables in the Hamiltonian (2.9) with their quantum counterparts. In other words, the Poisson bracket of the flux and charge in the circuit will be replaced by

$$\{\phi, q\} = \frac{\partial \phi}{\partial \phi}\frac{\partial q}{\partial q} - \frac{\partial q}{\partial \phi}\frac{\partial \phi}{\partial q} = 1. \tag{2.12}$$

As shown by Dirac the value of a classical Poisson bracket imposes its corresponding quantum commutator

$$\{\phi, q\} \rightarrow \frac{1}{i\hbar}[\hat{\phi}, \hat{q}]. \tag{2.13}$$

Thus, we can observe that the transfer of the classical Hamiltonian into its quantum version is supported by the uncertainty relation between flux and charge variables, as they correspond to position and momentum, respectively.

After quantizing the LC circuit, we aim to take it one step further by introducing dissipation into the aforementioned quantum circuit. Specifically, we include a resistor R in parallel to the existing circuit. However, the addition of a resistor leads to an irreversible time evolution of the system, which cannot be described by Hamilton's time-reversible equations of

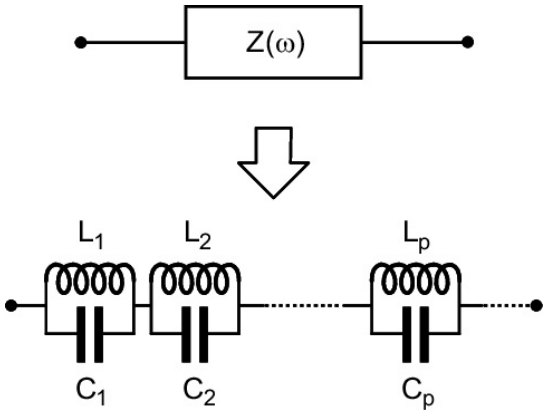

FIGURE 2.3: The Caldeira-Leggett model for Impedance.

motion. To address this issue, we employ the Caldeira-Leggett model of dissipation for systems interacting with the environment. In this model, the LC circuit acts as the system, while the resistor functions as the environment.

2.3 Caldeira-Leggett model and dissipation

In this section, we employ the Caldeira-Leggett model of resistors[25] to elucidate the role of dissipation in the quantum LC circuit. Essentially, the Caldeira-Leggett model replaces the resistor (impedance) in an RLC circuit with an infinite series of harmonic oscillators arranged in the form of an LC circuit in Fig. 2.3. If we write the electric impedance of each elements of parallel LC circuits we have

$$Z_{L_p} = j\omega L_p \tag{2.14}$$

$$Z_{C_p} = \frac{1}{j\omega C_p}. \tag{2.15}$$

Despite the pure imaginary impedance of the capacitor and inductance, the series LC circuit has a real part in impedance. In fact

$$\begin{aligned} Z_p(\omega) &= \left(\frac{1}{Z_{L_p}(\omega)} + \frac{1}{Z_{C_p}(\omega)} \right)^{-1} \\ &= -\frac{j}{2C_p} \left(\frac{1}{\omega - \omega_p} + \frac{1}{\omega + \omega_p} \right), \end{aligned} \tag{2.16}$$

where $\omega_p = \frac{1}{\sqrt{L_k C_p}}$. Before we obtain the real part of the above result, we need to go back to the definition of impedance which is responsible for the voltage response when a current

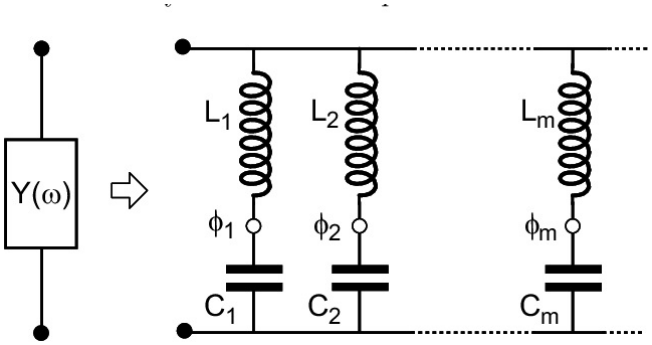

FIGURE 2.4: The Caldeira-Leggett model for Admittance.

is applied to the system

$$V(t) = \int_{-\infty}^{\infty} Z(t-\tau)I(\tau)d\tau. \tag{2.17}$$

Above relation must show the causality between the input ($I(\tau)$) and the output ($V(t)$), thus, we should have $Z(t) = 0$ for all $t < 0$. Going back to (2.16), we need to make sure that $Z_p(\omega)$ is analytic in the upper half plane so that its Fourier transformation $Z_p(t)$ remains causal. That said, we shift the poles of the $Z_p(\omega)$ slightly into the lower half plane by introducing $\omega \to \omega + j\epsilon$. Then we can use the identity $\frac{1}{x+j\epsilon} = PV(\frac{1}{x}) - j\pi\delta(x)$. Hence, we have,

$$\begin{aligned} Z_p(\omega) &= \lim_{\epsilon\to 0} \frac{-j}{2C_p}\left(\frac{1}{\omega-\omega_p+j\epsilon} + \frac{1}{\omega+\omega_p+j\epsilon}\right) \\ &= -Z_{0_p}\left\{\frac{\pi}{2}\omega_p[\delta(\omega-\omega_p)+\delta(\omega+\omega_p)] + \frac{j}{2}\left[PV(\frac{\omega_p}{\omega-\omega_p}) + PV(\frac{\omega_p}{\omega+\omega_p})\right]\right\}, \end{aligned} \tag{2.18}$$

where $Z_{0_p} = \frac{1}{C_p\omega_p}$, and we set it equal to the resistance of the corresponding RLC circuit. The total resistance of this model will be the sum of all LC circuits.

Alternatively, one can also model the admittance in terms of an infinite series of LC circuits (see Fig. 2.4). In fact, admittance Y represents the inverse of the impedance of an electrical circuit, which governs the current response when a voltage is applied to the system

$$I(t) = \int_{-\infty}^{\infty} Y(t-\tau)V(\tau)d\tau, \tag{2.19}$$

which is again causal in the sense that $Y(t) = 0$ for all $t < 0$. We can follow the same procedure that we had for modelling the impedance, however, with a modified series of LC circuit. Fig. 2.4 shows that, in contrast with the modelling of impedance, we need to use an

infinite series of parallel LC circuits. Thus, we have

$$Y_m(\omega) = \left(\frac{1}{Y_{L_m}(\omega)} + \frac{1}{Y_{C_m}(\omega)} \right)^{-1} \tag{2.20}$$

where

$$Y_{C_m} = j\omega C_m \tag{2.21}$$

$$Y_{L_m} = \frac{1}{j\omega L_m}. \tag{2.22}$$

are the admittance of the capacitor and inductance of the m-th LC circuit, respectively. Since each circuit is a parallel LC circuit, the impedance would be $Z_m = Z_{L_m} + Z_{C_m}$, so that the total admittance of each LC circuit would become $1/Y_m = 1/Y_{L_m} + 1/Y_{C_m}$. Hence, we have

$$Y_m(\omega) = -\frac{j}{2L_m} \left(\frac{1}{\omega - \omega_m} + \frac{1}{\omega + \omega_m} \right). \tag{2.23}$$

Following the same arguments that we used to obtain (2.18), we have

$$\begin{aligned} Y_m(\omega) &= \lim_{\epsilon \to 0} \frac{-j}{2L_m} \left(\frac{1}{\omega - \omega_m + j\epsilon} + \frac{1}{\omega + \omega_m + j\epsilon} \right) \\ &= -\frac{1}{Z_{0_P}} \left\{ \frac{\pi}{2} \omega_m [\delta(\omega - \omega_m) + \delta(\omega + \omega_m)] + \frac{j}{2} \left[PV(\frac{\omega_m}{\omega - \omega_m}) + PV(\frac{\omega_m}{\omega + \omega_m}) \right] \right\}. \end{aligned} \tag{2.24}$$

Therefore, we observed that both the impedance and admittance of a series of LC circuits will exhibit dissipation through their real parts. This observation is helpful in understanding the influence that such an element will have on the rest of the circuit. In that regard, the idea of the Caldeira-Leggett model is to replace the resistor in a circuit with large number of LC harmonic oscillators. Thus, we can express the Hamiltonian of the model by utilizing the Lagrangian of the system. To streamline the process, we derive the Lagrangian for the simplified circuit illustrated in Fig. 2.5, making it straightforward to extend it to the Caldeira-Leggett model. In Fig. 2.5, the flux variables Φ and ϕ_1 represent the *node* variables. Specifically, the node flux is defined as the integral of the voltage over the path connecting the node and the ground. For instance, in our example shown in Fig. 2.5, integrating the total voltage between the node ϕ_1 and the ground would yield the following result:

$$\dot{\phi}_1 = V_{C_1} + V_g = V_{C_1}. \tag{2.25}$$

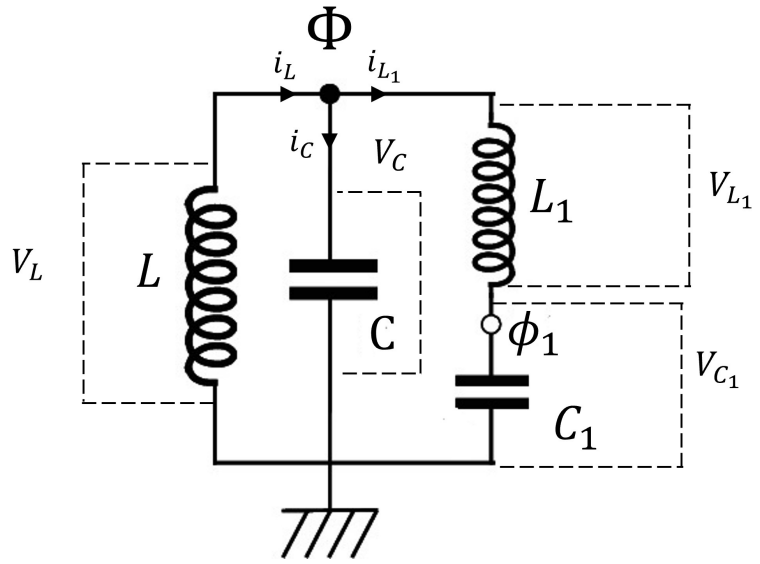

FIGURE 2.5: A simplified circuit.

where V_{C_1} is the voltage of the capacitance C_1 and $V_g = 0$ is the earth voltage. Therefore, we are relating the voltage of the capacitance to our node flux variable. Calculating the voltage between the node Φ and the ground we will obtain

$$\Phi = \int \dot{\phi}_{L_1} dt + \int \dot{\phi}_1 dt. \tag{2.26}$$

Hence,

$$\phi_{L_1} = \Phi - \phi_1. \tag{2.27}$$

By the same method we find that $\phi_L = \Phi$ and using Kirchhoff's circuit laws we may write

$$V_C = V_L, \tag{2.28}$$

where V_C and V_L are the voltages associated with the capacitance and inductance C and L, respectively. Thus, we have

$$q_C = C\dot{\Phi}. \tag{2.29}$$

According to Kirchhoff's current Law, the sum of all currents passing thorough the node Φ is zero. Hence,

$$i_L = i_C + i_{L_1}, \tag{2.30}$$

where i_L, i_C and i_{L_1} are the currents passing through L, C and L_1, respectively. Using (2.30) and (2.29), we have

$$\frac{\phi - \Phi}{L} + C\ddot{\Phi} = \frac{\Phi}{L} \tag{2.31}$$

$$\frac{\phi - \Phi}{L} = C_1\ddot{\phi}_1, \tag{2.32}$$

which they exhibit the equation of motion for this circuit. With that in hand, we can write the corresponding Lagrangian as

$$\mathcal{L} = \frac{1}{2}C\dot{\Phi}^2 + \frac{1}{2}C_1\dot{\phi}_1^2 - \frac{\Phi^2}{2L} - \frac{(\phi_1 - \Phi)^2}{2L_1}. \tag{2.33}$$

With the Lagrangian at our disposal, we can employ the Legendre transformation to compute the Hamiltonian. By substituting $q = C\dot{\Phi}$ and $q_1 = C_1\dot{\phi}_1$ into the Lagrangian, we can express the Hamiltonian as follows:

$$H = \frac{q^2}{2C} + \frac{q_1^2}{2C_1} + \frac{\Phi^2}{2L} + \frac{(\phi_1 - \Phi)^2}{2L_1}. \tag{2.34}$$

In this example, if we disregard the presence of inductance and capacitance on the left-hand side and solely focus on their existence at the corresponding flux node Φ, our Lagrangian and, consequently, the Hamiltonian will solely depend on C_1 and L_1. Thus, for the general scenario involving a large number of LC circuits, the Hamiltonian can be expressed as

$$H_d = \sum_m \frac{q_m^2}{2C_m} + \frac{(\phi_m - \Phi)^2}{2L_m}, \tag{2.35}$$

where Φ is the flux corresponds to the other terminal of the admittance. Indeed, we will see that it plays the role of the interaction between the dissipative part and the LC circuit.

Having modelled the dissipation in the LC circuit in terms of impedance and admittance, we are at the position to calculate the fluctuations in charge and flux variable of the circuit which can be obtained using the Hamiltonian of the Caldeira-Leggett model.

2.4 Fluctuations and dissipation

In the presence of dissipation, considering a damped LC circuit as shown in Fig. 2.6, we will employ equation (2.35) to calculate the fluctuations in the system variables. The total

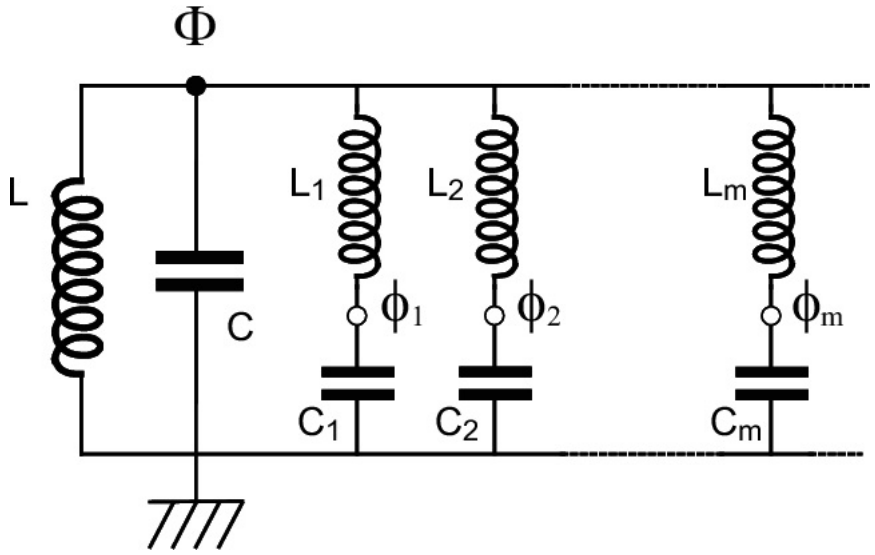

FIGURE 2.6: A damped LC circuit.

Hamiltonian of the circuit will be

$$H = \frac{\phi^2}{2L} + \frac{q^2}{2C} + \sum_m \frac{q_m^2}{2C_m} + \frac{(\phi_m - \phi)^2}{2L_m}. \tag{2.36}$$

Prior to computing the fluctuation relations for the entire circuit, our initial focus is on the dissipative component. If we were to exclude the dissipative part, we would be left with an infinite series of LC circuits ($\Phi = 0$ in (2.35)). In this context, we assume that all the harmonic oscillators are in a thermal state with a temperature of $1/\beta = T$. Consequently, we can determine the correlation function of the overall flux and charge within the circuit.

First of all we write the Hamiltonian in terms of ladder operators

$$\phi_m = \sqrt{\frac{\hbar Z_m}{2}}(a_m + a_m^\dagger) \tag{2.37}$$

$$q_m = \frac{1}{i}\sqrt{\frac{\hbar}{2Z_m}}(a_m - a_m^\dagger) \tag{2.38}$$

$$H_d = \sum_m \hbar\omega_m (a_m^\dagger a_m + \frac{1}{2}). \tag{2.39}$$

Since all the oscillators are independent, we can find the time evolution of the charge and flux variables at time t.

$$\frac{d\phi_m}{dt} = \frac{i}{\hbar}[\phi_m, H_d] = \frac{q_m}{c} \tag{2.40}$$

$$\frac{dq_m}{dt} = \frac{i}{\hbar}[q_m, H_d] = -\frac{\phi_m}{c}. \tag{2.41}$$

Hence, for the flux and charge variables we have

$$\phi_m(t) = \sqrt{\frac{\hbar Z_m}{2}}(a^\dagger e^{i\omega_m t} + a e^{-i\omega_m t}) \tag{2.42}$$

$$q_m(t) = \sqrt{\frac{\hbar}{2Z_m}}(a^\dagger e^{i\omega_m t} + a e^{-i\omega_m t}). \tag{2.43}$$

Writing Kirchhoff's laws for Fig. 2.6 we can see that the the voltage across all series LC circuits are equal while the total current i will be the sum of all currents i_m passing thorough each LC circuit. In other words we have

$$i = \sum_m i_m. \tag{2.44}$$

Thus, for the charges we can write

$$q = \sum_m q_m. \tag{2.45}$$

Now, we can calculate the correlation function for the total charge in the circuit as

$$\begin{aligned}
\langle q(t)q(0)\rangle &= \sum_m \langle q_m(t)q_m(0)\rangle \\
&= \sum_m \frac{\hbar}{2Z_m}\left(\langle a_m a_m^\dagger\rangle e^{-i\omega_m t} + \langle a_m^\dagger a_m\rangle e^{i\omega_m t}\right) \\
&= \sum_m \frac{\hbar}{2Z_m}\frac{1}{2}\left[\coth\left(\frac{\beta\hbar\omega}{2}\right) - 1\right] e^{-i\omega_m t} + \frac{1}{2}\left[\coth\left(\frac{\beta\hbar\omega}{2}\right) + 1\right] e^{i\omega_m t} \\
&= \sum_m \frac{\hbar}{2Z_m}\int_{-\infty}^{+\infty} d\omega \frac{\omega}{\omega_m}(\delta(\omega-\omega_m) + \delta(\omega+\omega_m))\left[\coth\left(\frac{\beta\hbar\omega}{2}\right) + 1\right] e^{-i\omega t} \\
&= \sum_m \frac{\hbar}{2\pi}\int_{-\infty}^{+\infty} d\omega \frac{1}{\omega}\left[\coth\left(\frac{\beta\hbar\omega}{2}\right) + 1\right] \mathrm{Re}(Y_m(\omega)) e^{-i\omega t} \\
&= \frac{\hbar}{2\pi}\int_{-\infty}^{+\infty} d\omega \frac{1}{\omega}\left[\coth\left(\frac{\beta\hbar\omega}{2}\right) + 1\right] \mathrm{Re}(Y(\omega)) e^{-i\omega t},
\end{aligned} \tag{2.46}$$

where in the forth line we used the real values of Y_m ($\mathrm{Re}(Y_m)$) in (2.24). To obtain the correlation functions for the flux variable, one needs to change the circuit for the dissipative part to the one in Fig. 2.3 where we have a collection of parallel LC circuits. For that circuit, all currents are equal while the total voltage is the sum over voltages in each LC circuit such that

$$V = \sum_m V_m. \tag{2.47}$$

Thus, for the fluxes ($V = \dot{\phi}$) we can write

$$\phi = \sum_m \phi_m. \tag{2.48}$$

Using the same steps we employed to calculate charge fluctuations, we can find the correlation function for the total flux in the circuit as

$$\begin{aligned}\langle \phi(t)\phi(0)\rangle =& \sum_m \langle \phi_m(t)\phi_m(0)\rangle \\ =& \sum_m \frac{\hbar Z_m}{2}\left(\langle a_m a_m^\dagger\rangle e^{-i\omega_m t} + \langle a_m^\dagger a_m\rangle e^{i\omega_m t}\right) \\ =& \frac{\hbar}{2\pi}\int_{-\infty}^{+\infty} d\omega \frac{1}{\omega}\left[\coth\left(\frac{\beta\hbar\omega}{2}\right)+1\right]\mathrm{Re}(Z(\omega))e^{-i\omega t},\end{aligned} \tag{2.49}$$

where we have used $\mathrm{Re}(Z_m)$ as the real part of the impedance. As we can see, equations (2.46) and (2.49) show the connection between fluctuations and the impedance or admittance in the circuit, hence they are called fluctuation-dissipation relations.

Returning to the circuit depicted in Fig. 2.6, our goal is to derive the correlation functions for the flux and charge variables. To achieve this, we must solve the Heisenberg equations of motion for the flux and charge variables using the Hamiltonian given in (2.36). However, there exists an alternative method to determine the correlation functions by utilizing the fluctuation-dissipation relation. In this approach, we treat the entire circuit shown in Fig. 2.6 as a dissipative element with an impedance $Z(\omega)$, which is defined as follows:

$$Z(\omega) = \frac{1}{\frac{1}{jL\omega} + jC\omega + Y(\omega)}. \tag{2.50}$$

Conservation of flux would also tell us that the flux ϕ through the dissipative part is equal to the flux Φ through the inductance of the system. Then using equation (2.49) we will replace the real value of (2.50) with $Y(\omega)$ inside that equation. Thus, at time $t = 0$ we have

$$\begin{aligned}\mathcal{R}(Z(\omega)) =& \frac{Y(\omega)}{Y^2(\omega) + (C\omega - \frac{1}{L\omega})^2} \\ =& \frac{\omega_0^4\omega^2 L^2}{y^2L^2\omega^2\omega_0^4 + \omega^4 + \omega_0^4 - 2\omega^2\omega_0^2} \\ =& \frac{Z_0^2\omega^2\omega_0^2 Y(\omega)}{\left(\omega^2-\omega_0^2\right)^2 + Z_0^2\omega_0^2\omega^2 Y(\omega)^2},\end{aligned} \tag{2.51}$$

where we have used the relation $Z_0 = \sqrt{\frac{L}{C}}$ and $\omega_0 = \frac{1}{\sqrt{LC}}$. Replacing (2.51) in (2.49) we will eventually have

$$\langle \Phi^2 \rangle = \frac{\hbar Z_0}{2} \int_{-\infty}^{+\infty} \frac{Z_0 \omega \omega_0^2 Y(\omega)}{\left(\omega^2 - \omega_0^2\right)^2 + Z_0^2 \omega_0^2 \omega^2 Y(\omega)^2} \coth\left(\frac{\beta\hbar\omega}{2}\right) d\omega. \tag{2.52}$$

The above result is valid with any choice of admittance $Y(\omega)$. Nevertheless, one should also be able to obtain the same result by solving the Caldeira-Leggett Hamiltonian (2.36). In the following subsection we will explicitly delineate this approach.

2.4.1 The Caldeira-Leggett model and fluctuations

The Hamiltonian (2.36) can be written in the alternative form as

$$H = \frac{\phi^2}{2L} + \frac{q^2}{2C} + \sum_m \frac{\phi^2}{2L_m} + \sum_m \frac{q_m^2}{2C_m} + \frac{\phi_m^2}{2L_m} - \sum_m \frac{1}{L_m} \phi_m \phi. \tag{2.53}$$

This Hamiltonian describes a harmonic oscillator interacting with a large number of harmonic oscillators (denoted by m), which serve as the degrees of freedom for the bath. The final term in the Hamiltonian explicitly represents the interaction between the system and the bath, which takes a bilinear form in terms of the flux operators of the interacting quantum systems. The coupling constant between the m-th oscillator of the bath and the system is given by $\frac{1}{L_m}$.

To solve this Hamiltonian, we utilize the Heisenberg equations of motion for both the system and bath variables. By doing so, we obtain

$$\frac{d\phi(t)}{dt} = \frac{1}{C} q(t), \quad \frac{dq(t)}{dt} = \sum_m \frac{1}{L_m} \phi_m(t) - \frac{\phi}{L} - \sum_m \frac{\phi}{L_m}, \tag{2.54}$$

$$\frac{d\phi_m(t)}{dt} = \frac{1}{C} q_m(t), \quad \frac{dq_m(t)}{dt} = -\frac{1}{L_m} \phi_m(t) + \frac{1}{L_m} \phi(t) \tag{2.55}$$

Taking the derivation of the above equations for ϕ and ϕ_m with respect to t and replacing the reciprocal momenta q and q_m we reach the equation of motion for ϕ as

$$C \frac{d^2\phi}{dt^2} + \int_0^t \gamma(t - t') \frac{d\phi(t')}{dt'} dt' + \frac{\phi}{L} = -\gamma(t)\phi(0) + \mathcal{F}, \tag{2.56}$$

where

$$\gamma(t) = \sum_m \frac{1}{L_m} \cos(\omega_m t), \tag{2.57}$$

and

$$F(t) = \sum_m \frac{1}{L_m} \phi_m(0) \cos(\omega_m t) + \omega_m q_m(0) \sin(\omega_m t). \tag{2.58}$$

$\gamma(t)$, known as the memory kernel, incorporates the influence of the system's history on its dynamics. In the case of Markovian dynamics, this memory kernel assumes the form of the Dirac delta function, which effectively separates the initial information of the system from its subsequent dynamics (yielding a memoryless kernel). Additionally, $\mathcal{F}$ represents a fluctuating force arising from the interaction between the system and the bath. The behavior of this force depends on the initial values of the bath variables.

Using the equation (2.56), we can find the flux variable at time t, which allows us to calculate its correlation function. To solve the equation of motion, we perform a Laplace transform on (2.56), yielding

$$\int_0^\infty dt e^{-st}\left(C\frac{d^2\phi}{dt^2}+\int_0^t \gamma(t-t')\frac{d\phi(t')}{dt'}dt'+\frac{\phi}{L}\right)=\int_0^\infty dt e^{-st}\left(-\gamma(t)\phi(0)+\mathcal{F}\right). \tag{2.59}$$

In order to address the assumption that the term $\gamma(t)\phi(0)$ vanishes in the long-time limit, we can incorporate this term into the fluctuating force $\mathcal{F}$. Consequently, we assume that all oscillators of the bath are in equilibrium around the point $\phi(0)$[15, 112]. This implies that the initial state of the bath is a thermal state centered around ϕ_0, such that

$$\rho_{bath}(0)=\mathcal{Z}^{-1}exp\left(\sum_m \frac{q_m^2}{2C_m}+\frac{(\phi_m-\phi(0))^2}{2L_m}\right). \tag{2.60}$$

Hence, we can still recover the fact that the average of the shifted fluctuating force, $F(t)=-\gamma(t)\phi(0)+\mathcal{F}(t)$, is still zero. With that in mind we have

$$\left(Cs^2+Cs\gamma(s)+\frac{1}{L}\right)\phi(s)=F(s), \tag{2.61}$$

where we have used $\mathcal{L}[h(\tau)g(t-\tau)]=H(s)G(s)$ where $H(s)$ and $G(s)$ are the Laplace transform of their reciprocal functions. Hence, we have

$$\phi(t)=\frac{1}{C}\int_{-\infty}^{\infty}\frac{F(j\omega+\sigma)e^{-(j\omega+\sigma)t}}{(j\omega+\sigma)^2+(j\omega+\sigma)\gamma(j\omega+\sigma)+\omega_0^2}d\omega. \tag{2.62}$$

We have replaced $s\rightarrow(j\omega+\sigma)$ in order to take the inverse Laplace transform. To solve the above integral, we choose the real axes $\sigma=0$ and the integration will be done along the

imaginary axis $j\omega$. For $t = 0$ we can calculate the correlation function $\langle\phi^2\rangle$ such that

$$\langle\phi^2\rangle = \frac{1}{C^2}\int_{-\infty}^{\infty}\int_{-\infty}^{\infty}\frac{\langle F(j\omega)F(j\omega')\rangle}{\left(-\omega^2+j\omega\gamma(j\omega)+\omega_0^2\right)\left(-\omega'^2+j\omega'\gamma(j\omega')+\omega_0^2\right)}d\omega d\omega'. \tag{2.63}$$

Thus, we need to calculate the fluctuation in the force term $F(t)$. According to (2.58) we can write

$$\begin{aligned}F(j\omega) =&\frac{1}{2}\sum_m\Bigg\{\frac{1}{L_m}\phi_m(0)\left(\delta(\omega_m-\omega)+\delta(\omega_m+\omega)\right)\\ &-j\omega_m q_m(0)\left(\delta(\omega_m+\omega)-\delta(\omega_m-\omega)\right)\Bigg\}.\end{aligned} \tag{2.64}$$

Since $\langle\phi_m(0)q_m(0)\rangle = 0$, we will have

$$\begin{aligned}&\langle F(j\omega)F(j\omega')\rangle\\ &=\frac{1}{4}\sum_m\frac{1}{L_m^2}\langle\phi_m^2(0)\rangle\left(\delta(\omega_m-\omega)+\delta(\omega_m+\omega)\right)\left(\delta(\omega_m-\omega')+\delta(\omega_m+\omega')\right)\\ &-\frac{1}{4}\sum_m\omega_m^2\langle q_m^2(0)\rangle\left(\delta(\omega_m+\omega)-\delta(\omega_m-\omega)\right)\left(\delta(\omega_m+\omega')-\delta(\omega_m-\omega')\right).\end{aligned} \tag{2.65}$$

Also, for the fluctuation in flux and charge variables of the bath we already obtained

$$\langle\phi_m^2(0)\rangle = \frac{\hbar Z_m}{2}\coth\left(\frac{\beta\hbar\omega_m}{2}\right) \tag{2.66}$$

$$\langle q_m^2(0)\rangle = \frac{\hbar}{2Z_m}\coth\left(\frac{\beta\hbar\omega_m}{2}\right). \tag{2.67}$$

Replacing the above equations into (2.63) we have

$$\langle\phi^2\rangle = \frac{1}{C^2}\sum_m\frac{\hbar\omega_m^2}{Z_m}\frac{coth(\frac{\beta\hbar\omega_m}{2})}{\left(-\omega_m^2+j\omega_m\gamma(j\omega_m)+\omega_0^2\right)\left(-\omega_m^2-j\omega_m\gamma(-j\omega_m)+\omega_0^2\right)}. \tag{2.68}$$

We can change the sum into integral such that

$$\langle\phi^2\rangle = \frac{1}{C^2}\sum_m\int_{-\infty}^{\infty}\frac{\hbar\omega_m^2}{Z_m}\frac{\omega_m}{\omega}\frac{\left(\delta(\omega_m-\omega)+\delta(\omega_m+\omega)\right)\coth\left(\frac{\beta\hbar\omega_m}{2}\right)}{\left(-\omega^2+j\omega\gamma(j\omega)+\omega_0^2\right)\left(-\omega^2-j\omega\gamma(-j\omega)+\omega_0^2\right)}. \tag{2.69}$$

Using (2.24) we have

$$\langle\phi^2\rangle = \frac{\hbar}{2C^2}\int_{-\infty}^{\infty}d\omega\frac{\omega Y(\omega)\coth\left(\frac{\beta\hbar\omega}{2}\right)}{\left(-\omega^2+j\omega\gamma(j\omega)+\omega_0^2\right)\left(-\omega^2-j\omega\gamma(-j\omega)+\omega_0^2\right)}. \tag{2.70}$$

Replacing $Z_0^2\omega_0^2 = \frac{1}{C^2}$ and $\gamma(j\omega) = Z_0\omega_0 Y(j\omega)$ we will obtain

$$\langle\phi^2\rangle = \frac{\hbar}{2C^2}\int_{-\infty}^{\infty} d\omega \frac{\omega Y(\omega)\coth\left(\frac{\beta\hbar\omega}{2}\right)}{\left(-\omega^2 + j\omega Z_0\omega_0 Y(j\omega) + \omega_0^2\right)\left(-\omega^2 - j\omega Z_0\omega_0 Y(j\omega) + \omega_0^2\right)}. \tag{2.71}$$

Therefore, by employing the Caldeira-Leggett model, we can successfully reproduce the result obtained in equation (2.52) using the fluctuation-dissipation theorem. In the subsequent section, we will utilize the aforementioned discussions on quantum RLC circuits and dissipation to investigate heat currents in a system composed of two magnetically coupled RLC circuits.

2.5 Two magnetically coupled RLC circuits

In this section, our objective is to derive the Hamiltonian describing two magnetically interacting RLC circuits. By utilizing this Hamiltonian, we will determine the fluctuations in relevant coordinates.

Before delving into the case of two coupled RLC circuits, let us first examine two simple coupled circuits as depicted in Fig. 2.7. The coupling between the two circuits arises when the flux produced in one circuit passes through the other circuit, generating current. Specifically, we can define ϕ_1 and ϕ_2 as the total fluxes passing through the left and right circuits, respectively. ϕ_{11} and ϕ_{22} represent the fluxes produced in inductances L_1 and L_2, while ϕ_{12} and ϕ_{21} are the mutual fluxes passing through the circuits. Thus, we obtain the following relations:

$$\phi_1 = \phi_{11} + \phi_{12} \tag{2.72}$$

$$\phi_2 = \phi_{22} + \phi_{21}. \tag{2.73}$$

Kirchhoff's law for voltages would be written as

$$v_1 = \dot{\phi}_1 = L_1\frac{di_1}{dt} + \dot{\phi}_{12} \tag{2.74}$$

$$v_2 = \dot{\phi}_2 = L_2\frac{di_2}{dt} + \dot{\phi}_{21}, \tag{2.75}$$

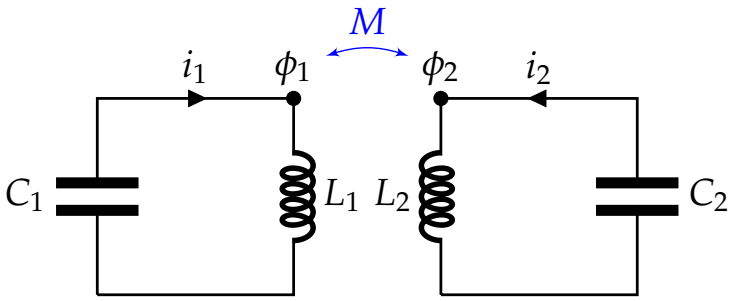

FIGURE 2.7: Two magnetically coupled circuits [61].

where v_1 and v_2 are the voltages associated with the two capacitances. For mutual flux $\phi_{12/21}$ we can write

$$\begin{aligned}\dot{\phi}_{12} &= \frac{d\phi_{12}}{di_2}\frac{di_2}{dt} = M_{12}\frac{di_2}{dt} \\ \dot{\phi}_{21} &= \frac{d\phi_{21}}{di_1}\frac{di_1}{dt} = M_{21}\frac{di_1}{dt},\end{aligned} \tag{2.76}$$

where $M_{12/21} = \frac{d\phi_{12/21}}{di_{2/1}}$ is the mutual inductance between the two circuits and it can be proved that $M_{12} = M_{21} = M$. To calculate the energy stored in the two coupled circuits, we first assume that $i_2 = 0$ and i_1 is increased up to an arbitrary value I_1. Then the power stored in the left circuit is

$$p_1 = v_1 i_1 = i_1 L_1 \frac{di}{dt}. \tag{2.77}$$

Next, we write the total energy as

$$E_1 = \int p_1 dt = \int_0^{I_1} i_1 di_1 = \frac{1}{2} L_1 I_1^2. \tag{2.78}$$

Now, we assume that $i_1 = I_1$ is constant and we change i_2 from zero to I_2. Since i_2 is changing, the mutual voltage induced in the left circuit is $M di_2/dt$ and therefore the total power would be

$$p_2 = v_2 i_2 + I_1 M \frac{di_2}{dt} = i_2 L_2 \frac{di}{dt} + I_1 M \frac{di_2}{dt}. \tag{2.79}$$

Thus, the energy stored in the circuit will be

$$E_2 = \int p_2 dt = \int_0^{I_2} i_2 di_2 + I \int_0^{I_2} M di_2 = \frac{1}{2} L_2 I_2^2 + M I_1 I_2. \tag{2.80}$$

The total energy of the inductance part of the circuit will be

$$E_1 + E_2 = \frac{1}{2} L_1 I_1^2 + \frac{1}{2} L_2 I_2^2 + M I_1 I_2. \tag{2.81}$$

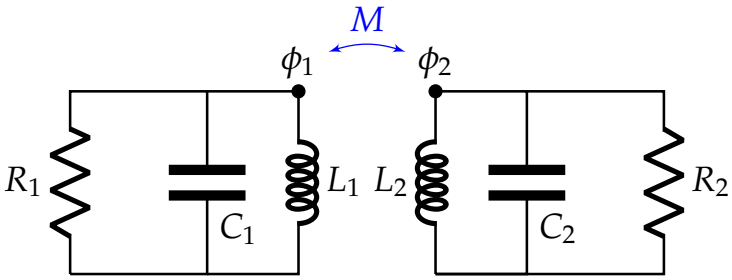

FIGURE 2.8: Two magnetically coupled RLC circuits.

Adding the energy with respect to the capacitances to this energy we can write the Hamiltonian as

$$H = \frac{q_1^2}{2C_1} + \frac{q_2^2}{2C_2} + \frac{1}{2}L_1 i_1^2 + \frac{1}{2}L_2 i_2^2 + M i_1 i_2, \tag{2.82}$$

where we have replaced arbitrary currents I_1 and I_2 by i_1 and i_2. We can see that M is playing the role of the coupling constant between the two circuits. Now we can find the Hamiltonian for two RLC circuits which are coupled by their mutual inductance (Fig. 2.8). We replace the resistors with the series of LC circuits, and using the Caldeira-Leggett Hamiltonian we can write

$$\begin{aligned} H =& \frac{q_1^2}{2C_1} + \frac{q_2^2}{2C_2} + \frac{\phi_{11}^2}{2L_1} + \frac{\phi_{22}^2}{2L_2} \\ &+ \frac{M}{L_1 L_2}\phi_{11}\phi_{22} + \sum_{m_1,m_2} \frac{q_{m_1}^2}{2C_{m_1}} + \frac{q_{m_2}^2}{2C_{m_2}} + \frac{(\phi_{m_1} - \phi_1)^2}{2L_{m_1}} + \frac{(\phi_{m_2} - \phi_2)^2}{2L_{m_2}}. \end{aligned} \tag{2.83}$$

ϕ_{m_1/m_2} and q_{m_1/m_2} are the flux and charge variables of each LC circuit in the Caldeira-Leggett representation of the resistors of the left and right circuits, respectively. Additionally, L_{m_1/m_2} represents the inductance and capacitance associated with the m-th LC circuit in the model. To express the Hamiltonian in terms of the total fluxes passing through the inductances (ϕ_1 and ϕ_2), we utilize equation (2.72). The fact that

$$\begin{aligned} \phi_{12} =& M_{12} i_2 = \frac{M_{12}}{L_2}\phi_2 \\ \phi_{21} =& M_{21} i_1 = \frac{M_{21}}{L_1}\phi_1, \end{aligned} \tag{2.84}$$

enables us to write

$$\begin{aligned} \phi_{11} =& \frac{L_1 L_2}{M^2 - L_1 L_2}\left(\frac{M}{L_2}\phi_2 - \phi_1\right) \\ \phi_{22} =& \frac{L_1 L_2}{M^2 - L_1 L_2}\left(\frac{M}{L_1}\phi_1 - \phi_2\right). \end{aligned} \tag{2.85}$$

Replacing the above relations into the Hamiltonian of the coupled circuits will yield

$$H = \frac{q_1^2}{2C_1} + \frac{q_2^2}{2C_2} + \frac{L_1 L_2}{L_1 L_2 - M^2}\left(\frac{\phi_1^2}{2L_1} + \frac{\phi_2^2}{2L_2} - \frac{M}{L_1 L_2}\phi_1\phi_2\right) + \sum_{m_1}\left(\frac{q_{m_1}^2}{2C_{m_1}} + \frac{(\phi_{m_1} - \phi_1)^2}{2L_{m_1}}\right) + \sum_{m_2}\left(\frac{q_{m_2}^2}{2C_{m_2}} + \frac{(\phi_{m_2} - \phi_2)^2}{2L_{m_2}}\right). \tag{2.86}$$

We can expand the terms inside the summations and write the Hamiltonian in terms of matrices in the following closed form:

$$H_s = \frac{1}{2}q^T(t)C^{-1}q(t) + \frac{1}{2}\phi^T(t)L^{-1}\phi(t) \tag{2.87}$$

$$H_{bath} = \sum_\alpha \frac{1}{2}q_\alpha^T(t)C_\alpha^{-1}q_\alpha(t) + \frac{1}{2}\phi_\alpha^T(t)L_\alpha^{-1}\phi_\alpha(t) \tag{2.88}$$

$$H_{int} = -\sum_\alpha \phi^T(t)\bar{L}_\alpha^{-1}\phi_\alpha, \tag{2.89}$$

Where, $\alpha = \{1,2\}$, $\phi = \begin{bmatrix}\phi_1 \\ \phi_2\end{bmatrix}$, ϕ_α and q_α are the vectors formed with the position and momentum of the α-th bath. $q = \begin{bmatrix}q_1 \\ q_2\end{bmatrix}$. L_α and C_α are $N \times N$ matrices while $\bar{L}_\alpha^{-1}$ is a $2 \times N_\alpha$ matrix. In fact $\bar{L}_1^{-1} = \begin{bmatrix}L_{11} & L_{12} & ... & L_{1N} \\ 0 & 0 & ... & 0\end{bmatrix}$ and $\bar{L}_2^{-1} = \begin{bmatrix}0 & 0 & ... & 0 \\ L_{21} & L_{22} & ... & L_{2N}\end{bmatrix}$. $C = \begin{bmatrix}C_1 & 0 \\ 0 & C_2\end{bmatrix}$, and $L^{-1} = \begin{bmatrix}L_1 & -M \\ -M & L_2\end{bmatrix}^{-1} + \sum_{m_1,m_2}\begin{bmatrix}L_{m_1} & 0 \\ 0 & L_{m_2}\end{bmatrix}^{-1}$. Once we have obtained the form of the Hamiltonian $H = H_s + H_{\text{bath}} + H_{\text{int}}$, we can analyze the fluctuations of the variables in our system by solving the equations of motion. In the upcoming section, we will delve into this topic extensively, discussing how these fluctuations can be associated with heat currents.

2.6 Heat currents and the Green's function method

Our main objective is to calculate the fluctuations in the system variables, which we have achieved by solving the equation of motion for the flux variable (2.56) using Laplace transform techniques. These fluctuations are crucial in determining the heat currents exchanged between the system and the baths.

To illustrate this, we introduce the variance matrix that captures all possible fluctuations

of the system variables. We will explicitly demonstrate the relationship between the covariance matrix and the heat currents flowing to or from the baths. Finally, we will utilize the Green's function to compute the covariance matrix and, consequently, the heat currents.

2.6.1 Covariance matrix and heat currents

The elements of the covariance matrix σ contain all the correlation functions of the system variables, i.e ϕ and q. For our system of interest, we first define the phase space variable $Z = \begin{bmatrix} \phi \\ q \end{bmatrix}$, where ϕ and q are two vectors. The covariance matrix in terms of phase space variable can be written as

$$\sigma(t) = \mathrm{Re}\left(\left\langle Z(t)Z(t)^T \right\rangle\right) - \langle Z(t)\rangle \left\langle Z(t)^T \right\rangle, \tag{2.90}$$

where expectation value of an operator $A(t)$ is given by $\langle A(t)\rangle = \mathrm{Tr}[A(t)\rho(0)]$, and $\rho(0)$ is the initial state of the total system. To justify the first term on r.h.s of (2.90) we calculate as an example $\sigma^{x_1 p_1}$ component of the covariance matrix. To do so, we need to consider that q and ϕ do not commute. Consequently, we have to account for the ordering of these operators, which results in the following expression:

$$\sigma^{x_1 p_1}(t) = \left\langle \frac{\phi_1(t)q_1(t) + q_1(t)\phi_1(t)}{2} \right\rangle - \langle \phi_1(t)\rangle \langle q_1(t)\rangle . \tag{2.91}$$

However, for the first term, we can use the commutation relation between the momentum and position $\phi_1(t)q_1(t) - q_1(t)\phi_1(t) = i\hbar$ and thus, we can write $\frac{\phi_1(t)q_1(t)+q_1(t)\phi_1(t)}{2} = \frac{2\phi_1(t)q_1(t)-i\hbar}{2}$. Therefore, $\mathrm{Re}(\langle \phi_1(t)q_1(t)\rangle) = \left\langle \frac{\phi_1(t)q_1(t)+q_1(t)\phi_1(t)}{2} \right\rangle$ which proves why we can write (2.91) in terms of (2.90). To find the relation between the covariance matrix and heat currents, we take the mean value of the Hamiltonian of the system H_s which gives

$$\langle H_s\rangle(t) = \frac{1}{2}\left\langle q^T(t)C^{-1}q(t)\right\rangle + \frac{1}{2}\left\langle \phi^T(t)L^{-1}\phi(t)\right\rangle . \tag{2.92}$$

Writing the above equation in terms of their matrices components we have

$$\langle H_s\rangle(t) = \frac{1}{2}\sum_{i,j} C^{-1}_{ij}\left\langle q_i^T(t)q_j(t)\right\rangle + \frac{1}{2}\sum_{ij} L^{-1}_{ij}\left\langle \phi_i^T(t)\phi_j(t)\right\rangle . \tag{2.93}$$

Using the definition of the covariance matrix (2.90) we have

$$\langle H_s \rangle (t) = \frac{1}{2} \sum_{i,j} C_{ij}^{-1} \sigma_{ij}^{pp}(t) + \frac{1}{2} \sum_{i,j} L_{ij}^{-1} \sigma_{ij}^{xx}(t). \tag{2.94}$$

We can change the above sums over the matrix elements to the trace by inserting an identity operator in the middle of each sum. In this way we obtain

$$\langle H_s \rangle (t) = \frac{1}{2} \mathrm{Tr} \left[C^{-1} \sigma^{pp}(t) \right] + \frac{1}{2} \mathrm{Tr} \left[L^{-1} \sigma^{xx}(t) \right]. \tag{2.95}$$

Taking the derivative of the above relation we have

$$\frac{d}{dt} \langle H_s \rangle (t) = \frac{1}{2} \mathrm{Tr} \left[C^{-1} \frac{d}{dt} \sigma^{pp}(t) \right] + \frac{1}{2} \mathrm{Tr} \left[L^{-1} \frac{d}{dt} \sigma^{xx}(t) \right]. \tag{2.96}$$

Before delving into the concept of heat, it is important to highlight a few points. In our system Hamiltonian, L plays the role of potential energy and, in general, it can be time-dependent. By varying L with time, we effectively exchange external work with our system. However, in our specific model of interest, we assume L to be constant. As a result, the change in the total energy of the system (2.96) corresponds solely to the heat exchange between the system and the baths, which is directly connected to the change in the covariance matrix of the system.

To calculate the heat exchange, we require the covariance matrix. In the next subsection, we will demonstrate how we can express the covariance matrix in terms of the Green's function of the system.

2.6.2 The Green's function approach

In the preceding section, we employed the Heisenberg equations of motion to describe the dynamics of the system variables. We expressed the Heisenberg equations of motion (2.54) in terms of the phase space variable Z for the system and z_α for the baths. This yields the following equations:

$$\dot{Z} + a_s Z = \sum_\alpha b_\alpha z_\alpha \tag{2.97}$$

$$\dot{z}_\alpha + a_\alpha z_\alpha = \bar{b_\alpha} Z, \tag{2.98}$$

where

$$a_s = \begin{bmatrix} 0 & -C^{-1} \\ L^{-1} & 0 \end{bmatrix},$$
$$b_\alpha = \begin{bmatrix} 0 & 0 \\ \bar{L}_\alpha^{-1} & 0 \end{bmatrix},$$
$$\bar{b}_\alpha = \begin{bmatrix} 0 & 0 \\ (\bar{L}_\alpha^{-1})^T & 0 \end{bmatrix},$$
$$a_\alpha = \begin{bmatrix} 0 & -C_\alpha^{-1} \\ L_\alpha^{-1} & 0 \end{bmatrix}.$$

To obtain the equation of motion for Z, one can solve equation (2.98) for z_α and substitute it back into equation (2.97) to obtain the desired result. In order to solve equation (2.98), we utilize the Green's function $g_\alpha(t,t')$, defined such that it satisfies:

$$\dot{g}_\alpha(t,t') + a_\alpha g_\alpha(t,t') = \delta(t-t'). \tag{2.99}$$

With the boundary condition $g_\alpha(t,t') = 0$ for $t < t'$, $g_\alpha(t,t')$ encodes the response of the α-th heat bath to a delta function impulse at time t'. Employing this, the solution for $z_\alpha(t)$ can be written as

$$z_\alpha(t) = g_\alpha(t,0)z_\alpha(0) + \int_0^t g_\alpha(t,t')b_\alpha Z(t')dt'. \tag{2.100}$$

For $t > t'$ and the aforementioned boundary condition that $g_\alpha(t,t') = 0$ for $t < t'$ we can find

$$g_\alpha(t,t') = \theta(t-t') \begin{bmatrix} \cos(\omega_\alpha(t-t')) & (\omega_\alpha C_\alpha)^{-1}\sin(\omega_\alpha(t-t')) \\ -(\omega_\alpha L_\alpha)^{-1}\sin(\omega_\alpha(t-t')) & \cos(\omega_\alpha(t-t')) \end{bmatrix}, \tag{2.101}$$

where, $\omega_\alpha^2 = L_\alpha^{-1}C_\alpha^{-1}$ and $\theta(t-t')$ is the Heaviside step function. Substituting (2.100) into (2.97) we can use $G(t,t')$ as the Green's function for the system phase variable to find Z, so that we have

$$\dot{Z} + a_s Z - \int_0^t \sum_\alpha b_\alpha g_\alpha(t,t')\bar{b}_\alpha Z(t')dt' = \sum_\alpha b_\alpha g_\alpha(t,0)z_\alpha(0). \tag{2.102}$$

Here we first find that

$$\eta_\alpha(t,t') := b_\alpha g_\alpha(t,t')\bar{b}_\alpha = \theta(t-t') \begin{bmatrix} 0 & 0 \\ \bar{L}_\alpha^{-1}(\omega_\alpha C_\alpha)^{-1}\sin(\omega_\alpha(t-t'))(\bar{L}_\alpha^{-1})^T & 0 \end{bmatrix}. \tag{2.103}$$

Next we can write the only component of this matrix as

$$\eta_\alpha^{xx}(t-t') = \bar{L}_\alpha^{-1}(\omega_\alpha C_\alpha)^{-1}\sin\big(\omega_\alpha(t-t')\big)(\bar{L}_\alpha^{-1})^T. \tag{2.104}$$

Finally we introduce the *spectral density* of the baths variables $I_\alpha(\omega)$ such that

$$\eta_\alpha^{xx}(t) = \int_0^\infty I_\alpha(\omega)\sin(\omega t)d\omega, \tag{2.105}$$

where we have

$$I_\alpha(\omega) = \bar{L}_\alpha^{-1}(\omega C_\alpha)^{-1}(\bar{L}_\alpha^{-1})^T\delta(\omega-\omega_\alpha). \tag{2.106}$$

Having defined the spectral density of the baths we can write (2.102) such that

$$\dot{Z} + a_s Z - \int_0^t \eta(t,t')Z(t')dt' = \sum_\alpha b_\alpha g_\alpha(t,0)z_\alpha(0), \tag{2.107}$$

where $\eta(t,t') = \sum_\alpha \eta_\alpha(t,t')$. Now we can find $Z(t)$ by using the Green's function method that we employed to find $z_\alpha(t)$. Hence,

$$Z(t) = G(t,0)Z(0) + \int_0^t G(t,t')\sum_\alpha b_\alpha g_\alpha(t',0)z_\alpha(0)dt', \tag{2.108}$$

where $G(t,t')$ is the Green's function associated with the previous equation and its given by

$$\frac{\partial}{\partial t}G(t,t') + a_s G(t,t') - \int_0^t \eta(t,\tau)G(\tau,t')d\tau = \delta(t-t'), \tag{2.109}$$

where we assume again that $G(t,t') = 0$ for $t < t'$. The above equations will give us the exact solutions for the time evolution of the phase space variable of the system. The above integro-differential equation contains the noise kernel $\eta(t,t')$, however, one can modify the equation in such a way to write it in terms of damping factor $\gamma(t,t')$ which we define such that $\eta(t,t') := \frac{\partial}{\partial t'}\gamma(t,t')$. To do so, we integrate by part the integral in the above equation

and we have

$$\frac{\partial}{\partial t}G(t,t') + a_s G(t,t') - \gamma(t,\tau)G(\tau,t')\Big|_0^t + \int_0^t \gamma(t,\tau)\frac{\partial}{\partial \tau}G(\tau,t')d\tau = \delta(t-t'). \tag{2.110}$$

Since $G(0,t') = 0$ and $\gamma(t,t) = \gamma(0)$ we can write the above equation as

$$\frac{\partial}{\partial t}G(t,t') + a_R G(t,t') + \int_0^t \gamma(t,\tau)\frac{\partial}{\partial \tau}G(\tau,t')d\tau = \delta(t-t'), \tag{2.111}$$

where $a_R = a_s - \gamma(0)$. We can also write the damping kernel in terms of the spectral density of the baths. First we should notice that $\gamma(t,t') = \sum_\alpha \gamma_\alpha(t,t')$ where $\gamma_\alpha(t,t') = \begin{bmatrix} 0 & 0 \\ \gamma_\alpha^{xx}(t-t') & 0 \end{bmatrix}$. Therefore, we have

$$\gamma_\alpha^{xx}(t) = \int_0^\infty \frac{I_\alpha(\omega)}{\omega}\cos(\omega t)d\omega, \tag{2.112}$$

which is reminiscent of the equation (2.57) yet in a matrix form.

Now we have all the requirements to calculate the covariance matrix σ in equation (2.90) using the phase space Green's function of the system and baths variables. Therefore, we replace (2.108) in (2.90) and we will have

$$\begin{aligned}
\sigma(t) &= G(t,0)\mathrm{Re}\left[\left\langle Z(0)Z(0)^T\right\rangle\right]G(t,0)^T \\
&+ \int_0^t \sum_\alpha G(t,0)\mathrm{Re}\left[\left\langle Z(0)z_\alpha(0)^T\right\rangle\right]g_\alpha(t',0)^T b_\alpha^T(0)G(t,t')^T dt' \\
&+ \left(\int_0^t \sum_\alpha G(t,0)\mathrm{Re}\left[\left\langle Z(0)z_\alpha(0)^T\right\rangle\right]g_\alpha(t',0)^T b_\alpha^T(0)G(t,t')^T dt'\right)^T \\
&+ \int_0^t\int_0^t G(t,t_1)\left[\sum_{\alpha,\beta} b_\alpha g_\alpha(t_1,0)\mathrm{Re}\left[\left\langle z_\alpha(0)z_\beta(0)^T\right\rangle\right]g_\beta(t_2,0)^T b_\beta^T(0)\right]G(t,t_2)^T dt_1 dt_2 \\
&+ \langle Z(t)\rangle\left\langle Z(t)^T\right\rangle.
\end{aligned} \tag{2.113}$$

Here we need to impose a few conditions on our problem. First of all, we assume that $\langle Z(0)\rangle = \langle z_\alpha(0)\rangle = 0$. Thus, according to (2.108) we will have $\langle Z(t)\rangle = 0$ so that the last term in the previous equation will vanish. Furthermore, we assume that there are no initial correlations between the system and the baths which means $\mathrm{Re}\left[\left\langle Z(0)z_\alpha(0)^T\right\rangle\right] = 0$. Thus, the second and third terms will also vanish.

We can calculate the fourth term in (2.6.2). Indeed, if we assume that the initial state of each bath is a thermal state with an inverse temperature β_α, such as $\rho_\alpha(0) = \mathcal{Z}_\alpha^{-1}e^{-\beta_\alpha H_\alpha}$,

where $\mathcal{Z}_\alpha$ is the partition function, we will be able to calculate the correlations between the initial states of each bath. This can be expressed as

$$\mathrm{Re}\left[\left\langle z_\alpha(0) z_\beta(0)^T \right\rangle\right] = \delta_{\alpha,\beta}\frac{\hbar}{2}\begin{bmatrix} (C_\alpha\omega_\alpha)^{-1}\coth\left(\frac{\hbar\beta_\alpha\omega_\alpha}{2}\right) & 0 \\ 0 & (L_\alpha\omega_\alpha)^{-1}\coth\left(\frac{\hbar\beta_\alpha\omega_\alpha}{2}\right)\end{bmatrix}. \tag{2.114}$$

Thus, we can write

$$\begin{aligned}\nu(t_1-t_2) &:= \left[\sum_{\alpha,\beta} b_\alpha g_\alpha(t_1,0)\mathrm{Re}\left[\left\langle z_\alpha(0) z_\beta(0)^T\right\rangle\right] g_\beta(t_2,0)^T \bar{b}_\beta(0)\right] \\ &= \sum_\alpha \begin{bmatrix} 0 & 0 \\ 0 & \bar{L}_\alpha^{-1}(C_\alpha\omega_\alpha)^{-1}\cos(\omega_\alpha(t_1-t_2))\coth\left(\frac{\hbar\beta_\alpha\omega_\alpha}{2}\right)(\bar{L}_\alpha^{-1})^T\end{bmatrix}. \end{aligned} \tag{2.115}$$

The only component of the matrix in the r.h.s is related to the spectral density $I_\alpha(\omega)$. We can write $\nu(t) = \sum_\alpha \begin{bmatrix} 0 & 0 \\ 0 & \nu_\alpha^{xx}(t)\end{bmatrix}$ where we have

$$\nu_\alpha^{xx}(t) = \int_0^\infty I_\alpha(\omega)\cos(\omega t)\coth\left(\frac{\hbar\beta_\alpha\omega}{2}\right)d\omega. \tag{2.116}$$

Therefore, we have

$$\sigma(t) = G(t,0)\sigma(0)G(t,o)^T + \frac{\hbar}{2}\int_0^t\int_0^t G(t,t_1)\nu(t_1-t_2)G(t,t_2)^T dt_1 dt_2. \tag{2.117}$$

Equation (2.117) explicitly illustrates the method for determining the time evolution of the covariance matrix. In order to investigate the behavior of the system in the long time limit, we make an additional assumption that the Green's function decays exponentially with time t. Consequently, the first term on the right-hand side of equation (2.117) will become negligible in this limit, indicating that the evolution of our system will eventually become independent of its initial state. Therefore, in the long time limit, we obtain

$$\sigma(t) = \frac{\hbar}{2}\int_0^t\int_0^t G(t,t_1)\nu(t_1-t_2)G(t,t_2)^T dt_1 dt_2. \tag{2.118}$$

We notice that $G(t,t')$ is the Green's function for the system phase space variables. Nevertheless, we can express (2.118) in terms of the Green's function for the configuration variables of the system $g(t,t')$. Indeed, our goal is to find the relation between $G(t,t')$ and $g(t,t')$. If we look at (2.107) we can expand it in terms of the momentum and position variables. We

have

$$\dot{\phi} - C^{-1}q = 0 \tag{2.119}$$

$$\dot{q} + L^{-1}\phi - \int_0^t \eta^{xx}(t,t,')\phi(t')dt' = \sum_\alpha \bar{L}_\alpha^{-1} g_\alpha^{11}(t,0)\phi_\alpha(0) + \bar{L}_\alpha^{-1} g_\alpha^{12}(t,0)q_\alpha(0). \tag{2.120}$$

Taking the time derivative of (2.119) and using (2.120) we will have

$$C\ddot{\phi} + L^{-1}\phi - \int_0^t \eta^{xx}(t,t,')\phi(t')dt' = \sum_\alpha \bar{L}_\alpha^{-1} g_\alpha^{11}(t,0)\phi_\alpha(0) + \bar{L}_\alpha^{-1} g_\alpha^{12}(t,0)q_\alpha(0). \tag{2.121}$$

We can solve this equation using the Green's function for the configuration variable $g(t,t')$ given by

$$C\frac{\partial^2}{\partial t^2}g(t,t') + L^{-1}g(t,t') - \int_0^t \eta^{xx}(t,\tau)g(\tau,t')d\tau = \delta(t-t'). \tag{2.122}$$

Again using the definition of damping kernel $\gamma(t)$ we can rewrite the above equation such that

$$C\frac{\partial^2}{\partial t^2}g(t,t') + L_R^{-1}g(t,t') + \int_0^t \gamma^{xx}(t-\tau)\frac{\partial}{\partial\tau}g(\tau,t')d\tau = \delta(t-t'), \tag{2.123}$$

where $L_R^{-1} = L^{-1} - \gamma^{xx}(0)$.

To find the relation between $G(t,t')$ and $g(t,t')$ we expand the equation (2.111) in a matrix form by defining $G = \begin{bmatrix} G_{xx} & G_{xp} \\ G_{px} & G_{pp} \end{bmatrix}$, so that we have

$$\frac{\partial}{\partial t}G_{xx} - C^{-1}G_{px} = \delta(t-t') \tag{2.124}$$

$$\frac{\partial}{\partial t}G_{px} + L_R^{-1}G_{xx} + \int_0^t \gamma^{xx}(t-\tau)\frac{\partial}{\partial\tau}G_{xx}(\tau,t')d\tau = 0. \tag{2.125}$$

One can easily solve these two coupled equations to see that $G_{xx}(t,t') = g(t,t')$ and consequently, $G_{pp}(t,t') = C\frac{\partial}{\partial t}g(t,t')$ and $G_{xp}(t,t') = g(t,t')$. That being said, we can find the components of the covariance matrix in a way that

$$\sigma^{xx}(t) = \frac{\hbar}{2}\int_0^t\int_0^t g(t,t_1)\nu^{xx}(t_1-t_2)g(t,t_2)^T dt_1 dt_2 \tag{2.126}$$

$$\sigma^{xp}(t) = \frac{\hbar}{2}\int_0^t\int_0^t g(t,t_1)\nu^{xx}(t_1-t_2)\frac{\partial}{\partial t}g(t,t_2)^T C dt_1 dt_2 \tag{2.127}$$

$$\sigma^{pp}(t) = \frac{\hbar}{2}\int_0^t\int_0^t C\frac{\partial}{\partial t}g(t,t_1)\nu^{xx}(t_1-t_2)\frac{\partial}{\partial t}g(t,t_2)^T C dt_1 dt_2. \tag{2.128}$$

Having calculated the components of the covariance matrix in terms of the Green's function of the system, we are able to find the relation for the heat currents. Going back to equation (2.96) we have

$$\dot{Q}(t) = \frac{1}{i\hbar}\langle[H_s, H_{int}]\rangle = \frac{1}{2}\mathrm{Tr}\left[C^{-1}\frac{d}{dt}\sigma^{pp}(t)\right] + \frac{1}{2}\mathrm{Tr}\left[L^{-1}\frac{d}{dt}\sigma^{xx}(t)\right]. \tag{2.129}$$

The above equation will give us the total amount of heat current exchanged between the system and the baths in terms of the covariance matrix of the system. One can also find the local heat currents exchanged between each LC circuit and the bath it is in contact with. Thus, we have

$$\begin{aligned}\dot{Q}_\alpha = \frac{1}{i\hbar}\langle[H_s, H^\alpha_{int}]\rangle &= -\frac{1}{2i\hbar}\langle[q^T C^{-1} q, \phi^T \bar{L}_\alpha^{-1}\phi_\alpha]\rangle \\ &= \langle q^T C^{-1}\bar{L}_\alpha^{-1}\phi_\alpha\rangle.\end{aligned} \tag{2.130}$$

To write the local heat current relation in terms of the system variables, we need to eliminate q_α using the Heisenberg equations of motion (2.54). However, this equation is a sum over all the environments. To get rid of the sum, we define an operator P_α which is a projector over the sites of the α-th bath. Indeed, its effect would be such that $P_\alpha\dot{q} = -P_\alpha L^{-1}\phi + \bar{L}_\alpha^{-1}\phi_\alpha$ assuming that $P_\alpha P_\beta = \delta_{\alpha,\beta}P_\alpha$ which ensures that, each system is coupled only with one bath directly. Applying this operator to (2.130) we will have

$$\dot{Q}_\alpha = \langle q^T C^{-1} P_\alpha L^{-1}\phi\rangle + \langle q^T C^{-1} P_\alpha \dot{q}\rangle. \tag{2.131}$$

Again as we did for the mean value of the Hamiltonian of the system, we can write (2.131) in terms of the covariance matrix. To do so we have

$$\dot{Q}_\alpha = \sum_{ijk} C^{-1}_{ij}(P_\alpha L^{-1})_{jk}\langle q_i\phi_k\rangle + \sum_{ijk} C^{-1}_{ij}(P_\alpha)_{jk}\langle q_i\dot{q}_k\rangle. \tag{2.132}$$

Therefore, we will obtain

$$\dot{Q}_\alpha = \mathrm{Tr}\left[P_\alpha\frac{d}{dt}\sigma^{pp}(t)C^{-1}\right] + \mathrm{Tr}\left[P_\alpha L^{-1}\sigma^{xp}(t)C^{-1}\right]. \tag{2.133}$$

For steady state limit of the covariance matrix at long time, the first term of (2.133) will vanish. To calculate the local heat current, we first rewrite $\sigma^{xp}(t)$ by using

$$\nu_\alpha^{xx}(t_1-t_2)=\int_0^\infty \nu_\alpha^{xx}(\omega)\cos(\omega(t_1-t_2))d\omega=\mathrm{Re}\int_0^\infty \nu_\alpha^{xx}(\omega)e^{-j\omega(t_1-t_2)}d\omega, \quad (2.134)$$

where $\nu_\alpha^{xx}(\omega)=I_\alpha(\omega)\coth\left(\frac{\hbar\beta_\alpha\omega}{2}\right)$. Replacing this into (2.126) we can see

$$\sigma^{xp}(t)=\mathrm{Re}\int_0^\infty \frac{\hbar}{2}\int_0^t\int_0^t g(t,t_1)e^{-j\omega t_1}\nu^{xx}(\omega)e^{-j\omega t_1}\frac{\partial}{\partial t}g(t,t_2)^T C dt_1 dt_2 d\omega. \quad (2.135)$$

In the limit $t\to\infty$ we can write

$$\int_0^\infty g(t,t_1)e^{-j\omega t_1}dt_1=g(j\omega), \quad (2.136)$$

Thus, we will have

$$\sigma^{xp}(t)=-\mathrm{Re}\int_0^\infty \frac{\hbar}{2}g(j\omega)\nu^{xx}(\omega)j\omega g(-j\omega)^T C d\omega. \quad (2.137)$$

Replacing this equation into (2.133) the local heat current expression for steady state limit can be obtained as

$$\dot{Q}_\alpha=\frac{\hbar}{2}\mathrm{Im}\sum_{\alpha'}\int_0^\infty \omega\coth\left(\frac{\hbar\beta_{\alpha'}\omega}{2}\right)\mathrm{Tr}\left[P_\alpha L^{-1}g(j\omega)I_{\alpha'}(\omega)g(-j\omega)^T\right]d\omega, \quad (2.138)$$

where we have used the fact that $\mathrm{Re}(-jX)=\mathrm{Im}(X)$. Here we define the *heat transfer matrix* $f_{\alpha\alpha'}$ such that

$$f_{\alpha\alpha'}=\mathrm{ImTr}\left[P_\alpha L^{-1}g(j\omega)I_{\alpha'}(\omega)g(-j\omega)^T\right]. \quad (2.139)$$

In case $P_\alpha L^{-1}=P_\alpha L_R^{-1}+L_\alpha^{-1}$, we can see that $\mathrm{Tr}\left[P_\alpha L_\alpha^{-1}g(j\omega)I_{\alpha'}(\omega)g(-j\omega)^T\right]=0$ because L_α^{-1} is a symmetric matrix and $g(j\omega)I_{\alpha'}(\omega)g(-j\omega)^T$ is anti-symmetric and the trace of their product will be vanishing. To prove the anti-symmetry of this term we define $B=\mathrm{Im}g(j\omega)I_{\alpha'}(\omega)g(-j\omega)^T=\left(g(j\omega)I_{\alpha'}(\omega)g(j\omega)^\dagger-g(j\omega)^*I_{\alpha'}(\omega)g(j\omega)^T\right)/2$. Thus, we can see that $B^T=-B$ which shows this matrix is anti-symmetric. That said we can rewrite the heat current matrix element as

$$f_{\alpha\alpha'}=\mathrm{ImTr}\left[P_\alpha L_R^{-1}g(j\omega)I_{\alpha'}(\omega)g(j\omega)^\dagger\right]. \quad (2.140)$$

To expand the above relation further, we first take the Laplace transform of (2.123) such that

$$g(s)^{-1} = Cs^2 + \gamma^{xx}(s)s + L_R^{-1}. \tag{2.141}$$

Writing L_R^{-1} in terms of $g(s)^{-1}$ we have

$$L_R^{-1} = g(s)^{-1} - Cs^2 + \gamma^{xx}(s)s. \tag{2.142}$$

Replacing the above equation into (2.140) with $s = j\omega$, we will have

$$\begin{aligned} f_{\alpha\alpha'} =& \mathrm{Im}\mathrm{Tr}\left[P_\alpha I_{\alpha'}(\omega) g(j\omega)^\dagger\right] \\ &+ \mathrm{Im}\omega^2 \mathrm{Tr}\left[C P_\alpha g(j\omega) I_{\alpha'}(\omega) g(j\omega)^\dagger\right] \\ &+ \mathrm{Im} j\omega \mathrm{Tr}\left[P_\alpha \gamma^{xx}(j\omega) g(j\omega) I_{\alpha'}(\omega) g(j\omega)^\dagger\right]. \end{aligned} \tag{2.143}$$

The first term vanishes because $P_\alpha I_{\alpha'}(\omega) = 0$ for $\alpha \neq \alpha'$. The second will also be vanishing because it is a product of two symmetric and anti-symmetric matrices. In the third term, the matrix $g(j\omega) I_{\alpha'}(\omega) g(j\omega)^\dagger$ is hermitian so that we only have to calculate $\mathrm{Im}(j\omega\gamma^{xx}(j\omega)) = \mathrm{Re}(\omega\gamma^{xx}(j\omega)) = \frac{\pi}{2} I(\omega)$. Thus, we have

$$f_{\alpha\alpha'} = \frac{\pi}{2} \mathrm{Tr}\left[I_\alpha(\omega) g(\omega) I_{\alpha'}(\omega) g(j\omega)^\dagger\right]. \tag{2.144}$$

Inserting this matrix back to the equation (2.138) we will have

$$\dot{Q}_\alpha = \hbar\pi \sum_{\alpha'} \int_0^\infty \omega d\omega \coth\left(\frac{\hbar\beta_{\alpha'}\omega}{2}\right) \mathrm{Tr}\left[I_\alpha(\omega) g(\omega) I_{\alpha'}(\omega) g(j\omega)^\dagger\right]. \tag{2.145}$$

Using $\sum_\alpha f_{\alpha\alpha'} = 0$, we have $\sum_{\alpha\neq\alpha'} f_{\alpha\alpha'} = -f_{\alpha\alpha}$. Thus, we can write the heat currents such that

$$\dot{Q}_\alpha = \frac{\hbar}{2} \sum_{\alpha'\neq\alpha} \int_0^\infty \omega d\omega f_{\alpha\alpha'}(\omega) \left(\coth\left(\frac{\hbar\beta_\alpha\omega}{2}\right) - \coth\left(\frac{\hbar\beta_{\alpha'}\omega}{2}\right)\right). \tag{2.146}$$

The linearity of the system implies that even if the model is fully quantum, its dynamics are equivalent to the classical case [87]. Consequently, the Green's function in Eq. (2.141), appearing in the heat transfer matrix of Eq. (2.139), is the solution to the classical equations of motion and does not depend on $\hbar$. The dependence on $\hbar$ only arises in the noise spectrum $2\hbar\omega\coth(\beta_\alpha\hbar\omega/2)$. It is worth noting that the expression in Eq. (2.146) can be obtained by computing the classical transfer function of the circuit connecting the two ports, treating the

resistors as sources of Johnson-Nyquist noise [95, 106]. However, an important distinction is that the exact equations of motion for the system, although classical, are non-local in time due to the non-Markovian effects caused by the environment. This aspect is not captured in a classical circuit treatment but is fully accounted for in our approach, as explained later.

We utilize the aforementioned result to calculate the heat exchanged between each bath and the interacting system. Specifically, we assume that our baths are Ohmic with Lorentz-Drude cutoff spectral densities given by $I_\alpha = \frac{2}{\pi}\gamma_0 P_\alpha \frac{\omega\omega_c^2}{\omega^2+\omega_c^2}$, where ω_c represents the cutoff frequency of the bath and γ_0 plays the role of the coupling to the bath, similar to $1/R$ in the previous chapter when defining the frequency-dependent admittance $Y(j\omega) = \frac{R^{-1}}{1-\frac{j\omega}{\omega_C}}$. In this case, the Laplace transform of the dissipation kernel is given by $\gamma(s)^{xx} = \gamma_0 \frac{\omega_c}{s+\omega_c}$.

Using this information, we can evaluate the heat current matrix $f_{\alpha,\alpha'}$ such that

$$\begin{aligned}
&\mathrm{Tr}\left[I_\alpha(\omega)g(\omega)I_{\alpha'}(\omega)g(j\omega)^\dagger\right] \\
&= \left(\frac{2}{\pi}\gamma_0\frac{\omega\omega_c^2}{\omega^2+\omega_c^2}\right)^2 \mathrm{Tr}\left[\begin{pmatrix}1&0\\0&0\end{pmatrix}\begin{pmatrix}g_{11}&g_{12}\\g_{21}&g_{22}\end{pmatrix}\begin{pmatrix}0&0\\0&1\end{pmatrix}\begin{pmatrix}g_{11}^*&g_{21}^*\\g_{12}^*&g_{22}^*\end{pmatrix}\right] \\
&= \left(\frac{2}{\pi}\gamma_0\frac{\omega\omega_c^2}{\omega^2+\omega_c^2}\right)^2 (g_{12}g_{12}^*)\,.
\end{aligned} \tag{2.147}$$

Thus, we only need to calculate the two off-diagonal elements of the Green's function in (2.141). Writing that equation in matrix form will result in

$$g(j\omega) = \begin{pmatrix} -C_1\omega^2 + \frac{L_2}{A} + j\frac{\omega\gamma_0\omega_c}{j\omega+\omega_c} & \frac{M}{A} \\ \frac{M}{A} & -C_2\omega^2 + \frac{L_1}{A} + j\frac{\omega\gamma_0\omega_c}{j\omega+\omega_c} \end{pmatrix}^{-1}, \tag{2.148}$$

where $A = L_1L_2 - M^2$. We need to find the inverse of the above matrix, however, we only need the off-diagonal terms. Thus we can write

$$\begin{aligned}
g_{12}(j\omega) =& \frac{\frac{M}{A}}{|g(j\omega)|} \\
=& \frac{M}{A}\left((-C_1\omega^2 + \frac{L_2}{A} + j\frac{\omega\gamma_0\omega_c}{j\omega+\omega_c})(-C_2\omega^2 + \frac{L_1}{A} + j\frac{\omega\gamma_0\omega_c}{j\omega+\omega_c}) - \left(\frac{M}{A}\right)^2\right)^{-1}
\end{aligned} \tag{2.149}$$

Substituting this result into (2.6.2) we will have

$$
\begin{aligned}
f_{1,2} = &-\frac{\pi}{2}\left(\frac{2}{\pi}\gamma_0\frac{\omega\omega_c^2}{\omega^2+\omega_c^2}\right)^2\left(\frac{M}{A}\right)^2 \\
&\times\left((-C_1\omega^2+\frac{L_2}{A}+j\frac{\omega\gamma_0\omega_c}{j\omega+\omega_c})(-C_2\omega^2+\frac{L_1}{A}+j\frac{\omega\gamma_0\omega_c}{j\omega+\omega_c})-\left(\frac{M}{A}\right)^2\right)^{-1} \\
&\times\left((-C_1\omega^2+\frac{L_2}{A}-j\frac{\omega\gamma_0\omega_c}{-j\omega+\omega_c})(-C_2\omega^2+\frac{L_1}{A}-j\frac{\omega\gamma_0\omega_c}{-j\omega+\omega_c})-\left(\frac{M}{A}\right)^2\right)^{-1}.
\end{aligned}
\tag{2.150}
$$

Employing this component of the heat current matrix, we can find the local heat current $\dot{Q}_1$ as

$$
\dot{Q}_1 = \frac{\hbar}{2}\int_0^\infty \omega d\omega f_{12}(\omega)\left(\coth\left(\frac{\hbar\beta_1\omega}{2}\right)-\coth\left(\frac{\hbar\beta_2\omega}{2}\right)\right). \tag{2.151}
$$

For the hyperbolic functions, we can write them in terms of digamma functions and the poles are obtained straightforwardly. For the hyperbolas we have

$$
\pi\coth\left(\frac{\hbar\beta_l\omega}{2}\right) = \frac{2\pi}{\hbar\beta_l\omega} - j\psi(1-\frac{j\hbar\beta_l\omega}{2\pi}) + j\psi(1+\frac{j\hbar\beta_l\omega}{2\pi}), \tag{2.152}
$$

where $l = \{1,2\}$. In the high-temperature regime, the digamma functions become negligible. Consequently, the heat current splits into two components: a classical contribution and a quantum correction. This splitting is achieved through the following equation:

$$
\dot{Q}_1 = \dot{Q}_1^{\mathrm{cl}} + \dot{Q}_1^{\mathrm{q}}, \tag{2.153}
$$

where $\dot{Q}_1^{\mathrm{cl}}$ and $\dot{Q}_1^{\mathrm{q}}$ denote the classical and quantum contributions to the heat current, respectively. The classical contribution is given by:

$$
\dot{Q}_1^{\mathrm{cl}} = \left(\frac{1}{\beta 1}-\frac{1}{\beta_2}\right)\int_0^\infty d\omega f_{12}(\omega), \tag{2.154}
$$

whereas the quantum contribution is expressed as:

$$
\dot{Q}_1^{\mathrm{q}} = \frac{i\hbar}{2\pi}\int_{-\infty}^\infty d\omega\omega f_{12}(\omega)\left[\psi\left(1-\frac{i\beta_2\hbar\omega}{2\pi}\right)-\psi\left(1-\frac{i\beta_1\hbar\omega}{2\pi}\right)\right]. \tag{2.155}
$$

The classical contribution is independent of $\hbar$ and corresponds to the high-temperature limit. On the other hand, the quantum contribution depends on $\hbar$ and represents the low-temperature correction.

To solve the integral in (2.155) we need to find the poles of f_{12} and also the digamma

functions. In fact the poles of the function $\psi(1-ix)$ are all located on the lower-half of the imaginary axis, i.e $x = -i, -2i, -3i, ...$ We write f_{12} in such a way that

$$f_{1,2}(\omega) = \frac{2}{\pi}\omega^2\omega_c^4\left(\frac{RM}{A}\right)^2 \frac{1}{|u_+(i\omega)\,u_-(i\omega)|^2}, \tag{2.156}$$

with

$$u_\pm(s) = (s^3 + \omega_c s^2)RC \;+\; \left(\frac{R}{L\pm M} + \omega_c\right) s \;+\; \frac{R}{L\pm M}\omega_c. \tag{2.157}$$

provided that $s = j\omega$, $C_1 = C_2 = C$ and $L_1 = L_2 = L$. Although exact evaluation of the integrals is possible [39], we will utilize the overdamped limit approximation to simplify the calculation. Additionally, we will discuss the frequency scales involved in this limit.

2.7 Overdamped limit of the heat currents

The equation of motion for a single parallel RLC circuit is given by a classical equation with flux variable ϕ in the inductance,

$$\ddot{\phi} + \gamma\dot{\phi} + \omega_0^2\phi = 0. \tag{2.158}$$

The damping rate $\gamma = 1/RC$ and the natural frequency $\omega_0 = 1/\sqrt{LC}$ are important frequency scales. The roots of the corresponding characteristic equation are given by $\Gamma_\pm = -(\gamma/2) \pm (\gamma^2/4 - \omega_0^2)^{1/2}$. If $\gamma \gg \omega_0$, the system is in the overdamped limit, which can be achieved by reducing the capacitance so that $C \ll L/R^2$. In this regime, the damping rates of magnetic flux and charge are $|\Gamma_+| \ll |\Gamma_-|$, where, $\Gamma_+ \simeq -\omega_0^2/\gamma$ and $\Gamma_- \simeq -\gamma + \omega_0^2/\gamma$, indicating that charge relaxes much faster than flux. The flux damping rate $\omega_d \simeq \omega_0^2/\gamma = R/L$ becomes independent of C. For the two coupled RLC circuits, a similar analysis can be performed by replacing L with $L \pm M$ for each normal mode. We can express the functions $u_\pm(s)$ in Eq. (2.157) in terms of γ and $\omega_\pm = \omega_d/(1 \pm M/L)$,

$$u_\pm(s) = (s^3 + \omega_c s^2)/\gamma + (\omega_\pm + \omega_c)\, s + \omega_\pm\omega_c. \tag{2.159}$$

In the overdamped limit, we observe that the cubic and quadratic terms in the equation are suppressed, although they still dominate at high frequencies. However, it is important to note that in the frequency integral of Eq. (2.151), the factor remains unaffected. $\coth(\beta_\alpha\hbar\omega/2) - \coth(\beta_{\alpha'}\hbar\omega/2)$ will cut off frequencies higher than $\omega_{\rm th} = k_b \max_\alpha\{T_\alpha\}/\hbar$. Therefore, we

(a) High temperatures:	$\omega_\pm \ll \gamma \ll \omega_{\rm th}$
(b) Intermediate temperatures:	$\omega_\pm < \omega_{\rm th} \ll \gamma$
(c) Low temperatures:	$\omega_{\rm th} < \omega_\pm \ll \gamma$

TABLE 2.1: Different temperature ranges can be distinguished within the overdamped regime, assuming that both baths have temperatures of the same order characterized by the thermal frequency $\omega_{\rm th}$. The first range, labeled as (a), corresponds to the classical Smoluchowski equation or overdamped Langevin equations. In the second range, labeled as (b), the bath temperatures lie between the frequency gap associated with the overdamped regime. The third range, labeled as (c), corresponds to low temperatures compared to the lowest frequency scale of the system. Additionally, mixed conditions can be considered, in which one bath has a low temperature and the other has a high temperature, or situations where $\omega_{\rm th}$ is comparable to γ.

see that the cubic and quadratic terms can be ignored with respect to the other two when we have

$$\omega_{\rm th} \ll \gamma, (\gamma\omega_\pm)^{1/2}, (\gamma\omega_\pm\omega_c)^{1/3}. \tag{2.160}$$

Thus, we can rewrite

$$u_\pm(s) \simeq (\omega_\pm + \omega_c)\, s + \omega_\pm\omega_c, \tag{2.161}$$

The only relevant frequency scales in this case are $\omega_\pm$ and ω_c. It is worth noting that the conditions described in Equation (2.160) can be met by increasing γ, and they do not impose any constraints on the ratios between $\omega_{\rm th}$, $\omega_\pm$, and ω_c. However, they limit the maximum temperature values, and Table 2.1 provides information on temperature ranges that are significant in the overdamped regime. Later on, we will demonstrate the persistence of quantum effects even when the temperatures are high relative to $\hbar\omega_\pm/k_b$.

Using the approximation of Eq. (2.161), the integrals in Eqs. (2.154) and (2.155) can be readily evaluated. For the classical contribution to the heat current, we obtain:

$$\dot{Q}_1^{\rm cl} = \frac{k_b}{2}(T_1 - T_2)\left(\frac{M}{L}\right)^2 \frac{\omega_c}{\omega_c + \omega_d}\frac{\lambda_+\lambda_-}{\omega_d}, \tag{2.162}$$

where $\lambda_\pm$ is the only root of $u_\pm(s)$,

$$\lambda_\pm = -\frac{\omega_c\,\omega_\pm}{\omega_c + \omega_\pm}. \tag{2.163}$$

To compute the quantum contribution to the heat currents, we need to consider the poles of both the digamma function and $f_{12}(\omega)$. The poles of $\psi(1-ix)$ are located on the lower half of the imaginary axis, at $x = -i, -2i, -3i, \ldots$. On the other hand, the poles of the heat

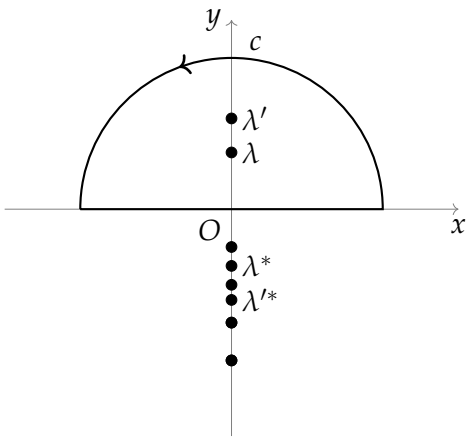

FIGURE 2.9: Upper-half plane contour. The dots are the poles of the digamma function [61].

transfer matrix element in the overdamped limit, $\lambda_{\pm}$, and their conjugates, $\lambda_{\pm}^{*}$, are on the imaginary axis. To exclude the contribution from the digamma function poles, we choose the integration contour to run on the upper half plane, covering only $\lambda_{\pm}$. Therefore, we can express the integral as:

$$\begin{aligned}\dot{Q}_1^{\mathrm{q}} = &\frac{i\hbar}{2\pi}\int_c d\omega\,\omega\, f_{12}(\omega)\left[\psi\left(1-\frac{i\beta_2\hbar\omega}{2\pi}\right)-\psi\left(1-\frac{i\beta_1\hbar\omega}{2\pi}\right)\right]\\ &+\frac{i\hbar}{2\pi}\int_\infty d\omega\,\omega\, f_{12}(\omega)\left[\psi\left(1-\frac{i\beta_2\hbar\omega}{2\pi}\right)-\psi\left(1-\frac{i\beta_1\hbar\omega}{2\pi}\right)\right].\end{aligned} \tag{2.164}$$

The integral over the contour c in Fig. 2.9 is computed using the residue theorem. The second integral is the contribution when ω tends to infinity. To evaluate this contribution, we need to expand the digamma function using a series representation such that

$$\psi\left(1\pm ix\right)\simeq\log\left(\pm ix\right)\mp\frac{i}{x}, \tag{2.165}$$

for $x\to\infty$. Since the integrand is vanishing as $1/\omega$ then we only need to keep the logarithmic term in the asymptotic digamma functions. Replacing this expansion into the second integral in Eq. (2.164) we will have

$$\begin{aligned}&\frac{i\hbar}{2\pi}\int_\infty d\omega\,\omega\, f_{12}(\omega)\left[\psi\left(1-\frac{i\beta_2\hbar\omega}{2\pi}\right)-\psi\left(1-\frac{i\beta_1\hbar\omega}{2\pi}\right)\right]\\ &=-\frac{i\hbar}{\pi}\left(\frac{M}{L}\right)^2\left(\frac{\lambda_+\lambda_-}{\omega_d}\right)^2\int d\omega\frac{1}{\omega}\log\left(\frac{\beta_1}{\beta_2}\right).\end{aligned} \tag{2.166}$$

We change the variable $\omega=\Lambda e^{i\theta}$ and we integrate over the semi-circle on the upper-half plane for $0\le\theta\le\pi$ and $\Lambda\to\infty$, thus we will have

$$\frac{i\hbar}{2\pi}\int_{\infty} d\omega\,\omega\, f_{12}(\omega)\left[\psi\left(1-\frac{i\beta_2\hbar\omega}{2\pi}\right)-\psi\left(1-\frac{i\beta_1\hbar\omega}{2\pi}\right)\right]$$
$$=\frac{\hbar}{\pi}\left(\frac{M}{L}\right)^2\left(\frac{\lambda_+\lambda_-}{\omega_d}\right)^2\log\left(\frac{T_2}{T_1}\right). \tag{2.167}$$

Hence, by adding the above result and the integral over the contour we will obtain

$$\dot{Q}_1^{\mathrm{q}}=\frac{\hbar}{\pi}\left(\frac{M}{L}\right)^2\left(\frac{\lambda_+\lambda_-}{\omega_d}\right)^2\log\left(\frac{T_2}{T_1}\right)$$
$$+\frac{\hbar}{4\pi}\frac{\omega_c}{\omega_c+\omega_d}\frac{M}{L}\times\left\{\lambda_+^2\left[\psi\left(1-\frac{\beta_1\hbar\lambda_+}{2\pi}\right)-\psi\left(1-\frac{\beta_2\hbar\lambda_+}{2\pi}\right)\right]\right.$$
$$\left.-\lambda_-^2\left[\psi\left(1-\frac{\beta_1\hbar\lambda_-}{2\pi}\right)-\psi\left(1-\frac{\beta_2\hbar\lambda_-}{2\pi}\right)\right]\right\}. \tag{2.168}$$

Equations (2.162) and (2.168) allow for the calculation of heat current in the overdamped regime without relying on the weak coupling or Markovian approximations. This is an important development as previous results in similar systems have either been limited by these approximations or have relied on numerical methods [45, 7, 81, 38]. By providing a way to calculate heat current without these limitations, the approach presented can be used to gain a better understanding of the behavior of such systems in the overdamped regime . The results show that the classical contribution to the heat current is proportional to the temperature difference between the two reservoirs, while the quantum contribution depends on both reservoir temperatures in a non-linear way. In order to compare the exact heat current obtained from numerical integration of Eqs.(2.162) and (2.168), we plot in Fig. 2.10 the heat current as a function of γ/ω_d for different values of T_1 and T_2, where $\omega_c = 5\omega_d$ and $M/L = 1/2$. It can be seen that the two results agree as γ/ω_d increases. This analysis allows us to compute the heat current in the overdamped regime without assuming weak coupling or Markovian approximations, thus complementing previous studies that were either numerical or limited by these approximations.

We will now consider some relevant limits to simplify the previous expressions. The Markovian limit, where $\omega_c \to \infty$, can be obtained by replacing the factors $\omega_c/(\omega_c+\omega_d)$ in Eqs. (2.162) and (2.168) with 1. We can then note that the roots $\lambda_\pm$ satisfy

$$\lim_{\omega_c\to\infty}\lambda_\pm = -\omega_\pm. \tag{2.169}$$

To examine the impact of a finite cutoff, we can use Eq. (2.163) to see that it is equivalent to reducing the values of the frequencies $\omega_\pm$ or ω_d.

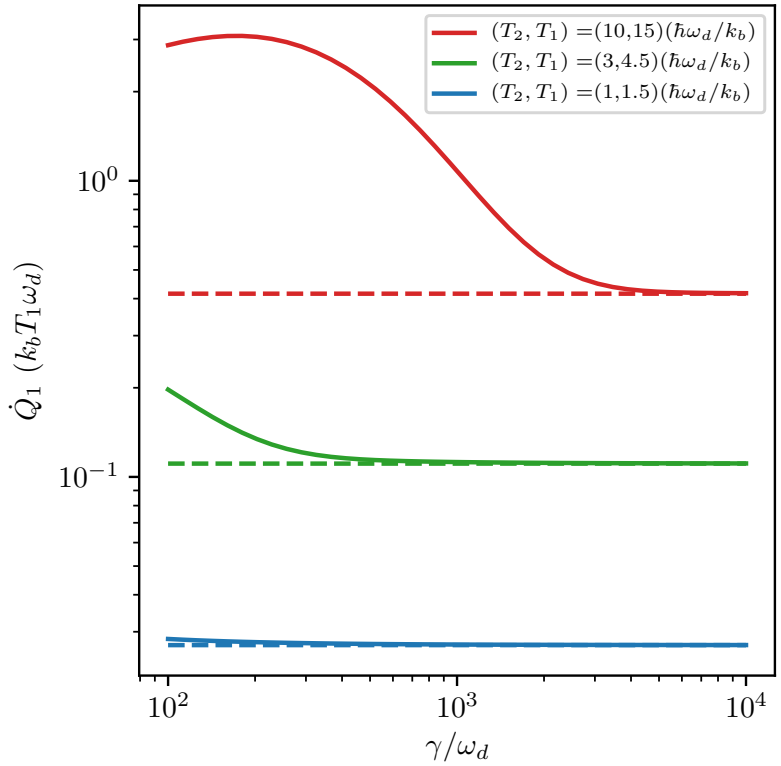

FIGURE 2.10: Heat current with respect to γ/ω_d. Solid lines show the exact heat current in terms of the different values of baths temperatures T_1 and T_2. The dashed lines are the heat current in the overdamped limit. This plot is sketched for $M = 1, L = 2, \omega_c = 5\omega_d, \omega_d = 1$ [61].

To analyze the low-temperature regime, we can take the limit $|\lambda_\pm|/\omega_{\rm th} \gg 1$ (which implies $\omega_{\rm th} \ll \omega_\pm, \omega_c$). In this case, we can use the following expansion for the digamma function when x is large

$$\psi(x) \approx \log x - \frac{1}{2x} - \frac{1}{12x^2} + \frac{1}{120x^4} + \mathcal{O}(x^5), \tag{2.170}$$

The contribution of the first logarithmic term cancels the first term in (2.162), while those coming from the third term vanish in the limit $|\lambda_\pm|/\omega_{\rm th} \gg 1$. Thus, the only remaining contributions originate from the term proportional to $1/x^4$, and the final result for the low-temperature heat current is given by

$$\dot{Q}_1^{\rm low} = \frac{2}{15}\left(\frac{\pi}{\hbar}\right)^3 \left(\frac{M}{L}\right)^2 \frac{k_b^4}{\omega_d^2}\left(T_1^4 - T_2^4\right) + \mathcal{O}(T_{1/2}^6). \tag{2.171}$$

To analyze the low-temperature regime, we consider $T_{1/2} = T \pm \Delta T/2$ and, to the first order in ΔT, we can express the heat current as $\dot{Q}1^{\rm low} = \mathcal{T} G_Q \Delta T$, where $G_Q = \pi k_b^2 T/3\hbar$ is the

fundamental unit of thermal conductance [84, 51, 95], and $\mathcal{T}=(4\pi^2/5)(M/L)^2(k_bT/\hbar\omega_d)^2$ is a temperature-dependent transmission coefficient. We note that Eq. (2.171) for the low-temperature heat current is independent of the cutoff frequency. This behavior arises because, at low temperatures, the heat current is predominantly influenced by low-frequency modes, while the cutoff frequency governs the high-frequency portion of the spectral densities. It is important to note that the same expression for the heat current in the low-temperature limit can also be obtained in the weak coupling regime, where $\gamma \ll \omega_\pm$. This is again attributed to the fact that, at low temperatures, only the low-frequency response of the system is significant. To further illustrate this point, let's consider the case of Ohmic dissipation in the Markovian limit ($\omega_c \to \infty$). In this scenario, both the spectral density and the dissipation kernel simplify to

$$I_\alpha(\omega) = \frac{2}{\pi}\frac{\omega}{R_\alpha}P_\alpha \tag{2.172}$$

$$\gamma(s) = \frac{1}{R}\left(P_1+P_2\right). \tag{2.173}$$

Replacing the above equations into the heat transfer matrix element $f_{\alpha\alpha'}(\omega)$ we will have

$$f_{1,2}(\omega) = \frac{2}{\pi}\left(\frac{M}{L}\right)^2\frac{\omega^2}{\omega_d^2}\left(\omega_+\omega_-\right)^2\frac{1}{|u_+(i\omega)\,u_-(i\omega)|^2}, \tag{2.174}$$

where in the weak coupling regime we have

$$u_\pm(\omega) = -\frac{1}{\gamma}\left(\omega - \frac{i\gamma}{2} + \sqrt{\gamma\omega_\pm}\right)\left(\omega - \frac{i\gamma}{2} - \sqrt{\gamma\omega_\pm}\right). \tag{2.175}$$

By utilizing the heat transfer matrix element, we can compute the classical and quantum contributions to the heat currents using the method described in the previous section. However, our focus is on the low temperature limit of the heat currents. As a result, the classical contribution becomes negligible, and the heat current, up to the first non-vanishing order of the quantum correction, can be expressed as

$$\dot{Q}_1^{\text{low}} = \frac{512}{15}\left(\frac{\pi}{\hbar}\right)^3\left(\frac{M}{L}\right)^2\frac{k_b^4}{\omega_d^2}\left(\frac{\omega_+\omega_-}{(\gamma+4\omega_+)\,(\gamma+4\omega_-)}\right)^2\left(T_1^4-T_2^4\right)+\mathcal{O}(T_{1/2}^6), \tag{2.176}$$

where in the weak coupling limit of $\gamma \ll \omega_\pm$ the above expression will be the same as (2.171). Figure 2.11 displays the behavior of the total heat current as a function of temperature. As temperature is decreased, we observe that the heat current can be accurately

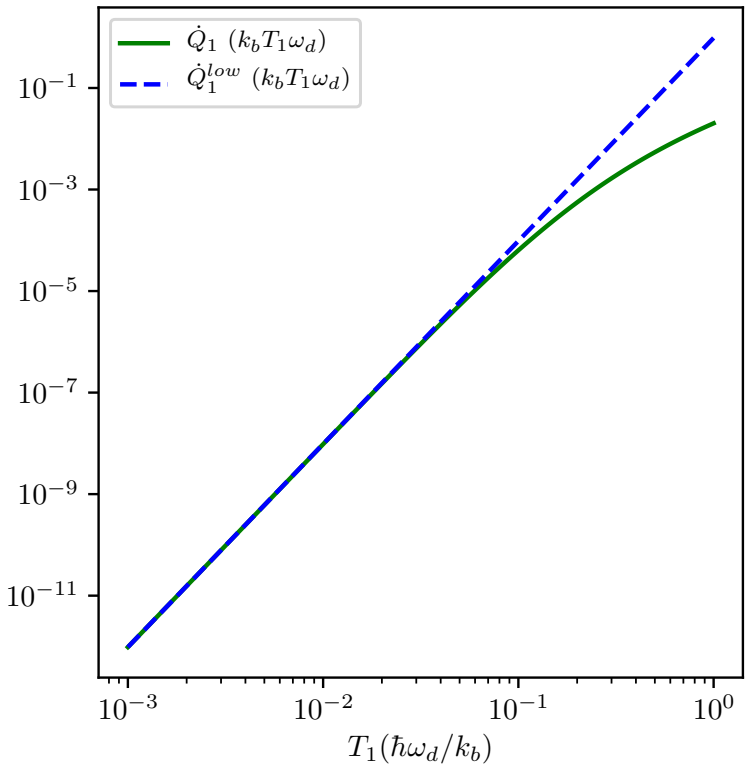

FIGURE 2.11: We compare the total heat current (represented by the green solid line) with the expression for the low-temperature regime (shown by the blue dashed line) for different values of T_1 [61]. In this comparison, we set $T_2 = T_1/2$, which means we decrease both temperatures simultaneously with a constant ratio. Interestingly, as the temperatures decrease, we observe that the two expressions converge and become indistinguishable. The parameters used for this comparison are $M = 1$, $L = 2$, $\omega_c = 5\omega_d$, and $\omega_d = 1$.

described by Eq. (2.171) in the low-temperature limit. This confirms the validity of the analytical result we obtained for the heat current in this regime. In the intermediate temperatures regime, where $|\lambda_\pm|/\omega_{\text{th}} \ll 1$, we employ the following expansion of the digamma function for small values of x,

$$\psi\,(1+x) = -\eta + \frac{\pi^2 x}{6} + \mathcal{O}(x^2), \tag{2.177}$$

where η is the Euler–Mascheroni constant. We then find the following high-temperature expansion of the quantum contribution

$$\begin{aligned}\dot{Q}_1^{\text{q}} = &\frac{\hbar}{\pi}\left(\frac{M}{L}\right)^2\left(\frac{\lambda_+\lambda_-}{\omega_d}\right)^2 \log\left(\frac{T_2}{T_1}\right)\\ &+\frac{\hbar^2}{48}\frac{\omega_c}{\omega_c+\omega_d}\frac{M}{L}(\lambda_+^3-\lambda_-^3)\left(\frac{1}{T_2}-\frac{1}{T_1}\right)+\mathcal{O}(T_{1/2}^{-2}).\end{aligned} \tag{2.178}$$

Remarkably, even under the constraints specified in Eq. (2.160), it is unexpected that the

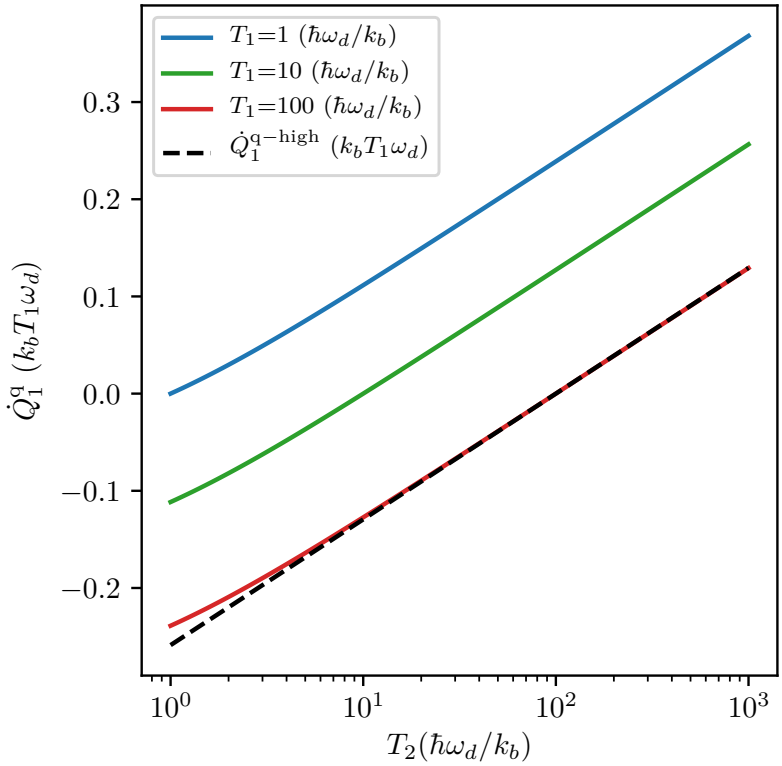

FIGURE 2.12: The quantum contribution to the heat currents for various values of T_1 is depicted as a function of T_2. It is observed that for high values of T_1 and T_2, the quantum correction does not vanish and aligns with a non-trivial logarithmic expression (represented by the black dashed line). This plot corresponds to the parameters $M = 1$, $L = 2$, $\omega_c = 5\omega_d$, and $\omega_d = 1$ [61].

dominant term in the expression for the heat current does not necessarily vanish as $|\lambda_\pm|/\omega_{\mathrm{th}} \to 0$. This occurrence can be attributed to the fact that the temperature is assumed to be high in comparison to the slow frequency scale ω_d, while it must still remain low in comparison to the fast frequency scale γ. Essentially, the temperature lies within the intermediate region of the time scale separation associated with the overdamped regime. Consequently, considering the first non-trivial order, the total heat current for high temperatures can be represented as:

$$\dot{Q}_1^{\mathrm{high}} = \dot{Q}_1^{\mathrm{cl}} + \frac{\hbar}{\pi}\left(\frac{M}{L}\right)^2\left(\frac{\lambda_+\lambda_-}{\omega_d}\right)^2 \log\left(\frac{T_2}{T_1}\right). \tag{2.179}$$

Figure 2.12 shows the behavior of the quantum contribution with respect to the growth of the temperature. When both bath temperatures are increased, we can still observe a non-zero quantum correction to the heat currents.

So far, we have covered the fundamentals of linear quantum RLC circuits, considering

the effects of dissipation. Expanding on this, we conducted an analysis of heat currents within a system comprising two magnetically coupled RLC circuits. As a result, we obtained analytical solutions for the overdamped heat currents in the steady state, which have been documented in the article [61]. In the forthcoming sections, we will provide an overview of the non-linear scenario in relation to the aforementioned study.

2.8 Non-linear quantum systems

Firstly, we will begin by revisiting some key aspects of superconductivity and the Josephson junction. From there, we will delve into the exploration of utilizing Josephson junctions to create qubits. This will involve studying different models for coupling these qubits and understanding how to effectively model dissipation in quantum electrodynamics (QED) circuits.

2.9 Josephson junction

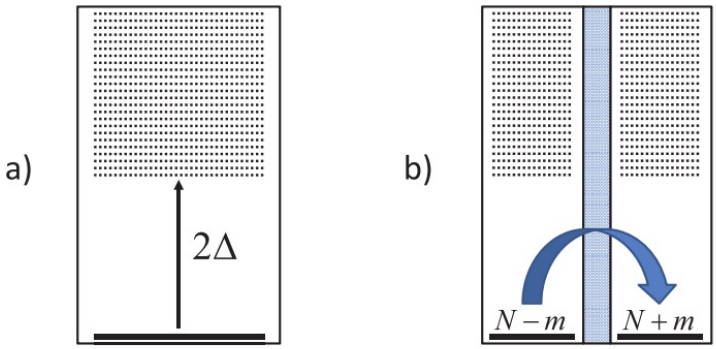

FIGURE 2.13: a- metal with superconducting gap 2Δ. b- JJ [48]

The Josephson junction (JJ) is a structure composed of two superconducting metallic electrodes brought into close proximity, separated only by a tunnel barrier [58, 24]. In contrast to normal metals, a superconducting electrode consists of paired electrons known as Cooper pairs. In the ground state of the superconducting electrode with an even number of electrons, there exists a unique non-degenerate state filled with Cooper pairs. This ground

state is separated from other excited states by the superconducting gap 2Δ, where Δ represents the energy required to break a Cooper pair into two normal electrons. In the low-temperature regime $k_B T \ll 2\Delta$, where k_B is Boltzmann's constant and T is the temperature, all Cooper pairs are predominantly located in the ground state and separated from the excited states.

We can represent the superconducting state of the electrode as $|N\rangle$, where N denotes the number of pairs in the metal. However, in the case of a Josephson junction, we have two superconductors. Therefore, we need to describe the state by the number of pairs tunneling between the two metals, denoted as m. Thus, the state of the Josephson junction can be expressed as:

$$|m\rangle = |N_L - m, N_R + m\rangle\,, \tag{2.180}$$

where N_L and N_R are the number of Cooper pairs on the left and right superconducting metals (Fig. 2.13).

The bare tunnelling Hamiltonian, without considering the Coulomb force could be written as

$$H_T = -\frac{E_J}{2}\sum_m |m\rangle\langle m+1| + |m+1\rangle\langle m|\,. \tag{2.181}$$

The Josephson coupling energy, denoted as E_J, characterizes the strength of the pairs' ability to tunnel through the barrier. The Hamiltonian mentioned above describes the process of annihilating one pair on the right side and creating another pair on the left side, while leaving a hole in the right superconductor. As a result, since the value of m changes by unity, we can represent the eigenfunctions of the tunneling Hamiltonian as wave functions with a phase factor φ. This can be expressed as follows

$$|\varphi\rangle = \sum_{m=-\infty,\infty} e^{im\varphi}\,|m\rangle\,. \tag{2.182}$$

This leads to the eigenvalue equation as

$$H_T\,|\varphi\rangle = -E_J\cos\varphi\,|\varphi\rangle\,. \tag{2.183}$$

Using the above equation, we can find the tunnelling current $I(\varphi)$. Indeed, we can use the expression $I(\varphi) = 2ev_g(\varphi)$ where $v_g(\varphi) = \frac{\partial\omega}{\partial k}$ is the group velocity of the pairs. We may write this with respect to the eigenvalues of H_T since $H_T = \hbar\omega$ and $\varphi = k$ as the wave

vector. Thus, it can be written as

$$v_g(\varphi) = \frac{1}{\hbar}\frac{\partial}{\partial\varphi}H_T = \frac{E_j}{\hbar}\sin\varphi. \tag{2.184}$$

Therefore, the current will be

$$I = 2ev_g(\varphi) = I_c\sin\varphi, \tag{2.185}$$

where $I_c = \frac{2eE_J}{\hbar}$ is the critical current or the maximum tunnelling current. In fact, adding more current will result in a voltage difference and breakage of the superconducting gap. One can alternately define the current operator by introducing two conjugate variables. First, we define the number operator $\hat{n}$ as

$$\hat{n} = \sum_m m\,|m\rangle\langle m|\,, \tag{2.186}$$

which indicates the number of tunnelling Cooper pairs. Furthermore, we can find $\langle\varphi|\hat{n}|\psi\rangle$ such that

$$\langle\varphi|\hat{n}|\psi\rangle = i\frac{\partial}{\partial\varphi}\langle\varphi|\psi\rangle\,. \tag{2.187}$$

Thus, we can see that the number operator is

$$\hat{n} = i\frac{\partial}{\partial\varphi}. \tag{2.188}$$

Indeed, the variables $\hat{n}$ and $\hat{\varphi}$ are conjugate variables that satisfy the commutation relation $[\hat{n},\hat{\varphi}] = i$. The phase variable $\hat{\varphi}$ can be related to the node flux variable introduced earlier in the RLC circuits, which represents the time integral of the voltage between a node and the ground. To establish this connection, we need to consider the influence of the Coulomb force in the junction.

The Josephson junction can be conceptualized as an LC circuit comprising a non-linear inductance and a capacitance C_J formed by the two superconducting plates. Therefore, the Hamiltonian of the junction can be expressed as follows

$$H = E_C\left(\hat{n} - \frac{Q_r}{2e}\right)^2 - E_J\hat{\cos}\,\varphi, \tag{2.189}$$

where $E_C = (2e)^2/2C_J$ is the Coulomb charging energy corresponding to one Cooper pair on the capacitance C_J. Q_r takes into account the offset charge existing in the capacitor. This

charge was also present when we wrote the Hamiltonian of a linear LC circuit. However, since the Hamiltonian was quadratic in flux variable, this term can be neglected. Using the Heisenberg equation of motion we can write (at this point, we drop the hats over the operators)

$$I = 2e\frac{dn}{dt} = -\frac{2e}{i\hbar}[H, n] = I_c \sin\varphi \tag{2.190}$$

$$\frac{d\varphi}{dt} = -\frac{1}{i\hbar}[H, \varphi] = \frac{2e}{\hbar}(V_{C_J} - V_r), \tag{2.191}$$

where V_{C_J} and V_r indicate the voltage with respect to the Cooper pairs and the offset charge on the capacitor. Equation (2.191) is indeed indicating the dependence of the phase variable on the node flux, such that $\phi = \int_0^t \left(V_{c_J} - V_r\right) dt$ or equivalently $\left(V_{c_J} - V_r\right) = \dot{\phi}$. Thus

$$\varphi = 2\pi\frac{\phi}{\phi_0}, \tag{2.192}$$

where $\phi_0 = \frac{2e}{\hbar}$ is the superconducting quantum flux. As a result, when the flux variable changes by one quantum flux, the superconducting phase undergoes a winding of 2π.

Our objective is to explore how Josephson junctions can be utilized to create qubits. However, before proceeding to that, it is important to address the fluctuations associated with the presence of offset charge in the capacitor. One approach to mitigate these fluctuations is to introduce a voltage source in series with a gate capacitor C_g, which gives rise to the construction of a Cooper pair box.

2.10 Cooper pair box

To obtain the Hamiltonian of the Cooper pair box (CPB) in terms of the flux and charge variables, we consider the CPB configuration shown in Figure 2.14. The CPB consists of a Josephson junction (JJ) in series with the gate capacitor C_g and a voltage source created by the capacitor C_B.

In this setup, we introduce the node fluxes Φ_1 and Φ_2 as shown in the figure, and the capacitor C_B creates the voltage source V_B. To derive the Hamiltonian, we treat the voltage source as a capacitor with a large capacitance, allowing us to consider it as a constant voltage term. According to the definition of the node flux we have

$$V_J = \dot{\Phi}_1 \tag{2.193}$$

$$V_B = \dot{\Phi}_2 \tag{2.194}$$

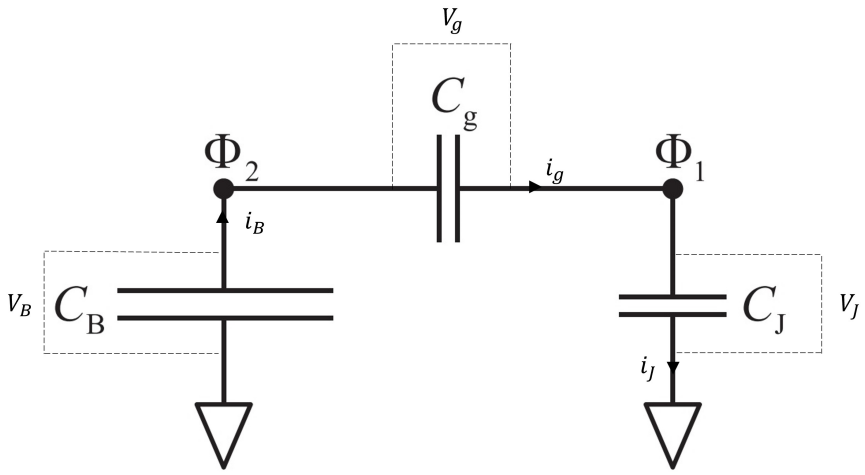

FIGURE 2.14: Circuit for the determining the electrostatic energy of a Cooper pair box [48]

$$V_g = \dot{\Phi}_1 - \dot{\Phi}_2, \tag{2.195}$$

where V_g and V_J are the voltages associated with capacitors C_g and C_J, respectively. Kirchhoff's current law for the currents i_g, i_B and i_J which pass through the capacitors C_g, C_B and C_J implies that

$$i_J = i_B = i_g, \tag{2.196}$$

Thus, we can find the equations of motion for the flux variables as

$$C_B\ddot{\Phi}_2 = C_J\ddot{\Phi}_1 \tag{2.197}$$

$$C_B\ddot{\Phi}_2 = C_g\left(\ddot{\Phi}_2 - \ddot{\Phi}_1\right) \tag{2.198}$$

$$C_J\ddot{\Phi}_1 = C_g\left(\ddot{\Phi}_2 - \ddot{\Phi}_1\right). \tag{2.199}$$

Based on the above equations we may construct the Lagrangian of the system such that

$$\mathcal{L} = \frac{1}{2}C_J\dot{\Phi}_1^2 + \frac{1}{2}C_g\left(\dot{\Phi}_1 - \dot{\Phi}_2\right)^2 + \frac{1}{2}C_B\dot{\Phi}_2^2. \tag{2.200}$$

Replacing the flux variable with their conjugate charge variable we can write the following Hamiltonian of the system in a matrix form:

$$H = \frac{1}{2}q^T C^{-1} q, \tag{2.201}$$

where $q = \begin{bmatrix} q_1 \\ q_2 \end{bmatrix}$ indicates the charge variables and the capacitance matrix defined as

$$C^{-1} = \frac{1}{C_g C_B + C_g C_J + C_J C_B} \begin{bmatrix} C_B + C_g & C_g \\ C_g & C_J + C_g \end{bmatrix}. \tag{2.202}$$

To simplify this matrix we define

$$C_{1\Sigma} \equiv C_g + C_{2s} \tag{2.203}$$

$$C_{2\Sigma} \equiv C_B + C_{1s}, \tag{2.204}$$

with

$$\frac{1}{C_{1s}} = \frac{1}{C_g} + \frac{1}{C_J} \tag{2.205}$$

$$\frac{1}{C_{2s}} = \frac{1}{C_g} + \frac{1}{C_B}. \tag{2.206}$$

Using the above relations the capacitance matrix can be written as

$$C^{-1} = \begin{bmatrix} \frac{1}{C_{1\Sigma}} & \frac{\kappa}{C_{2\Sigma}} \\ \frac{\kappa}{C_{2\Sigma}} & \frac{1}{C_{2\Sigma}} \end{bmatrix}, \tag{2.207}$$

with $\kappa = \frac{C_g}{C_g + C_J}$. Expanding the matrices in (2.201) together with including the tunnelling term we have

$$H = \frac{q_1^2}{2C_{1\Sigma}} + \kappa V_B q_1 - E_J \cos\left(2\pi \frac{\Phi_1}{\Phi_0}\right) + \frac{1}{2} C_{2\Sigma} V_B^2. \tag{2.208}$$

In the given equation, the last term is constant and can be disregarded. Firstly, we substitute $q_1 = 2en - Q_r$ into the equation and then utilize the fact that C_B is greater than the other two capacitances. In this scenario, where $C_B \gg C_j, C_g$, we obtain $C_{1\Sigma} = C_g + C_J$, which represents the total capacitance of the CPB. Therefore, we have

$$H = E_C \left(n^2 - 2n n_g\right) - E_J \cos\left(2\pi \frac{\Phi_1}{\Phi_0}\right) + \frac{1}{2} C_{2\Sigma} V_B^2 + \frac{Q_r^2}{2C_{1\Sigma}}, \tag{2.209}$$

where in the limit of $C_B \gg C_j, C_g$ we defined

$$n_g = \frac{1}{2e}\left(Q_r - \kappa C_{1\Sigma V_B}\right) \simeq \frac{1}{2e}\left(Q_r - C_g V_B\right). \tag{2.210}$$

On the other hand, unlike the integer value of n, the parameter n_g depends on both the voltage V_B and the capacitance C_g. This dependency allows us to manipulate and reduce the fluctuations in Q_r. Finally, by disregarding the constants in the aforementioned Hamiltonian, we can express the Hamiltonian of the CPB as follows:

$$H = E_C \left(n - n_g\right)^2 - E_J \cos\left(2\pi \frac{\Phi_1}{\Phi_0}\right). \tag{2.211}$$

After obtaining the Hamiltonian of the CPB, we will now explore how we can create a qubit using this Hamiltonian. Let us begin by examining the regime where the charging energy greatly exceeds the tunneling energy, denoted as $E_C \gg E_J$. In this regime, the dominant term in equation (2.211) is the Coulomb charging term. The eigenvalues of the Coulomb charging term $E_N = E_C \left(n - n_g\right)$, expressed in terms of n_g, exhibit a particular pattern for the first few energies. Notably, when $n_g = 1/2$, a degeneracy occurs at the states $N = 0$ and $N = 1$. The energy of this state is $E_C/4$, while the energy of the subsequent excited state is $9E_C/4$. This significant energy gap allows us to consider only the two degenerate states in this limit.

The presence of a small Josephson tunneling term acts as a perturbation, breaking the degeneracy and giving rise to a qubit. By utilizing equations (2.181) and (2.186), we can rewrite equation (2.211) as

$$H = E_C \sum_n \left(n - n_g\right)^2 |n\rangle\langle n| - \frac{E_J}{2} \sum_n |n\rangle\langle n+1| + |n+1\rangle\langle n|, \tag{2.212}$$

To find the Hamiltonian of the qubit we limit n_g to the vicinity of $1/2$ or we set $n_g = 1/2 + \Delta_g$ with Δ_g sufficiently small. Neglecting all the states except for $N = 0, 1$ in (2.212) we have

$$H = E_C \left(\left(\frac{1}{2} + \Delta_g\right)^2 |0\rangle\langle 0| + \left(\frac{1}{2} - \Delta_g\right)^2 |1\rangle\langle 1| \right) - E_J \left(|0\rangle\langle 1| + |1\rangle\langle 0|\right) \tag{2.213}$$

The above Hamiltonian can be written in terms of the Pauli matrices and the identity matrix $\mathbb{1}$ such that

$$H = E_C \left(\frac{1}{4} + \Delta_g^2\right) \mathbb{1} + E_C \Delta_g \sigma_z - \frac{E_J}{2} \sigma_x. \tag{2.214}$$

Since the first term is only an energy shift to the system, we can drop it from the Hamiltonian, yet we will take into account its presence at the end. Therefore, the Hamiltonian of the qubit

can be written as

$$H_q = E_C \Delta_g \sigma_z - \frac{E_J}{2}\sigma_x. \tag{2.215}$$

Applying a rotation to this Hamiltonian, it transforms into

$$H_q = E_C \Delta_g \sigma_x + \frac{E_J}{2}\sigma_z. \tag{2.216}$$

The control parameter available in the system is still Δ_g, given by $\Delta_g = n_g - 1/2$. When $n_g = 1/2$, we observe that the Hamiltonian becomes independent of both Δ_g and Q_r. Consequently, the fluctuations of the offset charge are eliminated at this particular point known as the "sweet spot". Therefore, the Hamiltonian can be expressed as

$$H_q = \frac{E_J}{2}\sigma_z, \tag{2.217}$$

with the eigenvalues $E_\pm = E_C/4 \pm E_J/2$. For non-zero n_g, one can find the eigenvalues of the full Hamiltonian of the qubit such that

$$E_q = E_C \left(\frac{1}{4} + \Delta_g^2\right) \pm \sqrt{E_C^2 \Delta_g^2 + E_J^2/4}. \tag{2.218}$$

For the higher order terms of the Hamiltonian (2.212), the energy gap between energy levels will become smaller and smaller due to the condition $E_C \gg E_J$. As a result, only the first two levels will remain well-separated and form a viable qubit. In the upcoming section, we explore an alternative form of qubit that operates in the opposite regime compared to the charge qubit.

2.11 Transmon qubit

So far, we have discussed how to create a charge qubit using a CPB in the regime where $E_C \gg E_J$. However, we should note that the Hamiltonian of the charge qubit (2.216) is directly influenced by the values of the gate charge n_g. While we were able to mitigate fluctuations caused by the offset charge Q_r, noise associated with the gate charge n_g remains a concern, which can negatively affect the system. Although setting $n_g = 1/2$ at the sweet spot can help, fluctuations in n_g still exist around this point.

To address the noise in the gate parameter, one approach is to increase the ratio E_J/E_C and enter the regime of a *transmon* qubit. This condition offers several advantages. First, it relaxes the impact of noisy offset charges. Additionally, it provides anharmonicity in the

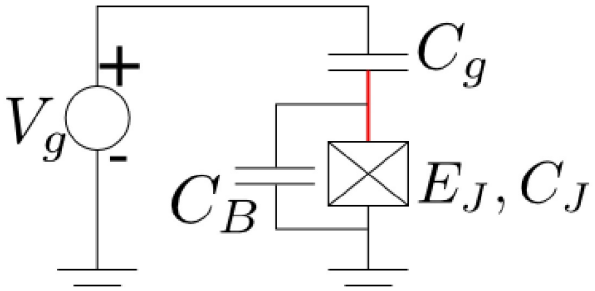

FIGURE 2.15: Circuit representation of the transmon qubit [47].

energy levels similar to what we had in the charge qubit with a small E_J/E_C ratio. By satisfying these requirements, we can alleviate the noise issue associated with the gate charge and enhance the performance of the qubit system.

The transmon qubit, as illustrated in Fig. 2.15, consists of a CPB and a large capacitor C_B connected in parallel to the junction. The purpose of adding C_B as a control parameter is to maintain E_C smaller than E_J, as the charging energy is inversely proportional to the junction capacitance. Consequently, the Hamiltonian of the transmon qubit retains the same form as that of the charge qubit. In order to demonstrate the effectiveness of $E_J \gg E_C$ in suppressing charge noise, one needs to solve the eigenvalue problem for the transmon Hamiltonian. This analysis will provide insight into the energy levels and behavior of the transmon qubit.

It has been demonstrated that the fluctuations in n_g decrease exponentially with $\sqrt{E_J/E_C}$ [68]. As shown in Fig. 2.16, increasing E_J/E_C reduces the dependence of energy levels on n_g and leads to a more harmonic oscillator-like behavior.

This phenomenon can be understood by drawing an analogy between the qubit Hamiltonian and a charged rotor in an external magnetic field. The Hamiltonian of a charged rotor, expressed in terms of its angular momentum L_z, can be written as follows:

$$H_r = \frac{L_z^2}{2ml^2} - mgl\cos\varphi, \tag{2.219}$$

where l is the length of the rotor. This Hamiltonian will be similar to the qubit if we turn the magnetic field B_0 on. Thus, the momentum of the rotor will change accordingly to

$$L_z \to L_z - qA = L_z + \frac{1}{2}qB_0l^2, \tag{2.220}$$

where q represents the rotor charge and $\frac{1}{2}qB_0l^2$ can be considered as the gate charge n_g, the limit of $E_J \gg E_C$ corresponds to a strong gravitational field. This leads to small oscillations around $\phi = 0$ and breaks the periodicity in ϕ. By expanding the cos term up to the fourth

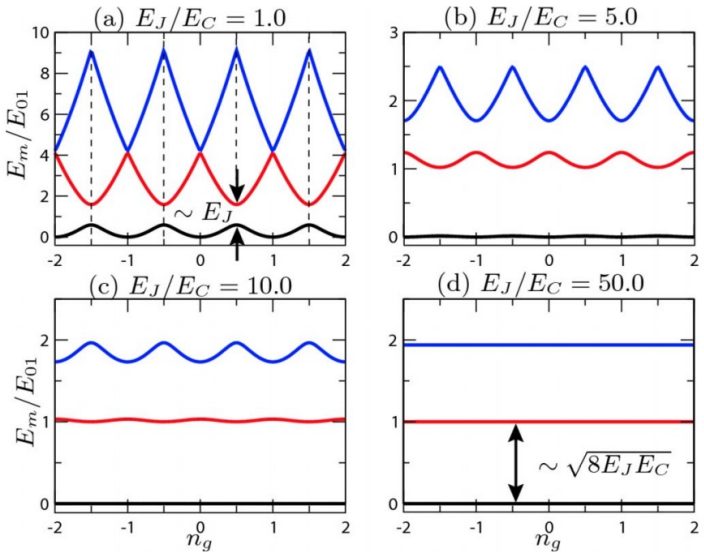

FIGURE 2.16: Eigenenergies E_m (first three levels) for the qubit Hamiltonian as a function of n_g [68].

order, the rotor transforms into an anharmonic oscillator. Since the oscillator is no longer periodic, we can apply a gauge transformation to eliminate the effect of the magnetic field, which is equivalent to reducing the influence of n_g in the problem.

The transmon qubit exhibits robust insensitivity to charge fluctuations, as we have observed. However, it is important to confirm the presence of level anharmonicity in the transmon qubit. To demonstrate this, we expand the cos term in the CPB Hamiltonian (2.211) up to the fourth order, resulting in

$$H = E_C \left(n - n_g\right)^2 - E_J \left(1 - \frac{\varphi^2}{2} + \frac{\varphi^4}{24}\right). \tag{2.221}$$

As we said before, with this expansion, one can remove n_g by gauge transformation due to elimination of periodicity in ϕ. Therefore, the Hamiltonian is merely a perturbed harmonic oscillator. Using the ladder operators a and $a^\dagger$ and also the relation $[n, \phi] = i$, we can write the Hamiltonian such that

$$H = \sqrt{8E_jE_C}\left(a^\dagger a + 1/2\right) - E_J - \frac{E_C}{12}\left(a^\dagger + a\right)^4. \tag{2.222}$$

To write the above Hamiltonian we first obtained

$$n = i\sqrt{\frac{\hbar\omega}{8E_C}}(a - a^\dagger) \tag{2.223}$$

$$\varphi = \sqrt{\frac{\hbar\omega}{4E_J}}(a + a^\dagger), \tag{2.224}$$

and then the commutation relation $[n, \phi] = i$ gives us $\hbar\omega = \sqrt{8E_J E_C}$. Considering the second term as a perturbation, we can find the eigenvalues of the above Hamiltonian. The first non-zero order correction using the perturbation theory gives the energies as

$$E_n^{(1)} = \frac{E_C}{12}\left(6n^2 + 6n + 3\right). \tag{2.225}$$

Thus, we may write the total energy as

$$E_n = -E_J + \sqrt{8E_j E_C}\,(n + 1/2) - \frac{E_C}{12}\left(6n^2 + 6n + 3\right). \tag{2.226}$$

From the above relation, we can define the relative and absolute anharmonicity as

$$\alpha \equiv E_{12} - E_{01} \quad \alpha_r \equiv \frac{\alpha}{E_{01}}. \tag{2.227}$$

Therefore, for large E_J/E_C we will have

$$\alpha = -E_C \quad \alpha_r = -\left(\frac{E_J}{E_C}\right)^{-\frac{1}{2}}. \tag{2.228}$$

Indeed, the parameter α_r plays a crucial role in determining the range of good anharmonicity in the transmon regime. In practice, it is often tuned by adjusting the pulse duration applied to the qubit [68]. For instance, if the transition frequency is approximately $\omega_{01}/2\pi \approx 10GHz$, the pulse duration can be estimated as $\tau_p = |\omega_{01}\alpha_r|^{-1}$. To ensure that the pulse duration is shorter than the inverse of the transition frequency ($\tau_p < \omega_{01}$), we can derive a lower limit for α_r as $\alpha_r^{min} \sim 1/(200\pi)$.

With a pulse duration of $\tau_p \approx 10ns$, this lower limit for α_r corresponds to a range of $20 \lesssim E_J/E_C \ll 5 \times 10^4$. This range provides a significant span with reduced sensitivity to charge fluctuations and sufficient anharmonicity, making it suitable for transmon qubit operations.

The transmon qubit and the charge qubit share a similar structure. In both cases, the two superconducting islands are not directly connected to each other, and only tunnelling current is present. As a result, the superconducting phase ϕ is compact and restricted to the range $0 \leq \phi \leq 2\pi$. However, if we design a circuit where the islands are connected and can be influenced by an external flux or current, we can create another type of qubit known as a *flux*

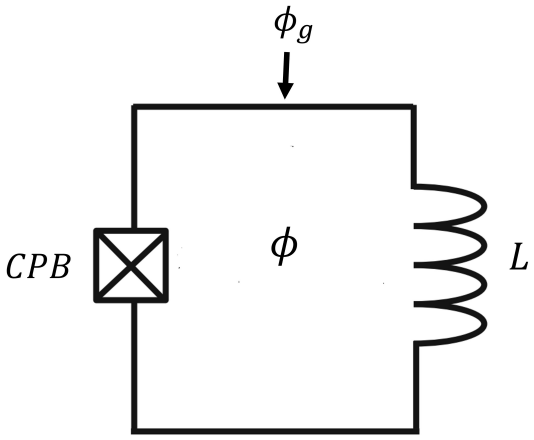

FIGURE 2.17: Flux qubit circuit.

qubit which we will study in the next section.

2.12 Flux qubit

The corresponding circuit for the flux qubit is shown in Fig. (2.17), where a CPB is connected to an inductance L and ϕ represents the node flux of the inductance.

Similar to the approach used for the CPB, we can derive the Hamiltonian that describes the circuit. Specifically, we combine the Hamiltonian of the inductance in the circuit shown in Fig. 2.17 with the Hamiltonian of the CPB in equation (2.211). In this case, the inductance acts as the control parameter and also provides the voltage applied to the junction. Therefore, the combined Hamiltonian can be expressed as follows

$$H = E_C \left(n - n_g\right)^2 - E_J \cos\varphi + \frac{1}{2L}\left(\phi - \phi_g\right)^2, \tag{2.229}$$

where ϕ_g is the and extremal flux which is a control parameter. In the above Hamiltonian, we can observe that the distinction between the charge and flux qubits lies in the element they are shunted by. In the case of the charge qubit, a capacitor couples to the charge variable, whereas in the flux qubit, an inductance is utilized to achieve flux coupling. Additionally, similar to the charge qubit, the dependence on n_g can be eliminated through a gauge transformation, rendering the flux qubit insensitive to charge fluctuations. By employing equation (2.192), we can express the inductive energy in terms of the phase variable, leading to the following expression

$$H = E_C n^2 - E_J \cos\varphi + E_L \left(\varphi - \varphi_g\right)^2, \tag{2.230}$$

where $E_L = \frac{\phi_0^2}{4\pi^2 L}$ is the inductive energy. The regime in which the flux qubit operates is characterized by $E_J \gg E_C$, similar to the transmon qubit. However, in the case of the flux qubit, we also need to consider another condition, namely $\lambda = E_J/E_L \sim 1$. This condition ensures that the third term in the Hamiltonian cannot be neglected; otherwise, the phase qubit would behave as a charge qubit. By satisfying these conditions, we can expand the Josephson term up to the fourth order, similar to the expansion performed for the transmon qubit. Choosing the external flux parameter as $\varphi_e = \varphi_g - 1/2$, while ϕ_g approaches $1/2$, we obtain the following:

$$H = E_C n^2 + \frac{1}{2}\left(E_J + 2E_L\right)\varphi^2 - E_J\frac{\varphi^4}{24} - 2E_L\varphi\varphi_e - \left(E_J - E_L\varphi_e^2\right). \tag{2.231}$$

To find the eigenvalues and eigenvectors of the above Hamiltonian we use perturbation theory once more. We first define

$$n = i\sqrt{\frac{\hbar\omega}{8E_C}}(a - a^\dagger) \tag{2.232}$$

$$\varphi = \sqrt{\frac{\hbar\omega}{4(E_J + 2E_L)}}(a + a^\dagger), \tag{2.233}$$

where $\hbar\omega = \sqrt{8(E_J + 2E_L)E_C}$. By substituting the expression above into the Hamiltonian, we can calculate the energy eigenvalues up to the first order such that

$$E_n^{(1)} = -\frac{E_C}{24\left(1/2 + 1/\lambda\right)}\left(6n^2 + 6n + 3\right) - \left(E_J - E_L\varphi_g^2\right). \tag{2.234}$$

We can determine the corresponding eigenstates, but it is sufficient to consider only the first two lowest states to form a qubit state. Therefore, we have the following expression for the eigenstates:

$$|\tilde{n}\rangle = |n\rangle - E_L\varphi_e\sqrt{\frac{\hbar\omega}{E_J + 2E_L}}\left(\frac{\sqrt{n}}{E_{n-1} - E_n}|n-1\rangle + \frac{\sqrt{n+1}}{E_{n+1} - E_n}|n+1\rangle\right). \tag{2.235}$$

Hence, the first two eigenvectors are

$$|\tilde{0}\rangle = |0\rangle - \varphi_e I_p |1\rangle \tag{2.236}$$

$$|\tilde{1}\rangle = |1\rangle + \varphi_e I_p |0\rangle, \tag{2.237}$$

where $I_p/2 = E_L \langle 0|\varphi|1\rangle / \hbar\omega = \frac{E_L}{2\hbar\omega}\sqrt{\frac{\hbar\omega}{E_J + 2E_L}}$. We can utilize the above states to calculate

the matrix elements of the Hamiltonian (2.231) up to the first order in ϕ_e. This allows us to express the Hamiltonian as follows

$$H = \frac{E_0 + E_1}{2}\mathbb{1} + \frac{E_0 - E_1}{2}\sigma_z + \frac{1}{2}\varphi_e I_p \left(E_0 - E_1 - \hbar\omega\right)\sigma_x, \tag{2.238}$$

where $E_0 = \langle 0| H + 2E_L\varphi\varphi_e |0\rangle$ and $E_1 = \langle 1| H + 2E_L\varphi\varphi_e |1\rangle$. We can see that the above Hamiltonian is very similar to the one we had for the charge qubit. Thus, neglecting the Identity term, in the limit $\varphi_e \to 0$ we have

$$H = \frac{E_0 - E_1}{2}\sigma_z. \tag{2.239}$$

The next step after understanding the basic architecture of superconducting qubit will concern how they can be operational. In the next section, we will investigate the coupling between superconducting qubits, which is essential for understanding their heat transport behavior and their operation in a quantum information processing setting. It is particularly important when considering the construction of an array of these artificial atoms for various purposes. By studying the different forms of qubit coupling, we can gain valuable insights into their behavior and performance.

2.13 Qubit couplings

To couple multiple qubits together, there exist number of ways. Here we consider the coupling structure named inductive coupling.

2.13.1 Inductive coupling

The inductive coupling between two circuits is analogous to the magnetic coupling between two LC circuits, as illustrated in Fig. 2.7. When two flux qubit circuits are placed in close proximity, they become coupled through their mutual inductance M. Fig. 2.18 represents the circuit configuration for the coupling between two flux qubits. As we have previously solved this circuit, we can express the Hamiltonian of the linearly coupled LC circuit by incorporating the Josephson tunneling term. Therefore, we obtain the following expression

$$\begin{aligned} H =& E_{C_1} n_1^2 + E_{C_2} n_2^2 - E_{J_1}\cos\varphi_1 - E_{L_1}\left(\varphi_1 - \varphi_{g_1}\right)^2 + E_{J_2}\cos\varphi_2 + E_{L_2}\left(\varphi_2 - \varphi_{g_2}\right)^2 \\ &+ E_M\left(\varphi_1 - \varphi_{g_1}\right)\left(\varphi_2 - \varphi_{g_2}\right), \end{aligned} \tag{2.240}$$

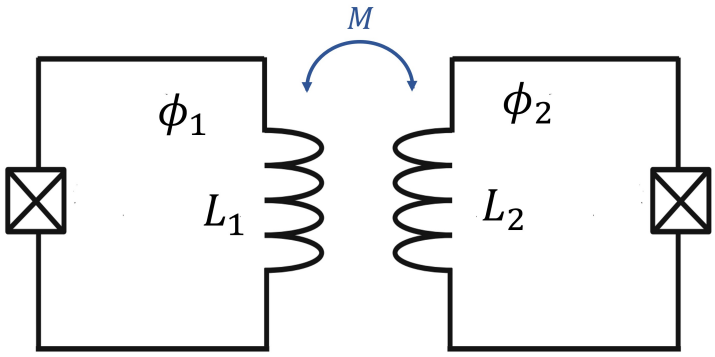

FIGURE 2.18: Two coupled flux qubit circuits.

where $E_{L_{1/2}} = \frac{L_{2/1}}{L_1L_2-M^2}\phi_0^2$ and $E_M = \frac{M}{L_1L_2-M^2}\phi_0^2$. To derive the Hamiltonian of the qubit in terms of the Pauli matrices, we will employ the same perturbation method as before. This time, we treat the interaction term $H_I = E_M\left(\varphi_1 - \varphi_{g_1}\right)\left(\varphi_2 - \varphi_{g_2}\right)$ as a perturbation for small values of $\varphi_{e_{1/2}} = 1/2 - \varphi_{g_{1/2}}$. By expanding the Hamiltonian up to the first order in $\varphi_{e_{1/2}}$, we obtain the following expressions

$$|\hat{00}\rangle = |00\rangle + E_M I_M^2 \frac{|11\rangle}{E_{11}-E_{00}} - E_M I_M\left(\varphi_{e_1}\frac{|10\rangle}{E_{10}-E_{00}} + \varphi_{e_2}\frac{|01\rangle}{E_{01}-E_{00}}\right) \tag{2.241}$$

$$|\hat{01}\rangle = |01\rangle + E_M I_M^2 \frac{|10\rangle}{E_{10}-E_{01}} - E_M I_M\left(\varphi_{e_1}\frac{|11\rangle}{E_{11}-E_{01}} + \varphi_{e_2}\frac{|00\rangle}{E_{00}-E_{01}}\right) \tag{2.242}$$

$$|\hat{10}\rangle = |10\rangle + E_M I_M^2 \frac{|01\rangle}{E_{01}-E_{10}} - E_M I_M\left(\varphi_{e_1}\frac{|00\rangle}{E_{00}-E_{10}} + \varphi_{e_2}\frac{|11\rangle}{E_{11}-E_{10}}\right) \tag{2.243}$$

$$|\hat{11}\rangle = |11\rangle + E_M I_M^2 \frac{|00\rangle}{E_{00}-E_{11}} - E_M I_M\left(\varphi_{e_1}\frac{|01\rangle}{E_{01}-E_{11}} + \varphi_{e_2}\frac{|10\rangle}{E_{10}-E_{11}}\right), \tag{2.244}$$

where $I_M = \langle nn|\,\varphi_{1/2}\,|nn\rangle$ and $E_{nm} = \langle nm|\,H - H_I\,|nm\rangle$ for $n,m = \{0,1\}$. In case we set $\varphi_g = 1/2$ we will have the Hamiltonian such that

$$H = \left(\frac{E_{00}-E_{01}}{2} + E_M\frac{A_{11}E_{11}-A_{10}E_{10}}{2}\right)\sigma_{z_1} + \left(\frac{E_{10}-E_{11}}{2} - E_M\frac{A_{01}E_{01}-A_{11}E_{00}}{2}\right)\sigma_{z_2}$$
$$+E_M^2 I_M^2\left(\frac{A_{11}+A_{10}}{2}\mathbb{1} + \frac{A_{11}-A_{10}}{2}\sigma_{z_1}\right)\left(-\frac{A_{11}+A_{10}}{2}\mathbb{1} + \frac{A_{11}-A_{10}}{2}\sigma_{z_2}\right), \tag{2.245}$$

where $A_{11} = \frac{I_M^2}{E_{11}-E_{00}}$ and $A_{10} = \frac{I_M^2}{E_{10}-E_{01}}$. Above Hamiltonian describes the inductive coupling between two qubits. In the next section, we will investigate the effect of dissipation on the qubits by introducing resistors, which act as heat baths in a similar manner to our previous discussions. This will allow us to study the heat transport behavior in the context of the coupled qubits and gain insights into the dynamics and stability of the system in the presence of dissipation.

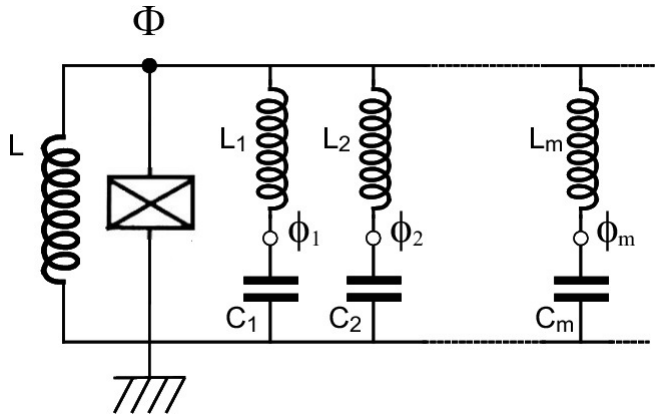

FIGURE 2.19: Spin-Boson model of the coupling between a flux qubit and a resistor

2.14 Environment coupling

In this section, we will investigate the dissipation in a qubit system. Similar to our approach with linear systems such as the harmonic oscillator, we can utilize the Caldeira-Leggett model to describe the coupling between the qubit system and a bath. Specifically, we couple the flux qubit circuit to a resistor and then represent it using the Caldeira-Leggett formalism (as shown in Fig. 2.19). Since we are now dealing with a spin system coupled to a bath of harmonic oscillators, this model is commonly referred to as the "spin-boson" model.

Let us examine Eq. (2.238). Neglecting the identity term, we define $\epsilon = E_0 - E_1$ as the energy splitting between the previously degenerate levels and $\Delta = \varphi_e I_p \left(E_1 - E_0 - \hbar\omega\right)$ as the tunneling energy. With these definitions, we can express the Hamiltonian of the two-level system as follows

$$H_{\mathrm{TLS}} = -\frac{1}{2}\hbar\Delta\sigma_x + \frac{1}{2}\hbar\epsilon\sigma_z. \tag{2.246}$$

One more time we would mention that the condition for this Hamiltonian to be valid is that

$$V_b \gg \hbar\Delta, \hbar\epsilon, k_b T, \tag{2.247}$$

where V_b is the barrier height in the double well potential. The eigenstates of the Hamiltonian are denoted as $|L\rangle$ and $|R\rangle$, which correspond to the eigenvectors of σ_z. Since we are dealing with a double-well potential, the two minima are located at positions $\pm\varphi_0$. To truncate the system, we express the phase operator in terms of σ_z, which represents the position of each localized state $|L\rangle$ and $|R\rangle$. In other words, we truncate the position operator (phase in our setup) into a 2×2 Hilbert space, which can be written as $\varphi = \frac{1}{2}\varphi_0\sigma_z$.

Using this operator, we can couple the two-level system (TLS) to a bath of harmonic oscillators. As we have seen in the Caldeira-Leggett model, the bath is coupled to the position operator of the system. The same principle applies here, and the bath is coupled to φ, effectively measuring the position of the localized states during the interaction. By employing the Caldeira-Leggett representation, we can write the Hamiltonian of the damped TLS as

$$H = H_{\mathrm{TLS}} + \sum_m \left(\frac{q_m^2}{2C_m} + E_{L_m}(\varphi_m - \varphi)^2 \right). \tag{2.248}$$

Here $E_{L_m} = \phi_0^2/2L_m$. Expanding the Hamiltonian we will have

$$H = H_{\mathrm{TLS}} + \sum_m \left(\frac{q_m^2}{2C_m} + E_{L_m}\varphi_m^2 \right) - \sigma_z \sum_m 2E_{L_m}\varphi_0\varphi_m + \sum_m \varphi_0^2 E_{L_m}. \tag{2.249}$$

The above Hamiltonian represents the spin-boson model, which describes the interaction between a two-level system (TLS) and its surrounding environment. The last term in the Hamiltonian is a constant term that represents the zero-point energy of the TLS and can be disregarded in many cases since it only contributes a constant offset to the energy. Thus, it does not affect the dynamics of the system and can be dropped when considering the system's behavior and dissipation.

2.15 Solving spin-boson model

Most studies on the spin-boson model focus on the regime of weak coupling between the system and the bath. For example, in [74], the authors investigated the problem of two TLS and two harmonic oscillators interacting with two thermal baths simultaneously. They derived an analytical expression for the heat currents, showing that weak internal coupling between the qubits can lead to a violation of the second law of thermodynamics. Similarly, in [111, 67], the authors studied the steady-state entanglement generation in a similar system using Markovian master equations. These studies primarily consider weak system-bath couplings.

In the regime beyond weak coupling, numerical techniques have been employed to study the dynamics of two interacting qubits [63]. However, analytical works on this subject mostly focus on a single TLS interacting with a non-equilibrium environment [8, 97, 110], employing methods based on path integrals.

Given the challenges of obtaining exact analytical results, it is beneficial to explore the path integral approach and approximate methods to analyze the behavior of the spin-boson model in the regime of strong system-bath coupling.

To begin, we can apply the path integral method to solve the spin-boson model and find the time evolution of the system state for arbitrary couplings. However, obtaining exact analytical results may still be challenging. To overcome this, we can employ the non-interacting blip approximation (NIBA) technique, which is particularly effective in exploring the overdamped limit of the system. In the overdamped regime, the system reaches an equilibrium state without exhibiting oscillations [73, 16].

In our study, we will first explore the propagator technique to analyze the time evolution of the system state in the spin-boson model. This technique allows us to calculate the transition probabilities between different states of the system. Next, we will employ the Feynman-Vernon path integral method to find the time evolution of the density matrix of the system. This technique incorporates the influence of the surrounding environment through a path integral formalism.

Finally, we will utilize the NIBA technique to study the regime of strong coupling between the qubit and the environment. NIBA is particularly useful in exploring the overdamped limit of the system, where the system reaches an equilibrium state without exhibiting oscillatory behavior.

It is important to note that while NIBA can provide insights into the system's dynamics in the strong coupling regime, it may not be suitable for describing a system of two interacting qubits and environments. However, the analytical solution using NIBA in such a scenario could be a subject of interest for future research.

2.15.1 Propagator method

One approach to determining the evolution of a system's state involves the utilization of a propagator, and subsequently, the Feynman path integral technique.

Assuming a system-bath interaction described by the Hamiltonian $H = H_S + H_B + H_I$, let us consider the initial state of the system as a factorized state, denoted as $\rho_0 = \rho_S \otimes \rho_B$. The temporal evolution of the entire state can be expressed as follows

$$\rho(t) = e^{-iHt}\rho_0 e^{iHt}. \tag{2.250}$$

We can write the above equation in terms of the system and bath coordinates by projecting the density matrix using the state $|x, R\rangle$, where x denotes the system coordinates and R does

the bath. Thus, we have

$$\rho(x,R,y,Q,t) = \langle x,R|\, e^{-iHt}\rho_0 e^{iHt}\, |y,Q\rangle\,, \tag{2.251}$$

where $\rho(x,R,y,Q,t) = \langle x,R|\,\rho(t)\,|y,Q\rangle$. Defining Identity operators of form

$$\mathbb{1} = \int dx\,|x\rangle\,\langle x|\,, \tag{2.252}$$

we may write Eq. (2.251) in terms of propagators. Thus, we will have

$$\rho(x,R,y,Q,t) = \int dx'dR'dy'dQ'K(x,R,t;x',R',0)K^*(y,R,t;y',Q',0)\rho_0(x',R',y',Q'). \tag{2.253}$$

$K(x,R,t;x',R',0)$ and $K^*(y,Q,t;y',Q',0)$ are the propagators written such that

$$K(x,R,t;x',R',0) = \langle x,R|\, e^{-iHt}\,|x',R'\rangle \tag{2.254}$$

$$K^*(y,Q,t;y',Q',0) = \langle y',Q'|\, e^{iHt}\,|y,Q\rangle\,. \tag{2.255}$$

Writing the density matrix in this manner will help us find the time evolution of the system state by taking the partial trace over the bath degrees of freedom. In fact, we should put $R = Q$ and integrate over R. We first take into account that the initial state is factorized so that $\rho_0(x',R',y',Q') = \rho_S(x',y',0)\rho_B(R',Q',0)$. Replacing this state into Eq. (2.253) we will have

$$\rho_S(x,y,t) = \int dx'dy'\mathcal{J}(x,y,t;x',y',0)\rho_S(x',y',0), \tag{2.256}$$

for which we have

$$\mathcal{J}(x,y,t;x',y',0) = \int dRdR'dQ'K(x,R,t;x',R',0)K^*(y,Q,t;y',Q',0)\rho_B(R',Q',0). \tag{2.257}$$

The aforementioned equations indicate that we can determine the temporal evolution of the system's state at any given time by obtaining the propagators. This process involves two essential steps. Firstly, we need to establish a model that describes the bath and its interaction with the system. Secondly, we employ the Feynman path integral approach to calculate the propagators.

2.15.2 Path integral

Considering the propagator $K(x,t;x',0) = \langle x| e^{-iHt/\hbar} |x'\rangle$ where we assume the system is described by the Hamiltonian $H = P^2/2M + V(q)$. We subdivide the time interval $[0,t]$ into small partitions such that $[0,t] = \bigcup_{k=1}^{i=N}[t_{k-1},t_k]$ where $t_0 = 0$ and $t_N = t$. In this way we can write the propagator such that

$$K(x,t;x',0) = \langle x| e^{-iH(t-t_{N-1})/\hbar}...e^{-iH(t_k-t_{k-1})/\hbar}....e^{-iHt/\hbar} \left|x'\right\rangle . \tag{2.258}$$

Adding identity operators in between the expectation values, i.e $\mathbb{1} = \int dx_k \, |x_k\rangle \, \langle x_k|$, we can reduce the problem to finding $K(x_k,t_k;x_{k-1},t_{k-1})$. Moreover, we assume that $t_k - t_{k-1} = \epsilon = t/N \to 0 \quad (N \to \infty)$. Thus, we have

$$K(x_k,t_k;x_{k-1},t_{k-1}) = \langle x_k| \, 1 - \frac{i\epsilon}{\hbar} H \, |x_{k-1}\rangle . \tag{2.259}$$

This time, we add the identity operator in terms of the momenta to simplify above equation. Therefore, we will obtain

$$K(x_k,t_k;x_{k-1},t_{k-1}) = \int dp_k \, \langle x_k|p_k\rangle \, \langle p_k| \, 1 - \frac{i\epsilon}{\hbar} H \, |x_{k-1}\rangle . \tag{2.260}$$

Utilizing the fact that the Hamiltonian is $H = P^2/2M + V(q)$ we will have

$$K(x_k,t_k;x_{k-1},t_{k-1}) = \int dp_k \, \langle x_k|p_k\rangle \, \langle p_k|x_{k-1}\rangle \left(1 - \frac{i\epsilon}{\hbar}\left(\frac{p_k^2}{2M} + V(x_k)\right)\right). \tag{2.261}$$

Using $\langle x_k|p_k\rangle = 1/\sqrt{2\pi\hbar} e^{ip_k x_k/\hbar}$, and writing the expression of the energy term in exponential form we can write

$$K(x_k,t_k;x_{k-1},t_{k-1}) = \frac{1}{\sqrt{2\pi\hbar}} \int dp_k \exp\frac{ip_k}{\hbar}(x_k - x_{k-1}) \exp\frac{-i\epsilon}{\hbar}\left(\frac{p_k^2}{2M} + V(x_k)\right). \tag{2.262}$$

After calculating the integral over p_k one obtains

$$K(x_k,t_k;x_{k-1},t_{k-1}) = \sqrt{\frac{M}{2\pi i\hbar\epsilon}} \exp\frac{i\epsilon}{\hbar}\left(\frac{M}{2}\frac{(x_k - x_{k-1})^2)}{\epsilon^2} - V(x_k)\right). \tag{2.263}$$

Now, we can write the propagator in terms of the above expression

$$K(x,t;x',0)=\prod_{k=1}^{N}\sqrt{\frac{M}{2\pi i\hbar\epsilon}}\int dx_1...d_{x_k}...dx_{N-1}\exp\sum_{k=1}^{N}\frac{i\epsilon}{\hbar}\left(\frac{M}{2}\frac{(x_k-x_{k-1})^2)}{\epsilon^2}-V(x_k)\right). \tag{2.264}$$

Here, x_k denotes the different paths that the system can follow and we are summing over all those paths. Changing the sum into integral we can write it in terms of the action so that we will have

$$K(x,t;x',0)=\prod_{t'=0}^{t}\int\frac{dx(t')}{\mathcal{N}}\exp\frac{i}{\hbar}S[x(t')], \tag{2.265}$$

where

$$S[x(t')]=\int_0^t dt'\left(\frac{1}{2}M\dot{x}^2-V(x)\right). \tag{2.266}$$

We may write (2.265) in simpler from such that

$$K(x,t;x',0)=\int_{x'}^{x}\mathcal{D}x\left(t'\right)\exp\frac{i}{\hbar}S[x(t')]. \tag{2.267}$$

Going back to the calculation of $\mathcal{J}(x,y,t;x',y',0)$, we first write

$$K(x,R,t;x',R',0)=\int_{x'}^{x}\int_{R'}^{R}\mathcal{D}x\left(t'\right)\mathcal{D}R\left(t'\right)\exp\frac{i}{\hbar}S[x(t'),R(t')]. \tag{2.268}$$

The definition of the action $S[x,R]=\int_0^t dt'\mathcal{L}(x,\dot{x};R,\dot{R},t')$ enables us to write the total action in terms of the action of the system, reservoir and interaction terms using their corresponding Lagrangian in a way that

$$S[x,R]=S_0[x]+S_{\mathrm{B}}[R]+S_I[x,R]. \tag{2.269}$$

By combining the previous equation with equation (2.268), we can rephrase the expression for $\mathcal{J}(x,y,t;x',y',0)$ in equation (2.257) in a more comprehensible manner using the actions. Therefore, we will have

$$\mathcal{J}(x,y,t;x',y',0)=\int_{x'}^{x}\int_{y'}^{y}\mathcal{D}x\left(t'\right)\mathcal{D}y\left(t'\right)e^{\frac{i}{\hbar}S_0[x(t')]}e^{-\frac{i}{\hbar}S_0[y(t')]}\mathcal{F}[x\left(t'\right),y\left(t'\right)]. \tag{2.270}$$

Here we have

$$\mathcal{F}[x(t'), y(t')] = \int\int\int dR dR' dQ' \rho_{\mathrm{B}}(R', Q', 0) \int_{R'}^{R}\int_{Q'}^{R} \mathcal{D}R(t')\,\mathcal{D}Q(t')$$
$$\times \exp\left\{\frac{i}{\hbar}\left[S_I[x(t'), R(t')] - S_I[y(t'), Q(t')] + S_{\mathrm{B}}[R(t')] - S_{\mathrm{B}}[Q(t')]\right]\right\}, \quad (2.271)$$

which is the so-called *influence functional*. This carries essential information regarding the time evolution of the initial state of the environment when it interacts with the system and its time-reversed counterpart.

To compute the influence functional, we make the assumption that the initial state of the environment is thermal and that all degrees of freedom in the bath are independent of one another. We begin by expressing the total Hamiltonian using the Caldeira-Leggett model of environment interaction. This allows us to write the Hamiltonian as follows:

$$H = \frac{1}{2}M\dot{x}^2 + V(x) + \sum_n \left\{\frac{1}{2}m_n\dot{r}_n^2 + \frac{1}{2}m_n\omega_n^2 r_n^2 - c_n x r_n + x^2\frac{c_n^2}{2m_n\omega_n^2}\right\}. \quad (2.272)$$

Above Hamiltonian describes the interaction between a system with potential energy $V(x)$ and an environment consisting of independent harmonic oscillators. Based on that we can proceed to switch back to our system and express everything in terms of charge and flux variables. By utilizing the aforementioned Hamiltonian, we can express $S_{\mathrm{I}} + S_{\mathrm{B}}$ in terms of the Lagrangian. Since the bath oscillators are independent, we can focus on the Lagrangian of the n-th bath oscillator. By calculating its action and subsequently the propagator, we can obtain the total bath propagator by multiplying them together. In other words, according to equation (2.268), we can express the Lagrangian for the n-th oscillator of the bath as follows:

$$K_{\mathrm{BI}}^n = \int_{R'}^{R} \mathcal{D}R(t') \exp\left[\frac{i}{\hbar}\int_o^t dt' \left\{\frac{1}{2}m_n\dot{r}_n^2 - \frac{1}{2}m_n\omega_n^2 r_n^2 + c_n x r_n - x^2\frac{c_n^2}{2m_n\omega_n^2}\right\}\right]. \quad (2.273)$$

Above integral is the reminiscent of finding the propagator of a forced harmonic oscillator [36]. We technically assume that $r_n = \tilde{r}_n + \chi_n$ where $\tilde{r}_n$ denotes the classical path and χ_n is the quantum deviation from that. Based on this we can write the above integral such that

$$K_{\mathrm{BI}}^n = \exp\left[\frac{i}{\hbar}S_{\mathrm{cl}}\right]\int_{R'}^{R} \mathcal{D}R(t') \exp\left[\frac{i}{\hbar}\int_o^t dt' \left(\frac{1}{2}m_n\left(\dot{\chi_n}^2 - \omega_n^2\chi_n^2\right)\right)\right]. \quad (2.274)$$

The classical action can thus be calculate by taking advantage of the Euler-Lagrange equations. To solve the quantum deviation, we first write χ_n in terms of its Fourier series such that

$$\chi_n(t') = \sum_\alpha \chi_n^\alpha \sin(\nu_\alpha t'); \quad \nu_\alpha = \pi\alpha/t. \quad (2.275)$$

Replacing this back to (2.287) we can take the time integral and we will have

$$K_{\mathrm{BI}}^{n}=\exp\left[\frac{i}{\hbar}S_{\mathrm{cl}}\right]\int_{R'}^{R}\mathcal{D}R\left(t'\right)\exp\left[i\frac{m_n t}{4\hbar}\sum_{\alpha}\left(\chi_n^{\alpha^2}\left(\nu_\alpha^2-\omega_n^2\right)\right)\right]. \tag{2.276}$$

Having this in hand, we can calculate the integrals over the different paths by changing the sum into a product. Then it will become a Gaussian integral which is already given for a free particle when $\omega_n \to 0$. We can calculate this for each path and we will obtain

$$\int_{R'}^{R}\mathcal{D}R\left(t'\right)\exp\left[i\frac{m_n t}{4\hbar}\sum_{\alpha}\left(\chi_n^{\alpha^2}\left(\nu_\alpha^2-\omega_n^2\right)\right)\right]=C\prod_{\alpha=1}^{\infty}\left(1-\omega_n^2/\nu_\alpha^2\right)^{-1/2}, \tag{2.277}$$

where $C=\left(m_n/2\pi i\hbar t\right)^{1/2}$ is merely the free particle normalization constant. Using

$$\prod_{\alpha=1}^{\infty}\left(1-\frac{\omega_n^2 t^2}{\pi^2\alpha^2}\right)=\frac{\sin(\omega_n t)}{\omega_n t}, \tag{2.278}$$

we finally have

$$K_{\mathrm{BI}}^{n}=\sqrt{\frac{m_n\omega_n}{2\pi i\hbar\sin\omega_n t}}\exp\frac{i}{\hbar}S_{\mathrm{cl}}^{n}, \tag{2.279}$$

where

$$\begin{aligned}S_{\mathrm{cl}}^{n}=\frac{m_n\omega_n}{2\sin\omega_n t}\Bigg[&\left(R_n^2+R_n'^2\right)\cos\omega_n t-2R_nR_n'\\&-\frac{2c_nR_n}{m_n\omega_n}\int_0^t x(t')\sin\omega_n t'dt'-\frac{2c_nR_n'}{m_n\omega_n}\int_0^t x(t')\sin\omega_n(t-t')dt'\\&-\frac{2c_n^2}{m_n^2\omega_n^2}\int_0^t dt'\int_0^t dt''x(t')x(t'')\sin\omega_n(t-t')\sin\omega_n t''\Bigg].\end{aligned} \tag{2.280}$$

The time reversed counterpart of the above propagator can be obtained by changing $i\to -i$, $x(t')\to y(t')$ and $R'\to Q'$. Next, we should multiply those two and then take the average over the bath density matrix. We notice that, because all the bath degrees of freedom are independently thermal with the temperature T, we may still decompose the bath density matrix into the form

$$\rho_{\mathrm{B}}(R',Q',0)=\prod_i\rho_{\mathrm{B}}^{i}(R_i',Q_i',0). \tag{2.281}$$

In this way we can rewrite (2.271) such that

$$\mathcal{F}[x\left(t'\right),y\left(t'\right)]=\prod_{ijl}\iiint dRdR'dQ'\rho_{\mathrm{B}}^{i}(R_i',Q_i',0)K_{\mathrm{BI}}^{j}(x(t'),R_i;R_i',t)K_{\mathrm{BI}}^{l^*}(y(t'),R_i;Q_i',t). \tag{2.282}$$

The integral mentioned above is Gaussian in nature and can be solved. However, before

proceeding with its solution, we must first derive the expression for the density matrix of the bath. To accomplish this, we employ the imaginary time path integral technique, wherein we utilize the Euclidean action instead of the usual Minkowski action. The bath density matrix $\rho_{\mathrm{B}}^{i}(R_i', Q_i', 0)$ can be written as

$$\rho_{\mathrm{B}}^{i}(R_i', Q_i', 0) = \frac{1}{\mathcal{Z}} \left\langle R_i' \right| e^{-H_{\mathrm{B}}\beta} \left| Q_i' \right\rangle, \tag{2.283}$$

with $\mathcal{Z}$ as the partition function. Comparing to (2.254) we can see that this can be similarly written in terms of the action if we have $t = -i\hbar\beta$. Thus, one can follow the procedure that we had before to obtain

$$\rho_{\mathrm{B}}^{i}(R_i', Q_i', 0) = \frac{1}{\mathcal{Z}} \int_{R_i'}^{Q_i'} \mathcal{D}R_i'\left(t'\right) \exp -\frac{1}{\hbar} S_{\mathrm{E}}[R_i'(t')], \tag{2.284}$$

where S_{E} denotes the Euclidean action written as

$$S_{\mathrm{E}}[R_i'(t')] = \int_0^{\hbar\beta} \left(\frac{1}{2} M \dot{R}_i'^2 + V(R_i'(\tau)) \right) d\tau. \tag{2.285}$$

Indeed, in the expression above, we observe the insertion of the Euclidean Lagrangian L_{E}, which differs from the system Lagrangian due to the negative potential V. Utilizing the aforementioned action, we can compute the density matrix of the bath, following a similar approach to what was done to obtain equation (2.277). We can begin by writing

$$S_{\mathrm{E}}[R_i'(t')] = \int_0^{\hbar\beta} \left(\frac{1}{2} m_i \left(\dot{r}_i^2 + \omega_i^2 r_i^2 \right) \right) d\tau. \tag{2.286}$$

Once again, we divide the path r_i into its classical and quantum deviations, as we did in the previous case. This yields the expression

$$\rho_{\mathrm{B}}^{i}(R_i', Q_i', 0) = \exp\left[-\frac{1}{\hbar} S_{\mathrm{E}}^{\mathrm{cl}} \right] \int_{R_i'}^{Q_i'} \mathcal{D}R_i'\left(t'\right) \exp\left[\frac{i}{\hbar} \int_o^t dt' \left(\frac{1}{2} m_i \left(\dot{\chi}_i^2 + \omega_i^2 \chi_i^2 \right) \right) \right]. \tag{2.287}$$

We have already solved this integral in (2.287) with the negative sign. by changing $\nu_\alpha \to i\nu_\alpha$ in (2.277) we will have

$$\rho_{\mathrm{B}}^{i}(R_i', Q_i', 0) = \frac{m_i \omega_i}{2\pi i\hbar \sinh \omega_i t} \exp \frac{-1}{\hbar} S_{\mathrm{E}}^{\mathrm{cl}}, \tag{2.288}$$

where we have

$$S_{\mathrm{E}}^{\mathrm{cl}} = -\frac{m_i\omega_i}{2\hbar\sinh\left(\frac{\hbar\omega_i}{K_bT}\right)}\left[\left(R_i'^2+Q_i'^2\right)\cosh\left(\frac{\hbar\omega_i}{K_bT}\right)-2Q_i'R_i'\right]. \tag{2.289}$$

Having obtained this, we can go back to the influence functional and write it in terms of noise and dissipation kernel such that

$$\mathcal{F}[x(\tau),y(\tau)] = e^{\frac{-1}{\pi\hbar}\int_0^t\int_0^\tau d\tau d\sigma\{-i\eta(\tau-\sigma)[x(\tau)-y(\tau)][x(\sigma)+y(\sigma)]+\nu(\tau-\sigma)[x(\tau)-y(\tau)][x(\sigma)-y(\sigma)]\}}, \tag{2.290}$$

where the noise kernel $\nu(\tau-\sigma) = \int_0^\infty d\omega J(\omega)\cos\omega(\tau-\sigma)\coth(\beta\hbar\omega/2)$ and the dissipation kernel $\eta(\tau-\sigma) = \int_0^\infty d\omega J(\omega)\sin\omega(\tau-\sigma)$ are written in terms of the spectral density of the bath $J(\omega) = \sum_k \frac{c_k(\omega_k)}{2m_k\omega_k}\delta(\omega-\omega_k)$.

To proceed, we can apply the expression for the influence functional to the spin-boson Hamiltonian in order to determine the evolved state of the system at time t. Since we are dealing with a two-level system, the paths $(x(t),y(t))$ it takes correspond to the states $|\uparrow\rangle$ and $|\downarrow\rangle$ exclusively. In other words, for instance, $x(s)$ only takes on the values $\pm\varphi_0$ for $|\uparrow\rangle$ and $|\downarrow\rangle$, respectively. Consequently, the spin double path can be viewed as a single path that jumps among four distinct states: $|\uparrow\uparrow\rangle$, $|\uparrow\downarrow\rangle$, $|\downarrow\uparrow\rangle$, and $|\downarrow\downarrow\rangle$. In this sense, we can construct two functions of these paths, one symmetric and one antisymmetric, such that

$$\chi(s) = \frac{1}{\varphi_0}(x(s)+y(s)) \tag{2.291}$$

$$\xi(s) = \frac{1}{\varphi_0}(x(s)-y(s)). \tag{2.292}$$

For example, for the two states $\{|\uparrow\uparrow\rangle,|\downarrow\downarrow\rangle\}$ we will have $\chi = \pm1$ while $\xi = 0$. For the other two paths we have the opposite situation that $\xi = \pm1$ while $\chi = 0$. Based on this construction of these paths, we regard them as *sojourns* that refer to the diagonal states $a = |\uparrow\uparrow\rangle$ and $d = |\downarrow\downarrow\rangle$, and *blips* that refer to the off-diagonal states $b = |\uparrow\downarrow\rangle$ and $c = |\downarrow\uparrow\rangle$. As a final remark about the two paths, one may notice that χ describes the classical path that the system would take because it refers to the diagonal elements of density matrix. ξ also refers to the quantum paths taken due to it being related to the off-diagonal elements of the density matrix.

Before solving the integral in (2.290), let us first consider the free paths in (2.270). To calculate the action for the two-level system, we construct its kernel using the same procedure that we had to obtain (2.265). Hence, the amplitude to stay in the state $|\uparrow\rangle(|\downarrow\rangle)$ during time

dt may be written as

$$K(x_k(\tau), dt; x_{k-1}, 0) = \langle x_{k-1}| 1 - iH_{\text{TLS}}dt/\hbar \, |x_k\rangle \,. \tag{2.293}$$

If the system remains in state $|\uparrow\rangle$ ($|\downarrow\rangle$), the amplitude will be $\exp\left(-i\frac{\epsilon dt}{2\hbar}\right)$ ($\exp\left(i\frac{\epsilon dt}{2\hbar}\right)$). In the case of a switch between the two states, the amplitude becomes $\langle\uparrow(\downarrow)| 1 - i\frac{H_{\text{TLS}}dt}{\hbar} |\downarrow(\uparrow)\rangle = i\frac{\Delta dt}{2}$. Applying this to the four states (a, b, c, d), we can find the amplitude for the double path as follows

$$\begin{aligned} &K(x_k(\tau), y_k(\tau), dt; x_{k-1}, y_{k-1}, 0) \\ &= \langle x_{k-1}, y_{k-1}| \left(1 - iH_{\text{TLS}}dt/\hbar\right)\left(1 + iH_{\text{TLS}}dt/\hbar\right) |x_k, y_k\rangle \,. \end{aligned} \tag{2.294}$$

Therefore, the amplitude to stay in the same state will be $\exp\left(-i\frac{\epsilon\xi(t)dt}{\hbar}\right)$, and for the "blips" or transitions between states, we will have $i\lambda\left(\frac{\Delta}{2}\right)dt$, where $\lambda = 0$ for $a \rightleftarrows d$ and $b \rightleftarrows c$, -1 for $a \rightleftarrows b$ and $d \rightleftarrows c$, and $+1$ for $a \rightleftarrows c$ and $b \rightleftarrows d$. These amplitudes are chosen such that, for example, the contribution to staying in state a is given by $\langle\uparrow| 1 - iH_{\text{TLS}} |\uparrow\rangle \langle\uparrow| 1 + iH_{\text{TLS}} |\uparrow\rangle = 1$ when ignoring dt^2.

To determine the total amplitude, we need to multiply the amplitude for each flip in the path taken through the four states a, b, c, and d. Considering a path that starts from a at time zero and returns to it at time t, consisting of $2n$ flips, the time it takes for the system to undergo the k-th flip is denoted as t_k. We subdivide this time interval into small partitions of dt and use the same method as in equation (2.265) to calculate the propagator for the k-th flip. By multiplying all the propagators (a total of $2n$), we obtain the propagator for the $2n$-flip path. Summing over all possible values of n will yield the probability of finding the system in state a when it started in state a.

Based on the amplitudes obtained during dt, we find that the total non-zero contribution to the amplitude after $2n$ flips will have a factor of $(-1)^n \left(\frac{\Delta}{2}\right)^{2n}$. We then have $2n$ integrals over all transitions that occur along the path. We will write this explicitly later. For now, let us derive the influence functional from equation (2.290). We express the symmetric and antisymmetric functions in equation (2.291) in the following form:

$$\chi(s) = \sum_{j=0}^{n} \eta^j \left(\theta(s - t_{2j}) - \theta(s - t_{2j+1})\right) \tag{2.295}$$

$$\xi(s) = \sum_{j=1}^{n} \zeta^j \left(\theta(s - t_{2j-1}) - \theta(s - t_{2j})\right) . \tag{2.296}$$

From the above equations, we observe that when $t_{2j} \leq t \leq t_{2j+1}$, $\chi(t)$ takes the values $\eta^j = \pm 1$ while $\xi(t) = 0$. This indicates that the system is in a diagonal state (a, d). Conversely, when $t_{2j-1} \leq t \leq t_{2j}$, $\xi(t)$ takes the values $\zeta^j = \pm 1$ while $\chi(t) = 0$. In this case, the system is in a blip state transition (b, c). We substitute these two functions into equation (2.290) to obtain

$$\mathcal{F}[x(t), y(t)] = \exp \frac{-\varphi_0^2}{\pi\hbar} \int_0^t \int_0^s ds ds' \left\{ -i\eta(s-s')\xi(s)\chi(s') + \nu(s-s')\xi(s)\xi(s') \right\}. \tag{2.297}$$

Hence, we will have

$$\begin{aligned} \mathcal{F}[\chi(t), \xi(t)] = &\exp \frac{i\varphi_0^2}{\pi\hbar} \sum_{j>0,k\geq 0} \zeta^j \eta^k \int_{t_{2j-1}}^{t_{2j}} \int_{t_{2k}}^{t_{2k+1}} ds ds' \eta(s-s') \\ &\times \exp \frac{-\varphi_0^2}{\pi\hbar} \sum_{j>0,k\geq 0} \zeta^j \zeta^k \int_{t_{2j-1}}^{t_{2j}} \int_{t_{2k-1}}^{t_{2k}} ds ds' \nu(s-s'). \end{aligned} \tag{2.298}$$

Since we have the noise and dissipation kernels functions, we can proceed with solving the time integrals. For the first one we have

$$\int_{t_{2j-1}}^{t_{2j}} \int_{t_{2k}}^{t_{2k+1}} ds ds' \eta(s-s') = \int_0^\infty d\omega J(\omega) \int_{t_{2j-1}}^{t_{2j}} \int_{t_{2k}}^{t_{2k+1}} ds ds' \sin\omega(s-s'). \tag{2.299}$$

Solving the above integral results in defining a function such that

$$Q_1(t) = \int_0^\infty d\omega \frac{J(\omega)}{\omega^2} \sin\omega t \tag{2.300}$$

We may follow the same procedure for the noise kernel $\nu(t)$ so that we have

$$\int_{t_{2j-1}}^{t_{2j}} \int_{t_{2k-1}}^{t_{2k}} ds ds' \nu(s-s') = \int_0^\infty d\omega J(\omega) \coth(\beta\hbar\omega/2) \int_{t_{2j-1}}^{t_{2j}} \int_{t_{2k-1}}^{t_{2k}} ds ds' \cos\omega(s-s'). \tag{2.301}$$

Similarly we define another function in a way that

$$Q_2(t) = \int_0^\infty d\omega \frac{J(\omega)}{\omega^2} (1 - \cos\omega t) \coth(\beta\hbar\omega/2). \tag{2.302}$$

Replacing the above functions into (2.298) we will have

$$\begin{aligned} \mathcal{F}[\chi(t), \xi(t)] = e^{\frac{i\varphi_0^2}{\pi\hbar}\left\{\sum_{j>0,k\geq 0} \zeta^j\eta^k \left(Q_1(t_{2j}-t_{2k+1}) - Q_1(t_{2j-1}-t_{2k+1}) - Q_1(t_{2j}-t_{2k}) + Q_1(t_{2j-1}-t_{2k})\right)\right\}} \\ \times e^{\frac{-\varphi_0^2}{\pi\hbar}\left\{\sum_{j=1}^{n} Q_2(t_{2j}-t_{2j-1}) + \sum_{j>0,k\geq 0, j>k} \zeta^j\zeta^k \left(Q_2(t_{2j}-t_{2k-1}) - Q_2(t_{2j-1}-t_{2k-1}) - Q_2(t_{2j}-t_{2k}) + Q_2(t_{2j-1}-t_{2k})\right)\right\}}, \end{aligned} \tag{2.303}$$

where we have used the fact that $\xi^j\xi^k = 1$ for $j = k$. Moreover, the propagator for staying at the blip ζ^j during the interval $t_{2j} - t_{2j-1}$ is $\exp -i\epsilon \int_{t_{2j-1}}^{t_{2j}} \xi(s)ds$. Thus, the contribution of n blips is accumulated in the bias factor $\exp -\frac{i\epsilon}{\hbar}\sum_j \zeta^j(t_{2j} - t_{2j-1})$ that will be multiplied to the influence functional.

Now we can find the probability of the system starting and ending in a which would be $p(t) = \langle a|\, \rho_s(t)\, |a\rangle$. Using (2.256) we will have

$$p(t) = 1 + \sum_n (-1)^n \left(\Delta/2\right)^{2n} K_n(t), \tag{2.304}$$

where

$$K_n(t) = \sum_{\eta,\zeta} \int_0^t dt_{2n} \int_0^{t_{2n}} dt_{2n-1} .... \int_0^{t_2} dt_1 F_n\left(t_1, t_2, ..., t_{2n}; \zeta_1, \zeta_2, ..., \zeta_n; \eta_1, \eta_2, ..., \eta_n\right). \tag{2.305}$$

We note that the time integrals in the above are time-ordered. One can simplify the influence functional by first defining

$$X_{jk} = Q_1(t_{2j} - t_{2k+1}) - Q_1(t_{2j-1} - t_{2k+1}) - Q_1(t_{2j} - t_{2k}) + Q_1(t_{2j-1} - t_{2k}). \tag{2.306}$$

Next, we will sum over all $\eta = \pm 1$. Since their values are limited to ± 1, the first term in (2.15.2) together with the blip amplitude can thus be written as

$$\begin{aligned}
&\sum_{\eta^k} \exp \frac{i\varphi_0^2}{\pi\hbar} \left(\sum_{j>0, k\geq 0} \eta^k \zeta^j X_{jk} \right) \times \exp -\frac{i\epsilon}{\hbar} \sum_j \zeta^j (t_{2j} - t_{2j-1}) \\
&= 2^{n-1} \prod_{k=1}^{n-1} \cos \left[\frac{\varphi_0^2}{\pi\hbar} \sum_{j=k+1} \zeta^j X_{jk} \right] \cos \left[\sum_j \zeta^j \left((t_{2j} - t_{2j-1}) \frac{\epsilon}{\hbar} - \frac{\varphi_0^2}{\pi\hbar} X_{j0} \right) \right].
\end{aligned} \tag{2.307}$$

With this in hand we may write

$$F_n\left(t_m; \zeta^m; \epsilon\right) = F_1\left(t_m\right) F_2\left(t_m; \zeta^m\right) F_3\left(t_m; \zeta^m\right) F_4\left(t_m; \zeta^m; \epsilon\right), \tag{2.308}$$

where

$$F_1 = \exp\left(\frac{-\varphi_0^2}{\pi\hbar} \sum_j S_j \right) \tag{2.309}$$

$$F_2 = \exp\left(\frac{-\varphi_0^2}{\pi\hbar} \sum_{j,k\geq 0} \zeta^j \zeta^k \Lambda_{jk}) \right) \tag{2.310}$$

$$F_3 = 2^{n-1}\prod_{k=1}^{n-1}\cos\left[\frac{\varphi_0^2}{\pi\hbar}\sum_{j=k+1}\zeta^j X_{jk}\right] \tag{2.311}$$

$$F_4 = \cos\left[\sum_j \zeta^j\left((t_{2j}-t_{2j-1})\frac{\epsilon}{\hbar}-\frac{\varphi_0^2}{\pi\hbar}X_{j0}\right)\right], \tag{2.312}$$

with

$$S_j = Q_2(t_{2j}-t_{2(j-1)}) \tag{2.313}$$

$$\Lambda_{jk} = Q_2(t_{2j}-t_{2k-1}) - Q_2(t_{2j-1}-t_{2k-1}) - Q_1(t_{2j}-t_{2k}) + Q_1(t_{2j-1}-t_{2k}). \tag{2.314}$$

It is worth noting a few remarks about the relations presented above. F_1 represents intrablip correlations since it arises from the term with $k = j$ in $\zeta^j\zeta^k$. F_2 denotes interblip correlations, representing correlations between ζ^j and ζ^k for $j \neq k$. On the other hand, F_3 and F_4 capture correlations between the entire blip sequence and the k-th sojourn.

The equations presented, including equation (2.304), provide essential insights into the dynamics of the spin-boson model. However, obtaining an analytical solution for the probability function given by equation (2.304) is challenging without suitable approximations. One successful approach is to employ the Noninteracting Blip Approximation (NIBA). This approximation assumes that the time intervals associated with blips are much smaller than the time interval for sojourns, implying that the system predominantly resides in diagonal states. By making this assumption, the influence functional can be significantly simplified by neglecting many interaction terms between blips and sojourns. In the following sections, we will provide a detailed exposition of NIBA, focusing on its application to derive analytical solutions for heat currents.

2.16 Heat currents

To calculate the heat transport between the system and the bath, we employ the functional method and utilize the standard definition of heat. This definition involves measuring the change in energy of the bath degrees of freedom at the initial and final times of the evolution [44, 8]. In essence, we perform two projective energy measurements on the reservoir, one at $t = 0$ and the other at the final time t. The difference between these measurements corresponds to the heat exchanged between the system and the bath during the evolution. By repeating this process multiple times, we can construct the probability density function (PDF) for the exchanged heat.

To investigate non-equilibrium heat currents, we consider a system interacting with two heat baths at different temperatures. Additionally, we assume no initial correlations between the system and the baths, leading to the following initial density matrix for the combined system-bath configuration:

$$\rho(0) = \rho_S(0) \otimes_\alpha \rho_\alpha^{\text{th}}, \tag{2.315}$$

where ρ_α^{th} denotes the thermal state of the two baths with temperature $\beta_\alpha = (k_b T_\alpha)^{-1}$ for $\alpha = \{1,2\}$.

To construct the PDF for the heat current, we introduce two projection operators, P_1^α and P_2^α, which correspond to measurements on the α-th bath degrees of freedom. P_1^α measures the α-th bath at the initial time ($t = 0$), while P_2^α measures the same bath at time t. With these projection operators, the PDF for the heat current can be expressed as follows

$$P(Q_\alpha, t) = \sum_{e_1^\alpha, e_2^\alpha} \delta(Q_\alpha + e_1^\alpha - e_2^\alpha) p[e_2^\alpha; e_1^\alpha] p[e_1^\alpha], \tag{2.316}$$

where $p[e_1^\alpha]$ is the probability of finding the energy e_1^α, and $p[e_2^\alpha; e_1^\alpha]$ is the conditional probability of finding the energy e_2^α given that the α-th bath was initially in the state with energy e_1^α. These probabilities can be expressed in terms of the density matrix and the unitary time evolution operators $U(t)$ generated by the total Hamiltonian $H = H_S + H_{B\alpha} + H_{I_\alpha}$ as

$$[e_2^\alpha; e_1^\alpha] p[e_1^\alpha] = \text{Tr}\left[P_2^\alpha U(t) P_1^\alpha \rho(0) P_1^\alpha U^\dagger(t) P_2^\alpha\right]. \tag{2.317}$$

To find the average heat current, we introduce the generating function (GF) $G_\alpha(\nu, t)$ which will generate all the moments of heat currents. It is defined such that

$$G_\alpha(\nu, t) = \int_{-\infty}^{\infty} dQ_\alpha P(Q_\alpha, t) e^{iQ_\alpha \nu_\alpha}. \tag{2.318}$$

Using the GF, we can find the average heat current $\langle Q_\alpha(t) \rangle$ such that

$$\langle Q_\alpha(t) \rangle = -i \frac{dG_\alpha(\nu, t)}{d\nu}\bigg|_{\nu=0}. \tag{2.319}$$

To proceed further we first use Eq.(2.316) to write

$$G(\nu_\alpha, t) = \sum_{e_1^\alpha, e_2^\alpha} p[e_2^\alpha; e_1^\alpha] p[e_1^\alpha] e^{i\nu_\alpha (e_2^\alpha - e_1^\alpha)}. \tag{2.320}$$

Due to the initial state of the total system being a product state, the projection operators commute with the initial state. Therefore, we can write the generating function as

$$G(\nu_\alpha, t) = \mathrm{Tr}\left[U^\dagger(t) e^{i\nu_\alpha H_\alpha} U e^{-i\nu_\alpha H_\alpha} \rho(0)\right], \tag{2.321}$$

where we have used that $\sum_{e_j^\alpha} P_j^\alpha e^{\pm i\nu_\alpha e_j^\alpha} = e^{\pm i\nu_\alpha H_{\mathrm{B}_\alpha}}$. To determine the GF, we performed simultaneous measurements on the α-th bath. The final measurement result can be expressed as $\mathrm{Tr}\left[P_{21}P_{22}U(t)P_{11}P_{12}\rho(0)P_{11}P_{12}U^\dagger(t)P_{21}P_{22}\right]$, where P_{ij} are the projection operators corresponding to the i-th energy of the j-th bath. Based on this, we can define the probability density function (PDF) as follows

$$\begin{aligned} P(Q_1, Q_2, t) = &\sum_{e_{11}, e_{12}, e_{21}, e_{22}} \delta(e_{11} - e_{12} + Q_1)\delta(e_{21} - e_{22} + Q_2) \\ &\times \mathrm{Tr}\left[P_{21}P_{22}U(t)P_{11}P_{12}\rho(0)P_{11}P_{12}U^\dagger(t)P_{21}P_{22}\right]. \end{aligned} \tag{2.322}$$

Thus, we will have

$$G(\vec{\alpha}, t) = \mathrm{Tr}\left[U^\dagger(t) e^{i(\nu_1 H_1 + \nu_2 H_2)} U e^{-i(\nu_1 H_1 + \nu_2 H_2)} \rho(0)\right], \tag{2.323}$$

where $\vec{\nu} = \{\nu_1, \nu_2\}$. In this way the heat current would be

$$\langle Q_\alpha(t)\rangle = -i \frac{dG_(\nu, t)}{d\nu_\alpha}\bigg|_{\vec{\nu}=0}, \tag{2.324}$$

which would be similar to what we had in (2.319).

Finding the GF in (2.323) is the main purpose of this section because it will help us calculate the heat currents at the end. Eq. (2.323) can be written in terms of the Feynman-Vernon path integral. First, we define

$$\rho(0) = \rho_{\mathrm{S}_1}(0) \otimes \rho_{\mathrm{S}_2}(0) \otimes \rho_L^{\mathrm{th}} \otimes \rho_R^{\mathrm{th}}, \tag{2.325}$$

where R and L indicate the right and left baths. With this definition of the initial state of the total system, we can find the Feynman-Vernon representation of the GF using the same procedure of the previous sections. Indeed, the only difference is the counting terms coming from the energy measurement. This term can still be dealt with using the Euclidean action technique that we employed to find the density operator of the bath in (2.287). Moreover, we need to take into account that we have now two qubits as our system. Therefore, one can

write the GF as

$$G(\vec{\alpha},t)=\int dX_1dX_2dY_1dY_2\mathbf{E}(X_1,X_2;Y_1,Y_2)F_{\vec{v}}(X_1,X_2,Y_1,Y_2), \tag{2.326}$$

where

$$\mathbf{E}(X_1,X_2;Y_1,Y_2)=e^{\frac{i}{\hbar}(S_0[X_1]+S_0[X_2]+S_{0I}[X_1,X_2])-\frac{i}{\hbar}(S_0[Y_1]+S_0[Y_2]+S_{0I}[Y_1,Y_2])}. \tag{2.327}$$

$X_{1,2}$ and $Y_{1,2}$ denote the forward and backward paths of the qubits and $\mathcal{F}_{\vec{v}}(X_1,X_2,Y_1,Y_2)$ is the influence functional. S_{0I} is the interaction action between the two qubits. To write this action we look at the interaction term in the Hamiltonian which is $\sigma_{1z}\otimes\sigma_{2z}$. Using the same method that we used to obtain the action for the free qubit in the previous section we can write the action of the interacting part such that

$$S_{0I}=\frac{E_m\varphi_0^2}{2}\int ds\left[\chi_1(s)\xi_2(s)+\chi_2(s)\xi_1(s)\right], \tag{2.328}$$

where we have $\chi_{1,2}=\pm1$ for sojourns and 0 for blips and $\xi_{1,2}=\pm1$ for blips and 0 for sojourns. The influence functional can also be written as

$$\mathcal{F}_{\vec{v}}(X_1,X_2,Y_1,Y_2)=e^{\frac{i}{\hbar}\left(S^L_{i,\alpha_L}[X_1,Y_1]+S^R_{i,\alpha_R}[X_2,Y_2]\right)}e^{\frac{-1}{\hbar}\left(S^L_{r,\alpha_L}[X_1,Y_1]+S^R_{r,\alpha_R}[X_2,Y_2]\right)}, \tag{2.329}$$

where we have

$$\begin{aligned}S^{R/L}_{r,\alpha_{R/L}}[X^R,Y^L]=\int_{t_i}^{t_f}dt\Bigg\{\int_{t_i}^{t}ds\left(X^R_tX^R_s+Y^L_tY^L_s\right)k_r^{R/L}(t-s)\\ -X^R_tY^L_sk_r^{R/L}(t-s+\alpha_{R/L})-X^R_sY^L_tk_r^{R/L}(t-s-\alpha_{R/L})\Bigg\},\end{aligned} \tag{2.330}$$

and for the imaginary part we obtain

$$\begin{aligned}S^{R/L}_{i,\alpha_{R/L}}[X^R,Y^L]=\int_{t_i}^{t_f}dt\int_{t_i}^{t}ds\Bigg\{\left(X^R_tX^R_s-Y^L_tY^L_s\right)k_i^{R/L}(t-s)\\ +X^R_tY^L_sk_i^{R/L}(t-s+\alpha_{R/L})-X^R_sY^L_tk_i^{R/L}(t-s-\alpha_{R/L})\Bigg\},\end{aligned} \tag{2.331}$$

where the kernels are

$$k_i^{R/L}(t-s)=\int d\omega J_{R/L}(\omega)\sin\left(\omega_{R/L}(t-s)\right) \tag{2.332}$$

$$k_r^{R/L}(t-s)=\int d\omega J_{R/L}(\omega)\coth\left(\frac{\hbar\omega_{R/L}\beta_{R/L}}{2}\right)\cos\left(\omega_{R/L}(t-s)\right). \tag{2.333}$$

To find the expression for the GF, we again use the same method of the previous sections. First we define

$$\begin{aligned}\chi_t &= X_t + Y_t \\ \xi_t &= X_t - Y_t.\end{aligned} \tag{2.334}$$

To calculate the real and imaginary parts of the actions as expressed in equations (2.16) and (2.16), we need to perform double integrals over interacting paths at different times. As mentioned earlier, these paths can be either blips or sojourns. Additionally, in order to obtain analytical solutions, we will make use of the Noninteracting Blip Approximation (NIBA). The assumptions underlying NIBA are as follows

1. The blips time interval Δt_B is much smaller than the sojourns Δt_S. In the other words $\Delta t_B \ll \Delta t_S$.

2. Bath correlations decay over times much shorter than the sojourn interval.

Under these two assumptions the only non-zero contribution of paths interaction could be listed as

1. t and s are in the same blip interval.

2. t and s are in the same sojourn interval.

3. t is in a sojourn and s is in an adjacent blip interval.

4. t and s are both in sojourn intervals separated by one blip.

Furthermore, we need to make an additional assumption regarding the system interaction action (2.328). It is worth noting that the integral in (2.328) considers both qubit paths simultaneously. However, each qubit can independently be in a blip interval or a sojourn. If the two qubits are in the same state (blip or sojourn), the action will be unity, resulting in no contribution. Therefore, the non-zero contributions arise from the interactions between qubits in different states.

For example, if the first qubit is in a sojourn state during the time interval Δt_S, the second qubit may have transition between m sojourns ($\Delta t'_S$) and n blips ($\Delta t'_B$) within this interval, satisfying $m\Delta t'_S + n\Delta t'_B = \Delta t_S$. As mentioned before, we assume that the blip intervals are much smaller than the sojourns.

In practice, we can separate the interaction between sojourns and blips into different orders. In the first order, we consider only one blip in the path of the second qubit. The

second order introduces an additional blip, and so on for subsequent orders. To establish a more rigorous framework, we define the following relations:

$$\chi_{1,2}(t) = \sum_{i=0} \eta_i^{1,2} \left[\theta(t_{2i+1}^{1,2} - t) - \theta(t_{2i}^{1,2} - t)\right] \tag{2.335}$$

$$\xi_{1,2}(t) = \sum_{i=1} \zeta_i^{1,2} \left[\theta(t_{2i}^{1,2} - t) - \theta(t_{2i-1}^{1,2} - t)\right]. \tag{2.336}$$

Using the above relations we may write the integral in (2.328) such that

$$S_{0I} = \frac{E_m \varphi_0^2}{2} \int ds \, [\chi_1(s)\xi_2(s) + \chi_2(s)\xi_1(s)] = \frac{E_m \varphi_0^2}{2} \left(\sum_{i,k} \Delta_{2i}^2 \zeta_i^2 f_{ik} \eta_k^1 + \sum_{i,k} \Delta_{2i}^1 \zeta_i^1 f_{ik} \eta_k^2 \right). \tag{2.337}$$

$\Delta_{2i}^{1,2} = t_{2i}^{1,2} - t_{2i-1}^{1,2}$ is the blip interval in the first or the second qubit. f_{ik} takes care of the number of existing blips on the first and second qubits. For the first order approximation stating that there is only one blip interacting with the sojourn, $f_{ik} = \delta_{ik}$. Therefore, we can write

$$S_{0I} = \frac{E_m \varphi_0^2}{2} \sum_i \left(\Delta_{2i}^2 \zeta_i^2 \eta_i^1 + \Delta_{2i}^1 \zeta_i^1 \eta_i^2 \right). \tag{2.338}$$

Now we may use the assumptions of NIBA and the four mentioned regimes of non-zero contributions to find the the free particles action and the influence functional. This is pretty much the same calculations that we did in previous sections. Therefore, one can write the GF such that

$$\begin{aligned} G(\vec{\alpha}, t) = \sum_n^\infty \left(\frac{\Delta}{2}\right)^{2n} \int dt_1^1 ... dt_{2n}^1 \int dt_1^2 ... dt_{2n}^2 \\ \times \sum_{\substack{\eta_1^1,...,\eta_n^1=\pm 1 \\ \eta_1^2,...,\eta_n^2=\pm 1 \\ \zeta_1^1,...,\zeta_n^1=\pm 1 \\ \zeta_1^2,...,\zeta_n^2=\pm 1}} \exp\left(\frac{-i}{\hbar}\epsilon_1 \sum_i^n \zeta_i^1 \Delta_{2i}^1\right) \exp\left(\frac{-i}{\hbar}\epsilon_2 \sum_i^n \zeta_i^2 \Delta_{2i}^2\right) \\ \times e^{\left(\frac{i}{\hbar}\sum_{j=\substack{(R,1)\\(L,2)}} \sum_{i=0}^{n-1} \eta_i^j \zeta_{i+1}^j X_+^j(\alpha_j, \Delta_{2i+2}^j) + \sum_{i=1}^n \eta_i^j \zeta_i^j X_-^j(\alpha_j, \Delta_{2i}^j) + \sum_{i=0}^{n-1} \eta_i^j \eta_{i+1}^j \Lambda^j(\alpha_j, \Delta_{2i+2}^j) + R^j(\alpha_j, \Delta_{2i}^j) + B^j(\alpha_j, \Delta_{2i}^j)\right)} \\ \times e^{\left(\frac{-i}{\hbar} U \sum_{i=1}^n \left(\Delta_{2i}^2 \zeta_i^2 \eta_i^1 + \Delta_{2i}^1 \zeta_i^1 \eta_i^2\right)\right)} \\ \times e^{\left(\frac{-1}{\hbar}\sum_{j=\substack{(R,1)\\(L,2)}} \sum_{i=0}^{n-1} \eta_i^j \zeta_{i+1}^j F_+^j(\alpha_j, \Delta_{2i+2}^j) + \sum_{i=1}^n \eta_i^j \zeta_i^j F_-^j(\alpha_j, \Delta_{2i}^j) + \sum_{i=0}^{n-1} \eta_i^j \eta_{i+1}^j \Sigma^j(\alpha_j, \Delta_{2i+2}^j) + C^j(\alpha_j, \Delta_{2i}^j) + D^j(\alpha_j, \Delta_{2i}^j)\right)}, \end{aligned} \tag{2.339}$$

where $U = \frac{E_m \varphi_0^2}{2}$. Moreover, all the other functions are as follows

$$
\begin{aligned}
X^j_{\pm}(\alpha_j, \Delta^j_B) =& \frac{1}{2}\int_0^\infty d\omega \frac{J(\omega)}{\omega^2} \sin\left(\omega\Delta^j_B\right)\left(1 \pm \cos(\omega\alpha_j)\right)\\
F^j_{\pm}(\alpha_j, \Delta^j_B) =& \pm\frac{1}{2}\int_0^\infty d\omega \frac{J(\omega)}{\omega^2} \sin\left(\omega\Delta^j_B\right)\sin(\omega\alpha_j)\coth\left(\frac{\hbar\omega\beta^j}{2}\right)\\
\Lambda^j(\alpha_j, \Delta^j_B) =& -\frac{1}{2}\int_0^\infty d\omega \frac{J(\omega)}{\omega^2} \cos\left(\omega\Delta^j_B\right)\sin(\omega\alpha_j)\\
\Sigma^j(\alpha_j, \Delta^j_B) =& \frac{1}{2}\int_0^\infty d\omega \frac{J(\omega)}{\omega^2} \cos\left(\omega\Delta^j_B\right)\left(\cos(\omega\alpha_j) - 1\right)\coth\left(\frac{\hbar\omega\beta^j}{2}\right)\\
B^j(\alpha_j, \Delta^j_B) =& \frac{1}{2}\int_0^\infty d\omega \frac{J(\omega)}{\omega^2} \sin(\omega\alpha_j)\\
C^j(\alpha_j, \Delta^j_B) =& \frac{1}{2}\int_0^\infty d\omega \frac{J(\omega)}{\omega^2} \left(\cos(\omega\alpha_j) + 1\right)\left(1 - \cos\left(\omega\Delta^j_B\right)\right)\coth\left(\frac{\hbar\omega\beta^j}{2}\right)\\
D^j(\alpha_j, \Delta^j_B) =& \frac{1}{2}\int_0^\infty d\omega \frac{J(\omega)}{\omega^2} \left(1 - \cos(\omega\alpha_j)\right)\coth\left(\frac{\hbar\omega\beta^j}{2}\right)\\
R^j(\alpha_j, \Delta^j_B) =& -\Lambda^j(\alpha_j, \Delta^j_B).
\end{aligned}
\tag{2.340}
$$

The GF in (2.339) can be written in terms of the transport matrix. To that end, we first write (2.339) in terms of cosh functions. Shifting the sum indices to start at $i = 1$ for all the summations, we can sum over all ζ^j so that we will have

$$
\begin{aligned}
G(\vec{\alpha}, t) = \sum_n^\infty \left(\frac{\Delta}{2}\right)^{2n} \int dt^1_1 ... dt^1_{2n} \int dt^2_1 ... dt^2_{2n} \sum_{\substack{\eta^1_1,...,\eta^1_n=\pm1\\ \eta^2_1,...,\eta^2_n=\pm1}}\\
\prod_j\prod_{i=0}^n 2\cosh\frac{i}{\hbar}\Big\{\epsilon^j\Delta^j_{2i} + \eta^j_{i-1}\left[X^j_+(\alpha_j, \Delta^j_{2i}) + iF^j_+(\alpha_j, \Delta^j_{2i})\right]\\
+\eta^j_i\left[X^j_-(\alpha_j, \Delta^j_{2i}) + iF^j_-(\alpha_j, \Delta^j_{2i})\right] - U\eta^{\bar{j}}_i\Delta^{\bar{j}}_{2i}\Big\}\\
\times e^{\frac{i}{\hbar}\left(\eta^j_{i-1}\eta^j_i\left[\Lambda^j(\alpha_j,\Delta^j_{2i}) + i\Sigma^j(\alpha_j,\Delta^j_{2i})\right] + R^j(\alpha_j,\Delta^j_{2i}) + B^j(\alpha_j,\Delta^j_{2i}) + i\left(C^j(\alpha_j,\Delta^j_{2i}) + D^j(\alpha_j,\Delta^j_{2i})\right)\right)},
\end{aligned}
\tag{2.341}
$$

where $\bar{j} \neq j$. To write the above relation in terms of the transfer matrix, we should first find the 16 matrix elements by summing over all η^j. Rewriting the expression we will have

$$
\begin{aligned}
G(\vec{\alpha}, t) = \sum_{n=0}^\infty \left(\frac{\Delta}{2}\right)^{2n} \int dt^1_1 ... dt^1_{2n} \int dt^2_1 ... dt^2_{2n} \sum_{\substack{\eta^1_1,...,\eta^1_n=\pm1\\ \eta^2_1,...,\eta^2_n=\pm1}}\\
\prod_j\prod_{i=0}^n 2\cosh\frac{i}{\hbar}\Big\{\epsilon^j\Delta^j_{2i} + \left(\frac{\eta^j_{i-1} + \eta^j_i}{2}\right)\left[X^j_+ + X^j_- + i\left(F^j_+ + F^j_-\right)\right]\\
+\left(\frac{\eta^j_{i-1} - \eta^j_i}{2}\right)\left[X^j_+ - X^j_- + i\left(F^j_+ - F^j_-\right)\right] - U\eta^{\bar{j}}_i\Delta^{\bar{j}}_{2i}\Big\}
\end{aligned}
$$

$$\times e^{\frac{-i}{\hbar}\left(\eta_{i-1}^{j}\eta_{i}^{j}\left[\Lambda^{j}(\alpha_j,\Delta_{2i}^{j})+i\Sigma^{j}(\alpha_j,\Delta_{2i}^{j})\right]+R^{j}(\alpha_j,\Delta_{2i}^{j})+B^{j}(\alpha_j,\Delta_{2i}^{j})+i\left(C^{j}(\alpha_j,\Delta_{2i}^{j})+D^{j}(\alpha_j,\Delta_{2i}^{j})\right)\right)}. \tag{2.342}$$

To consider all possible transition states of the two qubits at each interval, we need to account for all combinations of η_i^j values. For example, the first matrix element can be constructed by assuming the transition $(1,1) \rightarrow (1,1)$. This means that both qubits start and end with a sojourn, represented by $\eta_i^j = 1$. By substituting this transition into the expression, we observe that the asymmetric term vanishes, resulting in the first element of the transfer matrix $\mathbf{M}$ as follows

$$\begin{aligned} M_{(1,1,1,1)}\left(\Delta_{2i}\right) = &\cosh\frac{i}{\hbar}\left(\epsilon^1\Delta_{2i}^1+\left[X_+^1+X_-^1+i\left(F_+^1+F_-^1\right)\right]-U\Delta_{2i}^2\right)\\ &\times\cosh\frac{i}{\hbar}\left(\epsilon^2\Delta_{2i}^2+\left[X_+^2+X_-^2+i\left(F_+^2+F_-^2\right)\right]-U\Delta_{2i}^1\right)\\ &\times e^{\frac{i}{\hbar}\left(\left[\Lambda^1(\alpha_1,\Delta_{2i}^1)+i\Sigma^1(\alpha_1,\Delta_{2i}^1)\right]+R^1(\alpha_1,\Delta_{2i}^1)+B^1(\alpha_1,\Delta_{2i}^1)+i\left(C^1(\alpha_1,\Delta_{2i}^1)+D^1(\alpha_1,\Delta_{2i}^1)\right)\right)}\\ &\times e^{\frac{i}{\hbar}\left(\left[\Lambda^2(\alpha_2,\Delta_{2i}^2)+i\Sigma^2(\alpha_2,\Delta_{2i}^2)\right]+R^2(\alpha_2,\Delta_{2i}^2)+B^2(\alpha_2,\Delta_{2i}^2)+i\left(C^2(\alpha_2,\Delta_{2i}^2)+D^2(\alpha_2,\Delta_{2i}^2)\right)\right)}. \end{aligned} \tag{2.343}$$

Proceeding with this approach, we may write all the other transport matrix elements which would shape a 4×4 matrix. Next we assume that at the beginning, we start with a sojourn state $(1,0,0,0)$ and at the end of the process, we sum over all possible states (trace) $(1,1,1,1)$. Therefore, one may write the GF in a matrix form such that

$$G(\vec{\alpha},t) = \prod_j \begin{pmatrix}1 & 1 & 1 & 1\end{pmatrix} \sum_{n=0}^{\infty}\left(\frac{\Delta}{2}\right)^{2n}\int dt_1^j...dt_{2n}^j \prod_{i=0}^{n}\mathbf{M}(\alpha_j,\Delta_{2i}^j) \begin{pmatrix}1\\0\\0\\0\end{pmatrix}. \tag{2.344}$$

To find the GF, we will Laplace transform the above equation. This could help us to do the summation and write the transfer matrix in terms of its eigenvalues. Thus, we will have

$$G(\vec{\alpha},\lambda) = \prod_j \begin{pmatrix}1 & 1 & 1 & 1\end{pmatrix} \sum_{n=0}^{\infty}\left(\frac{\Delta}{2}\right)^{2n}\int_0^{\infty}e^{-\lambda t}dt\int dt_1^j...dt_{2n}^j \prod_{i=0}^{n}\mathbf{M}(\alpha_j,\Delta_{2i}^j) \begin{pmatrix}1\\0\\0\\0\end{pmatrix}. \tag{2.345}$$

At this point, we encounter a limitation in our approach. In equation (2.343), we observe that the interaction term inside the coth function depends on the time interval of the second

qubit. This arises due to the approximations we made regarding how the blips and sojourns of one qubit interact with the other qubit (equation (2.338)). As a result, while it is possible to perform the Laplace transformation, the resulting steady state and subsequent heat currents become unphysical.

Specifically, the steady state density matrix should have a unit trace. However, after performing the Laplace transformation and setting the counting fields to zero ($\alpha_j = 0$), the generating function does not become equal to 1. This implies that the trace of the steady state density matrix will not be unity. Furthermore, the steady state heat currents become time-dependent. Therefore, we conclude that NIBA and the approximations made to derive equation (2.338) fail to produce a physically valid result.

It is worth noting that it is possible to obtain analytical solutions by removing one of the qubits [8]. However, for the case of two interacting qubits, finding analytical solutions using NIBA remains a subject of interesting future research.

2.17 Conclusions

In this chapter, we began by discussing the quantization of LC circuits and introduced the Caldeira-Leggett model to incorporate dissipation. This model replaces the resistor in the circuit with a large number of series LC circuits, allowing us to study the heat current between two overdamped quantum harmonic oscillators coupled to local thermal baths. Importantly, we derived closed analytical expressions for the heat current that account for both quantum and classical contributions, without resorting to weak coupling or Markovian approximations.

Next, we explored the nonlinear dynamics of two interacting qubits coupled to baths at different temperatures. We introduced superconducting qubits and discussed their implementation using Josephson junctions. To study the heat currents in this setup, we employed Feynman path integrals and described the qubit dynamics in terms of blips and sojourns. However, finding closed analytical solutions for the heat currents in this case remains a challenging task. While analytical expressions for heat currents in a reduced system of one qubit are possible [8], the case of two or more interacting qubits fails to yields physical results and can be a subject to the future study.

Overall, this chapter has provided a comprehensive exploration of heat transport in quantum systems, ranging from harmonic oscillators to interacting qubits. While analytical solutions have been obtained in certain cases, the study of heat currents in more complex systems

remains an active area of research, often relying on numerical methods to gain insights into the thermal behavior of these systems.

Chapter 3

Dynamical Casimir effect and refrigeration

3.1 Introduction

The objective of this chapter is to develop an autonomous quantum refrigerator, consisting of two cavities connected by a SQUID (Superconducting Quantum Interference Device). Similar to its classical counterpart, the quantum refrigerator is an engine that can cool down the cold bath while heating up the hot bath by absorbing work. Our goal is to demonstrate that our setup can exhibit this behavior in the appropriate regime.

This setup is similar to previous studies on the dynamical Casimir effect [34, 116] and transmission lines interrupted by SQUIDs [117, 37, 76, 46, 109, 12]. As mentioned in the previous chapter, a SQUID is a highly sensitive device used for measuring magnetic fields [21]. It consists of two Josephson junctions, which are superconducting devices that allow electrical current to flow without resistance. The two junctions are connected in a loop, with a thin insulating barrier between two superconducting wires. When a magnetic field passes through the loop, it induces a change in the superconducting current, which can be measured as a voltage across the junctions, enabling precise detection of magnetic fields.

In our setup, the cavities are represented by a large number of parallel LC circuits. Each cavity consists of identical inductances $L_0^{r/l}$ and capacitors $C_0^{r/l}$. The primary variables used to describe the cavities are the node flux variables $\Phi_n^{r/l}$ associated with each node in the cavity. The SQUID is modeled by two parallel Josephson junctions with the same energy E_J and capacitance C_J. The SQUID is characterized by the node flux at $x = 0$, denoted as Φ_0, and the phase drop $2f$ related to the self-inductance L of the SQUID. This phase drop can also be influenced by an external flux.

The resistors $R^{l/r}$ located at each end of the setup play the role of heat baths connected

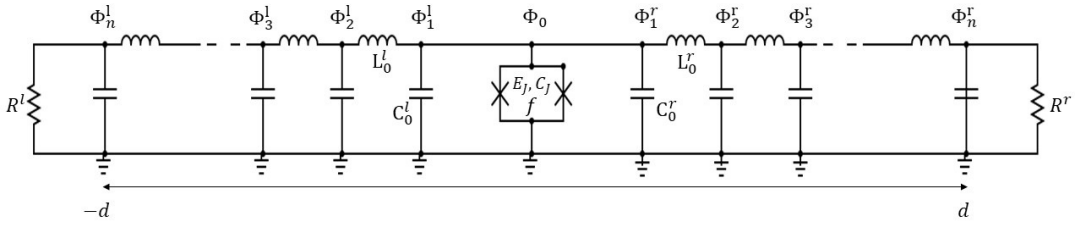

FIGURE 3.1: The Schematic of the model.

to the cavities, to which we can assign temperatures later on. It is important to note that the resistors can also be replaced by the Caldeira-Leggett representation of the bath, which essentially corresponds to an infinite cavity with the same structure as described above.

3.2 Lagrangian of the system of cavities and the SQUID

To write the Lagrangian of the circuit of the cavities and SQUID, we use the node flux representation. First we describe the Lagrangian of the two cavities.

$$L_c = \left(\frac{\hbar}{2e}\right)^2 \frac{1}{2}\sum_i \left\{ \Delta x C_0^l \left(\dot{\Phi}_i^l\right)^2 + \frac{1}{L_0^l \Delta x}\left(\Phi_{i+1}^l - \Phi_i^l\right)^2 \right\} + \left(\frac{\hbar}{2e}\right)^2 \frac{1}{2}\sum_i \left\{ \Delta x C_0^r \left(\dot{\Phi}_i^r\right)^2 + \frac{1}{L_0^r \Delta x}\left(\Phi_{i+1}^r - \Phi_i^r\right)^2 \right\}. \tag{3.1}$$

In the continuum limit of $\Delta x \to 0$ it can be written as

$$L_c = \left(\frac{\hbar}{2e}\right)^2 \frac{C_0^l}{2}\int_{-L_1}^{0} (\dot{\Phi}^2 - v_l^2 \Phi'^2) dx + \left(\frac{\hbar}{2e}\right)^2 \frac{C_0^r}{2}\int_{0}^{L_2} (\dot{\Phi}^2 - v_r^2 \Phi'^2) dx. \tag{3.2}$$

where $\nu_{l/r} = 1/\sqrt{L_0^r C_0^r}$. We notice that C_0 and L_0 have the units of $[C_J]/[x]$ and $[L]/[x]$, or in the other words they are capacitance and inductance per unit length. Next we consider the Lagrangian of the SQUID that is written as

$$L_s = \left(\frac{\hbar}{2e}\right)^2 \frac{C_J}{2}(\dot{\Phi}_0 - \dot{f})^2 + \left(\frac{\hbar}{2e}\right)^2 \frac{C_J}{2}(\dot{\Phi}_0 + \dot{f})^2 + E_J \cos(\Phi_0 - f) + E_J \cos(\Phi_0 + f) - \left(\frac{\hbar}{2e}\right)^2 \frac{1}{2L}\left(4f^2 + 8\frac{M}{L_{ext}} f f_{ext}\right). \tag{3.3}$$

The term $\frac{M}{L_{\text{ext}}}$ represents the presence of an external circuit with an inductance L_{ext}. This external circuit is magnetically coupled to the SQUID through a mutual inductance M and it introduces an external flux f_{ext}.

Let us write the equation of motion for the total Lagrangian $L = L_c + L_s$, assuming $\nu_l =$

$v_r = v$. We can redefine the following parameters: $C_0^l = C_0^r = \left(\frac{\hbar}{2e}\right)^2 C_0$, $C_J = \left(\frac{\hbar}{2e}\right)^2 C_J$, and $E_L = \left(\frac{\hbar}{2e}\right)^2 \frac{1}{2L}$. Therefore, the equations of motion become:

$$\ddot{\Phi} - v^2\Phi'' = 0 \tag{3.4}$$

$$2\left(\frac{\hbar}{2e}\right)^2 C_J\ddot{\Phi}_0 - \left(\frac{\hbar}{2e}\right)^2 C_0 v^2(\Phi'_{0+} - \Phi'_{0-}) + 2E_J\cos(f)\Phi_0 = 0 \tag{3.5}$$

$$\left(\frac{\hbar}{2e}\right)^2 C_J\ddot{f} + E_J\cos\Phi_0\sin f + E_L\left(f + \frac{M}{L_{ext}}f_{ext}\right) = 0. \tag{3.6}$$

As we can observe, the above equations represent two coupled non-linear oscillators. To simplify the analysis, we assume that $\Phi_0 \ll 1$, which corresponds to the Transmon condition $E_J \gg E_{C_J}$ discussed in Chapter 2. Under this condition, the last two equations decouple, and the effective Lagrangian for the SQUID and cavities can be written as follows

$$L_{sys} = L_c + \left(\frac{\hbar}{2e}\right)^2 C_J\dot{\Phi}_0^2 - E_J\Phi_0^2\cos f. \tag{3.7}$$

In a more unified form this Lagrangian can be written as

$$L_{sys} = \left(\frac{\hbar}{2e}\right)^2 \frac{C_0}{2}\int_{-L_1}^{L_2}\left[(1 + \frac{2C_J}{C_0}\delta(x))\dot{\Phi}^2 - v^2\Phi'^2 + 2\frac{E_J}{\left(\frac{\hbar}{2e}\right)^2 C_0}\delta(x)\cos(\Phi)\cos(f)\right]dx, \tag{3.8}$$

where the equation of motion for f reads

$$\left(\frac{\hbar}{2e}\right)^2 C_J\ddot{f} + E_J\sin f + E_L\left(f + \frac{M}{L_{ext}}f_{ext}\right) = 0. \tag{3.9}$$

where for small values of f will describe a harmonic oscillator. We can solve equation of motion (3.4) by separation of variables. This means that we can write

$$\Phi(x,t) = \sum_n \phi(t)\psi_n(x,t) \tag{3.10}$$

where $\psi_n(x)$ is an instantaneous basis satisfying the bellow boundary conditions:

$$\psi_n'' + k_n^2(t)\psi_n = 0 \tag{3.11}$$

$$\psi'(-L_1) = \psi'(L_2) = 0 \tag{3.12}$$

$$\psi_n'(0^+) - \psi_n'(0^-) = \frac{2}{v^2}(-\frac{C_J v^2 k_n^2}{C_0} + \frac{E_J}{\left(\frac{\hbar}{2e}\right)^2 C_0}\cos f)\psi_n. \tag{3.13}$$

Therefore, plugging (3.10) into the equation (3.4) we will have

$$\ddot{\phi}_n\psi_n(x) - v^2\phi_n(t)\psi_n''(x) = 0. \tag{3.14}$$

To rewrite the Lagrangian in terms of the new variables, we first find the time and position derivatives of $\Phi(x,t)$ such that

$$\dot{\Phi}(x,t) = \sum_n \dot{\phi}_n\psi_n + \phi_n\dot{\psi} \tag{3.15}$$

$$\Phi'(x,t) = \sum_n \phi_n\psi_n' \tag{3.16}$$

Consequently, we can obtain

$$\dot{\Phi}^2(x,t) = \sum_{n,m} \dot{\phi}_n\dot{\phi}_m\psi_n\psi_m + \sum_{n,m}\phi_n\phi_m\dot{\psi}_n\dot{\psi}_m + 2\sum_{n,m}\dot{\phi}_n\phi_m\psi_n\dot{\psi}_m \tag{3.17}$$

$$\Phi'^2(x,t) = \sum_{mn}\phi_n\phi_m\psi_n'\psi_m' \tag{3.18}$$

We then replace these terms inside the Lagrangian and from the first term we will have

$$\begin{aligned}\left(\frac{\hbar}{2e}\right)^2 C_0\int_{-L_1}^{L_2}(1+2C_J/C_0\delta(x))\dot{\Phi}^2 =& \left(\frac{\hbar}{2e}\right)^2 C_0\sum_{n,m}\dot{\phi}_n\dot{\phi}_m\int_{-L_1}^{L_2}(1+2C_J/C_0\delta(x))\psi_n\psi_m \\ &+\left(\frac{\hbar}{2e}\right)^2 C_0\sum_{n,m}\phi_n\phi_m\int_{-L_1}^{L_2}(1+2C_J/C_0\delta(x))\dot{\psi}_n\dot{\psi}_m \\ &+2\left(\frac{\hbar}{2e}\right)^2 C_0\sum_{n,m}\dot{\phi}_n\phi_m\int_{-L_1}^{L_2}(1+2C_J/C_0\delta(x))\psi_n\dot{\psi}_m.\end{aligned} \tag{3.19}$$

To simplify above equations further, we define the inner product as

$$\frac{1}{d}\int_{-L_1}^{L_2}(1+2C_J/C_0\delta(x))\psi_n\psi_m = \delta_{mn}, \tag{3.20}$$

where $d = L_1 + L_2$ is length of the system (This is added to make δ function dimensionless). Applying this to the first term in the Lagrangian we obtain

$$\begin{aligned}\left(\frac{\hbar}{2e}\right)^2 C_0\int_{-L_1}^{L_2}(1+2C_J/C_0\delta(x))\dot{\Phi}^2 =& \left(\frac{\hbar}{2e}\right)^2 C\sum_n\dot{\phi}_n^2 + 2\left(\frac{\hbar}{2e}\right)^2 C\sum_{n,m}A_{mn}\dot{\phi}_n\phi_m \\ &+\left(\frac{\hbar}{2e}\right)^2 C\sum_{n,m}B_{mn}\phi_n\phi_m,\end{aligned} \tag{3.21}$$

where we defined $C_0 = C/d$ and

$$A_{mn} = \frac{1}{d}\int_{-L_1}^{L_2} dx(1 + 2C_J/C_0\delta(x))\psi_n\dot{\psi}_m \tag{3.22}$$

$$B_{mn} = \frac{1}{d}\int_{-L_1}^{L_2} dx(1 + 2C_J/C_0\delta(x))\dot{\psi}_n\dot{\psi}_m = \sum_k A_{mk}A_{nk} = \sum_k A_{mk}A_{nk}. \tag{3.23}$$

The next term in the Lagrangian will give rise to

$$-\int_{-L_1}^{L_2} dx v^2\Phi'^2 = -v^2\sum_{mn}\phi_n(t)\phi_m(t)\int_{-L_1}^{L_2} dx\psi_n'(x,t)\psi_m'(x,t) = \\ -v^2\sum_{mn}k_n^2\phi_n^2(t) + E_J\cos f\Phi_0, \tag{3.24}$$

where to obtain the last equality we have used the boundary condition (3.13) together with the inner product. Therefore the Lagrangian will be written as

$$L_{sys} = \frac{1}{2}\left(\frac{\hbar}{2e}\right)^2 C\sum_n\left(\dot{\phi_n}^2 - \omega_n^2\phi_n^2\right) + \left(\frac{\hbar}{2e}\right)^2 C\dot{f}\sum_{n,m}M_{nm}\dot{\phi}_n\phi_m \\ + \left(\frac{\hbar}{2e}\right)^2 C\frac{\dot{f}^2}{2}\sum_{n,m,k}M_{nk}M_{mk}\phi_n\phi_m, \tag{3.25}$$

with

$$M_{nm} = \frac{1}{d}\int_{-L_1}^{L_2} dx(1 + 2C_J/C_0\delta(x))\psi_m\frac{d\psi_n}{df}. \tag{3.26}$$

The time dependence of the ψ_n functions is related to the field f. This Lagrangian describes the interaction among the fields inside the cavity. We notice that the source of this interaction is the time dependence of f or, equivalently, the existence of the SQUID, which resembles a moving mirror in the middle of the cavity [71]. Next, we will study the Lagrangian of the SQUID.

3.3 The SQUID Lagrangian

The phase drop of the SQUID over its inductance L follows the equation of motion

$$\left(\frac{\hbar}{2e}\right)^2 C_J\ddot{f} + E_J\sin f + \left(\frac{\hbar}{2e}\right)^2\frac{2}{L}\left(f + \frac{M}{L_{ext}}f_{ext}\right) = 0. \tag{3.27}$$

Therefore its Lagrangian can be written as

$$L = \left(\frac{\hbar}{2e}\right)^2\frac{C_J}{2}\dot{f}^2 - V(f), \tag{3.28}$$

where

$$V(f) = -E_J \cos f + \left(\frac{\hbar}{2e}\right)^2 \frac{1}{L}\left(f^2 + \frac{M}{L_{ext}} f f_{ext}\right), \tag{3.29}$$

is the potential energy. This Lagrangian is exact up to the assumption that $\Phi_0 \ll 1$. However, we can also look at the limit of small displacement of f around f_0 namely assuming

$$\begin{aligned} f &= f_0 + \delta f(t) \\ f_{ext} &= F_{ext} + \delta f_{ext}(t). \end{aligned} \tag{3.30}$$

where $\delta f \ll 1$ and $\delta f_{ext} \ll 1$. This limit will be useful once we write the full Hamiltonian and we need to make the linear interaction approximation. Therefore the equation of motion for f can be rewritten as

$$\begin{aligned} \left(\frac{\hbar}{2e}\right)^2 C_J \ddot{\delta f} + E_J \cos f_0 + \left(\frac{\hbar}{2e}\right)^2 \frac{2}{L}\delta f + E_J \sin f_0 + \left(\frac{\hbar}{2e}\right)^2 \frac{2}{L} f_0 \\ = -\left(\frac{\hbar}{2e}\right)^2 \frac{2M}{LL_{ext}}\delta f_{ext} - \left(\frac{\hbar}{2e}\right)^2 \frac{2M}{LL_{ext}} F_{ext} \end{aligned} \tag{3.31}$$

The stationary solution where we set $\delta f = 0$ and $\delta f_{ext} = 0$ gives

$$E_J \sin f_0 + \left(\frac{\hbar}{2e}\right)^2 \frac{2}{L}\left(f_0 + \frac{M}{L_{ext}} F_{ext}\right) = 0. \tag{3.32}$$

This indicates the relation between f_0 and F_{ext}. Using it we obtain

$$\left(\frac{\hbar}{2e}\right)^2 C_J \ddot{\delta f} + \left(E_J \cos f_0 + \left(\frac{\hbar}{2e}\right)^2 \frac{2}{L}\right)\delta f = -\left(\frac{\hbar}{2e}\right)^2 \frac{2M}{LL_{ext}}\delta f_{ext}, \tag{3.33}$$

which is basically a forced oscillator. Furthermore, one can rewrite the Lagrangian of f according to its equation of motion in (3.27). In this way we will obtain

$$L_f = \left(\frac{\hbar}{2e}\right)^2 C_J \frac{\dot{\delta f}^2}{2} - \left(\frac{\hbar}{2e}\right)^2 \frac{1}{2} C_J \omega_f^2 \delta f^2 - \left(\frac{\hbar}{2e}\right)^2 \frac{2M}{LL_{ext}} \delta f \delta f_{ext}, \tag{3.34}$$

where

$$\omega_f^2 = \frac{1}{\left(\frac{\hbar}{2e}\right)^2 C_J}\left(E_J \cos f_0 + \left(\frac{\hbar}{2e}\right)^2 \frac{2}{L}\right), \tag{3.35}$$

is the frequency of the oscillation in δf. The above discussion and approximations will be essential when we will investigate the interaction between the SQUID and the cavities. However, In the next section, we will use this Lagrangian and the Lagrangian of the cavities

to study the total system.

3.4 Full Lagrangian and Hamiltonian

Previously we studied the Lagrangian of the Cavity and the SQUID part separately. To find the Hamiltonian description of the system we will first find the Lagrangian of the total system by combining the Lagrangian of the cavities and the SQUID. This allows to write

$$L_{sys} = \frac{1}{2}\left(\frac{\hbar}{2e}\right)^2 C\sum_n \left(\dot{\phi_n}^2 - \omega_n^2\phi_n^2\right) + \left(\frac{\hbar}{2e}\right)^2 C\dot{f}\sum_{n,m} M_{nm}\dot{\phi_n}\phi_m + \left(\frac{\hbar}{2e}\right)^2 C\frac{\dot{f}^2}{2}\sum_{n,m,k} M_{nk}M_{mk}\phi_n\phi_m + \left(\frac{\hbar}{2e}\right)^2 C_J\frac{\dot{f}^2}{2} - V(f). \tag{3.36}$$

The next step in our analysis is to derive the Hamiltonian for the system. Following a similar approach to the previous chapter, we begin by obtaining the momentum variables for both the cavity and the SQUID. This allows us to express the Lagrangian in terms of these momenta, enabling a straightforward transformation to the corresponding Hamiltonian formalism. The momentum variables for the cavity and SQUID are given by

$$q_n = \frac{1}{\hbar}\frac{\partial L}{\partial\dot{\phi}_n} = \hbar\left(\frac{1}{2e}\right)^2 C\dot{\phi}_n + \hbar\left(\frac{1}{2e}\right)^2 C\dot{f}\sum_m M_{nm}\phi_m \tag{3.37}$$

$$p_f = \hbar\left(\frac{1}{2e}\right)^2 C\sum_{n,m} M_{nm}\dot{\phi_n}\phi_m + \hbar\left(\frac{1}{2e}\right)^2 C\dot{f}\sum_{n,m,k} M_{nk}M_{mk}\phi_n\phi_m + \hbar\left(\frac{1}{2e}\right)^2 C_J\dot{f}, \tag{3.38}$$

Next, we proceed to write the Hamiltonian. Following the approach used in the previous chapter, we introduce the momentum variables for both the cavity modes and the SQUID, denoted by q_n and p_f, respectively. It is worth noting that the inclusion of the factor $1/\hbar$ ensures that the momenta are dimensionless. Consequently, the Hamiltonian can be expressed as

$$H = \frac{1}{2}\left(\frac{\hbar}{2e}\right)^2 C\sum_n \left(\dot{\phi_n}^2 + \omega_n^2\phi_n^2\right) + \hbar\left(\frac{1}{2e}\right)^2 C\dot{f}\sum_{n,m} M_{nm}\dot{\phi_n}\phi_m + \left(\frac{\hbar}{2e}\right)^2 C_J\frac{\dot{f}^2}{2} + \left(\frac{\hbar}{2e}\right)^2 C\frac{\dot{f}^2}{2}\sum_{n,m,k} M_{nk}M_{mk}\phi_n\phi_m + V(f). \tag{3.39}$$

This Hamiltonian still does not contain the momenta. Therefore we first write

$$\dot{\phi}_n = \frac{1}{\hbar\left(\frac{1}{2e}\right)^2 C}q_n - \dot{f}M_{nm}\phi_m, \tag{3.40}$$

where using this we can write

$$p_f = \sum_{n,m} M_{nm} q_n \phi_m + \hbar \left(\frac{1}{2e}\right)^2 C_J \dot{f}, \tag{3.41}$$

and hence

$$\dot{f} = \frac{1}{\hbar \left(\frac{1}{2e}\right)^2 C_J} p_f - \frac{1}{\hbar \left(\frac{1}{2e}\right)^2 C_J} \sum_{n,m} M_{nm} q_n \phi_m. \tag{3.42}$$

Replacing $\dot{\phi}_n$ inside the Hamiltonian (3.4) we will have

$$H = \sum_n \left[\frac{(2e)^2}{2C} q_n^2 + \frac{1}{2} \left(\frac{\hbar}{2e}\right)^2 C \omega_n^2 \phi_n^2 \right] + \left(\frac{\hbar}{2e}\right)^2 C_J \frac{\dot{f}^2}{2} + V(f). \tag{3.43}$$

Therefore the final Hamiltonian after also replacing $\dot{f}$ from (3.42) will take the following form

$$H = \sum_n \left[\frac{(2e)^2}{2C} q_n^2 + \frac{1}{2} \left(\frac{\hbar}{2e}\right)^2 C \omega_n^2 \phi_n^2 \right] + \frac{(2e)^2}{2C_J} \left(p_f - \sum_{n,m} M_{nm} q_n \phi_m \right)^2 + V(f). \tag{3.44}$$

Eq. (3.47) represents the total Hamiltonian of the system. We notice that the interaction between the SQUID and cavities are contained in the second term. To study the nature of interaction we rewrite the above Hamiltonian in terms of Ladder operators by first defining

$$\phi_n = \sqrt{\frac{\hbar \omega_n}{2E_C}} \left[a_n + a_n^\dagger \right] \tag{3.45}$$

$$q_n = -i \sqrt{\frac{E_C}{2\hbar \omega_n}} \left[a_n - a_n^\dagger \right]. \tag{3.46}$$

Thus, the Hamiltonian will become

$$H = \sum_n \hbar \omega_n a_n^\dagger a_n + \frac{(2e)^2}{2C_J} \left(p_f + \Gamma(f) \right)^2 + V(f), \tag{3.47}$$

where the operator $\Gamma(f)$ is defined as

$$\Gamma(f) = \frac{i}{2} \sum_{n,m} M_{nm} \left[a_n - a_n^\dagger \right] \left[a_n + a_n^\dagger \right]. \tag{3.48}$$

We observe that the operators a_n and $a_n^\dagger$ exhibit a dependence on f through ω_n. This implies the presence of an interaction between the cavity fields and the SQUID degrees of freedom, f. Thus, we can proceed with the first linear approximation of the Hamiltonian. This approximation assumes that the position of the SQUID, denoted as f, undergoes small oscillations

around its equilibrium position, f_0.

Concretely, we employ the same approximation as in equation (3.3), expressing $f(t)$ as $f(t) \approx f_0 + \delta f(t)$, where $\delta f(t)$ is a small deviation satisfying $\delta f(t) \ll 1$. Consequently, up to first order in δf, the frequency ω_n can be approximated as

$$\omega_n(f) \approx \omega_n(f_0) + \delta f \omega_n'(f_0). \tag{3.49}$$

For the ladder operators we can also write

$$a_n \approx \sqrt{\frac{E_C}{2\hbar\omega_n(f_0)}}\phi_n + i\sqrt{\frac{\hbar\omega_n(f_0)}{2E_C}}q_n - \frac{1}{2}\delta f \frac{\omega_n'(f_0)}{\omega_n(f_0)}\left(\sqrt{\frac{E_C}{2\hbar\omega_n(f_0)}}\phi_n - i\sqrt{\frac{\hbar\omega_n(f_0)}{2E_C}}q_n\right), \tag{3.50}$$

which can be written as

$$a_n \approx a_n(f_0) - \frac{1}{2}\delta f \frac{\omega_n'(f_0)}{\omega_n(f_0)} a_n^\dagger(f_0). \tag{3.51}$$

Moreover, we notice that in this limit using equation (3.26) we have

$$M_{nm} = M_{nm0} + \delta f M'_{nm0}. \tag{3.52}$$

with $M'_{mn0} = \sum_k M_{nk0}M_{mk0}$ and

$$M_{nm0} = \frac{1}{d}\int_{-L_1}^{L_2} dx(1 + 2C_J/C_0\delta(x))\psi_m(f_0)\frac{dk_n}{df_0}\frac{d\psi_n(f_0)}{dk_n}. \tag{3.53}$$

Now, we need to substitute these terms back into the bare Hamiltonian and $\Gamma(f)$ in equation (3.47). These terms contribute non-linearly to the interaction Hamiltonian. However, since we have $\delta f \ll 1$, we can make a linear approximation. We express $\Gamma(f)$ as $\Gamma(f) \approx \Gamma(f_0) + \delta f \Gamma'(f_0)$, where Γ' is determined by substituting the aforementioned expansions of creation and annihilation operators and M_{nm} into $\Gamma(f)$, while keeping only the terms linear in δf. Therefore, we will have

$$\Gamma'(f_0) = \sqrt{\frac{\omega_m(f_0)}{\omega_n(f_0)}}\left[M'_{nm} + M_{nm}\frac{\omega_n'(f_0)}{\omega_n(f_0)}\right]\left(a_m(f_0) + a_m^\dagger(f_0)\right)\left(a_n(f_0) - a_n^\dagger(f_0)\right). \tag{3.54}$$

Replacing this into the Hamiltonian we will obtain

$$H = \hbar \sum_n \left(\omega_n + \omega_n' \delta f\right) \left(a_n^\dagger - \delta f \frac{\omega_n'}{2\omega_n} a_n\right) \left(a_n - \delta f \frac{\omega_n'}{2\omega_n} a_n^\dagger\right) + \frac{(2e)^2}{2C_J} \left(p_f + \Gamma_0 + \delta f \Gamma_0'\right)^2 + V(\delta f). \tag{3.55}$$

where, for simplicity, we have replaced $\Gamma(f_0)$ with Γ_0, and similarly for Γ'. Moreover

$$V(\delta f) = \left(\frac{\hbar}{2e}\right)^2 \frac{1}{2} C_J \omega_f^2 \delta f^2 + \left(\frac{\hbar}{2e}\right)^2 \frac{2M}{LL_{ext}} \delta f f_{ext}. \tag{3.56}$$

In the Hamiltonian (3.55), the ladder operators are independent of δf. To find the form of interaction, we perform a unitary transformation $H' = T^\dagger H T$ where

$$T = \exp\left\{i\delta f(\Gamma_0 + \frac{1}{2}\delta f \Gamma_0')\right\}. \tag{3.57}$$

We first apply this on the second term of the Hamiltonain and the result will be

$$T^\dagger \left(p_f + \Gamma_0 + \delta f \Gamma_0'\right)^2 T = p_f^2. \tag{3.58}$$

Therefore we are shifting the momentum by $\Gamma_0 + \delta f \Gamma_0'$. Next we need to trasnfrom the first term in the Hamiltonian;

$$\begin{aligned}
&T^\dagger \hbar \sum_n \left(\omega_n + \omega_n' \delta f\right) \left(a_n^\dagger - \delta f \frac{\omega_n'}{2\omega_n} a_n\right) \left(a_n - \delta f \frac{\omega_n'}{2\omega_n} a_n^\dagger\right) T \approx \\
&\hbar \sum_n \omega_n \left(a_n^\dagger a_n - \delta f \frac{\omega_n'}{2\omega_n} (a_n^{\dagger 2} + a_n^2) + \delta f^2 \left(\frac{\omega_n'}{2\omega_n}\right)^2 a_n a_n^\dagger\right) \\
&+\hbar \sum_n \omega_n' \left(\delta f a_n^\dagger a_n - \delta f^2 \frac{\omega_n'}{2\omega_n} (a_n^{\dagger 2} + a_n^2)\right) \\
&\frac{-\hbar}{2} \delta f \sum_{n,m} M_{nm} \sqrt{\frac{\omega_m}{\omega_n}} \left[\omega_m \left(a_m - a_m^\dagger\right) \left(a_n - a_n^\dagger\right) + \omega_n \left(a_m + a_m^\dagger\right) \left(a_n + a_n^\dagger\right)\right] \\
&-\frac{\hbar}{4} \delta f^2 \sum_{n,m} \tilde{M}_{nm} \sqrt{\frac{\omega_m}{\omega_n}} \left[\omega_m \left(a_m - a_m^\dagger\right) \left(a_n - a_n^\dagger\right) + \omega_n \left(a_m + a_m^\dagger\right) \left(a_n + a_n^\dagger\right)\right] \\
&-\frac{\hbar}{2} \delta f^2 \sum_{mn} M_{nm} \sqrt{\frac{\omega_m}{\omega_n}} \left[\omega_n \frac{\omega_n'}{\omega_n} \left(a_m + a_m^\dagger\right) \left(a_n^\dagger + a_n\right) + \omega_m \frac{\omega_m'}{\omega_m} \left(a_m^\dagger - a_m\right) \left(a_n - a_n^\dagger\right)\right] \\
&-\frac{\hbar}{2} \delta f^2 \sum_{n,m} M_{nm} \sqrt{\frac{\omega_m}{\omega_n}} \left[\omega_m' \left(a_m - a_m^\dagger\right)\left(a_n - a_n^\dagger\right) + \omega_n' \left(a_m + a_m^\dagger\right)\left(a_n + a_n^\dagger\right)\right] + O(\delta f^3),
\end{aligned} \tag{3.59}$$

where $\tilde{M}_{nm} = \left[M_{nm}' + M_{nm} \frac{\omega_n'}{\omega_n}\right]$. Now, these terms represent the interaction between the cavities and the SQUID, expressed as powers of δf. In our analysis, we have considered terms up to second order in δf. However, we can simplify the Hamiltonian by employing

two approaches.

Firstly, since δf is very small, we can neglect all the second-order terms in δf. Notably, there is a second-order term in $V(\delta_f)$ given by $\left(\frac{\hbar}{2e}\right)^2 \frac{1}{2} C_J \omega_f^2 \delta f^2$. Nevertheless, the prefactor of this term, $\left(\frac{\hbar}{2e}\right)^2 \frac{1}{2} C_J \omega_f^2 = \frac{\hbar^2 \omega_f^2}{4E_{C_J}} \propto E_J$, is large. Consequently, we can neglect this term in comparison to other dominant terms in the Hamiltonian.

Secondly, we can utilize the rotating wave approximation (RWA). By applying the RWA, we can show that all the second-order terms in δf cancel out. This approximation helps simplify the Hamiltonian further.

To outline the implementation of the RWA, let us first write

$$\delta f = \sqrt{\frac{E_{C_J}}{\hbar \omega_f}} \left[a_f + a_f^\dagger \right] \tag{3.60}$$

$$p_f = -i \frac{1}{2} \sqrt{\frac{\hbar \omega_f}{E_{C_J}}} \left[a_f - a_f^\dagger \right]. \tag{3.61}$$

Replacing them in to the Hamiltonian will result in writing the bare Hamiltonian as

$$H_0 = \hbar \sum_n \omega_n a_n^\dagger a_n + \hbar \omega_f a_f^\dagger a_f. \tag{3.62}$$

Therefore we can use the above Hamiltonian and move to the rotating frame by applying the unitary

$$U = \exp it/\hbar \left[\sum_n \hbar \omega_n a_n^\dagger a_n + \hbar \omega_f a_f^\dagger a_f \right] \tag{3.63}$$

on the interaction Hamiltonian of equation (3.59). Therefore one can show that after doing the RWA, applying the resonant condition $\omega_f = \omega_n + \omega_m$ to any two modes when $m \neq n$ and finally going back to the Schrödinger picture, we obtain

$$\begin{aligned} H_{rwa} = \hbar \sum_n \omega_n a_n^\dagger a_n + \hbar \omega_f a_f^\dagger a_f + \hbar \sum_n \omega_n \frac{E_{C_J}}{\hbar \omega_f} \left(\frac{\omega_n'}{2\omega_n} \right)^2 a_n a_n^\dagger a_f a_f^\dagger \\ - \frac{\hbar}{2} \sqrt{\frac{E_{C_J}}{\hbar \omega_f}} \sum_{n,m} M_{nm} \sqrt{\frac{\omega_m}{\omega_n}} \left(\omega_m + \omega_n \right) \left(a_f^\dagger a_m a_n + a_f a_m^\dagger a_n^\dagger \right). \end{aligned} \tag{3.64}$$

Moreover, we can neglect the third term of the first line by reasoning that, the constant $E_{C_J}/\hbar\omega_f \propto \sqrt{E_{C_J}/E_J} \ll 1$. Therefore that term is negligible and we write the final Hamiltonian as

$$H_{rwa} = \hbar \sum_n \omega_n a_n^\dagger a_n + \hbar\omega_f a_f^\dagger a_f$$
$$-\frac{\hbar}{2}\sqrt{\frac{E_{C_J}}{\hbar\omega_f}} \sum_{n,m} M_{nm} \sqrt{\frac{\omega_m}{\omega_n}} (\omega_m + \omega_n) \left(a_f^\dagger a_m a_n + a_f a_m^\dagger a_n^\dagger \right). \tag{3.65}$$

Considering that there are only two modes of the cavity which satisfy the resonant condition, we can write from (3.65)

$$H_{rwa} = \hbar \sum_n \omega_n a_n^\dagger a_n + \hbar\omega_f a_f^\dagger a_f$$
$$-\frac{\hbar}{2}\sqrt{\frac{E_{C_J}}{\hbar\omega_f}} \left(M_{12}\sqrt{\frac{\omega_2}{\omega_1}} + M_{21}\sqrt{\frac{\omega_1}{\omega_2}} \right) (\omega_2 + \omega_1) \left(a_f^\dagger a_2 a_1 + a_f a_2^\dagger a_1^\dagger \right). \tag{3.66}$$

The Hamiltonian presented here is commonly known as an "absorption refrigerator" [54, 82, 80]. In this setup, one can achieve autonomous cooling of one mode by utilizing the other two modes. The concept of absorption refrigeration has attracted significant interest in the field of quantum thermodynamics.

In the next section, we will delve further into this topic, exploring the principles and dynamics of the absorption refrigerator.

3.5 Absorption refrigerator

As mentioned earlier, the Hamiltonian given by Eq. (3.66) can serve as a quantum refrigerator. This is evident from the interaction term among the three modes, $a_f^\dagger a_2 a_1$. This interaction implies that one photon is created in the SQUID while two photons are simultaneously absorbed in the other two cavity modes. As a result, the energy of the SQUID is increase, while the energy of the two other modes is decreased. It is important to note that the conjugate of this Hamiltonian describes the reverse process.

To promote the refrigeration process, one can manipulate the energy levels of each oscillator. One approach is to connect each mode to a heat bath, allowing them to reach a thermal equilibrium state with temperatures T_i for $i \in f, 1, 2$. By adjusting the temperatures, the occupation probabilities of the oscillators can be tuned. The initial occupation number n_i of the i-th oscillator can be expressed as

$$n_i = Tr[\rho_{T_i} a_i^\dagger a_i] \tag{3.67}$$

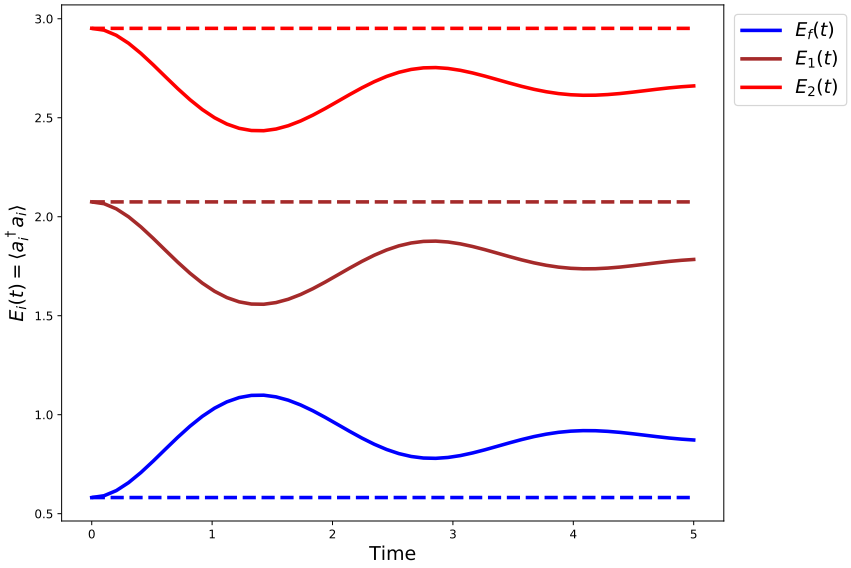

FIGURE 3.2: Averaged energies of each mode after time t, showing the increase in energy of the SQUID and the decrease in energy of the other two modes. The solid lines show the average energy of each oscillator at time t. Dashed lines indicate the average energy at the initial time.

where

$$\rho_{T_i} = \frac{\exp\left(-\frac{1}{K_b T_i} a_i^\dagger a_i\right)}{\mathrm{Tr}\left[\exp\left(-\frac{1}{K_b T_i} a_i^\dagger a_i\right)\right]}. \tag{3.68}$$

is thermal initial state.

In the general scenario, the system can function as both a refrigerator and a heat engine. By applying the resonant condition $\omega_f = \omega_1 + \omega_2$, one can adjust the temperatures of the three modes (corresponding to the initial occupation probabilities) in a way that allows the SQUID to cool down the other two cavities. This occurs when the temperature of the SQUID is higher than that of the other two modes, i.e., $T_1 < T_2 < T_f$. This is because, in this temperature regime, the state of SQUID will have a lower occupation probability comparing to the other modes. Therefore, in this configuration, we observe that the final average energy of the SQUID, denoted as $E_f(t) = \mathrm{Tr}[\omega_f a_f^\dagger a_f \rho(t)]$, exceeds its initial average energy obtained from the thermal state $E_f(t) = \mathrm{Tr}[\omega_f a_f^\dagger a_f \rho_{T_f}(0)]$. To explore this case, there are two approaches. The first approach involves connecting each mode to separate heat baths initially, allowing them to reach their respective temperatures. Subsequently, the modes interact with each other while still being influenced by the baths. In this scenario, the dynamics at time t can be obtained by solving the master equation, as demonstrated in [54].

Another simpler approach is to disconnect the modes from the heat baths once they have

reached their respective temperatures. Subsequently, the modes interact with each other without the influence of the baths. In this case, the dynamics are determined by the unitary time evolution. This approach is considered in our analysis. In Figure 3.2, we observe the average energy of each mode at time t. The comparison with their initial values clearly indicates that the energy of the SQUID increases while the other two modes become colder. This confirms that this configuration operates as a refrigerator, consistent with the findings in [82, 80].

3.6 Conclusions

In this chapter, we studied a setup that is used as a realization of the dynamical Casimir effect. By quantizing the SQUID degrees of freedom, we obtained the Lagrangian of the quantized system in terms of the modes inside the cavity. After switching to the Hamiltonian representtion, we obtained a three-body interaction term consisting of the cavity modes operators and the SQUID. By assuming a weak coupling between the cavities and the SQUID and the rotating wave approximation, we reduced the Hamiltonian into the form of the absorption refrigerator interaction. In this way we showed that by heating up the SQUID one can cool down the two modes of the cavity.

This result is significant as it demonstrates the versatility of the architecture depicted in Figure 3.1. The system offers the flexibility to work with multiple cavity modes and their interactions with the SQUID. In the refrigerator configuration, we focused on two of these modes. However, to enhance the cooling process, we can explore the influence of the other available modes. This will be the next step in advancing this research project, as we aim to fully investigate the impact of these additional modes on the cooling dynamics.

Chapter 4

Work statistics in quantum systems

4.1 Introduction

This chapter concerns itself with the work that has been done in the paper *A convenient Keldysh contour for thermodynamically consistent perturbative and semiclassical expansions* [20]. In this paper, we have introduced a modified version of the Keldysh contour that is specifically tailored for studying work statistics in quantum thermodynamics. By employing this modified contour, we have developed a perturbation expansion of the moment generating function (MGF), which allows us to investigate work fluctuations and their statistical properties.

The perturbative approach we have presented exhibits a similar structure to conventional perturbative expansions based on non-equilibrium Green's functions (GFs) [90]. However, the key difference lies in the building blocks, namely the GFs and the contour itself. By employing the modified contour, we are able to derive a perturbative expansion that satisfies the fluctuation theorem (FT) [5, 4, 56, 29] at all perturbative orders.

As an application of this method, we have computed the work statistics for a scenario where a slight non-linear perturbation of a quadratic Hamiltonian is activated after an initial measurement and deactivated prior to a final energy measurement. The resulting probability distribution of work can be expressed as a combination of Poisson processes, providing insights into the statistical behavior of work fluctuations in this specific scenario.

Furthermore, we have investigated the semiclassical limit of the work MGF. Building upon the usual Feynman path integral technique [35], we have extended it to the modified contour framework. To achieve this, we have considered a generalization of the Keldysh rotation and demonstrated that a convenient way to achieve it is through the introduction of a symmetrization of the modified contour. By performing this symmetrization, we have adapted procedures similar to those in [88, 86, 89, 27] to obtain a semiclassical expansion of

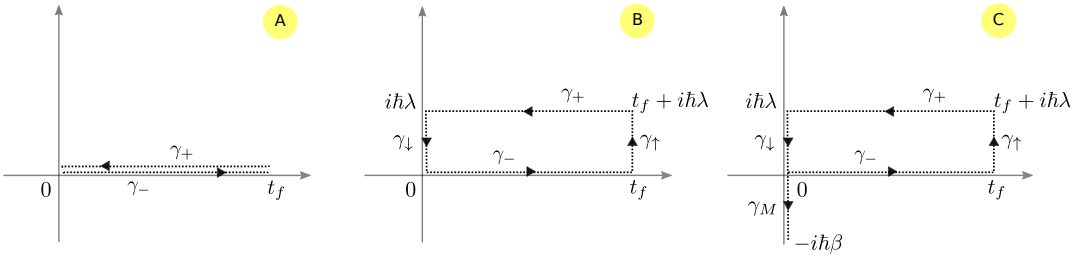

FIGURE 4.1: There are three distinct time integration contours commonly used in calculations: a) The Keldysh contour γ_K, which consists of two branches denoted as γ_- and γ_+. The γ_- branch corresponds to the forward time evolution, while the γ_+ branch represents the backward evolution. b) The contour γ_C, obtained by extending the Keldysh contour with two additional vertical tracks, $\gamma_\uparrow$ and $\gamma_\downarrow$. These vertical tracks serve to encode specific initial conditions. c) The contour γ, constructed by further augmenting the γ_C contour with an additional track, γ_M, that carries information about the initial condition. These various time integration contours provide a framework for handling calculations in different scenarios and enable the analysis of quantities of interest in a systematic manner. [20].

the MGF. Specifically, we have explicitly computed the classical order (zeroth order) and the first quantum correction to the work MGF, shedding light on the interplay between classical and quantum contributions to work fluctuations.

4.2 The Contour idea

The Schwinger-Keldysh contour is employed as a useful technique to streamline calculations in open and many-body quantum systems. This concept can also be extended to the realm of counting statistics within a double measurement setup. In this section, we provide a brief overview of the Keldysh approach and its application to counting statistics, before delving into more specific topics such as work generating functions. In many-body quantum theory, a general quantity can be represented as a correlator of the following form

$$G = \mathrm{Tr}\left\{\left[\mathcal{T}\prod_{j=1}^{M} A_H^{(j,-)}(t_j^-)\right]\rho_0\left[\bar{\mathcal{T}}\prod_{i=1}^{K} A_H^{(i,+)}(t_i^+)\right]\right\}, \tag{4.1}$$

where ρ_0 is the initial-state density matrix and $A_H^{(i,\pm)}(t)$ are a set of quantum operators in the Heisenberg picture, with $\mathcal{T}$ and $\bar{\mathcal{T}}$ indicating, respectively, the time ordering and anti-time ordering operators. An elegant way to simplify Eq. (4.1) is to introduce a generalized version of the time-ordering operator: the *contour ordering* operator, which orders the operators according to the position of their time arguments on a new domain, called the Schwinger-Keldysh contour [90, 103, 62]. This contour is composed of two branches, which we call lower $(-)$ and upper $(+)$ branch: the first one leads from time 0 to a final time t, while the

second goes backward from t to time 0 (see Fig. 4.1 A). Equation (4.1) can be rewritten in terms of the new ordering operator in the much simpler form

$$G = \mathrm{Tr}\left\{\left[\mathcal{T}_K \prod_i A_H^{(i)}(z_i)\rho_0\right]\right\}, \tag{4.2}$$

where the time arguments z_i for $i = 1, \ldots, M+K$ are chosen on the Keldysh contour γ_K and hence belong to the forward or backward branch. Writing the evolution operator explicitly we can also cast the equation above as (setting $\hbar = 1$)

$$G = \mathrm{Tr}\left[\left\{\mathcal{T}_K e^{-i\int_{\gamma_K} H(z)dz} \prod_i A^{(i)}(z_i)\rho_0\right\}\right], \tag{4.3}$$

where the operators $A^{(i)}$ are in the Schrödinger picture and $H(z)$ denotes the system Hamiltonian. Eq. (4.3) is written in terms of a single ordering operator instead of two different operators $\mathcal{T}, \bar{\mathcal{T}}$ like in eq. (4.1) and this represents a huge advantage [103, 90]. In a double measurement process the simplification achieved with the contour idea is even greater. In this framework a generic observable Λ is measured at time 0 and time t_f, and in between the system evolves under the action of a time dependent Hamiltonian $H(t)$ [29]. The generating function for the statistics of the difference of the outcomes between the first and second measurement is given by

$$M_\Lambda(\lambda, t_f) = \mathrm{Tr}\left[e^{\lambda\Lambda_H(t_f)} e^{-\lambda\Lambda_H(0)}\rho_0\right]. \tag{4.4}$$

This representation holds under the assumption that the initial measurement operator commutes with the initial state density matrix ρ_0. Now let us write Eq. (4.4) in the form of Eq. (4.3) by using the dummy integrals $A^{(1)} = e^{\lambda\Lambda(t)} = e^{-i\int_0^{i\lambda}\Lambda(t_f)dz}$ and $A^{(0)} = e^{-\lambda\Lambda(0)} = e^{-i\int_{i\lambda}^0\Lambda(0)dz}$. Then, we find

$$\begin{aligned} &M_\Lambda(\lambda, t_f) = \\ &\mathrm{Tr}\left\{\mathcal{T}_K\left[e^{-i\int_{\gamma_K} H(z)dz} e^{-i\int_0^{i\lambda}\Lambda(t_f)dz} e^{-i\int_{i\lambda}^0\Lambda(0)dz}\rho_0\right]\right\}. \end{aligned} \tag{4.5}$$

By examining the sum of the three integrals, it becomes evident that it can be consolidated into a single integration along an alternate contour called γ_C. This modified contour is derived from the Schwinger-Keldysh contour but includes two additional vertical branches at

times 0 and t (Fig. 4.1 B). As a result, the ordering operator must also be extended to accommodate this new contour. Consequently, we can express the given expression as

$$M_\Lambda(\lambda, t_f) = \mathrm{Tr}\left\{\mathcal{T}_C\left[e^{-i\int_{\gamma_C} H_C(z)dz}\rho_0\right]\right\}, \tag{4.6}$$

where now the Hamiltonian H_C is naturally extended as

$$H_C(z) = \begin{cases} H(t) & \text{for } z = t \in \gamma_K, \\ \Lambda(0), \Lambda(t_f) & \text{for } z = \tau \in \gamma_{\uparrow,\downarrow}, \end{cases} \tag{4.7}$$

where we labelled the vertical tracks of the contour drawn in Fig. 4.1 B by $\gamma_\uparrow$. As a last step, we point out that the dependence on the initial state ρ_0 can also be cast as an integration on an additional track of the contour. Indeed, if we define $H_M + \log(Z)/\beta \equiv -(1/\beta)\log\rho_0$ with $Z = Tr[e^{-\beta H_M}]$, we can always write $\rho_0 = \exp\left[-i\int_0^{-i\beta} H_M(z)dz\right]/Z$ and express Eq. (4.6) as [33]

$$M(\lambda, t_f) = \frac{\mathrm{Tr}\left[\mathcal{T}_\gamma\left\{e^{-i\int_\gamma H_\gamma(z)dz}\right\}\right]}{\mathrm{Tr}\left[\mathcal{T}_\gamma\left\{e^{-i\int_\gamma H_{\gamma,0}(z)dz}\right\}\right]}, \tag{4.8}$$

where γ is the contour defined in Fig. 4.1 C, built by adding an additional track γ_M, $\mathcal{T}_\gamma$ denotes the time-ordering operator along this contour, and the extended Hamiltonian $H_\gamma(z)$ is defined as

$$H_\gamma(z) = \begin{cases} H(t) & \text{for } z = t \in \gamma_K, \\ \Lambda(0), \Lambda(t_f) & \text{for } z = \tau \in \gamma_{\uparrow,\downarrow}, \\ H_M & \text{for } z \in \gamma_M. \end{cases} \tag{4.9}$$

Moreover, we have used $H_{\gamma,0} := H_\gamma|_{\Lambda=0}$. If the initial state is a Gibbs state, we have $H_M = H(0)$ and β assumes the role of the inverse physical temperature.

To write the work MGF, we will study the case in which the measurement operator $\Lambda(t)$ coincides with the system Hamiltonian. Therefore, the difference of the outcomes of measurements will be the difference of the final and initial energies, i.e. *work* in a closed quantum system. This corresponds to Eq. (4.4) with $\Lambda_H(0) = H(0)$ and $\Lambda_H(t) = H_H(t)$

$$M(\lambda, t_f) = \mathrm{Tr}[e^{\lambda H_H(t_f)} e^{-\lambda H_H(0)}\rho(0)]. \tag{4.10}$$

Indeed Eq. (4.10) can be written in terms of equation (4.8), where in eq. (4.9) we have $\Lambda(0), \Lambda(t_f) = H(0), H(t_f)$.

By employing the modified contour γ, it becomes feasible to construct perturbative expansions for work generating functions in weakly perturbed quantum systems. In the upcoming section, we study the perturbation expansion of the MGF.

4.3 Perturbation theory

In order to apply the standard perturbation theory approach, the contour Hamiltonian can be decomposed as $H_\gamma(z) = H_0(z) + \chi(z)H_1(z)$, where $H_0(z)$ and $H_1(z)$ correspond to the unperturbed Hamiltonian and the perturbation, respectively. These Hamiltonians are defined on the contour γ, while $\chi(z)$ represents a switching function. Two scenarios will be explored for work extraction.

In the first scenario, the final Hamiltonian is identical to the initial Hamiltonian, which implies $\chi(0) = \chi(t_f) = 0$. This protocol is called the *switching on/off* protocol because the perturbation $H_1(z)$ is activated after the initial measurement and deactivated before the final measurement. Bochkov and Kuzovlev derived the first integral fluctuation theorem ([11]) for this setting, and the corresponding switching function is expressed as

$$\chi(z) = \begin{cases} \chi(t) & \text{for } z = t \in \gamma_K, \\ 0 & \text{for } z \in \gamma_{\uparrow,\downarrow}, \\ 0 & \text{for } z \in \gamma_M. \end{cases} \tag{4.11}$$

In the second scenario, the final Hamiltonian is arbitrary, i.e., $\chi(0) = 0$ but $\chi(t_f) \neq 0$. This is the general setting considered by Jarzynski [56] and the associated contour Hamiltonian is

$$\chi(z) = \begin{cases} \chi(t) & \text{for } z = t \in \gamma_K, \\ \chi(t_f) \neq 0 & \text{for } z \in \gamma_\uparrow, \\ 0 & \text{for } z \in \gamma_{M,\downarrow}. \end{cases} \tag{4.12}$$

The customary approach to time-dependent perturbation theory is done in the interaction picture [94]. To generalize this concept to the modified contour we use the following relation

$$U_\gamma(z,0) \equiv \mathcal{T}_\gamma\{e^{-\frac{i}{\hbar}\int_\gamma^z dz H_\gamma(z)}\} = U_{\gamma 0}(z,0)\tilde{U}_{\gamma,1}(z,0), \tag{4.13}$$

where we denoted with $\int_\gamma^z$ the integration between the initial point of the modified contour and the point z and defined

$$U_{\gamma 0} = \mathcal{T}\{e^{-\frac{i}{\hbar}\int_\gamma dz H_0(z)}\}; \qquad \tilde{U}_{\gamma,1} = \mathcal{T}\{e^{-\frac{i}{\hbar}\int_\gamma dz \chi(z)\tilde{H}_1(z)}\}, \tag{4.14}$$

with the contour interaction Hamiltonian defined as $\tilde{H}_1(z) = U_{\gamma 0}(0,z)H_1(z)U_{\gamma 0}(z,0)$. To derive equation (4.13) we first take the derivative of $U_\gamma(z,0)$ with respect to z. Thus we will have

$$\frac{d}{dz}U_\gamma(z,0) = -\frac{i}{\hbar}H_\gamma(z)U_\gamma(z,0). \tag{4.15}$$

Above equation can be obtained by an infinitesimal displacement of the generator. Expanding to the first order we will have

$$\begin{aligned} U_\gamma(z+\epsilon,0) \equiv \mathcal{T}_\gamma\{e^{-\frac{i}{\hbar}\int_\gamma^{z+\epsilon} H_\gamma(z)dz}\} &= (\mathbb{I} - i\frac{\epsilon}{\hbar}H_\gamma(z))\mathcal{T}_\gamma\{e^{-\frac{i}{\hbar}\int_\gamma^{z} H_\gamma(z)dz}\} + O(\epsilon^2) \\ &= (\mathbb{I} - i\frac{\epsilon}{\hbar}H_\gamma(z))U_\gamma(z,0) + O(\epsilon^2). \end{aligned} \tag{4.16}$$

Next we will show that the r.h.s of Eq. (4.13) coincides Eq. (4.16).

$$\begin{aligned} \frac{d}{dz}U_{\gamma 0}(z,0)\tilde{U}_{\gamma,1}(z,0) &= -iH_0(z)U_{\gamma 0}(z,0)\tilde{U}_{\gamma,1}(z,0) - i\chi(z)U_{\gamma 0}(z,0)\tilde{H}_1(z)\tilde{U}_{\gamma,1}(z,0) \\ &= -iH_0(z)U_{\gamma 0}(z,0)\tilde{U}_{\gamma,1}(z,0) - i\chi(z)U_{\gamma 0}(z,0)\tilde{H}_1(z)U_{\gamma 0}(0,z)U_{\gamma 0}(z,0)\tilde{U}_{\gamma,1}(z,0) \\ &= -iH_0(z)U_{\gamma 0}(z,0)\tilde{U}_{\gamma,1}(z,0) - i\chi(z)H_1(z)U_{\gamma 0}(z,0)\tilde{U}_{\gamma,1}(z,0), \end{aligned} \tag{4.17}$$

and the last term is equal to the r.h.s. of (4.15) after regrouping $H_0(z)$ and $\chi(z)H_1(z)$. Note now that the numerator of Eq. (4.8) in terms of $U_\gamma(z,0)$ is simply given by

$$\mathrm{Tr}\left[\mathcal{T}_\gamma\{e^{-\frac{i}{\hbar}\int_\gamma H_\gamma(z)dz}\}\right] = \mathrm{Tr}[U_\gamma(-i\hbar\beta,0)], \tag{4.18}$$

and we can use Eq. (4.13) to write

$$\mathrm{Tr}[U_\gamma(-i\hbar\beta,0)] = \mathrm{Tr}[U_{\gamma 0}(-i\hbar\beta,0)\tilde{U}_{\gamma,1}(-i\hbar\beta,0)] = \mathrm{Tr}[e^{-\beta H_0}\tilde{U}_{\gamma,1}(-i\hbar\beta,0)]. \tag{4.19}$$

Expanding $\tilde{U}_{\gamma,1}$ as a contour ordered exponential and dividing by the proper normalization, we obtain

$$M_W(\lambda,t_f) = \frac{\mathrm{Tr}[e^{-\beta H_M}\mathcal{T}_\gamma\{e^{-\frac{i}{\hbar}\int_\gamma dz\chi(z)\tilde{H}_1(z)}\}]}{\mathrm{Tr}[e^{-\beta H_M}]}, \tag{4.20}$$

where we used that $H_0(z) = H_M$ on the γ_M branch of the contour. Equation (4.20) can also be written as an explicit function of $H_1(z)$

$$M_W(\lambda, t_f) = \frac{\mathrm{Tr}[\mathcal{T}_\gamma\{e^{-\frac{i}{\hbar}\int_\gamma dz H_0(z)} e^{-\frac{i}{\hbar}\int_\gamma dz \chi(z) H_1(z)}\}]}{\mathrm{Tr}[\mathcal{T}_\gamma\{e^{-\frac{i}{\hbar}\int_\gamma dz H_0(z)}]}. \tag{4.21}$$

The significance of the aforementioned equation lies in the fact that when $H_1(z)$ is a minor perturbation of $H_0(z)$, we can expand the second exponential in the numerator and obtain a series of perturbations for the generating function. However, before delving into this, let us first concentrate on the crucial component of perturbation theory, which is known as *Green's function*.

4.4 The Green's function on the modified contour

Consider a generic two-point correlation function on the contour in the Schrodinger picture. This can be found as

$$\begin{aligned} G_{A_1,A_2}(z_1, z_2) &\equiv \langle \mathcal{T}_\gamma\{A_1(z_1)A_2(z_2)\}\rangle \\ &= \theta(z_1 - z_2)\langle A_1(z_1)A_2(z_2)\rangle + \theta(z_2 - z_1)\langle A_1(z_2)A_2(z_1)\rangle \\ &= \theta(z_1 - z_2)\mathrm{Tr}[U_\gamma(-i\hbar\beta, z_1)A_1(z_1)U_\gamma(z_1, z_2)A_2(z_2)U_\gamma(z_2, 0)] \\ &+\theta(z_2 - z_1)\mathrm{Tr}[U_\gamma(-i\hbar\beta, z_2)A_2(z_2)U_\gamma(z_2, z_1)A_1(z_1)U_\gamma(z_1, 0)]. \end{aligned} \tag{4.22}$$

This can be rewritten the as

$$\begin{aligned} G_{A_1,A_2}(z_1, z_2) =& \theta(z_1 - z_2)\mathrm{Tr}[U_\gamma(-i\hbar\beta, 0)U_\gamma(0, z_1)A_1(z_1)U_\gamma(z_1, z_2)A_2(z_2)U_\gamma(z_2, 0)] \\ &+\theta(z_2 - z_1)\mathrm{Tr}[U_\gamma(-i\hbar\beta, 0)U_\gamma(0, z_2)A_2(z_2)U_\gamma(z_2, z_1)A_1(z_1)U_\gamma(z_1, 0)]. \end{aligned} \tag{4.23}$$

To take the the derivatives with respect to z_1 and z_2, we use the equations bellow which come from (4.16)

$$\begin{aligned} \frac{d}{dz_1}U_\gamma(z_1, z_2) &= -\frac{i}{\hbar}H_\gamma(z_1)U_\gamma(z_1, z_2) \\ \frac{d}{dz_1}U_\gamma(z_2, z_1) &= \frac{i}{\hbar}U_\gamma(z_2, z_1)H_\gamma(z_1). \end{aligned} \tag{4.24}$$

Using above equations we can take the derivative of (4.23) to obtain the equations of motion for the two-point correlation function

$$\begin{aligned}
&\frac{\partial}{\partial z_1} G_{A_1,A_2}(z_1,z_2) = \\
&\frac{i}{\hbar}\theta(z_1-z_2)\mathrm{Tr}[U_\gamma(-i\hbar\beta,0)U_\gamma(0,z_1)[H_\gamma(z_1),A_1(z_1)]U_\gamma(z_1,z_2)A_2(z_2)U_\gamma(z_2,0)] \\
&+\frac{i}{\hbar}\theta(z_2-z_1)\mathrm{Tr}[U_\gamma(-i\hbar\beta,0)U_\gamma(0,z_2)A_2(z_2)U_\gamma(z_2,z_1)[H_\gamma(z_1),A_1(z_1)]U_\gamma(z_1,0)] \\
&+\delta(z_1-z_2)\mathrm{Tr}\left\{U_\gamma(-i\hbar\beta,0)U_\gamma(0,z_1)A_1(z_1)U_\gamma(z_1,z_2)A_2(z_2)U_\gamma(z_2,0)\right\} \\
&-\delta(z_1-z_2)\mathrm{Tr}\left\{U_\gamma(-i\hbar\beta,0)U_\gamma(0,z_2)A_2(z_2)U_\gamma(z_2,z_1)A_1(z_1)U_\gamma(z_1,0)\right\}, \\
&\frac{\partial}{\partial z_2} G_{A_1,A_2}(z_1,z_2) = \\
&\frac{i}{\hbar}\theta(z_1-z_2)\mathrm{Tr}[U_\gamma(-i\hbar\beta,0)U_\gamma(0,z_1)A_1(z_1)U_\gamma(z_1,z_2)[H_\gamma(z_2),A_2(z_2)]U_\gamma(z_2,0)] \\
&+\frac{i}{\hbar}\theta(z_2-z_1)\mathrm{Tr}[U_\gamma(-i\hbar\beta,0)U_\gamma(0,z_2)[H_\gamma(z_2),A_2(z_2)]U_\gamma(z_2,z_1)A_1(z_1)U_\gamma(z_1,0)] \\
&-\delta(z_1-z_2)\mathrm{Tr}\left\{U_\gamma(-i\hbar\beta,0)U_\gamma(0,z_1)A_1(z_1)U_\gamma(z_1,z_2)A_2(z_2)U_\gamma(z_2,0)\right\} \\
&+\delta(z_1-z_2)\mathrm{Tr}\left\{U_\gamma(-i\hbar\beta,0)U_\gamma(0,z_2)A_2(z_2)U_\gamma(z_2,z_1)A_1(z_1)U_\gamma(z_1,0)\right\}. \qquad (4.25)
\end{aligned}$$

More general correlation functions can be obtained by including more operators in the trace (4.22). For instance, we introduce the n-operator correlation function as

$$G_{A_1,\ldots A_n}(z_1,\ldots z_n) = \mathrm{Tr}\left[\mathcal{T}_\gamma\left\{e^{-\frac{i}{\hbar}\int_\gamma H_\gamma(z)dz}A_1(z_1)\ldots A_n(z_n)\right\}\right]. \qquad (4.26)$$

The primary focus of this chapter is on scenarios where the operators A_i are composed of bosonic or fermionic creation and annihilation operators. However, the equations of motion (4.25) can only be solved in certain instances, such as when H_γ is quadratic, and $A_{1,2}$ are single creation/annihilation operators. Conversely, when H_γ is non-quadratic, the equations (4.25) are not self-contained in G_{A_1,A_2} and depend on higher-order correlation functions, which leads to the Martin Schwinger hierarchy [103].

That said for systems consisting of coupled bosons and fermions, the two point correlation function is given by the *Green's function* defined as

$$G(z,z') \equiv -i\langle\mathcal{T}_\gamma\{\tilde{c}(z)\tilde{c}^\dagger(z')\}\rangle = -i\mathrm{Tr}[\mathcal{T}_\gamma\{e^{-\frac{i}{\hbar}\int_\gamma dz H_0(z)}c(z)c^\dagger(z')\}], \qquad (4.27)$$

The expression in equation (4.27) involves a bosonic/fermionic annihilation operator c, and the angular brackets denote averaging over the density matrix of the initial state. This equation is a straightforward extension of the Keldysh contour GFs [62], but it is important to

note that z and z' are defined on the contour shown in Fig. 4.1C, as opposed to the standard Keldysh contour.

By utilizing the aforementioned derivatives of the two-point correlation function G_{A_1,A_2}, it is possible to derive expressions for a bosonic operator a that is governed by the Hamiltonian $H_0 = \omega a^\dagger a$. Specifically, we obtain:

$$\begin{aligned} -i\frac{d}{dz'}\langle \mathcal{T}_\gamma\{a(z)a^\dagger(z')\}\rangle &= \langle \mathcal{T}_\gamma\{a(z)[\omega a^\dagger(z')a(z'), a^\dagger(z')]\}\rangle + i[a(z), a^\dagger(z')]\delta(z-z') \\ &= \omega\langle \mathcal{T}_\gamma\{a(z)a^\dagger(z')\}\rangle + i\delta(z-z'), \end{aligned} \tag{4.28}$$

where the δ-term appears because, if $z' > z$, the ordering operator switches the position of a and $a^\dagger$. Substituting the definition of the Green's function into the equation above, we have for a bosonic Green's function,

$$\frac{d}{dz'}G_b^{(0)}(z,z') = i\omega G_b^{(0)}(z,z') + i\delta(z-z'). \tag{4.29}$$

We can derive the same equation for a fermionic operator c as follows,

$$\begin{aligned} -i\frac{d}{dz'}\langle \mathcal{T}_\gamma\{c(z)c^\dagger(z')\}\rangle &= \langle \mathcal{T}_\gamma\{c(z)[\omega c^\dagger(z')c(z'), c^\dagger(z')]\}\rangle + i[c(t'), c^\dagger(t')]\delta(z-z') \\ &= \omega\langle \mathcal{T}_\gamma\{c(z)c^\dagger(z')\}\rangle + i\delta(z-z'), \end{aligned} \tag{4.30}$$

which is formally identical to Eq. (4.29). The solution of Eq. (4.29) for a generic GF reads

$$G_{b,f}^{(0)}(z,z') = -ie^{-i\omega(z-z')}\left\{A\left[\Theta(z-z') + \Theta(z'-z)\right] + \Theta(z-z')\right\}. \tag{4.31}$$

The value of the constant A in the aforementioned equation can be calculated using boundary conditions [103]. Specifically, if we substitute either of the contour arguments with the earliest and latest time instances on the contour, the results should be identical for bosons or differ by a sign for fermions. For a two-point GF, we can therefore derive:

$$\begin{aligned} G_{b,f}^{(0)}(-i\hbar\beta, t') &= \pm G_{b,f}^{(0)}(0,t'), \\ G_{b,f}^{(0)}(t, -i\hbar\beta) &= \pm G_{b,f}^{(0)}(t,0), \end{aligned} \tag{4.32}$$

which leads to obtaining

$$G_{b,f}^{(0)}(z,z') = -ie^{-i\omega(z-z')}\left[\pm n\Theta_\gamma(z'-z) + \bar{n}\Theta_\gamma(z-z')\right]. \tag{4.33}$$

In the equation above, the upper (lower) sign corresponds to bosons (fermions), $\bar{n} = 1 \pm n$, and $n = n_{b,f}(\omega) = (e^{\hbar\beta\omega} \mp 1)^{-1}$ represents the Bose (Fermi) distribution function associated with frequency ω. Similar to standard Schwinger-Keldysh theory, the contour Green's function lacks a clear physical interpretation. However, its components can be obtained by restricting the z and z' variables to specific branches of the contour (denoted by $\pm$ subscripts) such as

$$\begin{aligned} G^{(0)}_{b,f}(t_+, t'_-) &= G^{(0)>}_{b,f}(t_+, t'_-) = -i\bar{n}e^{\hbar\omega\lambda}e^{-i\omega(t-t')}, \\ G^{(0)}_{b,f}(t_-, t'_+) &= G^{(0)<}_{b,f}(t_-, t'_+) = \mp ine^{-\hbar\omega\lambda}e^{-i\omega(t-t')}, \end{aligned} \tag{4.34}$$

The components of the contour Green's function $G_{A_1,A_2}(z, z')$ have physical meaning only when we restrict z and z' to selected branches of the contour. The greater ($>$) and lesser ($<$) components are obtained by restricting the domain of z and z' to γ_- and γ_+ branches, respectively, and are given by Eq.(4.34). The λ-dependent displacement between γ_- and γ_+ tracks gives rise to the dependence of the components on λ. Other components can be obtained by choosing different contour arguments, such as the time-ordered and anti-time-ordered components, which are λ-independent and are defined as $G^{(0)T}_{b,f}(t-, t'-) \equiv G^{(0)}_{b,f}(t_-, t'-)$ and $G^{(0)\bar{T}}_{b,f}(t_+, t'+) \equiv G^{(0)}_{b,f}(t_+, t'_+)$, respectively. When $\lambda = 0$ and $t = t'$, the Eqs.(4.34) represent the components of the non-interacting density matrix [90]. Choosing instead both time arguments on γ_- or γ_+ we obtain the time ordered and anti-time ordered GF

$$\begin{aligned} G^{(0)T}_{b,f}(t_-, t'_-) &= -ie^{-i\omega(t-t')}\big[\pm n\Theta(t'-t) + \bar{n}\Theta(t-t')\big], \\ G^{(0)\bar{T}}_{b,f}(t_+, t'_+) &= -ie^{-i\omega(t-t')}\big[\pm n\Theta(t-t') + \bar{n}\Theta(t'-t)\big], \end{aligned} \tag{4.35}$$

where Θ is the Heaviside step function on the real axis. These functions coincide with the conventional Green's functions, and other components can be obtained by choosing different arguments on the contour. For example, one can define mixed non-interacting Green's functions such as $G^{(0)}_{b,f}(t, i\tau)$ for $t \in \gamma_\pm$ and $i\tau \in \gamma_\uparrow$, which are relevant when considering the more general assumption (4.12). However, these new Green's functions do not play a role in discussing the work statistics in the switching on/off scenario (4.11).

As a matter of fact, we can define a non-interacting GF with both arguments on the vertical track, $G^{(0)\uparrow\uparrow}_{b,f}(r, r') \equiv G^{(0)}_{b,f}(ir, ir')$ with $ir, ir' \in \gamma_\uparrow$. As a consequence we have

$$G^{(0)\uparrow\uparrow}_{b,f}(r, r') = -ie^{\omega(r-r')}\big[\pm n\Theta(r'-r) + \bar{n}\Theta(r-r')\big]. \tag{4.36}$$

Another possibility is represented by the case in which one argument is on the horizontal branches and one on $\gamma_\uparrow$. We can identify four different cases $G_{b,f}^{(0)\uparrow+}(r,t) = G_{b,f}^{(0)}(ir,t)$, $G^{(0)\uparrow-}(r,t) = G_{b,f}^{(0)}(ir,t)$, $G_{b,f}^{(0)+\uparrow}(t,r) = G_{b,f}^{(0)}(t,ir)$, $G_{b,f}^{(0)-\uparrow}(t,r) = G_{b,f}^{(0)}(t,ir)$. We explicitly write this four new components below

$$\begin{aligned} G_{b,f}^{(0)\uparrow+}(r,t') &= \mp i n e^{\omega(r-\lambda)+i\omega(t_f-t')}; \quad G_{b,f}^{(0)\uparrow-}(r,t') = -i\bar{n}e^{\omega r+i\omega(t'-t_f)}; \\ G_{b,f}^{(0)+\uparrow}(t,r') &= -i\bar{n}e^{-\omega(r-\lambda)-i\omega(t_f-t')}; \quad G_{b,f}^{(0)-\uparrow}(t,r') = \mp i n e^{-\omega r-i\omega(t'-t_f)}. \end{aligned} \tag{4.37}$$

These definitions enable the extension of the theory to protocols that go beyond the switching on/off paradigm, where the function $\chi(z)$ is defined as in Eq. (4.12). With the Green's functions now defined on the modified contour, we can proceed to explore the perturbation theory of the work generating function.

4.5 Cumulant generating function of work for a weak perturbation

Within the perturbative framework we can expand the second integral in the numerator of Eq. (4.21) in terms of correlation functions of arbitrary order, and obtain an expression of the form

$$\begin{aligned} M_W(\lambda,t_f) = \sum_{n=0}^{\infty}\frac{1}{n!}\left(-\frac{i}{\hbar}\right)^n\int_\gamma dz_1\ldots dz_n\times \\ \times\frac{\mathrm{Tr}[\mathcal{T}_\gamma\{e^{-\frac{i}{\hbar}\int_\gamma dz H_0(z)}\chi(z_1)H_1(z_1)\ldots\chi(z_n)H_1(z_n)\}]}{\mathrm{Tr}[\mathcal{T}_\gamma e^{-\frac{i}{\hbar}\int_\gamma dz H_0(z)}]}. \end{aligned} \tag{4.38}$$

Each order n corresponds to an n-point correlation function of the Hamiltonian H_1. Assuming H_1 to be a linear combination of fermionic and bosonic creation and annihilation operators, Wick's theorem can be used to decompose these correlation functions into non-interacting Green's functions [103, 90]. Importantly, the expansion of the correlation functions in non-interacting Green's functions is identical to standard perturbation theory because Wick's theorem follows from the commuting (or anti-commuting) algebra of the operators $c, c^\dagger$, which holds regardless of the integration contour.

The diagrammatic representation of the discussion follows standard perturbation theory, with the Feynman diagrams in Eq. (4.38) being identical except for the contour of integration for the vertex variables $z_1,\ldots,z_n$ and the non-interacting Green's functions from Eq. (4.33). For instance, let us consider the second-order perturbation theory of the Hamiltonian

$H_1 = \hbar\omega_\chi(a + a^\dagger)c^\dagger c$, where c and a are the annihilation operators for a fermionic and a bosonic mode, respectively. The second-order contribution ($n = 2$) in Eq.(4.38) comprises two connected Feynman diagrams, represented by the upper and lower panel diagrams in Fig. 4.2a. Focusing on the former, denoted as $M_W^{(2),1}(\lambda, t)$, we find

$$M_W^{(2),1}(\lambda, t_f) = -i\omega_\chi^2 \iint_\gamma dz_1 dz_2 \chi(z_1)\chi(z_2) G_b^{(0)}(z_1, z_2) G_f^{(0)}(z_1, z_2) G_f^{(0)}(z_2, z_1). \quad (4.39)$$

For the switching on/off protocol of in Eq. (4.11), we divide the integration over γ into two contributions of integration over γ_- and γ_+ (similar approach has been introduced before by Langreth [70]), we rewrite the above integral in terms of the components of the GFs such that

$$\begin{aligned} M_W^{(2),1}(\lambda, t_f) &= i\omega_\chi^2 \iint_0^{t_f} dt_1 dt_2 \chi(t_1)\chi(t_2) \times \\ \times \Big\{ & G_b^{(0)\bar{T}}(t_1, t_2) G_f^{(0)\bar{T}}(t_1, t_2) G_f^{(0)\bar{T}}(t_2, t_1) + G_b^{(0)T}(t_1, t_2) G_f^{(0)T}(t_1, t_2) G_f^{(0)T}(t_2, t_1) \\ & - G_b^{(0)>}(t_1, t_2) G_f^{(0)>}(t_1, t_2) G_f^{(0)<}(t_2, t_1) - G_b^{(0)<}(t_1, t_2) G_f^{(0)<}(t_1, t_2) G_f^{(0)>}(t_2, t_1) \Big\}. \end{aligned} \quad (4.40)$$

In a similar manner to the correspondence between Eq. (4.39) and Fig. 4.2a, we can establish a relationship between the four terms in Eq. (4.40) and specific Feynman diagrams. These diagrams incorporate a "charge" $\pm$ that reflects the position of the vertex variables on the contour. An illustration of these diagrams can be seen in Fig. 4.2b.

Among these terms, the time-ordered and anti-time-ordered components remain independent of the parameter λ. On the other hand, the $G^{<,>}$ functions include an exponential factor of $e^{\pm\hbar\omega\lambda}$ that encodes the frequency $\hbar\omega$ (as indicated in Eq. (4.34)). This factor captures the energy transfer associated with the corresponding propagator.

The diagrammatic representation thus allows us to visually connect the mathematical expressions with the underlying physical processes, highlighting the role of the vertex variables and the significance of the frequency-dependent terms in the Green's functions.

The simplicity of this dependence allows us to introduce the concept of energy transferred in a "charged" diagram d, denoted as E^d. This energy transfer is defined as $E^d = \hbar \sum_i s_i^d \omega_i$, where the sum runs over all propagators in the diagram, and s_i^d takes on values of 0, -1, or 1 depending on the nature of the propagator i in diagram d. Specifically, if the propagator is a $G^<$ function, we set $s_i^d = -1$; if it is a $G^>$ function, we set $s_i^d = 1$; and if it is a $G^{T,\bar{T}}$ function, we set $s_i^d = 0$.

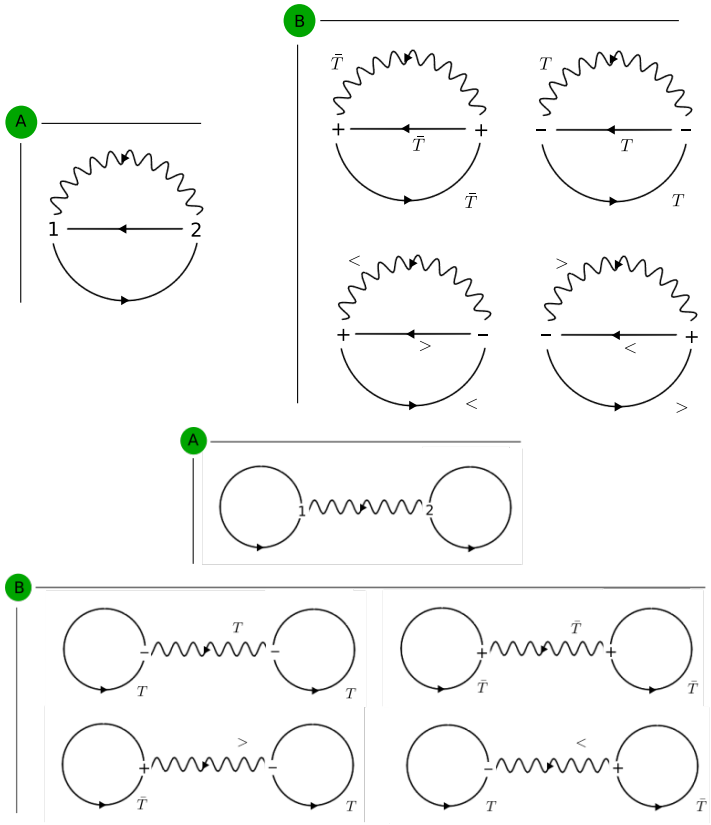

FIGURE 4.2: An example of how different Keldysh components appears in the form of Feynman diagram. In both top and bottom figures, the diagram on the left denotes the Fyenman diagram while the diagrams on the right are the diagrams related to the components of the Green's functions. The solid and wiggly lines denote the fermionic and bosonic non-interacting GFs, respectively [20].

Each diagram contributes to the generating function with a factor of $\Gamma_d(t)e^{\lambda E^d}$, where $\Gamma_d(t)$ represents a prefactor associated with the contribution of the diagram. This prefactor can be determined by evaluating the contribution of the diagram itself, typically through the calculation of a corresponding double integral over the time variables. For example, in the case of Eq. (4.40), one can obtain $\Gamma_d(t)$ by computing the relevant double integral.

For convenience we introduce the cumulant generating function (CGF), given by the logarithm of Eq. (4.8),

$$C_W(\lambda, t_f) = \log \mathrm{Tr}[\mathcal{T}_\gamma\{e^{-\frac{i}{\hbar}\int_\gamma dz H_\gamma(z)}\}] - \log \mathrm{Tr}[\mathcal{T}_\gamma\{e^{-\frac{i}{\hbar}\int_\gamma dz H_0(z)}\}]. \tag{4.41}$$

As a consequence of the linked cluster theorem, above diagrammatic expansion of each of the two logarithms contains only connected diagrams (see for example [103], chapter 11). Therefore we obtain the following general formula for the CGF

$$C_W(\lambda, t_f) = \sum_{d,\text{conn.}} \Gamma_d(t)(e^{\lambda E_d} - 1). \tag{4.42}$$

The index d in the sum in Eq.(4.42) runs over all the connected charged diagrams. The cumulative generating function (CGF) in Eq.(4.42) can be understood as a sum of independent Poisson processes that are rescaled with average rates $\Gamma_d(t)$ and energy jumps given by E_d. Each diagram represents a distinct channel that enables the exchange of quantized energy E_d with a Poissonian rate $\Gamma_d(t)$. The universality of Eq. (4.42) is a consequence of the Poisson law of rare events since, within the perturbative framework, the rates of energy exchange processes are small. In the next subsections, we study two examples that can be used as a verification of this result.

4.5.1 Dispersive coupling

In the case of the dispersive coupling model $H_1 \approx (a + a^\dagger)c^\dagger c$ we can verify the result of Eq. (4.42) by direct calculation of the CGF using the matrix form of the time evolution operator. The total Hamiltonian is given by

$$H = \hbar\omega_b a^\dagger a + \hbar\omega_f c^\dagger c + \hbar\chi\omega_\chi c^\dagger c(a^\dagger + a). \tag{4.43}$$

The bosonic and fermionic annihilation operators are denoted by a and c, respectively. The CGF can be obtained using Eq.4.42, with the Feynman diagram for the second-order expansion of Eq.(4.38) shown in Fig. 4.2a. The diagrams in Fig. 4.2b on the top are labeled as

$d = 1,\ldots,4$, while those on the bottom are labeled as $d = 5,\ldots,8$. The diagrams with $E_d = 0$ for $d = 1,2,5,6$ contribute nothing to the CGF (4.42).

The contribution to the cumulant generating function comes from the three propagators in the third and fourth diagrams of Fig. 4.2:

$$C_W^{(2)}(\lambda,t_f)_{d=3,4} =$$
$$i\chi^2\omega_\chi^2\int_0^{t_f}\int_0^{t_f} dt_1dt_2 G_f^{(0)<}(t_1,t_2)G_f^{(0)>}(t_2,t_1)[G_b^{(0)>}(t_1,t_2) - G_b^{(0)>}(t_1,t_2)|_{\lambda=0}]$$
$$i\chi^2\omega_\chi^2\int_0^{t_f}\int_0^{t_f} dt_1dt_2 G_f^{(0)<}(t_1,t_2)G_f^{(0)>}(t_2,t_1)[G_b^{(0)<}(t_1,t_2) - G_b^{(0)<}(t_1,t_2)|_{\lambda=0}]. \tag{4.44}$$

The prefactor $-\frac{1}{2}\times 2\times -1\times i^3\times -1 = i$ arises due to various factors. The term $-\frac{1}{2}$ appears in every second-order diagram, while the factor of 2 accounts for the two possible ways of exchanging the two vertices in Fig. 4.2. The single $+$ in Fig. 4.2*b* contributes a factor of -1, and the factor of i^3 comes from the definition of many-body Green's function (refer to Eqs. (4.27) and (4.39)). Lastly, the factor of -1 is prescribed by the Wick theorem (see, for instance, [103]).

The energy jumps for these diagrams $d = 3,4$ are $E_3 = -\hbar\omega_b$ and $E_4 = \hbar\omega_b$, respectively, where we can verify them directly by replacing the components in Eq. (4.44),

$$C_W^{(2)}(\lambda,t_f)_{d=3,4} = \frac{2\chi^2\omega_\chi^2}{\omega_b^2}(1-\cos(\omega_b t_f))[n_f(\omega_f) - n_f(\omega_f)^2]$$
$$\times[(1+n_b(\omega_b))(e^{\hbar\omega_b\lambda}-1) + n_b(e^{-\hbar\omega_b\lambda}-1))]. \tag{4.45}$$

By direct comparison with Eq. (4.42), we find

$$\Gamma_3(t_f) = \gamma_{\omega_b}(t_f)[n_f(\omega_f) - n_f^2(\omega_f)][1+n_b(\omega_b)],$$
$$\Gamma_4(t_f) = \gamma_{\omega_b}(t_f)[n_f(\omega_f) - n_f^2(\omega_f)]n_b(\omega_b), \tag{4.46}$$

with $\gamma_{\omega_b}(t_f) = \frac{2\chi^2\omega_\chi^2}{\omega_b^2}[1-\cos(\omega_b t_f)]$. The diagrams $d = 7,8$ represented in Fig. 4.2 give the same contributions as the ones computed for $d = 3,4$ with only change that the prefactor $(-n_f^2 + n_f)$ will be exchanged with n_f^2. Summing all the contributions, we obtain

$$C_W^{(2)}(\lambda,t_f) = \sum_{\pm}\gamma_{\omega_b}(t_f)n_f(\omega_f)n_b(\mp\omega_b)(e^{\pm\hbar\omega_b\lambda}-1). \tag{4.47}$$

To verify this result we calculate the CGF directly. In fact, the fermionic operators in the

Hamiltonian (4.43) can be expressed as Pauli matrices acting over a two dimensional Hilbert space, by defining $\sigma^+ = c^\dagger$, $\sigma^z = 2c^\dagger c - 1$. The anticommutation relations $\{\sigma^-, \sigma^+\} = \{c, c^+\} = 1$ are preserved and we obtain

$$H = \hbar\omega_b a^\dagger a + \hbar\left(\frac{\sigma_z}{2} + \frac{1}{2}\right)(\omega_f + \chi\omega_\chi a^\dagger + \chi\omega_\chi a). \tag{4.48}$$

The Hamiltonian commutes with σ_z, so we can write the time evolution operator as

$$U(t,0) = \mathcal{T}\{e^{-\frac{i}{\hbar}\int_0^t H(s)ds}\} = \begin{pmatrix} e^{-\frac{i}{\hbar}(\hbar\omega_b a^\dagger a + \hbar\omega_f + \hbar\chi\omega_\chi a^\dagger + \hbar\chi\omega_\chi a)t} & 0 \\ 0 & e^{-i\omega_b a^\dagger a t} \end{pmatrix}. \tag{4.49}$$

The top-left element of the matrix (4.49) is the same as from a driven harmonic oscillator. We can define $H_b = \hbar\omega_b(a^\dagger a + 1/2)$ and

$$\langle 1|e^{-\frac{i}{\hbar}Ht}|1\rangle = e^{-i(\omega_f - \omega_b)t} e^{-\frac{i}{\hbar}H_b t - i\chi\omega_\chi(a+a^\dagger)t}, \tag{4.50}$$

the exponential above can be written in terms of displacement operators [19]

$$e^{-\frac{i}{\hbar}H_b t - i\chi\omega_\chi(a+a^\dagger)t} = e^{\frac{i}{\hbar}\theta(t)} D[\delta(t)] e^{-\frac{i}{\hbar}H_b t}, \tag{4.51}$$

where $\theta(t)$ is a phase factor and

$$D[\delta(t)] = \exp\Big\{(\delta(t)a^\dagger - \delta^*(t)a)\Big\}, \tag{4.52}$$

is the displacement operator of argument $\delta(t)$. The time dependent parameter $\delta(t)$ is connected to the classical solution for the Hamilton equations for the variable $\alpha(t) = \frac{x(t)+ip(t)}{\sqrt{2}}$, with $\alpha(0) = 0$. This variable evolve as $\alpha(t) = \alpha e^{-i\omega t} + \delta(t)$, where $\delta(t) = \frac{\chi\omega_\chi}{\omega_b}(1 - e^{-i\omega t})$. For counting the work statistics in the sudden quench scenario we have the following generating function

$$M_W(\lambda, t_f) = \frac{1}{Z}\mathrm{Tr}[e^{\lambda H_0} U(t_f,0) e^{-(\lambda+\beta)H_0} U^\dagger(t_f,0)], \tag{4.53}$$

so that it is clear using Eq. (4.49) that we have to evaluate the tilted displacement operator $D[\delta(t_f), \lambda] = e^{\lambda H_0} D[\delta(t_f)] e^{-\lambda H_0}$. Since $e^{\lambda H_0} e^{-\lambda H_0} = 1$ we can bring the two matrices at the exponent in the displacement operator and obtain

$$D[\delta(t_f),\lambda] = \exp\left[\delta(t_f)e^{\lambda H_0}a^\dagger e^{-\lambda H_0} - \delta^*(t_f)e^{\lambda H_0}ae^{-\lambda H_0}\right]$$
$$= \exp\left[\delta(t_f)e^{\hbar\lambda\omega_b}a^\dagger - \delta^*(t_f)e^{-\hbar\lambda\omega_b}a\right]. \tag{4.54}$$

Using Eq. (4.53) we find

$$M_W(\lambda,t_f) = \frac{1}{Z}\mathrm{Tr}[U^\dagger(t_f,0)U_\lambda(t_f,0)\begin{pmatrix} e^{-\hbar\beta\omega_b a^\dagger a}e^{-\hbar\beta\omega_f} & 0 \\ 0 & e^{-\hbar\beta\omega_b a^\dagger a}\end{pmatrix}]$$
$$= \frac{1}{Z}\mathrm{Tr}[\begin{pmatrix} D[-\delta(t_f)]D[\delta(t_f),\lambda] & 0 \\ 0 & 1\end{pmatrix}\begin{pmatrix} e^{-\hbar\beta\omega_b a^\dagger a}e^{-\hbar\beta\omega_f} & 0 \\ 0 & e^{-\hbar\beta\omega_b a^\dagger a}\end{pmatrix}], \tag{4.55}$$

Our focus lies in obtaining a weak perturbation expansion for the equation mentioned above. This entails considering the condition $\delta(t_f) \ll \omega_b$, allowing us to perform a Taylor expansion of $D[-\delta(t_f)]D[\delta(t_f),\lambda]$. In this expansion, we retain only the terms that contain an equal number of a and $a^\dagger$ operators. Meanwhile, terms with unequal numbers of these operators average out to zero, thereby playing no significant role in the expansion. Thus, we have

$$D[-\delta(t_f)]D[\delta(t_f),\lambda] = 1 + |\delta(t_f)|^2[(e^{\hbar\lambda\omega_b}-1)aa^\dagger + (e^{-\hbar\omega_b\lambda}-1)a^\dagger a] + O(\chi^3). \tag{4.56}$$

The final expression for $M(\lambda,t)$ thus reads

$$M_W(\lambda,t_f) = \frac{1}{Z_f}(1+e^{-\hbar\beta\omega_f}\{1+|\delta(t_f)|^2[(e^{\hbar\lambda\omega_b}-1)(1+n_b)+(e^{-\hbar\omega_b\lambda}-1)n_b]\})$$
$$= 1 + 4\frac{\chi^2\omega_\chi^2}{\omega_b^2}\sin^2\left(\frac{\omega_b t_f}{2}\right)n_f[(e^{\hbar\lambda\omega_b}-1)(1+n_b)+(e^{-\hbar\omega_b\lambda}-1)n_b], \tag{4.57}$$

computing the logarithm to find the expansion for the CGF and noting that $2\sin^2(\frac{\omega_b t_f}{2}) = 1-\cos(\omega_b t_f)$ we obtain and confirm the result of the Eq. (4.47).

4.5.2 Anharmonic oscillator

Another example of the application of our result is the anharmonic oscillator with Hamiltonian

$$H = \hbar\omega_b a^\dagger a + \hbar\chi\omega_\chi(a^{\dagger 2} + a^2). \tag{4.58}$$

The standard protocol involves preparing the system in a Gibbs state of the unperturbed Hamiltonian, turning on the anharmonic term at time zero, measuring the system's energy at times 0 and t before and after the perturbation, respectively. The vertex in Eq. (4.58) corresponds to two lines pointing inward or outward, which in the second order generates a single diagram in the form of a loop with two bosonic propagators between times t_1 and t_2. The contribution of this diagram yields the second-order cumulant generating function will be

$$C_W^{(2)}(\lambda, t_f) = 2\gamma_{2\omega_b}(t_f)[(e^{-2\hbar\lambda\omega_b} - 1)n_b^2 + (1+n_b)^2(e^{2\hbar\lambda\omega_b} - 1)]. \tag{4.59}$$

Similar to Eq. (4.42), this cumulant generating function contains two rescaled Poissonian energy jumps with energies $E_d = \pm 2\hbar\omega_b$ and rates given by $\gamma_{2\omega_b}(t_f)n_b^2$ and $\gamma_{2\omega_b}(t_f)(1+n_b)^2$, respectively.

4.5.3 Beyond switching on/off protocols

As we mentioned before, the other components of the Green's function (4.37) are useful when we want to deal with a scenario other than switching on/off. Considering a generic integral of a function in the modified contour we have

$$\begin{aligned}\int_\gamma \chi(z)f(z)dz &= \int_{\gamma_+} \chi(z)f(z)dz + \int_{\gamma_-} \chi(z)f(z)dz + \int_{\gamma_\uparrow} \chi(z)f(z)dz \\ &= \int_0^{t_f} \chi(t)f_-(t)dt - \int_0^{t_f} \chi(t)f_+(t)dt + i\chi(t_f)\int_0^{\hbar\lambda} f_\uparrow(r)dr,\end{aligned} \tag{4.60}$$

where $f_\uparrow, f_\pm$ are the components of the function f in the modified contour. Notice that the contribution of the downward and Matsubara tracks is absent. This is because we are implicitly assuming that $\chi(z) = 0$ on $\gamma_{M,\downarrow}$ as prescribed by the protocols (4.11) and (4.12). The same decomposition of the integral can be done for the equations arising from the perturbative expansion, such as Eq. (4.39).

For the ease of calculations, let us do them in the case in which the switching function is given by

$$\chi(z) = \begin{cases} 0 & \text{for } z \in \gamma_K, \\ 0 & \text{for } z \in \gamma_{M,\downarrow}, \\ \chi & \text{for } z \in \gamma_\uparrow. \end{cases} \tag{4.61}$$

In this scenario, the system undergoes a quench of the Hamiltonian $\omega_\chi H_1$, followed by an immediate measurement without allowing the system to evolve over time. We can compute the generating function for the Hamiltonian given in Eq. (4.43). The involved diagrams are the same as shown in panels A of Fig. 4.2, but we integrate over the vertical branch, and only the Green's function $G_{b,f}^{(0)\uparrow\uparrow}$ appears in the calculations. The integrals in Eq.(4.39) are then simplified to

$$\begin{aligned}
C_W^{(2)}(\lambda,t_f)_{d=1} &= i\chi^2\omega_\chi^2\int_0^\lambda\int_0^\lambda dr_1dr_2G_b^{(0)\uparrow\uparrow}(r_1,r_2)G_f^{(0)\uparrow\uparrow}(r_1,r_2)G_f^{(0)\uparrow\uparrow}(r_2,r_1)\\
&= -\chi^2\omega_\chi^2\int_0^\lambda\int_0^\lambda dr_1dr_2(-n_f\bar{n}_f)e^{\omega_b(r_1-r_2)}[n_b\Theta(r_2-r_1)+\bar{n}_b\Theta(r_1-r_2)]\\
&= \chi^2\omega_\chi^2n_f\bar{n}_f[n_b\frac{\hbar\lambda\omega_b+e^{-\hbar\lambda\omega_b}-1}{\omega_b^2}+\bar{n}_b\frac{-\hbar\lambda\omega_b+e^{\hbar\lambda\omega_b}-1}{\omega_b^2}]\\
&= \chi^2\omega_\chi^2\frac{n_f-n_f^2}{\omega_b^2}[n_b(e^{-\hbar\lambda\omega_b}-1)+(1+n_b)(e^{\hbar\lambda\omega_b}-1)-\hbar\lambda\omega_b].
\end{aligned}\tag{4.62}$$

$d=1$ indicates that the contribution of the diagram in Fig. 4.2 assumes the value of the vertex variables to be chosen in $\gamma_\uparrow$. The contribution of the dumbbell diagram is instead given by

$$\begin{aligned}
M_W^{(2)}(\lambda,t_f)_{d=2} &= -i\chi^2\omega_\chi^2\int_0^\lambda\int_0^\lambda dr_1dr_2G_b^{(0)\uparrow\uparrow}(r_1,r_2)G_f^{(0)\uparrow\uparrow}(r_1,r_1^+)G_f^{(0)\uparrow\uparrow}(r_2,r_2^+)\\
&= \chi^2\omega_\chi^2\int_0^\lambda\int_0^\lambda dr_1dr_2n_f^2e^{\omega_b(r_1-r_2)}[n_b\Theta(r_2-r_1)+\bar{n}_b\Theta(r_1-r_2)]\\
&= \chi^2\omega_\chi^2n_f^2[n_b\frac{\hbar\lambda\omega_b+e^{-\hbar\lambda\omega_b}-1}{\omega_a^2}+\bar{n}_b\frac{-\hbar\lambda\omega_b+e^{\hbar\lambda\omega_b}-1}{\omega_b^2}]\\
&= \frac{\chi^2\omega_\chi^2n_f^2}{\omega_b^2}[n_b(e^{-\hbar\lambda\omega_b}-1)+(1+n_b)(e^{\hbar\lambda\omega_b}-1)-\hbar\lambda\omega_b].
\end{aligned}\tag{4.63}$$

The CGF at second order can be obtained by summing the two contributions in (4.62) and (4.63).

We have examined the perturbation expansion for the work MGF in two distinct scenarios thus far. To establish the reliability of this perturbative expansion, we investigate the symmetries of the modified contour as a means to demonstrate its consistency.

4.6 Fluctuation theorems

In this section, we will explore a fluctuation symmetry that connects the MGF of the work extraction process, M_W, with that of the time-reversed process, M_W^{rev}. We assume that the

system is initially in the Gibbs state, so that the Hamiltonian at $t = 0$ is equal to the unperturbed Hamiltonian, $H_M = H(0) = H_0$. To compute M_W^{rev}, we introduce the time-reversed process, where the system is initialized in the Gibbs state $\rho_{\text{rev}}(0) = e^{-\beta H(t_f)}/Z(t_f)$ and undergoes a time-reversed evolution. The time-reversed evolution consists of a time-reversal operation Ξ, such that $\Xi = \Xi^{-1}$ and $\Xi i = -i\Xi$, and a forward evolution in which the driving protocol is reversed, i.e., $H_{\text{rev}}(s) = H(t_f - s)$ (assuming that the Hamiltonian does not depend on a magnetic field B)

$$\Xi\rho_{\text{rev}}(t_f)\Xi = U_{\text{rev}}(t_f,0)\Xi\rho_{\text{rev}}(0)\Xi U_{\text{rev}}^{\dagger}(t_f,0), \tag{4.64}$$

where $U_{\text{rev}}(t_f,0) = \mathcal{T}[\exp\left(-i\int_0^{t_f} H_{\text{rev}}(s)ds\right)]$. Using Eq. (4.64) and $\Xi U^{\text{rev}}(t_f,0)\Xi = U^{\dagger}(t_f,0)$ we can write the following chain of equalities

$$\begin{aligned} M_W(\lambda,t_f) &= \frac{1}{Z(0)}\text{Tr}[Ue^{-\beta H(0)}e^{-\lambda H(0)}U^{\dagger}e^{\lambda H(t_f)}] \\ &= \frac{1}{Z(0)}\text{Tr}[Ue^{-\beta H(0)}e^{-\lambda H(0)}U^{\dagger}e^{(\lambda+\beta)H(t_f)}e^{-\beta H(t_f)}] \\ &= \frac{1}{Z(0)}\text{Tr}[U^{\dagger}e^{(\lambda+\beta)H(t_f)}e^{-\beta H(t_f)}Ue^{-(\lambda+\beta)H(0)}] \\ &= \frac{Z(t)}{Z(0)}M_W^{\text{rev}}(-\beta-\lambda,t_f). \end{aligned} \tag{4.65}$$

After introducing the free energy difference as $Z(t_f)/Z(0) = e^{-\beta\Delta F}$ the above result leads to the fluctuation symmetry

$$M_W(\lambda,t_f) = e^{-\beta\Delta F}M_W^{\text{rev}}(-\beta-\lambda,t_f). \tag{4.66}$$

To express the symmetry in the contour framework, it is important to note that the dependence of Eq. (4.8) on the counting field and final time is incorporated through the modified contour γ shown in Fig. 4.1C. Thus, each step in the derivation of Eq. (4.65) can be viewed as a transformation of the contour itself, as illustrated in Fig. 4.2. The geometric symmetry can be expressed by explicitly showing the dependence on λ, i.e., $\gamma_\lambda = \gamma^{\text{rev}}_{-\lambda-\beta}$, and the ratio between the weighted generating function of the forward and time-reversed processes becomes

$$\frac{M_W(\lambda,t_f)Z(t_f)}{M_W^{\text{rev}}(-\lambda-\beta,t_f)Z(0)} = \frac{\text{Tr}[\mathcal{T}_\gamma\{e^{-i\int_{\gamma_\lambda}H(z)dz}\}]}{\text{Tr}[\mathcal{T}_{\gamma^{\text{rev}}_{-\lambda-\beta}}\{e^{-i\int_{\gamma^{\text{rev}}_{-\lambda-\beta}}H(z)dz}\}]} = 1, \tag{4.67}$$

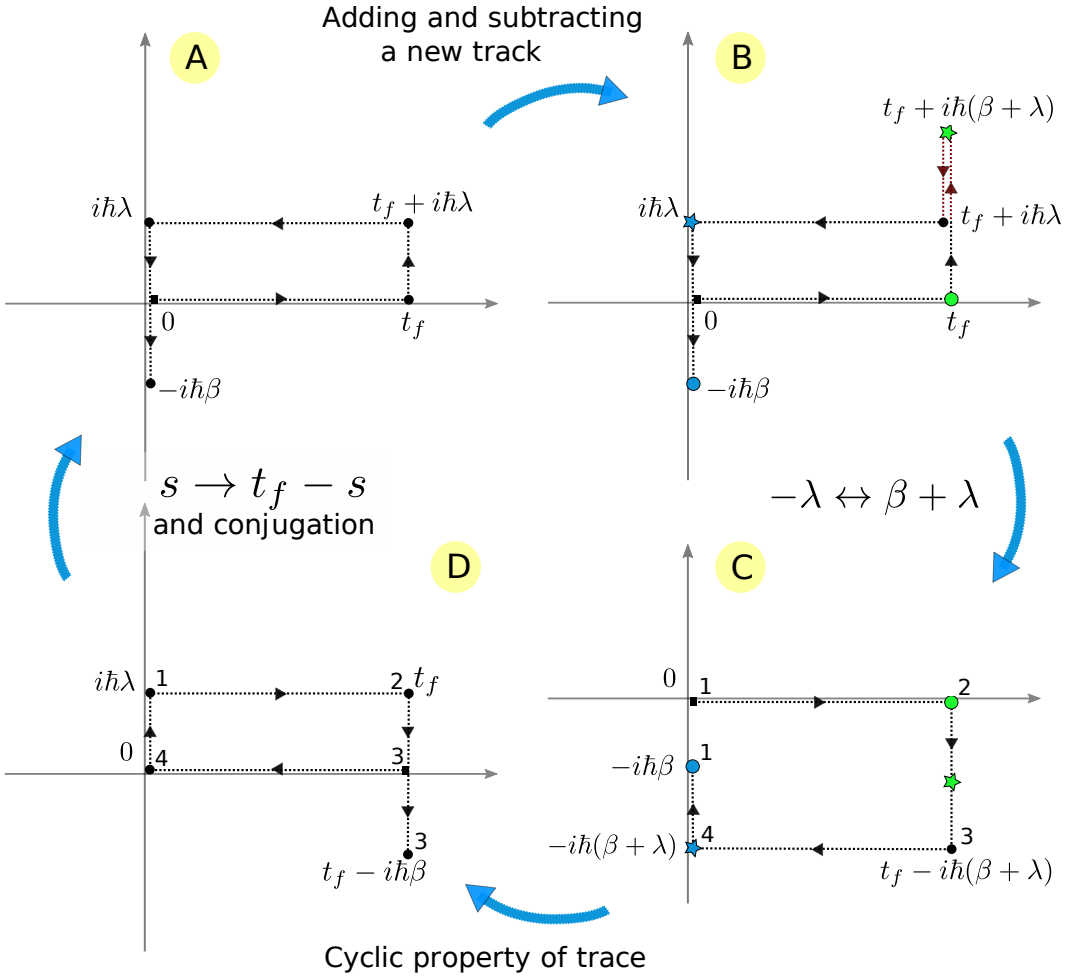

FIGURE 4.3: A visual representation illustrating the proof of Eq. (4.65) is presented. The connection between exponentials of time-dependent Hamiltonians and contour tracks enables a convenient analogy. By multiplying and dividing by the exponential of $-\beta H(t)$, we can equivalently add and subtract a new track ($1 \to 2$) in the graphical depiction. The exchange of $-\lambda$ with $\beta + \lambda$ corresponds to an inversion of the blue and green dots ($2 \to 3$). The cyclic property of the trace, employed in the last step of the equalities (4.65), can be visualized as removing slices from the end of the contour and attaching them at $z = 0$ ($3 \to 4$). The final step demonstrates that contour 4 is indeed associated with the backward evolution of the original contour ($4 \to 1$) [20].

that is equivalent to the result (4.66). The proof of the FT based on the contour γ depicted in Fig. 4.1 C is a fundamental structural symmetry of any theory that relies on this contour, and is essential to demonstrate the thermodynamic consistency of the perturbation theory explained in the subsequent sections. This symmetry guarantees that the FT holds for all orders of the perturbation in equation (4.38), since the Green's function (4.33) and the integrations in (4.38) are all defined on the modified contour. Consequently, the fluctuation symmetry implies that the perturbation expansion of the time-reversed MGF will coincide with that of the forward MGF for the switching on/off scenario, thereby preserving this symmetry at all orders of the expansion.

At this point we may also discuss fluctuation theorem at the level of the single Feynman diagrams.We can introduce time-reversed diagrams by examining the time-reversed generating function. Suppose we have two points z and z' on the contour used to calculate M_W in Fig. 4.1c or Fig. 4.3a. We can also choose the same two points on the contour used for M_W^{rev}, as shown in Fig. 4.3d. If we take $z = t$ and $z' = t' + i\lambda$, then we obtain

$$G_{b,f}^{(0)}(z,z') = G_{b,f}^{(0)<}(t,t') = G_{b,f\,\text{rev}}^{(0)>}(t,t'). \tag{4.68}$$

Let us consider $G_{\text{rev}}^{(0)>}$ as the greater component of the Green's function (GF) on the contour of M_W^{rev}. The relationship in equation (4.68) is derived from the inversion of the forward and backward branches in the two contours depicted on the left side of Fig. 4.3. However, the time-ordered and anti-time-ordered components remain unaffected by the relative positions of the branches. Thus, we have $G_{b,f}^{(0)T}(t,t') = G_{b,f\text{rev}}^{(0)T}(t,t')$ and $G_{b,f}^{(0)\bar{T}}(t,t') = G_{b,f\text{rev}}^{(0)\bar{T}}(t,t')$.

If we interpret z and z' as vertex variables in a switching-on/off protocol, similar to Eq.(4.11), then Eq.(4.68) implies that for every diagram involved in the calculation of M_W, there exists a corresponding diagram in the calculation of M_W^{rev} with the time arguments chosen in the same branches. However, the two diagrams have different weights due to the exchange of the lesser and greater Green's functions in Eq.(4.68). The ratio of the contributions from these two diagrams can be computed using Eq.(4.34) and the properties of the GFs.

$$\frac{G_{b,f}^{(0)<}(t,t')}{G_{b,f}^{(0)>}(t,t')} = \pm e^{-\beta\hbar\omega} e^{-2\lambda\hbar\omega}. \tag{4.69}$$

In summary, the ratio of the contribution of a "charged" diagram and its time-reversed counterpart is multiplied by a factor of $\pm e^{\beta\hbar\omega} e^{-2\lambda\hbar\omega}$ for every lesser GF, and a factor of $\pm e^{-\beta\hbar\omega} e^{+2\lambda\hbar\omega}$ for every greater GF present in the original diagram, where ω represents the

frequency of the corresponding fermionic/bosonic mode. In Section 4.5, we introduced E_d and setting $\lambda = 0$, resulting in the relationship between the weights $\Gamma_d(t_f)$ and $\Gamma_d^{\text{rev}}(t_f)$ of a given diagram and its time-reversed counterpart:

$$\frac{\Gamma_d(t_f)}{\Gamma_d^{\text{rev}}(t_f)} = e^{\beta E_d}, \tag{4.70}$$

where the sign contribution $\pm$ in Eq. (4.69) can be neglected by assuming that the interaction Hamiltonian contains an even number of fermionic fields. The Crooks fluctuation relation in Eq. (4.70) can be interpreted as a diagrammatic representation of the detailed balance conditions [1, 69, 91, 101]. It is worth noting that the requirement in Eq. (4.70) is more stringent than the FT for the CGF, $C_W(\lambda, t_f) = C_W^{\text{rev}}(\lambda, t_f)$, since it applies to individual transitions rather than the overall statistics. Furthermore, one can derive the FT for the CGF from Eqs. (4.70) and (4.42) in a straightforward manner.

In conclusion, we have developed a perturbative expansion on the modified contour that is consistent at all perturbative orders, satisfying the fluctuation theorem. However, as we have also discussed in chapter 2 regarding heat generating functions, it is also possible to study the Feynman path integral representation of the generating functions. Therefore, In the upcoming sections, we will investigate the application of Feynman path integral techniques to the modified contour framework.

4.7 Path integrals on the modified contour

To go beyond perturbation theory, one can express Eq. (4.8) in terms of path integrals [41, 42, 9]. which can be considered as an extension of the usual Feynman path integral approach on the Keldysh contour [113, 100, 35]. Employing this approach, we will find out that the modified contour is in fact particularly suitable for work statistics and for describing the semiclassical limit of the MGF by performing an expansion for small values of $\hbar$ of the generating function [86]. Considering the Hamiltonian of a single particle in an external potential we can write,

$$H(t) = \frac{P^2}{2m} + V[\alpha(t), X], \tag{4.71}$$

where P is the momentum operator, m is mass and $V[\alpha(t), X]$ is a single particle potential in the particle position X, which depends parametrically on an external driving parameter $\alpha(t)$. Inserting the Hamiltonian (4.71) into Eq. (4.8) and performing a Trotter decomposition of the contour-ordered exponentials, we obtain the path integral form of the moment generating

function,

$$M_W(\lambda, t_f) = \frac{1}{Z(0)} \int \mathcal{D}x(z)\mathcal{D}p(z) e^{\frac{i}{\hbar}S[x(z),p(z)]}, \tag{4.72}$$

where $p(z)$ and $x(z)$ are the momentum and position fields defined on the modified contour γ, $Z(0)$ is the partition function corresponding to the Hamiltonian at time 0 and S is the classical action

$$S = \int_\gamma dz \left\{ \frac{dx(z)}{dz} p(z) - H_\gamma[x(z), p(z)] \right\}. \tag{4.73}$$

In this presentation, we demonstrate the derivation of a measurement operator denoted as Λ, which corresponds to the total energy. It is given by the equation $\Lambda = \frac{P^2}{2m} + V(X)$. However, it should be noted that the formalism described can be applied to alternative measurement operators as well.

To facilitate the analysis, we divide the fields on the contour by assigning components to them, following a similar approach to that employed for the Green's functions (GFs). By defining the variable z as $z = t + i\tau$, we can express the aforementioned division as

$$x(z) = \begin{cases} x_-(t) & \text{for } z = t \in \gamma_-, \\ x_+(t) & \text{for } z = t + i\lambda \in \gamma_+, \\ x_\uparrow(\tau) & \text{for } z = t_f + i\tau \in \gamma_\uparrow, \\ x_\downarrow(\tau), x_M(\tau) & \text{for } z = i\tau \in \gamma_{\downarrow,M}, \end{cases} \tag{4.74}$$

and analogously for $p(z)$. To write the path integral in terms of the position coordinates we consider the quantity $\mathcal{S} = (i/\hbar S)$ in the exponent of the Eq. (4.72). We have

$$\mathcal{S} = \frac{i}{\hbar} \int_\gamma \left\{ \frac{d}{dz} x(z) p(z) - \frac{p(z)^2}{2m} - V[x(z)] \right\} dz, \tag{4.75}$$

where to simplify the notation, we omit the parameter α from the argument of V. The integration of the momentum variables yields different outcomes depending on the branch under consideration. Using discrete notation, the exponent of the path integral can be expressed as follows:

$$\text{on } \gamma_- \;\to\; -\frac{i}{\hbar}\frac{p^2(t)}{2m}\Delta t + \frac{i}{\hbar}\frac{dx(t)}{dt}p(t)\Delta t; \quad \text{on } \gamma_+ \;\to\; \frac{i}{\hbar}\frac{p^2(t)}{2m}\Delta t - \frac{i}{\hbar}\frac{dx(t)}{dt}p(t)\Delta t; \tag{4.76}$$

$$\text{on } \gamma_\uparrow \to \frac{p_\uparrow^2(\tau)}{2m}\Delta\tau - i\frac{dx_\uparrow(\tau)}{d\tau}p_\uparrow(\tau)\Delta\tau; \;\; \text{on } \gamma_{\downarrow,M} \to -\frac{p_{\downarrow,M}^2(\tau)}{2m}\Delta\tau + i\frac{dx_{\downarrow,M}(\tau)}{d\tau}p(\tau)\Delta\tau, \tag{4.77}$$

where we have assumed $z = t + i\tau$. After eliminating the momentum variables from the action of the path integral via gaussian integration, the new exponents on the different branches of the contour read

$$\begin{aligned} \text{on } \gamma_- \ &\rightarrow \ \frac{i}{2\hbar} m \left[\frac{dx(t)}{dt}\right]^2 \Delta t; \quad \text{on } \gamma_+ \ \rightarrow \ -\frac{i}{2\hbar} m \left[\frac{dx(t)}{dt}\right]^2 \Delta t; \\ \text{on } \gamma_\uparrow \ &\rightarrow \ \frac{1}{2} m \left[\frac{dx(\tau)}{d\tau}\right]^2 \Delta \tau; \quad \text{on } \gamma_\downarrow, \gamma_M \ \rightarrow \ -\frac{1}{2} m \left[\frac{dx(\tau)}{d\tau}\right]^2 \Delta \tau. \end{aligned} \tag{4.78}$$

The terms mentioned above contribute to the exponent in the path integral and can be expressed as iT, $-iT$, T, and $-T$, where T represents the kinetic energy. Upon reverting to the contour variable z, this contribution from the kinetic term combines with the potential energy and yields a modified expression:

$$\begin{aligned} \text{on } \gamma_- \ &\rightarrow \ (iT - iV)\Delta t = (iT - iV)\Delta z = i\mathcal{L} dz; \\ \text{on } \gamma_+ \ &\rightarrow \ (-iT + iV)\Delta t = (-iT + iV)(-\Delta z) = i\mathcal{L} dz; \\ \text{on } \gamma_\uparrow \ &\rightarrow \ (T + V)\Delta \tau = -i(T + V)\Delta z = i\mathcal{L}_\uparrow dz; \\ \text{on } \gamma_\downarrow, \gamma_M \ &\rightarrow -(T + V)\Delta \tau = i(T + V)(-\Delta z) = i\mathcal{L}_{\downarrow/M} dz. \end{aligned} \tag{4.79}$$

In total we can write the exponent of the path integral as

$$\mathcal{S} = \frac{i}{\hbar} \int_\gamma \mathcal{L}_\gamma \left[x(z), x'(z)\right] dz, \tag{4.80}$$

where $\mathcal{L}$ is defined on the contour as

$$\mathcal{L}_\gamma(z) = \begin{cases} \mathcal{L}[x(t), \dot{x}(t)] & \text{for } z \in \gamma_K, \\ \mathcal{L}_\uparrow, \mathcal{L}_\downarrow, \mathcal{L}_M & \text{for } z \in \gamma_{\uparrow,\downarrow,M}. \end{cases} \tag{4.81}$$

Therefore we will write

$$M_W(\lambda, t_f) = \frac{1}{Z(0)} \int \mathcal{D}' x(z) e^{\frac{i}{\hbar} S[x(z)]}, \tag{4.82}$$

where $\mathcal{D}' x(z)$ is the new measure of integration following the elimination of the momenta, and the Lagrangian action reads

$$S = \int_\gamma dz \ \mathcal{L}_\gamma \left[\alpha(z), x(z)\right], \tag{4.83}$$

where $\mathcal{L}_\gamma$ is the Lagrangian on the modified contour that according to the portion of the contour of interest can assume different forms as

$$\mathcal{L}_\gamma[\alpha(z), x(z)] = \begin{cases} \mathcal{L}[\alpha(t), x_-(t)] & z = t \in \gamma_-, \\ \mathcal{L}[\alpha(t), x_+(t)] & z = t + i\lambda \in \gamma_+, \\ \mathcal{L}_\uparrow[\alpha(t_f), x_\uparrow(\tau)] & z = t_f + i\tau \in \gamma_\uparrow \\ \mathcal{L}_{\downarrow,M}[\alpha(0), x_{\downarrow,M}(\tau)], & z = i\tau \in \gamma_{\downarrow,M}, \end{cases} \tag{4.84}$$

where we have

$$\begin{aligned} \mathcal{L}[\alpha(t), x(t)] &= \frac{1}{2}m\left[\frac{dx(t)}{dt}\right]^2 - V[\alpha(t), x(t)], \\ \mathcal{L}_\uparrow[\alpha(t_f), x_\uparrow(\tau)] &= -\frac{1}{2}m\left[\frac{dx_\uparrow(\tau)}{d\tau}\right]^2 - V[\alpha(t_f), x_\uparrow(\tau)], \\ \mathcal{L}_{\downarrow,M}[\alpha(0), x_{\downarrow,M}(\tau)] &= -\frac{1}{2}m\left[\frac{dx_{\downarrow,M}(\tau)}{d\tau}\right]^2 - V[\alpha(0), x_{\downarrow,M}(\tau)]. \end{aligned} \tag{4.85}$$

This observation suggests that the Lagrangian on the vertical branches corresponds to the negation of the classical energy. By utilizing the action-based generating function mentioned in Eq. (4.73), one can analyze the characteristics of work fluctuations at the path integral level and explore its semi-classical limit.

4.7.1 Symmetrization of the contour and Keldysh rotation

As per the quantum-classical correspondence principle [57], the generating function's semi-classical limit should yield its classical analogue at the first non-zero order in $\hbar$. Therefore, the path integral representation of the generating function (4.82) on the contour γ must replicate its stochastic path integral counterpart in an appropriate limit [105, 72, 53]. However, there exists a disparity between the domains of integration of the stochastic path integral, which is $[0, t_f]$, and the Keldysh contour [22, 77, 2]. In the path integral formulation of dynamics, this obstacle is surmountable since the forward (γ_-) and backward (γ_+) branches are identical. Consequently, integration on the Keldysh contour becomes integration on the segment $[0, t_f]$ of the forward and backward actions' difference [62]. To apply this reasoning to the contour depicted in Fig. 4.1c, we need to transform it to divide it equally into two halves. To achieve this symmetrization, we assign half of the vertical lines of $\gamma_\uparrow$, $\gamma_\downarrow$ and γ_M to an upper branch called $\gamma_\oplus$, while the other half of the lines goes to a lower branch,

$\gamma_\ominus$ (refer to Fig. 4.4 for a detailed description of this process). Subsequently, for the symmetrized contour in Fig. 4.4c, an argument $z \in \gamma_\oplus$ maps to $\gamma_\ominus$ via complex conjugation, which enables us to represent the action in Eq.(4.83) as

$$\begin{aligned} S &= \int_{\gamma_\ominus} \mathcal{L}_\gamma \left[x_\ominus(z), \alpha(z)\right] dz + \int_{\gamma_\oplus} \mathcal{L}_\gamma \left[x_\oplus(z), \alpha(z)\right] dz \\ &= \int_{\gamma_\ominus} \mathcal{L}_\gamma \left[x_\ominus(z), \alpha(z)\right] dz - \int_{\gamma_\ominus} \mathcal{L}_\gamma [x_\oplus(z^*), \alpha(z^*)] dz^* \\ &= \int_{\gamma_\ominus} \{\mathcal{L}_\gamma [x_\ominus(z), \alpha(z)] - \mathcal{L}_\gamma [x_\oplus(z^*), \alpha(z^*)]\}\, d\,\mathrm{Re}\; z \\ &+ i \int_{\gamma_\ominus} \{\mathcal{L}_\gamma [x_\ominus(z), \alpha(z)] + \mathcal{L}_\gamma [x_\oplus(z^*), \alpha(z^*)]\} d\,\mathrm{Im}\; z, \end{aligned} \tag{4.86}$$

In the last equation, we have split the differential dz into its real and imaginary parts. Following a similar procedure to the Keldysh rotation [89, 86, 88, 99], we can introduce the classical and quantum fields as:

$$x_{cl}(z) = \frac{1}{2}\left[x_\ominus(z) + x_\oplus(z^*)\right], \qquad x_q(z) = \frac{1}{2}\left[x_\ominus(z) - x_\oplus(z^*)\right]. \tag{4.87}$$

By substituting the above expressions into the action in Eq. (4.86), we can rewrite the generating function as a path integral over $\gamma_\ominus$. It is worth noting that the integrand of the action in Eq. (4.86) depends on the specific branch of the contour. For instance, $\mathrm{Im} : z$ vanishes on $\gamma_{(\ominus,-)}$, while $\mathrm{Re}\, z$ vanishes on $\gamma_{(\ominus,\uparrow)}$, $\gamma_{(\ominus,\downarrow)}$, and $\gamma_{(\ominus,M)}$. Therefore, it is convenient to separate the contributions of the horizontal and vertical branches, resulting in:

$$\begin{aligned} M_W(\lambda, t_f) = &\frac{1}{Z(0)} \int \mathcal{D}' x_{cl/q}(z) e^{\frac{1}{\hbar}\int_{\gamma_{(\ominus,\downarrow),(\ominus,M)}} \Sigma[x_{cl}(z), x_q(z)] d\,\mathrm{Im}\, z} \\ &\times e^{\frac{i}{\hbar}\int_{\gamma_{(\ominus,-)}} \mathcal{M}[x_{cl}(z), x_q(z)] d\,\mathrm{Re}\, z} e^{\frac{1}{\hbar}\int_{\gamma_{(\ominus,\uparrow)}} \Sigma[x_{cl}(z), x_q(z)] d\,\mathrm{Im}\, z}, \end{aligned} \tag{4.88}$$

where $\mathcal{D}' x_{cl/q}(z) = \mathcal{D}' x_{cl}(z) \mathcal{D}' x_q(z)$ and we introduced the functions

$$\begin{aligned} \Sigma &= -m\left(\dot{x}_{cl}^2 + \dot{x}_q^2\right) + V(\alpha, x_{cl} + x_q) + V(\alpha, x_{cl} - x_q), \\ \mathcal{M} &= 2m\dot{x}_{cl}\dot{x}_q - V(\alpha, x_{cl} + x_q) + V(\alpha, x_{cl} - x_q). \end{aligned} \tag{4.89}$$

Note that in equation (4.86), the field domain of the path integral is denoted as $\gamma_\ominus$, with the starting and ending points represented by $z = i\beta\hbar/2$ and $z = t_f$, respectively. As the forward and backward fields are equal at these points, the boundary conditions for Equation (4.88) are given by $x_q(t_f) = x_q(i\beta\hbar/2) = 0$.

Drawing inspiration from the classical case, where the fluctuating work can be defined

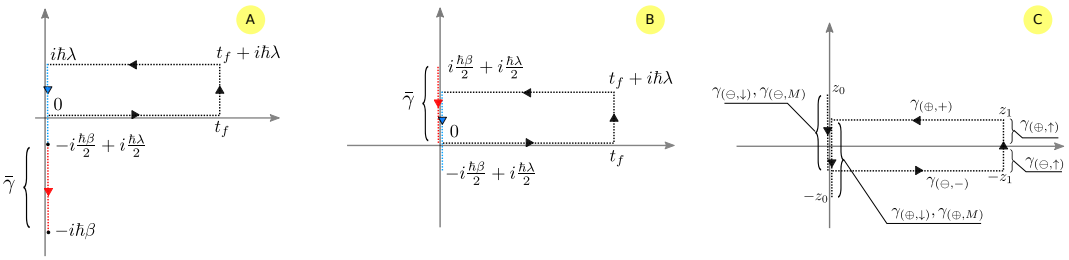

FIGURE 4.4: The contour in Fig. 4.1c can be transformed into a new symmetric contour by: a) Detaching the interval $[-i\frac{\hbar\beta}{2} + i\frac{\hbar\lambda}{2}, -i\hbar\beta]$ (labeled as $\bar{\gamma}$) and attaching it to the initial part using the cyclic property of the trace. b) Shifting the contour along the imaginary axis by $\frac{\hbar\lambda}{2}$, utilizing the translation invariance of the generating function. c) The resulting symmetric contour has $z_0 = i\frac{\hbar\beta}{2}$ and $z_1 = t_f + i\frac{\hbar\lambda}{2}$. The branches $\gamma_{\uparrow,\downarrow,M}$ in Fig. 4.1c can be divided into $\gamma_{(\ominus,\uparrow)}$,$\gamma_{(\oplus,\uparrow)}$, $\gamma_{(\ominus,\downarrow)}$, $\gamma_{(\oplus,\downarrow)}$, and $\gamma_{(\ominus,M)}$, $\gamma_{(\oplus,M)}$. The branch $\gamma_{(\ominus,M)}$ extends from z_0 to $z = 0$, while the branch $\gamma_{(\ominus,\downarrow)}$ extends from $z = 0$ to $z = -i\frac{\hbar\lambda}{2}$ [20].

based on the endpoints of stochastic trajectories, it is natural to introduce a quantum energy function at time t_f. This function is defined as follows:

$$E_Q(\lambda, t_f) = \frac{1}{\hbar\lambda} \int_{\gamma_{(\ominus,\uparrow)}} \Sigma[x_{cl}(z), x_q(z)] d\,\mathrm{Im}\, z, \tag{4.90}$$

and its analogue at the initial time $t = 0$, where $\gamma_{(\ominus,\uparrow)}$ is replaced by $\gamma_{(\ominus,\downarrow)}$. The difference between the initial and final energy functions gives a characterization of the fluctuating work at the trajectory level, and we can write the MGF as

$$M_W(\lambda, t_f) = \frac{1}{Z(0)} \int \mathcal{D}' x_{cl/q}(z) e^{\frac{1}{\hbar}\int_{\gamma_{(\ominus,M)}} \Sigma(z) d\,\mathrm{Im}\, z} e^{\frac{i}{\hbar}\int_{\gamma_{(\ominus,-)}} \mathcal{M}(z) d\,\mathrm{Re}\, z} e^{\lambda W(\lambda, t_f)}, \tag{4.91}$$

where $\mathcal{M}(z)$ and $\Sigma(z)$ are given in Eq. (4.89) and

$$W(\lambda, t_f) = E_Q(\lambda, t_f) - E_Q(\lambda, 0). \tag{4.92}$$

The specific symmetrization depicted in Fig. 4.4 plays a crucial role in obtaining a representation of the MGF (Moment Generating Function) where $W(\lambda, t_f)$ depends solely on the initial and final points of the trajectories.

If an alternative contour had been chosen instead of the contour shown in Fig. 4.4c and its lower half $\gamma_\ominus$ as the integration domain in the final equation set (4.86), the functional dependence of $W(\lambda, t_f)$ on the fields would have been different. A particularly noteworthy alternative is the one utilized by Funo and Quan [42], which will be summarized in the

subsequent section.

4.7.2 Comparison with an asymmetric contour

To highlight the distinction in our approach using an asymmetric contour, we opted for the contour presented in Reference [42]. In this paper, the authors have explored work statistics using Feynman path integral techniques applied to an asymmetric modification of the Keldysh contour. The key feature of this contour is that it does not have any vertical branches except for the γ_M branch. This is because the counting fields λ are purely imaginary. As a result, our modified contour can be transformed into the one introduced in [42] by replacing λ with $-i\lambda$. This substitution effectively replaces the original contour γ with a flat contour, as depicted in Fig. 4.5b.

With this chosen contour, it becomes possible to calculate the characteristic function of work using path integrals. The expression for the characteristic function of work is given by:

$$M_W(i\lambda, t_f) = \frac{1}{Z(0)} \int \mathcal{D}' x_M \mathcal{D}' x \mathcal{D}' y e^{-\frac{i}{\hbar}(S_1[x]-S_2[y])-\frac{1}{\hbar}S_M[x_M]}, \tag{4.93}$$

where S_1, S_2 and S_M are the the actions of the forward, backward and γ_M branches in the contour of Fig. 4.5b, respectively,

$$\begin{aligned} S_1 &= \int_0^{\hbar\lambda} ds\mathcal{L}\left[\alpha(0), x(s)\right] + \int_{\hbar\lambda}^{\hbar\lambda+t_f} ds\mathcal{L}\left[\alpha(s-\hbar\lambda), x(s)\right], \\ S_2 &= \int_0^{t_f} ds\mathcal{L}\left[\alpha(s), y(s)\right] + \int_{t_f}^{\hbar\lambda+t_f} ds\mathcal{L}\left[\alpha(t_f), y(s)\right], \\ S_M &= \int_0^{-\hbar\beta} ds\mathcal{L}_M\left[\alpha(0), x_M(s)\right]. \end{aligned} \tag{4.94}$$

The fields in the path integral equation (4.93) are subject to the following boundary conditions: $x(\hbar\lambda + t_f) = y(\hbar\lambda + t_f)$, $x_M(-\hbar\beta) = x(0)$, and $x_M(0) = y(0)$. These boundary conditions arise directly from the continuity requirement of the field $x(z)$ along the modified contour. In the context of Fig. 4.5b, where x, y, and x_M represent the components of the field on the contour, these boundary conditions differ from those specified by equation (4.74) in the case of Fig. 4.5a.

It should be noted that, unlike the contour shown in Fig. 4.5b, the Lagrangian in the forward and backward branches now exhibits differences. This is due to the definition of the work functional as a difference between the forward and backward action in terms of the

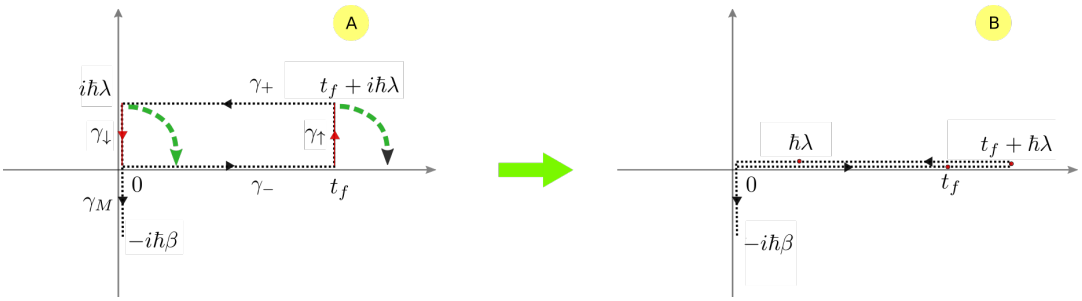

FIGURE 4.5: We can convert the modified contour into an asymmetric one by substituting λ with $-i\lambda$. a) The modified contour in its original form. b) The resulting asymmetric contour after the transformation. This contour can be utilized to define the work functional based on the forward paths. By employing this asymmetric contour, we can study the properties and characteristics of the work functional [42, 20].

forward path x (for details we refer to Ref. [42])

$$i\lambda W_\lambda[x] = \frac{i}{\hbar}\left(S_1^\lambda[x] - S_2^\lambda[x]\right), \tag{4.95}$$

which after some manipulations makes it possible to express the work functional at the level of quantum trajectories:

$$W_\lambda = \int_0^{t_f} dt \frac{1}{\hbar\lambda} \int_0^{\hbar\lambda} ds \dot{\alpha}(t) \frac{\partial V[\alpha(t), x(t+s)]}{\partial \alpha(t)}, \tag{4.96}$$

In the first integral, the integrand serves as a quantum extension of the concept of instantaneous power. This outcome differs from the representation (4.92), where the work is solely expressed as a function of the endpoints of the trajectories.

After highlighting the significance of contour symmetry, we can utilize the symmetrized contour to investigate the semiclassical limit of the work moment generating function. This semiclassical analysis allows us to derive classical and quantum corrections to the work MGF, shedding light on the interplay between classical and quantum dynamics in thermodynamic processes.

4.7.3 Semiclassical limit

For the analysis of the semiclassical limit, it is advantageous to express the path integral in the Hamiltonian convention, keeping the integration over the momentum fields p until the final stages of the calculation. In this scenario, we can replicate the procedure described in Section 4.7.1 and obtain an equivalent result to the equation (4.88), but with the inclusion of the momentum variables $\mathcal{D}p_{x/cl}$ in the path integral. To demonstrate this, we can write the

following;

$$\begin{aligned}
\frac{i}{\hbar}S &= \frac{i}{\hbar}\int_{\gamma} dz \left\{\frac{dx(z)}{dz}p(z) - H_\gamma[x(z),p(z)]\right\} \\
&= \frac{i}{\hbar}\int_{\gamma_\ominus} dz \left\{\frac{dx_\ominus(z)}{dz}p_\ominus(z) - H_\gamma[x_\ominus(z),p_\ominus(z)]\right\} \\
&-\frac{i}{\hbar}\int_{\gamma_\ominus} dz^* \left\{\frac{dx_\oplus(z^*)}{dz^*}p_\oplus(z^*) - H_\gamma[x_\oplus(z^*),p_\oplus(z^*)]\right\} \\
&= \frac{i}{\hbar}\int_{\gamma_\ominus} d\,\mathrm{Re}\, z \left\{\frac{dx_\ominus(z)}{dz}p_\ominus(z) - \frac{dx_\oplus(z^*)}{dz}p_\oplus(z^*) - \mathbf{H}_-\right\} \\
&-\frac{1}{\hbar}\int_{\gamma_\ominus} d\,\mathrm{Im}\, z \left\{\frac{dx_\ominus(z)}{dz}p_\ominus(z) - \frac{dx_\oplus(z^*)}{dz}p_\oplus(z^*) - \mathbf{H}_+\right\},
\end{aligned} \tag{4.97}$$

where we defined

$$\mathbf{H}_\pm = H_\gamma[x_\ominus(z),p_\ominus(z)] \pm H_\gamma[x_\oplus(z^*),p_\oplus(z^*)], \tag{4.98}$$

and we used that in the vertical branches, in which $d\,\mathrm{Im}\, z \neq 0$, we have $\frac{d}{dz^*} = -\frac{d}{dz}$, while in the horizotontal branches, in which $d\,\mathrm{Re}\, z \neq 0$, we have $\frac{d}{dz^*} = \frac{d}{dz}$. To write the action in terms of the quantum and classical components of the fields we apply the linear transformation (4.87) and substitute $x_{cl}(z) = 1/2[x_\ominus(z) + x_\oplus(z^*)]$, $x_q(z) = 1/2[x_\ominus(z) - x_\oplus(z^*)]$, $p_q(z) = 1/2[p_\ominus(z) - p_\oplus(z^*)]$ and $p_{cl}(z) = 1/2[p_\ominus(z) + p_\oplus(z^*)]$, therefore

$$\begin{aligned}
&\frac{dx_\ominus(z)}{dz}p_\ominus(z) - \frac{dx_\oplus(z^*)}{dz}p_\oplus(z^*) = \\
&\frac{dx_{cl}(z)}{dz}[p_\ominus(z) - p_\oplus(z^*)] + \frac{dx_q(z)}{dz}[p_\ominus(z) + p_\oplus(z^*)].
\end{aligned} \tag{4.99}$$

From it, using again Eq. (4.87), we obtain an expression only in terms of the quantum and classical components

$$\frac{dx_\ominus(z)}{dz}p_\ominus(z) - \frac{dx_\oplus(z^*)}{dz}p_\oplus(z^*) = 2\frac{dx_{cl}(z)}{dz}p_q(z) + 2\frac{dx_q(z)}{dz}p_{cl}(z). \tag{4.100}$$

If we replace the equation above in Eq. (4.97) we obtain the action in terms of the quantum and classical variables

$$\begin{aligned}
\frac{i}{\hbar}S &= \frac{i}{\hbar}\int_{\gamma_\ominus} d\,\mathrm{Re}z\left\{2\frac{dx_{cl}(z)}{dz}p_q(z) + 2\frac{dx_q(z)}{dz}p_{cl}(z)\right\} \\
-\frac{i}{\hbar}\int_{\gamma_\ominus} d\,\mathrm{Re}z&\left\{H_\gamma[x_{cl}(z)+x_q(z),p_{cl}(z)+p_q(z)] - H_\gamma[x_{cl}(z)-x_q(z),p_{cl}(z)-p_q(z)]\right\} \\
&-\frac{1}{\hbar}\int_{\gamma_\ominus} d\,\mathrm{Im}\, z\left\{2\frac{dx_{cl}(z)}{dz}p_q(z) + 2\frac{dx_q(z)}{dz}p_{cl}(z)\right\}
\end{aligned}$$

$$+\frac{1}{\hbar}\int_{\gamma_\ominus} d\,\mathrm{Im}\,z\Big\{H_\gamma[x_{cl}(z)+x_q(z),p_{cl}(z)+p_q(z)]+H_\gamma[x_{cl}(z)-x_q(z),p_{cl}(z)-p_q(z)]\Big\}. \tag{4.101}$$

Therefore, the functions $\mathcal{M}$ and Σ are replaced by

$$\begin{aligned}\Sigma_h &= \mathcal{K}+m\left(p_{cl}^2+p_q^2\right)+V[\alpha,x_{cl}+x_q]+V[\alpha,x_{cl}-x_q],\\ \mathcal{M}_h &= \mathcal{K}+\frac{2}{m}p_{cl}p_q-V[\alpha,x_{cl}+x_q]+V[\alpha,x_{cl}-x_q].\end{aligned} \tag{4.102}$$

Here, $\mathcal{K}=2p_q\left(\frac{dx_{cl}}{dz}\right)-2x_q\left(\frac{dp_{cl}}{dz}\right)$. In the classical limit, we anticipate that the final energy will depend on $x_{cl}(t_f)$ and $p_{cl}(t_f)$. Consequently, we assume that the contribution of x_q and p_q is negligible along the vertical branches. This assumption can be verified by considering the nonlinear contributions in x_q and p_q and demonstrating that they scale with higher powers of $\hbar$ (refer to [86] for further details).

Expanding both integrals over the quantum variables x_q and p_q up to second order in (4.101), we obtain the following expression for the horizontal track:

$$\begin{aligned}&H_\gamma[x_{cl}(z)+x_q(z),p_{cl}(z)+p_q(z)]-H_\gamma[x_{cl}(z)-x_q(z),p_{cl}(z)-p_q(z)]=\\ &2\frac{p_{cl}p_q}{m}+V[x_{cl}(z)+x_q(z)]-V[x_{cl}(z)-x_q(z)]\approx 2\frac{p_{cl}p_q}{m}+2x_q\frac{\partial}{\partial x_{cl}}V[x_{cl}],\end{aligned} \tag{4.103}$$

and for the vertical branches

$$\begin{aligned}&H_\gamma[x_{cl}(z)+x_q(z),p_{cl}(z)+p_q(z)]+H_\gamma[x_{cl}(z)-x_q(z),p_{cl}(z)-p_q(z)]=\\ &2H_\gamma[x_{cl}(z),p_{cl}(z)]+\frac{p_q^2(z)}{m}+x_q^2(z)\frac{\partial^2}{\partial x_{cl}^2}V[x_{cl}].\end{aligned}$$

After integrating by parts Eq. (4.101) and replacing the expansions (4.103) and (4.104) we obtain

$$\begin{aligned}\frac{i}{\hbar}S=\frac{2i}{\hbar}\int_{\gamma_\ominus} d\,\mathrm{Re}\,z\Big\{&\frac{dx_{cl}(z)}{dz}p_q(z)-\frac{dp_{cl}(z)}{dz}x_q(z)-\left[\frac{p_qp_{cl}}{m}+x_q\frac{\partial}{\partial x_{cl}}V[x_{cl}]\right]\Big\}\\ &-\frac{2}{\hbar}\int_{\gamma_\ominus} d\,\mathrm{Im}\,z\Big\{\frac{dx_{cl}(z)}{dz}p_q(z)-\frac{dp_{cl}(z)}{dz}x_q(z)\\ &-\left[H_\gamma[x_{cl}(z),p_{cl}(z)]+\frac{p_q^2(z)}{2m}+\frac{1}{2}x_q^2(z)\frac{\partial^2}{\partial x_{cl}^2}V[x_{cl}]\right]\Big\}.\end{aligned} \tag{4.104}$$

It is worth noting that the boundary terms resulting from the integration by parts vanish due to the boundary conditions $x_q(t_f)=x_q(i\hbar\beta/2)=0$.

Next, we decompose the integral over the vertical lines ($\int_{\gamma_\ominus} d\,\mathrm{Im}\, z$) into two distinct contributions represented by the vertical tracks $\gamma_{(\ominus,\uparrow)}$ and $\gamma_{(\ominus,\downarrow),(\ominus,M)}$. We express the components of the quantum and classical fields as follows:

$$x_{cl/q}(z) = \begin{cases} x_{cl/q\uparrow}(\tau) & \text{for } z = t_f + i\tau \in \gamma_{(\ominus,\uparrow)}, \\ x_{cl/q\downarrow}(\tau) & \text{for } z = i\tau \in \gamma_{(\ominus,\downarrow),(\ominus,M)}. \end{cases} \tag{4.105}$$

In equation (4.74), we denoted the components of the branches γ_M and $\gamma_\downarrow$ as $x_M(\tau)$ and $x_\downarrow(\tau)$, respectively. However, on the symmetrized contour, for the sake of simplicity in calculations, we represent the fields on the branches $\gamma_{(\ominus,\downarrow)}$ and $\gamma_{(\ominus,M)}$ as $x_{cl/q\downarrow}(\tau)$. In this way we will have

$$\begin{aligned} &-\frac{2}{\hbar}\int_{\gamma_\ominus} d\,\mathrm{Im}\, z \Bigg\{ \frac{dx_{cl}(z)}{dz} p_q(z) - \frac{dp_{cl}(z)}{dz} x_q(z) \\ &- \left[H_\gamma[x_{cl}(z), p_{cl}(z)] + \frac{p_q^2(z)}{2m} + \frac{1}{2} x_q^2(z) \frac{\partial^2}{\partial x_{cl}^2} V[x_{cl}] \right] \Bigg\} = \\ &-\frac{2}{\hbar}\int_{-\lambda\hbar/2}^{0} d\tau \Bigg\{ i\frac{dp_{cl\uparrow}(\tau)}{d\tau} x_{q\uparrow}(\tau) - i\frac{dx_{cl\uparrow}(\tau)}{d\tau} p_{q\uparrow}(\tau) \\ &- \left[\frac{p_{cl\uparrow}^2(\tau)}{2m} + V[x_{cl\uparrow}(\tau)] + \frac{p_{q\uparrow}^2(\tau)}{2m} + \frac{1}{2} x_{q\uparrow}^2(\tau) V''[x_{cl\uparrow}(\tau)] \right] \Bigg\} \\ &+\frac{2}{\hbar}\int_{-\lambda\hbar/2}^{\beta\hbar/2} d\tau \Bigg\{ i\frac{dp_{cl\downarrow}(\tau)}{d\tau} x_{q\downarrow}(\tau) - i\frac{dx_{cl\downarrow}(\tau)}{d\tau} p_{q\downarrow}(\tau) \\ &- \left[\frac{p_{cl\downarrow}^2(\tau)}{2m} + V[x_{cl\downarrow}(\tau)] + \frac{p_{q\downarrow}^2(\tau)}{2m} + \frac{1}{2} x_{q\downarrow}^2(\tau) V''[x_{cl\downarrow}(\tau)] \right] \Bigg\}. \end{aligned} \tag{4.106}$$

By utilizing the equation mentioned above, we observe that to first order in p_q and x_q, euation (4.102) yields $\Sigma_h \approx \mathcal{K} + 2E_{cl}(z) = \mathcal{K} + \frac{p_{cl}^2(z)}{m} + 2V[\alpha(t_f), x_{cl}(z)]$. Consequently, at this order, the path integrals over x_q and p_q become trivial. As the function $\mathcal{K}$ includes the first order of the quantum fields, the path integral over $\gamma_{(\ominus,\uparrow)}$ can be expressed as

$$\int \mathcal{D}x_q \mathcal{D}p_q e^{\int_{\gamma_{(\ominus,\uparrow)}} \mathcal{K}(x_{cl}, x_q, p_{cl}, p_q) dz} = \prod_{\xi=p,q} \delta[\xi_{cl}(z) - \xi_{cl}(t_f)]. \tag{4.107}$$

Consequently, in this limit, the only permissible classical paths are those in which $x_{cl}(z)$ and $p_{cl}(z)$ on the vertical branches are consistently equal to $x_{cl}(t_f)$ and $p_{cl}(t_f)$. Keeping this in

mind, the path integral over the classical fields can be straightforwardly evaluated as

$$\int \mathcal{D}x_{cl}\mathcal{D}p_{cl}e^{\int_{\gamma_{(\ominus,\uparrow)}}[\frac{1}{m}p_{cl}^2+2V(\alpha,x_{cl})]dz}\prod_{\xi}\delta[\xi_{cl}(z)-\xi_{cl}(t_f)] = e^{\lambda\left\{\frac{p_{cl}^2(t_f)}{2m}+V[\alpha(t_f),x_{cl}(t_f)]\right\}}. \tag{4.108}$$

Combining this result with the one we obtain doing the analogous calculation on $\gamma_{(\ominus,\downarrow)}$ and $\gamma_{(\ominus,M)}$, we finally conclude that

$$W(\lambda,t_f) = E_{cl}(t_f) - E_{cl}(0) + O(\hbar). \tag{4.109}$$

This expression corresponds to the classical counterpart of Equation (4.92). Notably, this outcome remains unaffected by the presence of λ and aligns with the fluctuations of work in classical driven isolated systems [65, 56].

To obtain the first quantum correction to this result, we retain the quadratic terms in x_q and p_q from the expansion of Equation (4.106). This leads to a Gaussian integral over the quantum fields. If we define $\frac{i}{\hbar}\tilde{S}$ as the exponent of the path integral following this Gaussian integration, we obtain

$$\begin{aligned}\frac{i\tilde{S}}{\hbar} &= \frac{1}{\hbar}\int_{-\hbar\lambda/2}^{0}\frac{d\tau}{V''[x_{cl\uparrow}(\tau)]}\left[\frac{dp_{cl\uparrow}(\tau)}{d\tau}\right]^2+\frac{1}{\hbar}\int_{-\hbar\lambda/2}^{0}d\tau m\left[\frac{dx_{cl\uparrow}(\tau)}{d\tau}\right]^2\\ &+\frac{2}{\hbar}\int_{-\lambda\hbar/2}^{0}d\tau\left\{\frac{p_{cl\uparrow}^2(\tau)}{2m}+V[x_{cl\uparrow}(\tau)]\right\}-\frac{1}{\hbar}\int_{-\hbar\lambda/2}^{\beta\hbar/2}\frac{d\tau}{V''[x_{cl\downarrow}(\tau)]}\left[\frac{dp_{cl\downarrow}(\tau)}{d\tau}\right]^2\\ &-\frac{1}{\hbar}\int_{-\hbar\lambda/2}^{\beta\hbar/2}d\tau m\left[\frac{dx_{cl\downarrow}(\tau)}{d\tau}\right]^2-\frac{2}{\hbar}\int_{-\hbar\lambda/2}^{\beta\hbar/2}d\tau\left\{\frac{p_{cl\downarrow}^2(\tau)}{2m}+V[x_{cl\downarrow}(\tau)]\right\}.\end{aligned} \tag{4.110}$$

It is important to note that a consequence of the path integration mentioned above is a change in the normalization factor proportional to $1/\sqrt{V''[x_{cl\downarrow}(\tau)]}$ and $1/\sqrt{V''[x_{cl\uparrow}(\tau)]}$. To facilitate further manipulations, we make the assumption that the quantities $V''[x_{cl\downarrow}(\tau)]$ and $V''[x_{cl\uparrow}(\tau)]$ can be replaced with $V''[x_{cl}(0)]$, $V''[x_{cl}(0)]$, $V''[x_{cl}(t_f)]$, and $V''[x_{cl}(t_f)]$ respectively, both in the kinetic terms of the action and in the normalization factor.

The rationale behind this replacement is that the vertical tracks are short in the semiclassical limit, allowing us to substitute the values of the fields at the boundaries of $\gamma_\uparrow$ and $\gamma_\downarrow$ with the values of the fields at those boundaries.

We now turn our attention to the integral involving the momentum variables. By defining $\tilde{m}(t_f) = 2/V''[x_{cl\uparrow}(t_f)]$ and $\omega(t_f) = \sqrt{V''[x_{cl\uparrow}(t_f)]/m}$, we obtain:

$$\int \mathcal{D}p_{cl\uparrow} \exp\left\{\frac{1}{\hbar}\int_{-\lambda\hbar/2}^{0} d\tau \frac{\tilde{m}(t_f)}{2}\left[\frac{dp_{cl\uparrow}(\tau)}{d\tau}\right]^2 + \frac{\tilde{m}(t_f)\omega^2(t_f)p_{cl\uparrow}^2(\tau)}{2}\right\} = \sqrt{\frac{\tilde{m}\omega}{2\pi\hbar\sinh(\hbar\omega\lambda/2)}} e^{\left\{\frac{\tilde{m}\omega}{2\hbar\sinh(\hbar\omega\lambda/2)}\left\{\left[p_{cl}^2(t_f)+p_{cl\uparrow}^2(0)\right]\cosh(\hbar\omega\lambda/2) - 2p_{cl}(t_f)p_{cl\uparrow}(0)\right\}\right\}}. \quad (4.111)$$

Let us for now restrict our analysis to $\gamma_\uparrow$. The integral over $p_{cl\uparrow}(0)$ will give

$$\int \mathcal{D}p_{cl\uparrow} \sqrt{\frac{\tilde{m}\omega}{2\pi\hbar\sinh(\hbar\omega\lambda/2)}} e^{\left\{\frac{\tilde{m}\omega}{2\hbar\sinh(\hbar\omega\lambda/2)}\left\{\left[p_{cl}^2(t_f)+p_{cl\uparrow}^2(0)\right]\cosh(\hbar\omega\lambda/2) - 2p_{cl}(t_f)p_{cl\uparrow}(0)\right\}\right\}} = \sqrt{\frac{1}{2\cosh(\hbar\omega\lambda/2)}} \exp\left\{\frac{p_{cl}^2(t_f)\tilde{m}\omega}{2\hbar\cosh(\hbar\omega\lambda/2)}\sinh(\hbar\omega\lambda/2)\right\}. \quad (4.112)$$

Similar to this we will do the integration on the other vertical branch. This will result in

$$\int \mathcal{D}p_{cl\downarrow} \exp\left\{\frac{-1}{\hbar}\int_{-\lambda\hbar/2}^{\beta\hbar/2} d\tau \frac{\tilde{m}(t_f)}{2}\left[\frac{dp_{cl\downarrow}(\tau)}{d\tau}\right]^2 + \frac{\tilde{m}(t_f)\omega^2(t_f)p_{cl\downarrow}^2(\tau)}{2}\right\} = \sqrt{\frac{\tilde{m}\omega}{2\pi\hbar\sinh(\hbar\omega(\lambda+\beta)/2)}} \exp\left\{-\frac{\tilde{m}\omega\cosh(\hbar\omega(\lambda+\beta)/2)}{2\hbar\sinh(\hbar\omega(\lambda+\beta)/2)}\left[p_{cl}^2(0)+p_{cl\downarrow}^2(\beta\hbar/2)\right]\right\} \times \exp\left\{\frac{\tilde{m}\omega}{2\hbar\sinh(\hbar\omega(\lambda+\beta)/2)}\left\{2p_{cl}(0)p_{cl\downarrow}(\beta\hbar/2)\right\}\right\}. \quad (4.113)$$

We are still missing the integration over $p_{cl\downarrow}(\beta\hbar/2)$. This will be in line with the above results and yields

$$\int \mathcal{D}p_{cl\downarrow} \exp\left\{\frac{-1}{\hbar}\int_{-\lambda\hbar/2}^{\beta\hbar/2} d\tau \frac{\tilde{m}(t_f)}{2}\left[\frac{dp_{cl\downarrow}(\tau)}{d\tau}\right]^2 + \frac{\tilde{m}(t_f)\omega^2(t_f)p_{cl\downarrow}^2(\tau)}{2}\right\} = \sqrt{\frac{1}{2\cosh(\hbar\omega(\lambda+\beta)/2)}} \exp\left\{\frac{-p_{cl}^2(0)\tilde{m}\omega}{2\hbar\cosh(\hbar\omega(\lambda+\beta)/2)}\sinh(\hbar\omega(\lambda+\beta)/2)\right\}. \quad (4.114)$$

Above calculations will pave the way to write the total contribution of the vertical branches to the path integral. One can write them such that

$$\int Dx_q Dp_q D_{p_{cl}} e^{\frac{1}{\hbar}\int_{(\gamma_{\ominus,\downarrow}),(\ominus,M)} \Sigma[x_{cl},x_q]d\,\mathrm{Im}\,z} e^{\frac{1}{\hbar}\int_{\gamma_{(\ominus,\uparrow)}} \Sigma[x_{cl},x_q]d\,\mathrm{Im}\,z} = e^{\frac{2}{\hbar}\int_{-\hbar\lambda/2}^{0} d\tau\left\{\frac{m}{2}\left[\frac{dx_{cl\uparrow}(\tau)}{d\tau}\right]^2 + V[x_{cl\uparrow}(\tau)]\right\}} e^{\frac{-2}{\hbar}\int_{-\hbar\lambda/2}^{\beta\hbar/2} d\tau\left\{\frac{m}{2}\left[\frac{dx_{cl\downarrow}(\tau)}{d\tau}\right]^2 + V[x_{cl\downarrow}(\tau)]\right\}} e^{\left\{\frac{p_{cl}^2(t_f)\tilde{m}\omega}{2\hbar}\tanh(\hbar\omega\lambda/2)\right\}}$$

$$\times\sqrt{\frac{1}{4\cosh(\hbar\omega\lambda/2)\cosh(\hbar\omega(\lambda+\beta)/2)}}e^{\left\{\frac{-p_{cl}^2(0)\tilde{m}\omega}{2\hbar}\tanh(\hbar\omega(\lambda+\beta)/2)\right\}}. \tag{4.115}$$

This relation gives us the semi-classical definition of the work function up to the second order in $\hbar$. For a generic potential we write the fields in the vertical branch as $x_{cl\uparrow}(\tau) = x_{cl}(t_f) + \delta x_{cl\uparrow}(\tau)$ and keep only the second order in $\delta x_{cl\uparrow}(\tau)$

$$\int \mathcal{D}x_{cl\uparrow}\exp\frac{2}{\hbar}\int_{-\hbar\lambda/2}^{0}d\tau\left\{\frac{m}{2}\left[\frac{dx_{cl\uparrow}(\tau)}{d\tau}\right]^2+V[x_{cl\uparrow}(\tau)]\right\}=$$
$$\int\mathcal{D}\delta x_{cl\uparrow}e^{\frac{2}{\hbar}\int_{-\hbar\lambda/2}^{0}d\tau\left\{\frac{m}{2}\left[\frac{d\delta x_{cl\uparrow}(\tau)}{d\tau}\right]^2+V[x_{cl}(t_f)]+V'[x_{cl}(t_f)]\delta x_{cl\uparrow}(\tau)+\frac{1}{2}V''[x_{cl}(t_f)]\delta x_{cl\uparrow}(\tau)^2\right\}}=$$
$$\exp\lambda\left\{V[x_{cl}(t_f)]-\frac{V'[x_{cl}(t_f)]^2}{2V''[x_{cl}(t_f)]}\right\}\int D\delta x_{cl\uparrow}e^{\frac{1}{\hbar}\int_{-\hbar\lambda/2}^{0}d\tau\left\{m\left[\frac{\delta x_{cl\uparrow}(\tau)}{d\tau}\right]^2+V''[x_{cl}(t_f)]\delta x_{cl\uparrow}(\tau)^2\right\}}. \tag{4.116}$$

To derive the final line, we completed the square in the last two terms of the second line and then redefined $\delta x_{cl\uparrow}+\frac{V'[x_{cl}]}{V''[x_{cl}]}\to\delta x_{cl\uparrow}$.

It is important to exercise caution when considering the integration domain of the path integral $\int D\delta x_{cl\uparrow}$. Prior to the change of variable, the integration limit was $\int_{\delta x_{cl\uparrow}(-\hbar\lambda/2)}^{\delta x_{cl\uparrow}(0)}D\delta x_{cl\uparrow}$. By utilizing $\delta x_{cl\uparrow}(\tau) = x_{cl\uparrow}(\tau) - x_{cl}(t_f)$, the limit of integration becomes $\int D\delta x_{cl\uparrow} = \int_0^{x_{cl\uparrow}(0)-x_{cl}(t_f)}D\delta x_{cl\uparrow}$. As a result, the change of variable in the equation leads to a modification in the integration domain

$$\int_0^{x_{cl\uparrow}(0)-x_{cl}(t_f)}D\delta x_{cl\uparrow}\to\int_{\frac{V'[x_{cl}(t_f)]}{V''[x_{cl}(t_f)]}}^{x_{cl\uparrow}(0)-x_{cl}(t_f)+\frac{V'[x_{cl}(t_f)]}{V''[x_{cl}(t_f)]}}D\delta x_{cl\uparrow}. \tag{4.117}$$

With this in mind (4.116) can be written as

$$\exp\lambda\left\{V[x_{cl}(t_f)]-\frac{V'[x_{cl}(t_f)]^2}{2V''[x_{cl}(t_f)]}\right\}\int D\delta x_{cl\uparrow}e^{\frac{1}{\hbar}\int_{-\hbar\lambda/2}^{0}d\tau\left\{m\left(\frac{d\delta x_{cl\uparrow}(\tau)}{d\tau}\right)^2+V''[x_{cl}(t_f)]\delta x_{cl\uparrow}(\tau)^2\right\}}$$
$$=\sqrt{\frac{1}{2\cosh\left(\hbar\omega(t_f)\lambda/2\right)}}e^{\lambda\left\{V[x_{cl}(t_f)]-\frac{V'[x_{cl}(t_f)]^2}{2V''[x_{cl}(t_f)]}\right\}}e^{\left\{\frac{m\omega(t_f)}{\hbar}\left(\frac{V'[x_{cl}(t_f)]}{V''[x_{cl}(t_f)]}\right)^2\tanh\hbar\omega(t_f)\lambda/2\right\}}. \tag{4.118}$$

We need to do similar integration for other vertical branch. The result will be the same except that we need to change $\lambda\to\lambda+\beta$ and $\omega(t_f)\to\omega(0)$.

At the end, calculating all the above equations, we can eventually obtain a solution for

(4.115). This in fact will help us find the semi-classical expansion of work. First we write (4.115) as

$$\begin{aligned}
&\int Dx_{cl}\int Dx_q Dp_q Dp_{cl} e^{\frac{1}{\hbar}\int_{\gamma_{(\ominus,\downarrow),(\ominus,M)}}\Sigma[x_{cl},x_q]d\,\mathrm{Im}\,z} e^{\frac{1}{\hbar}\int_{\gamma_{(\ominus,\uparrow)}}\Sigma[x_{cl},x_q]d\,\mathrm{Im}\,z} = \\
&\frac{1}{2\cosh\left(\hbar\omega(t_f)\lambda/2\right)} e^{\left\{\frac{p_{cl}^2(t_f)\tilde{m}\omega(t_f)}{2\hbar}\tanh\hbar\omega(t_f)\lambda/2\right\}} e^{\lambda\left[V[x_{cl}(t_f)]-\frac{V'[x_{cl}(t_f)]^2}{2V''[x_{cl}(t_f)]}\right]} \\
&\qquad\times\exp\left\{\frac{m\omega(t_f)}{\hbar}\left[\frac{V'[x_{cl}(t_f)]}{V''[x_{cl}(t_f)]}\right]^2\tanh\left(\hbar\omega(t_f)\lambda/2\right)\right\} \\
&\times\frac{1}{2\cosh(\hbar\omega(0)(\lambda+\beta)/2)}\exp\left\{\frac{-p_{cl}^2(0)\tilde{m}\omega(0)}{2\hbar}\tanh(\hbar\omega(0)(\lambda+\beta)/2)\right\} \\
&\times\exp\left\{-(\lambda+\beta)\,V[x_{cl}(0)]-\frac{V'[x_{cl}(0)]^2}{2V''[x_{cl}(0)]}\right\} e^{\left\{\frac{m\omega(0)}{\hbar}\left[\frac{V'[x_{cl}(0)]}{V''[x_{cl}(0)]}\right]^2\tanh(\hbar\omega(0)(\lambda+\beta)/2)\right\}}.
\end{aligned} \tag{4.119}$$

Expanding above equation in orders of $\hbar$ will yeilds the semi-classical expression of the work. If we introduce $W(\lambda,t_f) = W_0(t_f) + \lambda W_1(t_f) + \lambda^2 W_2(t_f) + O(\lambda^3,\hbar^2)$ with $W_0(t_f) = E_{cl}(t_f) - E_{cl}(0)$, we will therefore have

$$\begin{aligned}
W_1(t_f) &= -\frac{\hbar^2 V''[\alpha(t_f),x_{cl}(t_f)]}{4m} + \frac{\hbar^2 V''[\alpha(0),x_{cl}(0)]}{4m} \\
W_2(t_f) &= \frac{\hbar^2 V''[\alpha(t_f),x_{cl}(t_f)]}{12m}\left[\frac{p_{cl}^2(t_f)}{2m} + \frac{V'^2[\alpha(t_f),x_{cl}(t_f)]}{2V''[\alpha(t_f),x_{cl}(t_f)]}\right] \\
&\quad - \frac{\hbar^2 V''[\alpha(0),x_{cl}(0)]}{12m}\left[\frac{p_{cl}^2(0)}{2m} + \frac{V'^2[\alpha(0),x_{cl}(0)]}{2V''[\alpha(0),x_{cl}(0)]}\right],
\end{aligned} \tag{4.120}$$

where W_1 contributes to the variance of work that can be obtained from the second derivative of the generating function with respect to λ.

As a cross-check of the above result we will study the case of time-dependent harmonic potentials. This will show that the semi-classical limit will become exact in that case.

4.7.4 Work MGF for a harmonic oscillator

In the case of a time-dependent harmonic oscillator with potential energy given by $V[x,t] = \frac{1}{2}M\omega(t)x^2$, the potential simplifies for the vertical lines to $\omega(0) = \omega_0$ for the left vertical branch and $\omega(t_f) = \omega_1$ for the right vertical branch. In this case, both $\omega(t_f)$ and $m(t_f)$ are constant, so the approximation $V''[x_{cl\uparrow}(\tau)] \approx V''[x_{cl}(t_f)]$ becomes exact. Therefore, using

(4.115) and performing the path integral over x_{cl}, we obtain

$$\int Dx_{cl} \int Dx_q Dp_q D_{p_{cl}} e^{\frac{1}{\hbar}\int_{\gamma_{(\ominus,\downarrow),(\ominus,M)}} \Sigma[x_{cl},x_q]d\,\mathrm{Im}\,z} e^{\frac{1}{\hbar}\int_{\gamma_{(\ominus,\uparrow)}} \Sigma[x_{cl},x_q]d\,\mathrm{Im}\,z} =$$
$$\sqrt{\frac{1}{2\cosh(\hbar\omega_1\lambda/2)}} \exp\left\{\frac{x_{cl}^2(t_f)m\omega_1}{\hbar\cosh(\hbar\omega_1\lambda/2)}\sinh(\hbar\omega_1\lambda/2)\right\}$$
$$\times\sqrt{\frac{1}{2\cosh(\hbar\omega_0(\lambda+\beta)/2)}} \exp\left\{\frac{-x_{cl}^2(0)m\omega_0}{\hbar\cosh(\hbar\omega_0(\lambda+\beta)/2)}\sinh(\hbar\omega_0(\lambda+\beta)/2)\right\}$$
$$\sqrt{\frac{1}{2\cosh\hbar\omega_1\lambda/2}} \exp\left\{\frac{p_{cl}^2(t_f)}{m\omega_1\hbar\cosh(\hbar\omega_1\lambda/2)}\sinh(\hbar\omega_1\lambda/2)\right\}$$
$$\times\sqrt{\frac{1}{2\cosh(\hbar\omega_0(\lambda+\beta)/2)}} \exp\left\{\frac{-p_{cl}^2(0)}{m\omega_0\hbar\cosh(\hbar\omega_0(\lambda+\beta)/2)}\sinh(\hbar\omega_0(\lambda+\beta)/2)\right\} \tag{4.121}$$

Next we need to integrate over $p(t_f)$, $x(t_f)$, $p_{cl}(0)$ and $x_{cl}(0)$. We notice that the relation between them is given by the path integral over the horizontal line that results in the equation of motion for a time dependent harmonic oscillator as $x(t_f) = A(t_f)x(0) + B(t_f)p(0)/M$ and $p(t_f) = M\dot{A}(t_f)x(0) + \dot{B}(t_f)p(0)$. Therefore we can write the above relation as

$$M_W(\lambda,t) = \frac{\sinh(\beta\hbar/2)}{2\cosh(\hbar\omega_1\lambda/2)\cosh(\hbar\omega_0(\lambda+\beta)/2)} \tag{4.122}$$

$$exp\left\{\frac{-1}{2}\begin{pmatrix}x(0) & p(0)\end{pmatrix}\begin{pmatrix}C_{11} & C_{12}\\ C_{21} & C_{22}\end{pmatrix}\begin{pmatrix}x(0)\\ p(0)\end{pmatrix}\right\}, \tag{4.123}$$

with

$$\begin{aligned} C_{11} &= \frac{2m\omega_0}{\hbar}\tanh\left(\hbar\omega_0(\lambda+\beta)/2\right) - \frac{2m}{\hbar\omega_1}\left[A^2\omega_1^2 + \dot{A}^2\right]\tanh\left(\hbar\omega_1\lambda/2\right)\\ C_{22} &= \frac{2}{m\omega_0\hbar}\tanh\left(\hbar\omega_0(\lambda+\beta)/2\right) - \frac{2}{\hbar m\omega_1}\left[\omega_1^2B^2 + \dot{B}^2\right]\tanh\left(\hbar\omega_1\lambda/2\right)\\ C_{12} &= C_{21} = -\left[\frac{2\omega_1}{\hbar}AB + \frac{2}{\omega_1\hbar}\dot{A}\dot{B}\right]\tanh\left(\hbar\omega_1\lambda/2\right), \end{aligned} \tag{4.124}$$

where the term $\sinh\beta\hbar/2$ comes form the normalization of the generating function. Therefore the integration over p_0 and x_0 will result in $2\pi/\sqrt{\det(\mathbf{C})}$ which can be written as

$$M_W(\lambda,t_f) = \frac{\sinh(\beta\hbar/2)}{\cosh(\hbar\omega_1\lambda/2)\cosh(\hbar\omega_0(\lambda+\beta)/2)}$$
$$\times\frac{1}{\sqrt{Y_1^2(\lambda,\beta) - 2Q^*Y_2(\lambda)Y_1(\lambda,\beta) + \left[\dot{A}B - \dot{B}A\right]^2Y_2(\lambda)}}. \tag{4.125}$$

where $Y_1(\lambda,\beta) = \tanh\left(\hbar\omega_0(\lambda+\beta)/2\right)$ and $Y_2(\lambda) = \tanh\left(\hbar\omega_1\lambda/2\right)$. We notice that the last term under the square root is the Wronskian and for our given boundary conditions is 1. Also for Q^* we have

$$Q^* = \frac{1}{\omega_0\omega_1}\left\{\omega_0^2\left[\omega_1^2B^2+\dot{B}^2\right]+\left[\omega_1^2A^2+\dot{A}^2\right]\right\}. \tag{4.126}$$

Thus, setting the Wronskian to 1, (4.125) will coincide with the exact result in ref [23]. This cross-check will serve to verify the semiclassical expansion of the work functional. As a final step, we will examine the fluctuation relations within the path integral approach, similar to what we previously did for the perturbative expansion of the moment generating function.

4.7.5 Fluctuations and the Wigner function

The representation of work given by equations (4.91) and (4.92), which arises from the contour in Fig. 4.4c, offers a significant advantage. It allows for the isolation of the dynamics information in the forward branch $\gamma_{(\ominus,-)}$, while the λ dependence is confined to the vertical branches.

This separation between the dynamical contribution to the action and the "thermodynamical" contribution enables us to solve both aspects separately, at least in a formal sense. In contrast, representing work as in Eq. (4.96) is problematic because the fields used to define W_λ are the same ones appearing in the dynamical action (i.e., the fields in the forward branch).

Exploiting this advantage, we can explore a generalization of the concept of detailed balance at the level of quantum trajectories, following a conceptual approach similar to the one presented in Sec. 4.6 for the diagrammatic approach to perturbation theory.

To begin this analysis, we introduce the formal solution to the path integral over the vertical branch $\gamma_{(\ominus,\uparrow)}$. This involves dividing the path integration in Eq. (4.88) into three separate propagators, given by

$$\mathcal{E}_{\lambda,t_f}[y_q^f,y_{cl}^f,\alpha(t_f)] = \frac{1}{\lambda}\log\int_{B(y^f)}\mathcal{D}'x_{cl/q}\,e^{\frac{1}{\hbar}\int_{\gamma_{(\ominus,\uparrow)}}\Sigma[x_{cl}(z),x_q(z)]d\,\mathrm{Im}\,z}, \tag{4.127}$$

$$\mathcal{E}_{-\lambda-\beta,0}[y_q^i,y_{cl}^i,\alpha(0)] = \frac{1}{-\lambda-\beta}\log\int_{B'(y^i)}\mathcal{D}'x_{cl/q}\,e^{\frac{1}{\hbar}\int_{\gamma_{(\ominus,\downarrow),(\ominus,M)}}\Sigma[x_{cl}(z),x_q(z)]d\,\mathrm{Im}\,z}, \tag{4.128}$$

$$\mathcal{U}[y_q^f,y_{cl}^f,t_f;y_q^i,y_{cl}^i,0] = \int_{B''(y^i,y^f)}\mathcal{D}'x_{cl/q}\,e^{\frac{i}{\hbar}\int_{\gamma_{(\ominus,-)}}\mathcal{M}[x_{cl}(z),x_q(z)]d\,\mathrm{Re}\,z}, \tag{4.129}$$

where $B(y^i), B'(y^f), B''(y^i, y^f)$ are shortcuts to denote the boundary conditions of the path integrals and we made the dependence on $\alpha(t_f)$ explicit for convenience.. For Eq. (4.127) the boundary conditions are $x_{q\uparrow}(-\hbar\lambda/2) = y^f_q, x_{q\uparrow}(0) = 0, x_{cl\uparrow}(-\hbar\lambda/2) = y^f_{cl}$, for Eq. (4.128) we have[1] $x_{q\downarrow}(\hbar\beta/2) = 0, x_{q\downarrow}(-\hbar\lambda/2) = y^i_q$, $x_{cl\downarrow}(-\hbar\lambda/2) = y^i_{cl}$ while for Eq. (4.129) we have $x_q(0), x_{cl}(0) = y^i_q, y^i_{cl}$, $x_q(t_f), x_{cl}(t_f) = y^f_q, y^f_{cl}$.

$$\mathcal{E}_{\lambda,t_f}[y^f_q, y^f_{cl}, \alpha(t_f)] = \frac{1}{\lambda}\log\int \mathcal{D}' x_{cl/q} e^{\frac{1}{\hbar}\int_{\gamma_{(\ominus,\uparrow)}} \Sigma[x_{cl}(z), x_q(z)] d\,\mathrm{Im}\, z}, \tag{4.130}$$

We can write Eq. (4.88) as

$$M_W(\lambda, t_f) = \frac{1}{Z(0)}\int dy^f_q dy^f_{cl} dy^i_q dy^i_{cl} \frac{e^{\lambda\mathcal{E}_\lambda[y^f_q, y^f_{cl}, \alpha(t_f)]}}{e^{(\beta+\lambda)\mathcal{E}_{-\lambda-\beta}[y^i_q, y^i_{cl}, \alpha(0)]}} \mathcal{U}[y^f_q, y^f_{cl}, t_f; y^i_q, y^i_{cl}, 0], \tag{4.131}$$

With $\mathcal{U}$ denoting the propagator from the initial values of the fields (y^i_q, y^i_{cl}) to the final values (y^f_q, y^f_{cl}), which can be obtained by integrating the contribution of the forward branch in Eq.(4.88) with the appropriate boundary conditions mentioned below Eqs.(4.130), (4.128), (4.129), we define the integrand of Eq. (4.88) for $\lambda = 0$ as

$$K(y^f_q, y^f_{cl}, y^i_q, y^i_{cl}) = Z(0)^{-1}\mathcal{U}[y^f_q, y^f_{cl}, t_f; y^i_q, y^i_{cl}, 0] e^{-\beta\mathcal{E}_{-\beta}[y^i_q, y^i_{cl}, \alpha(0)]}. \tag{4.132}$$

The expression in Eq. (4.132) exhibits a similar structure to the joint probability distribution of a classical system with a two-dimensional configuration space spanned by (y_q, y_{cl}). In this analogy, the system is initially prepared in a Gibbs state characterized by the Hamiltonian $\mathcal{E}_{-\beta}[y^i_q, ycl^i, \alpha(0)]$ and undergoes a stochastic evolution that brings it to the final configuration (y^f_q, y^f_{cl}).

However, it should be noted that due to the general complex nature of $\mathcal{U}$, the quantity K lacks a direct probabilistic interpretation. Nevertheless, we can interpret Eq. (4.132) in terms of Wigner functions [115, 114, 50, 86, 88]. It has been shown that by considering appropriate phase space representations, the expression can be connected to Wigner functions, which provide a phase space formulation of quantum mechanics.

Indeed, it is possible to establish a connection and prove the relationship between the expression in Eq. (4.132) and Wigner functions. First we write

$$\int dy^i_q dy^f_q K(y^f_q, y^f_{cl}, y^i_q, y^i_{cl}) = C\int dp^i dp^f \Pi(p^f, y^f_{cl}, p^i, y^i_{cl}) W_\beta(p^i, y^i_{cl}) \tag{4.133}$$

[1] here we use the notation $x_{q/cl\downarrow}(\tau)$ for the fields on the branch $\gamma_{(\ominus,\downarrow),(\ominus,M)}$ (see Eq 4.105).

The variable W_β corresponds to the Wigner representation of the initial state, while Π represents the Weyl transform of the propagator. The constant C serves as a normalization factor. It is well-established that on the right-hand side of Eq. (4.133), W_β and Π can be interpreted as classical distributions in phase space. Specifically, W_β corresponds to a classical Gibbs state distribution, while Π represents a classical propagator that enforces the deterministic equations of motion in the phase space [115].

By considering both the integrand on the left-hand side and the integrand on the right-hand side of Eq. (4.133), we can introduce a generalization of the detailed balance conditions. Utilizing the notion of time-reversed trajectories introduced in Section 4.6, it can be shown that the propagators of the forward trajectory and the time-reversed trajectory coincide when we reverse the initial and final positions.

To proceed, let us focus on the classical expansion of the quantity $\mathcal{E}_{-\beta}$, which corresponds to the integral along the branch $\gamma_{(\ominus,M)}$. The action in this case is denoted by Σ and can be expanded in terms of small $x_{q\downarrow}$ [115] (see footnote 1). Therefore

$$\Sigma = m\left(\dot{x}_{cl\downarrow}^2 + \dot{x}_{q\downarrow}^2\right) + 2V(\alpha, x_{cl\downarrow}) + V''(\alpha, x_{cl\downarrow})x_{q\downarrow}^2 + O(\hbar^2). \tag{4.134}$$

In comparison to Eq. (4.89), there is a sign change in the kinetic term in the present case due to the use of $x_{cl\downarrow}(\tau)$ instead of $\gamma_{cl}(z)$. This arises from the relationship $\frac{d}{dz} = -i\frac{d}{d\tau}$ in the vertical branches. Considering that the branch $\gamma_{(\ominus,\downarrow)}$ is short for $\hbar \to 0$, the value of $x_{cl\downarrow}$ will not vary significantly from the value at the boundary with $\gamma_{(\ominus,-)}$, denoted as y_{cl}^i. Hence, we can define $x_{cl\downarrow}(s) = y_{cl}^i + \delta(s)$ and derive the following expression

$$\begin{aligned}\Sigma =& m\left(\dot{\delta}^2(s) + \dot{x}_{q\downarrow}^2(s)\right) + 2V(\alpha(0), y_{cl}^i) + 2V'(\alpha(0), y_{cl}^i)\delta(s) \\ &+ V''(\alpha(0), y_{cl}^i)[x_{q\downarrow}^2(s) + \delta^2(s)] + O(\hbar^2).\end{aligned} \tag{4.135}$$

Our primary focus lies in the scenario where the boundaries in the path integration described by Eq. (4.128) with $\lambda = 0$ are specified as $x_{q\downarrow}(\hbar\beta/2) = x_{q\downarrow}(0) = 0$. In this particular case, the contribution from the integral over the quantum variables becomes negligible. Consequently, the path integration involving $x_{cl\downarrow}$ simplifies to a path integration over $\delta(s)$ with boundary conditions $\delta(0) = 0$. While the initial value of δ remains arbitrary, we denote it as $\bar{\delta}$.

$$\int \mathcal{D}'\delta e^{\frac{1}{\hbar}\int_{-\hbar\frac{\beta}{2}}^{0} d\tau\left(m\dot{\delta}^2(s) + 2V(\alpha(0), y_{cl}^i) + 2V'(\alpha(0), y_{cl}^i)\delta(s) + V''(\alpha(0), y_{cl}^i)\delta^2(s)\right)}$$

$$= \int \mathcal{D}'\delta e^{\frac{1}{\hbar}\int_{-\hbar\frac{\beta}{2}}^{0} d\tau \left[m\dot{\delta}^2(s)+m\Omega^2\left(\delta+\Delta\right)^2-m\Omega^2\Delta^2\right]}, \tag{4.136}$$

where we introduced $\Omega = \sqrt{\frac{V''(\alpha(0),y^i_{cl})}{m}}$ and $\Delta = \frac{V'(\alpha(0),y^i_{cl})}{V''(\alpha(0),y^i_{cl})}$. After doing the change of variable $\delta \to \delta + \Delta$ and solving the path integral we obtain as a result

$$\left(\frac{m\Omega}{\pi\hbar\sinh\left(\frac{\beta\hbar\Omega}{2}\right)}\right)^{\frac{1}{2}} e^{-\beta[V(\alpha(0),y^i_{cl})-\frac{1}{2}m\Omega^2\Delta^2]} e^{\left\{-\frac{m\Omega}{\hbar}\frac{\cosh\left(\frac{\hbar\beta\Omega}{2}\right)[(\bar{\delta}+\Delta)^2+\Delta^2]-2\Delta(\bar{\delta}+\Delta)}{\sinh\left(\frac{\hbar\beta\Omega}{2}\right)}\right\}}$$
$$\approx e^{-\beta[V(\alpha(0),y^i_{cl})-\frac{1}{2}m\Omega^2\Delta^2]}\left(\frac{2m}{\pi\hbar^2\beta}\right)^{\frac{1}{2}}\exp\left\{-\frac{2m}{\hbar^2\beta}\bar{\delta}^2-\frac{2m}{\hbar^2\beta}\frac{\hbar^2\beta^2\Omega^2}{8}[2\Delta^2+2\bar{\delta}\Delta+\bar{\delta}^2]\right\}, \tag{4.137}$$

In the last exponential, the two contributions arise from the zeroth and second order expansions of the hyperbolic cosine with respect to $\hbar$. It is important to observe that the terms proportional to Δ^2 cancel out, resulting in an integral over $\bar{\delta}$ as the remaining contribution. Hence

$$\int_{-\infty}^{\infty} d\bar{\delta} e^{-\beta V(\alpha(0),y^i_{cl})}\left(\frac{2m}{\pi\hbar^2\beta}\right)^{\frac{1}{2}}\exp\left\{-\frac{2m}{\hbar^2\beta}\bar{\delta}^2-\frac{m\beta^2\Omega^2}{4}[2\bar{\delta}\Delta+\bar{\delta}^2]\right\}$$
$$\approx \int_{-\infty}^{\infty} d\bar{\delta} e^{-\beta V(\alpha(0),y^i_{cl})}\left(\frac{2m}{\pi\hbar^2\beta}\right)^{\frac{1}{2}}\exp\left\{-\frac{2m}{\hbar^2\beta}\bar{\delta}^2\right\} = e^{-\beta V(\alpha(0),y^i_{cl})}, \tag{4.138}$$

where the second term in the integrand in the first line can be neglected since it is of the next order in $\hbar$. This proves that

$$\frac{K(y^f_q,y^f_{cl},y^i_q,y^i_{cl})}{K^{\text{rev}}(y^i_q,y^i_{cl},y^f_q,y^f_{cl})} = \frac{e^{-\beta\mathcal{E}_{-\beta}[y^i_q,y^i_{cl},\alpha(0)]}}{e^{-\beta\mathcal{E}_{-\beta}[y^f_q,y^f_{cl},\alpha(t_f)]}}e^{-\beta\Delta F}. \tag{4.139}$$

The quantity $e^{-\beta\Delta F} = Z(t_f)/Z(0)$ represents the ratio of partition functions between the final time t_f and the initial time $t = 0$. As mentioned earlier, K is not necessarily real and does not have a direct operational interpretation in terms of measurements. However, if we set $y^i_q = y^f_q = 0$, then K corresponds to the joint probability distribution $P(y^f_{cl}, y^i_{cl})$ in a two-point measurement process of the position operator, where the initial and final measured values are given by y^i_{cl} and y^f_{cl}. This can be inferred from Eq. (4.133) that

$$\iint dy_q^i dy_q^f K(y_q^f, y_{cl}^f, y_q^i, y_{cl}^i) = \iint dy_q^i dy_q^f \iint dp^i dp^f \iint d\eta^i d\eta^f K(\eta^f, y_{cl}^f, \eta^i, y_{cl}^i) e^{ip^i(y_q^i-\eta^i)} e^{ip^f(y_q^f-\eta^f)}. \tag{4.140}$$

Let us focus on the dependence by η^i, y_q^i, p^i, after replacing the definition of K in the equation above we have a contribution of the form

$$Z(0)^{-1} \iint d\eta^i dy_q^i e^{ip^i(y_q^i-\eta^i)} \mathcal{U}[\eta^f, y_{cl}^f, t_f; \eta^i, y_{cl}^i, 0] e^{-\beta \mathcal{E}_{-\beta}[\eta^i, y_{cl}^i, \alpha(0)]}. \tag{4.141}$$

Remembering the definition of $\mathcal{E}_{-\beta}$ we can also write

$$e^{-i\eta^i p^i} Z(0)^{-1} e^{-\beta \mathcal{E}_{-\beta}[\eta^i, y_{cl}^i, \alpha(0)]} = e^{-i\eta^i p^i} \left\langle y_{cl}^i - \eta^i \right| \rho_0 \left| y_{cl}^i + \eta^i \right\rangle. \tag{4.142}$$

After integrating over η^i, the expression above, disregarding irrelevant prefactors, becomes proportional to the Wigner function associated with the initial state, denoted as W_β. Similarly, by integrating over y_q^i and y_q^f, the propagator $\mathcal{U}$ transforms into the quantum phase space propagator. In the classical limit, this reduces to

$$\frac{P(y_{cl}^f, y_{cl}^i)}{P^{\text{rev}}(y_{cl}^i, y_{cl}^f)} = e^{\beta[V(\alpha(t_f), y_{cl}^f) - V(\alpha(0), y_{cl}^i)] - \beta \Delta F} + O(\hbar). \tag{4.143}$$

This corresponds to a detailed balance condition for the exchanges of potential energy in the system. This result is consistent with the fact that in the initial measurement, there is no information about the initial momentum of the particle. To derive the classical form of detailed balance in the phase space representation, we need to consider the right-hand side of Eq. (4.133). In the classical limit, the Wigner function becomes non-positive, and we obtain

$$\frac{\Pi(p^f, y_{cl}^f, p^i, y_{cl}^i) W_\beta(p^i, y_{cl}^i)}{\Pi^{\text{rev}}(-p^i, y_{cl}^i, -p^f, y_{cl}^f) W_\beta^{\text{rev}}(-p^f, y_{cl}^f)} = \frac{W_\beta(p^i, y_{cl}^i)}{W_\beta^{\text{rev}}(-p^f, y_{cl}^f)} \approx e^{\beta(W_{cl} - \Delta F)} + O(\hbar), \tag{4.144}$$

The function W_{cl} is given by Eq. (4.109) following the classical results [65], while W_β^{rev} represents the Wigner function associated with the initial state of the time-reversed trajectory. The final equivalence can also be derived from the relationship between the Wigner function and classical Gibbs state in the classical limit [115]. It should be noted that the inclusion of minus signs in front of the final momentum is done for completeness, although in our calculations, where the Hamiltonian is always quadratic in p, this change of sign becomes

irrelevant.

4.8 Conclusions

In this chapter, our focus was on exploring the statistics of work using the concept of moment-generating functions (MGFs). To achieve this, we introduced a modified Keldysh contour, which proved to be a powerful tool for our analysis. The symmetry properties of this contour played a crucial role in ensuring the consistency of our perturbative approach and the emergence of fluctuation relations.

We demonstrated the versatility of the modified contour technique, particularly in the context of diagrammatic methods. By utilizing this technique, we derived the work distribution for a switch on/off scenario, revealing that the work can be represented as a linear combination of rescaled Poisson processes. Each process corresponds to a distinct channel through which energy is exchanged between the system and the experimental driving apparatus, taking the form of discrete energy packages.

By employing Feynman path integral techniques and symmetrizing the contour, we applied a generalized version of the Keldysh rotation approach. This allowed us to express the action in terms of classical and quantum fields, enabling us to extend the notion of detailed balance to quantum trajectories and establish connections with the Wigner function.

Lastly, we obtained the semi-classical expansion of the work MGF, which provided valuable insights into the behavior of the system under different perturbations and approximations. This expansion allowed us to explore the semiclassical regime and extract meaningful information about work statistics.

Chapter 5

Discussion and perspectives

In this thesis, we focused on two main concepts of quantum thermodynamics: work and heat. Specifically, we analyzed the behavior of heat currents in overdamped quantum systems by studying two magnetically coupled RLC circuits. We established the role of dissipation by employing the Caldeira-Leggett model, which replaces the resistor in the circuits with a large number of series LC circuits. This paved the way to examine the heat current between two quantum harmonic oscillators that are overdamped and coupled to local thermal baths. We derived closed analytical expressions for the heat current, taking into account both quantum and classical contributions, without resorting to weak coupling or Markovian approximations. These results can serve as a useful benchmark to test approximate methods, such as Markovian embedding schemes or the method developed in [79]. Our findings indicate that in the overdamped regime, there is an intermediate temperature range where significant quantum corrections to the classical heat current exist, even if the temperatures are high compared to the only relevant frequency scale of the system dynamics. This is a noteworthy observation as it broadens the temperature range where quantum effects are relevant in thermal transport.

Although our results apply to general harmonic systems, we have specifically focused on an electronic implementation as low-temperature electronic circuits are a promising platform for investigating quantum energy transport. In this regard we studied a set-up which is used in realization of dynamical Casimir effects [34, 116]. This set up was consisting of cavities that are interrupted by SQUID. By quantizing the SQUID degrees of freedom we showed that, one can find a three-body interaction Hamiltonian. The Hamiltonian can be reduced to a form of quantum absorption refrigerator interaction in which the SQUID can autonomously cool down the other two modes of the cavities.

In the last section, we discussed the statistics of work extraction for closed quantum systems. We utilized the modified Keldysh contour to investigate the perturbative approach to MGFs and their semi-classical limit, and demonstrated the consistency of the perturbative

expansion through the symmetry property of the extended contour. Our study showed the suitability of the modified contour technique for diagrammatic approaches, allowing us to derive the work distribution in a switch on/off scenario. Expressing the MGF in terms of a Feynman path integral and using the Keldysh rotation, we generalized the detailed balance to quantum trajectories and made contact with the Wigner function and classical phase space approaches to thermodynamics.

Interesting perspectives of this thesis may involve the study of non-linear RLC circuits. As we discussed in the second chapter, it is indeed a burdensome task to find analytical solution to the heat currents for interacting superconducting qubits. Therefore, developing a new methodology to study those systems will be essential for understanding heat currents in strong coupling regime.

In the concept of work statistics, a potential avenue for future research is to extend our approach to many-body open quantum systems [103, 102] and evaluate the effectiveness of our new contour in maintaining thermodynamic consistency while calculating work and heat counting statistics using established approximation schemes like GW or random phase (RPA) [92, 49, 55].

Bibliography

[1] Robert Alicki. “On the detailed balance condition for non-Hamiltonian systems”. In: *Reports on Mathematical Physics* 10.2 (1976), pp. 249–258. DOI: 10.1016/0034-4877(76)90046-X.

[2] Alexander Altland and Ben D. Simons. *Condensed matter field theory*. Cambridge University Press, 2010. DOI: https://doi.org/10.1017/CBO9780511789984.

[3] Gian Marcello Andolina et al. “Extractable work, the role of correlations, and asymptotic freedom in quantum batteries”. In: *Physical review letters* 122.4 (2019), p. 047702. DOI: https://doi.org/10.1103/PhysRevLett.122.047702.

[4] David Andrieux and Pierre Gaspard. “A fluctuation theorem for currents and non-linear response coefficients”. In: *Journal of Statistical Mechanics: Theory and Experiment* 2007.02 (2007), P02006. DOI: https://iopscience.iop.org/article/10.1088/1742-5468/2007/02/P02006.

[5] David Andrieux and Pierre Gaspard. “Quantum Work Relations and Response Theory”. In: *Phys. Rev. Lett.* 100 (23 2008), p. 230404. DOI: 10.1103/PhysRevLett.100.230404. URL: https://link.aps.org/doi/10.1103/PhysRevLett.100.230404.

[6] Joachim Ankerhold, Philip Pechukas, and Hermann Grabert. “Strong friction limit in quantum mechanics: The quantum Smoluchowski equation”. In: *Phys. Rev. Lett.* 87.8 (2001), p. 086802. DOI: 10.1103/PhysRevLett.87.086802.

[7] A Asadian et al. “Heat transport through lattices of quantum harmonic oscillators in arbitrary dimensions”. In: *Phy. Rev. E* 87.1 (2013), p. 012109. DOI: 10.1103/PhysRevE.87.012109.

[8] Erik Aurell, Brecht Donvil, and Kirone Mallick. “Large deviations and fluctuation theorem for the quantum heat current in the spin-boson model”. In: *Physical Review E* 101.5 (2020), p. 052116. DOI: https://journals.aps.org/pre/abstract/10.1103/PhysRevE.101.052116.

[9] Erik Aurell, Ryochi Kawai, and Ketan Goyal. "An operator derivation of the Feynman–Vernon theory, with applications to the generating function of bath energy changes and to an-harmonic baths". In: *Journal of Physics A: Mathematical and Theoretical* 53.27 (2020), p. 275303. DOI: 10.1088/1751-8121/ab9274.

[10] Nicolas Bergmann and Michael Galperin. "Green's functions perspective on nonequilibrium thermodynamics of open quantum systems strongly coupled to baths". In: *arXiv:2004.05175 [cond-mat]* (). DOI: arXiv:2004.05175. URL: http://arxiv.org/abs/2004.05175.

[11] G. N Bochkov and I. E. Kuzovlev. "General theory of thermal fluctuations in nonlinear systems". In: *Sov. Phys. JETP* 45 (1977), pp. 125–130. DOI: http://www.jetp.ras.ru/cgi-bin/dn/e_045_01_0125.pdf.

[12] J. Bourassa et al. "Josephson junction-embedded transmission-line resonators: from Kerr medium to in-line transmon". In: *Physical Review A* 86.1 (July 11, 2012), p. 013814. ISSN: 1050-2947, 1094-1622. DOI: 10.1103/PhysRevA.86.013814. arXiv: 1204.2237[cond-mat,physics:quant-ph]. URL: http://arxiv.org/abs/1204.2237 (visited on 01/26/2023).

[13] Anton Bruch, Caio Lewenkopf, and Felix von Oppen. "Landauer-Büttiker Approach to Strongly Coupled Quantum Thermodynamics: Inside-Outside Duality of Entropy Evolution". In: *Phys. Rev. Lett.* 120.10 (2018), p. 107701. DOI: 10.1103/PhysRevLett.120.107701. URL: https://link.aps.org/doi/10.1103/PhysRevLett.120.107701.

[14] Anton Bruch et al. "Quantum Thermodynamics of the Driven Resonant Level Model". In: *Phys. Rev. B* 93.11 (2016), p. 115318. DOI: 10.1103/PhysRevB.93.115318. URL: http://link.aps.org/doi/10.1103/PhysRevB.93.115318.

[15] Amir O Caldeira. *An introduction to macroscopic quantum phenomena and quantum dissipation*. Cambridge University Press, 2014. DOI: https://doi.org/10.1017/CBO9781139035439.

[16] Amir O Caldeira. *An introduction to macroscopic quantum phenomena and quantum dissipation*. Cambridge University Press, 2014. DOI: https://doi.org/10.1017/CBO9781139035439.

[17] Amir O Caldeira and Anthony J Leggett. "Quantum tunnelling in a dissipative system". In: *Annals of physics* 149.2 (1983), pp. 374–456. DOI: https://www.sciencedirect.com/science/article/abs/pii/0003491683902026.

[18] Francesco Campaioli et al. "Enhancing the charging power of quantum batteries". In: *Physical review letters* 118.15 (2017), p. 150601. DOI: https://link.springer.com/chapter/10.1007/978-3-319-99046-0_8.

[19] LO Castaños and A Zuñiga-Segundo. "The forced harmonic oscillator: Coherent states and the RWA". In: *American Journal of Physics* 87.10 (2019), pp. 815–823.

[20] Vasco Cavina et al. "A convenient Keldysh contour for thermodynamically consistent perturbative and semiclassical expansions". In: *arXiv preprint arXiv:2304.03681* (2023). DOI: https://doi.org/10.48550/arXiv.2304.03681.

[21] J. Clarke and A. I. Braginski, eds. *The SQUID handbook*. OCLC: ocm52746892. Weinheim: Wiley-VCH, 2004. 2 pp. ISBN: 978-3-527-40411-7 978-3-527-40408-7 978-3-527-40229-8.

[22] C. De Dominicis and L. Peliti. "Field-theory renormalization and critical dynamics above T_c: Helium, antiferromagnets, and liquid-gas systems". In: *Phys. Rev. B* 18 (1 1978), pp. 353–376. DOI: 10.1103/PhysRevB.18.353. URL: https://link.aps.org/doi/10.1103/PhysRevB.18.353.

[23] S. Deffner and E. Lutz. "Nonequilibrium work distribution of a quantum harmonic oscillator". In: *Physical Review A* 77 (2008). DOI: https://link.aps.org/doi/10.1103/PhysRevE.77.021128.

[24] Michel H Devoret, Andreas Wallraff, and John M Martinis. "Superconducting qubits: A short review". In: *arXiv preprint cond-mat/0411174* (2004). DOI: https://arxiv.org/abs/cond-mat/0411174.

[25] Michel H Devoret et al. "Quantum fluctuations in electrical circuits". In: *Les Houches, Session LXIII* 7.8 (1995), pp. 133–135. DOI: https://www.physique.usherbrooke.ca/tremblay/cours/PHY-731/Quantum_circuit_theory-1.pdf.

[26] Raoul Dillenschneider and Eric Lutz. "Quantum Smoluchowski equation for driven systems". In: *Phys. Rev. E* 80.4 (2009), p. 042101. DOI: 10.1103/PhysRevE.80.042101.

[27] Thomas Dittrich, Carlos Viviescas, and Luis Sandoval. "Semiclassical Propagator of the Wigner Function". In: *Physical Review Letter* 96 (2006), p. 070403. DOI: https://link.aps.org/pdf/10.1103/PhysRevLett.96.070403.

[28] Wenjie Dou et al. "Universal approach to quantum thermodynamics in the strong coupling regime". In: *Phys. Rev. B* 98.13 (2018), p. 134306. DOI: 10.1103/PhysRevB.98.134306.

[29] Massimiliano Esposito, Upendra Harbola, and Shaul Mukamel. "Nonequilibrium fluctuations, fluctuation theorems, and counting statistics in quantum systems". In: *Rev. Mod. Phys.* 81 (4 2009), pp. 1665–1702. DOI: 10.1103/RevModPhys.81.1665. URL: https://link.aps.org/doi/10.1103/RevModPhys.81.1665.

[30] Massimiliano Esposito, Katja Lindenberg, and Christian Van den Broeck. "Entropy production as correlation between system and reservoir". In: *New Journal of Physics* 12.1 (2010), p. 013013. DOI: 10.1088/1367-2630/12/1/013013. URL: https://doi.org/10.1088%2F1367-2630%2F12%2F1%2F013013.

[31] Massimiliano Esposito, Maicol A. Ochoa, and Michael Galperin. "Quantum thermodynamics: A nonequilibrium Green's function approach". In: *Phys. Rev. Lett.* 114.8 (2015), p. 080602. DOI: 10.1103/PhysRevLett.114.080602.

[32] Massimiliano Esposito and Michael Ochoa Maicol A. andGalperin. "Nature of heat in strongly coupled open quantum systems". In: *Phys. Rev. B* 92.23 (2015), p. 235440. DOI: 10.1103/PhysRevB.92.235440. URL: https://link.aps.org/doi/10.1103/PhysRevB.92.235440.

[33] Zhaoyu Fei et al. "Quantum work distributions associated with the dynamical Casimir effect". In: *Physical Review A* 99.5 (2019). ISSN: 2469-9934. DOI: 10.1103/physreva.99.052508. URL: http://dx.doi.org/10.1103/PhysRevA.99.052508.

[34] S. Felicetti et al. "Dynamical Casimir effect entangles artificial atoms". In: *Physical Review Letters* 113.9 (Aug. 27, 2014), p. 093602. ISSN: 0031-9007, 1079-7114. DOI: 10.1103/PhysRevLett.113.093602. arXiv: 1402.4451[cond-mat, physics:quant-ph]. URL: http://arxiv.org/abs/1402.4451 (visited on 12/12/2022).

[35] Richard P Feynman. *Statistical mechanics: a set of lectures*. CRC press, 2018.

[36] Richard P Feynman, Albert R Hibbs, and Daniel F Styer. *Quantum mechanics and path integrals*. Courier Corporation, 2010. DOI: https://books.google.lu/books?hl=en&lr=&id=JkMuDAAAQBAJ&oi=fnd&pg=PP1&dq=feynman+and+hibbs&ots=xHkMgHFq2r&sig=SLhfIG8uv04IdwcjiowceK-5xdY&redir_esc=y#v=onepage&q=feynman%20and%20hibbs&f=false.

[37] César D. Fosco, Fernando C. Lombardo, and Francisco D. Mazzitelli. "Vacuum fluctuations and generalized boundary conditions". In: *Physical Review D* 87.10 (May 10, 2013), p. 105008. ISSN: 1550-7998, 1550-2368. DOI: 10.1103/PhysRevD.87.105008. URL: https://link.aps.org/doi/10.1103/PhysRevD.87.105008 (visited on 01/02/2023).

[38] Nahuel Freitas, Esteban A Martinez, and Juan Pablo Paz. "Heat transport through ion crystals". In: *Physica Scripta* 91.1 (2015), p. 013007. DOI: 10.1088/0031-8949/91/1/013007.

[39] Nahuel Freitas and Juan Pablo Paz. "Analytic solution for heat flow through a general harmonic network". In: *Phys. Rev. E* 90.4 (2014), p. 042128. DOI: 10.1103/PhysRevE.90.042128.

[40] Nahuel Freitas and Juan Pablo Paz. "Fundamental limits for cooling of linear quantum refrigerators". In: *Phys. Rev. E* 95.1 (2017), p. 012146. DOI: 10.1103/PhysRevE.95.012146.

[41] Ken Funo and H. T. Quan. "Path integral approach to heat in quantum thermodynamics". In: *Physical Review E* 98.1 (2018). ISSN: 2470-0053. DOI: 10.1103/physreve.98.012113. URL: http://dx.doi.org/10.1103/PhysRevE.98.012113.

[42] Ken Funo and H.T. Quan. "Path Integral Approach to Quantum Thermodynamics". In: *Physical Review Letters* 121.4 (2018). ISSN: 1079-7114. DOI: https://doi.org/10.1103/PhysRevLett.121.040602. URL: http://dx.doi.org/10.1103/PhysRevLett.121.040602.

[43] CW Gardiner. "Quantum noise and quantum Langevin equations". In: *IBM Journal of Research and Development* 32.1 (1988), pp. 127–136. DOI: 10.1147/rd.321.0127.

[44] S Gasparinetti et al. “Heat-exchange statistics in driven open quantum systems”. In: *New Journal of Physics* 16.11 (2014), p. 115001. DOI: https://doi.org/10.48550/arXiv.1404.3507.

[45] Christopher Gaul and Helmut Büttner. “Quantum mechanical heat transport in disordered harmonic chains”. In: *Phys. Rev. E* 76.1 (2007), p. 011111. DOI: 10.1103/PhysRevE.76.011111.

[46] S. M. Girvin. “Circuit QED: superconducting qubits coupled to microwave photons”. In: *Quantum Machines: Measurement and Control of Engineered Quantum Systems*. Ed. by Michel Devoret et al. 1st ed. Oxford University PressOxford, June 12, 2014, pp. 113–256. ISBN: 978-0-19-968118-1 978-0-19-176145-4. DOI: 10.1093/acprof:oso/9780199681181.003.0003. URL: https://academic.oup.com/book/43704/chapter/367194888 (visited on 01/25/2023).

[47] S. M. Girvin. “Introduction to Quantum Electromagnetic Circuits”. In: *Oxford University Press* (2014). DOI: 10.1002/cta.2359.

[48] Steven M Girvin. “Circuit QED: superconducting qubits coupled to microwave photons”. In: *Quantum machines: measurement and control of engineered quantum systems* (2014), pp. 113–256. DOI: https://www.oxfordscholarship.com/view/10.1093/acprof:oso/9780199681181.001.0001/acprof-9780199681181-chapter-3.

[49] Gabriele Giuliani and Giovanni Vignale. *Quantum theory of the electron liquid*. Cambridge university press, 2005. DOI: https://doi.org/10.1017/CBO9780511619915.

[50] Roy J Glauber. *Quantum theory of optical coherence: selected papers and lectures*. John Wiley & Sons, 2007.

[51] Andreas Greiner et al. “Thermal conductivity and Lorenz number for one-dimensional ballistic transport”. In: *Physical review letters* 78.6 (1997), p. 1114.

[52] Patrick Haughian, Massimiliano Esposito, and Thomas L. Schmidt. “Quantum Thermodynamics of the Resonant-Level Model with Driven System-Bath Coupling”. In: *Phys. Rev. B* 97.8 (2018), p. 085435. DOI: 10.1103/PhysRevB.97.085435. URL: https://link.aps.org/doi/10.1103/PhysRevB.97.085435.

[53] Tim Herpich et al. “Stochastic thermodynamics of all-to-all interacting many-body systems”. In: *New Journal of Physics* 22.6 (2020), p. 063005. DOI: https://iopscience.iop.org/article/10.1088/1367-2630/ab882f.

[54] Patrick P. Hofer et al. "Autonomous quantum refrigerator in a circuit QED architecture based on a Josephson junction". In: *Physical Review B* 94.23 (Dec. 16, 2016), p. 235420. ISSN: 2469-9950, 2469-9969. DOI: 10.1103/PhysRevB.94.235420. URL: https://link.aps.org/doi/10.1103/PhysRevB.94.235420 (visited on 12/12/2022).

[55] Edvin G. Idrisov and Thomas L. Schmidt. "Entropy Production in One-Dimensional Quantum Fluids". In: *Physical Review B* 100.16 (Oct. 2019), p. 165404. DOI: 10.1103/PhysRevB.100.165404. URL: https://link.aps.org/doi/10.1103/PhysRevB.100.165404.

[56] C. Jarzynski. "Nonequilibrium Equality for Free Energy Differences". In: *Physical Review Letters* 78.14 (1997), 2690–2693. ISSN: 1079-7114. DOI: 10.1103/physrevlett.78.2690. URL: http://dx.doi.org/10.1103/PhysRevLett.78.2690.

[57] Christopher Jarzynski, HT Quan, and Saar Rahav. "Quantum-classical correspondence principle for work distributions". In: *Physical review X* 5.3 (2015), p. 031038. DOI: https://link.aps.org/doi/10.1103/PhysRevX.5.031038.

[58] Brian David Josephson. "Possible new effects in superconductive tunnelling". In: *Physics letters* 1.7 (1962), pp. 251–253. DOI: https://www.sciencedirect.com/science/article/abs/pii/0031916362913690?via%3Dihub.

[59] Sergi Julià-Farré et al. "Bounds on the capacity and power of quantum batteries". In: *Physical Review Research* 2.2 (2020), p. 023113. DOI: https://doi.org/10.1103/PhysRevResearch.2.023113.

[60] Leo P Kadanoff and Gordon Baym. *Quantum statistical mechanics: Green's function methods in equilibrium and nonequilibrium problems*. CRC Press, 2018. DOI: https://doi.org/10.1201/9780429493218.

[61] Sadeq S Kadijani et al. "Heat transport in overdamped quantum systems". In: *Physical Review B* 102.23 (2020), p. 235422. DOI: https://doi.org/10.1103/PhysRevB.102.235422.

[62] A. Kamenev. *Field Theory of Non-Equilibrium Systems*. Cambridge University Press, 2011. ISBN: 9781139500296. URL: https://books.google.lu/books?id=CwlrUepnla4C.

[63] Akihito Kato and Yoshitaka Tanimura. "Quantum heat transport of a two-qubit system: Interplay between system-bath coherence and qubit-qubit coherence". In: *The Journal of Chemical Physics* 143.6 (2015), p. 064107. DOI: https://doi.org/10.1063/1.4928192.

[64] Gil Katz and Ronnie Kosloff. "Quantum thermodynamics in strong coupling: Heat transport and refrigeration". In: *Entropy* 18.5 (2016), p. 186. DOI: 10.3390/e18050186.

[65] Ryoichi Kawai, Juan MR Parrondo, and Christian Van den Broeck. "Dissipation: The phase-space perspective". In: *Physical review letters* 98.8 (2007), p. 080602.

[66] Leonid V Keldysh et al. "Diagram technique for nonequilibrium processes". In: *Sov. Phys. JETP* 20.4 (1965), pp. 1018–1026. DOI: http://jetp.ras.ru/cgi-bin/e/index/e/20/4/p1018?a=list.

[67] Shishir Khandelwal et al. "Critical heat current for operating an entanglement engine". In: *New Journal of Physics* 22.7 (2020), p. 073039. DOI: 10.1088/1367-2630/ab9983.

[68] Jens Koch et al. "Charge-insensitive qubit design derived from the Cooper pair box". In: *Physical Review A* 76.4 (2007), p. 042319. DOI: https://doi.org/10.1103/PhysRevA.76.042319.

[69] Andrzej Kossakowski et al. "Quantum detailed balance and KMS condition". In: *Commun.Math. Phys.* 57 (1977), 97—110. DOI: 10.1007/BF01625769.

[70] David C Langreth et al. *Linear and nonlinear electron transport in solids*. 1976. DOI: https://link.springer.com/book/10.1007/978-1-4757-0875-2.

[71] C. K. Law. "Interaction between a moving mirror and radiation pressure: A Hamiltonian formulation". In: *Physical Review A* 51.3 (Mar. 1, 1995), pp. 2537–2541. ISSN: 1050-2947, 1094-1622. DOI: 10.1103/PhysRevA.51.2537. URL: https://link.aps.org/doi/10.1103/PhysRevA.51.2537 (visited on 03/09/2023).

[72] Alexandre Lazarescu et al. "Large deviations and dynamical phase transitions in stochastic chemical networks". In: *The Journal of Chemical Physics* 151.6 (2019), p. 064117. DOI: https://doi.org/10.1063/1.5111110.

[73] Anthony J Leggett et al. "Dynamics of the dissipative two-state system". In: *Reviews of Modern Physics* 59.1 (1987), p. 1. DOI: https://doi.org/10.1103/RevModPhys.59.1.

[74] Amikam Levy and Ronnie Kosloff. "The local approach to quantum transport may violate the second law of thermodynamics". In: *Europhysics Letters* 107.2 (2014), p. 20004. DOI: 10.1209/0295-5075/107/20004.

[75] Goran Lindblad. "On the generators of quantum dynamical semigroups". In: *Communications in Mathematical Physics* 48 (1976), pp. 119–130. DOI: https://doi.org/10.1007%2FBF01608499.

[76] A. Lupascu, C. J. P. M. Harmans, and J. E. Mooij. "Quantum state detection of a superconducting flux qubit using a DC-SQUID in the inductive mode". In: *Physical Review B* 71.18 (May 13, 2005), p. 184506. ISSN: 1098-0121, 1550-235X. DOI: 10.1103/PhysRevB.71.184506. arXiv: cond-mat/0410730. URL: http://arxiv.org/abs/cond-mat/0410730 (visited on 01/20/2023).

[77] Paul Cecil Martin, ED Siggia, and HA Rose. "Statistical dynamics of classical systems". In: *Physical Review A* 8.1 (1973), p. 423. DOI: https://doi.org/10.1103/PhysRevA.8.423.

[78] Esteban A Martinez and Juan Pablo Paz. "Dynamics and thermodynamics of linear quantum open systems". In: *Phys. Rev. Lett.* 110.13 (2013), p. 130406. DOI: 10.1103/PhysRevLett.110.130406.

[79] F. Mascherpa et al. "Optimized auxiliary oscillators for the simulation of general open quantum systems". In: *Phys. Rev. A* 101.5 (2020), p. 052108. ISSN: 2469-9934. DOI: 10.1103/PhysRevA.101.052108.

[80] Gleb Maslennikov et al. "Quantum absorption refrigerator with trapped ions". In: *Nature Communications* 10.1 (Jan. 14, 2019). Number: 1 Publisher: Nature Publishing Group, p. 202. ISSN: 2041-1723. DOI: 10.1038/s41467-018-08090-0. URL: https://www.nature.com/articles/s41467-018-08090-0%C2%A0 (visited on 04/04/2023).

[81] F Nicacio et al. "Thermal transport in out-of-equilibrium quantum harmonic chains". In: *Phys. Rev. E* 91.4 (2015), p. 042116. DOI: 10.1103/PhysRevE.91.042116.

[82] Stefan Nimmrichter et al. “Quantum and classical dynamics of a three-mode absorption refrigerator”. In: *Quantum* 1 (Dec. 11, 2017), p. 37. ISSN: 2521-327X. DOI: 10.22331/q-2017-12-11-37. arXiv: 1709.08353[quant-ph]. URL: http://arxiv.org/abs/1709.08353 (visited on 04/04/2023).

[83] Philip Pechukas, Joachim Ankerhold, and Hermann Grabert. “Quantum Smoluchowski equation”. In: *Annalen der Physik* 9.9-10 (2000), pp. 794–803. DOI: 10.1002/1521-3889(200010)9:9/10<794::AID-ANDP794>3.0.CO;2-J.

[84] JB Pendry. “Quantum limits to the flow of information and entropy”. In: *Journal of Physics A: Mathematical and General* 16.10 (1983), p. 2161.

[85] Martí Perarnau-Llobet et al. “Strong coupling corrections in quantum thermodynamics”. In: *Phys. Rev. Lett.* 120.12 (2018), p. 120602. DOI: 10.1103/PhysRevLett.120.120602.

[86] Anatoli Polkovnikov. “Phase space representation of quantum dynamics”. In: *Annals of Physics* 325.8 (2010), 1790–1852. ISSN: 0003-4916. DOI: 10.1016/j.aop.2010.02.006. URL: http://dx.doi.org/10.1016/j.aop.2010.02.006.

[87] Anatoli Polkovnikov. “Phase space representation of quantum dynamics”. In: *Annals of Physics* 325.8 (2010), pp. 1790–1852.

[88] Anatoli Polkovnikov. “Quantum corrections to the dynamics of interacting bosons: Beyond the truncated Wigner approximation”. In: *Physical Review A* 68.5 (2003), p. 053604. DOI: https://link.aps.org/doi/10.1103/PhysRevA.68.053604.

[89] Roberto Raimondi et al. “Quasiclassical approach to the spin Hall effect in the two-dimensional electron gas”. In: *Physical Review B* 74.3 (2006), p. 035340. DOI: https://doi.org/10.1103/PhysRevB.74.035340.

[90] Jørgen Rammer. *Quantum field theory of non-equilibrium states*. Vol. 22. Cambridge University Press Cambridge, 2007. DOI: https://doi.org/10.1017/CBO9780511618956.

[91] Riccardo Rao and Massimiliano Esposito. “Detailed fluctuation theorems: A unifying perspective”. In: *Entropy* 20.9 (2018), p. 635. DOI: 10.3390/e20090635.

[92] Xinguo Ren et al. "Random-phase approximation and its applications in computational chemistry and materials science". In: *Journal of Materials Science* 47.21 (2012), pp. 7447–7471. DOI: https://link.springer.com/article/10.1007/s10853-012-6570-4.

[93] Hannes Risken and Hannes Risken. *Fokker-planck equation*. Springer, 1996. DOI: https://link.springer.com/book/10.1007/978-3-642-61544-3.

[94] Jun John Sakurai and Eugene D Commins. *Modern quantum mechanics, revised edition*. 1995. DOI: https://doi.org/10.1119/1.17781.

[95] DR Schmidt, RJ Schoelkopf, and AN Cleland. "Photon-mediated thermal relaxation of electrons in nanostructures". In: *Physical review letters* 93.4 (2004), p. 045901.

[96] Julian Schwinger. "Brownian motion of a quantum oscillator". In: *Journal of Mathematical Physics* 2.3 (1961), pp. 407–432. DOI: https://doi.org/10.1063/1.1703727.

[97] Dvira Segal. "Qubit-mediated energy transfer between thermal reservoirs: Beyond the Markovian master equation". In: *Physical Review B* 87.19 (2013), p. 195436. DOI: https://doi.org/10.1103/PhysRevB.87.195436.

[98] Udo Seifert. "First and second law of thermodynamics at strong coupling". In: *Phys. Rev. Lett.* 116.2 (2016), p. 020601. DOI: 10.1103/PhysRevLett.116.020601.

[99] Lukas M Sieberer, Michael Buchhold, and Sebastian Diehl. "Keldysh field theory for driven open quantum systems". In: *Reports on Progress in Physics* 79.9 (2016), p. 096001. DOI: 10.1088/0034-4885/79/9/096001.

[100] C Morais Smith and AO Caldeira. "Generalized Feynman-Vernon approach to dissipative quantum systems". In: *Physical Review A* 36.7 (1987), p. 3509. DOI: https://link.aps.org/doi/10.1103/PhysRevA.36.3509.

[101] Ariane Soret, Vasco Cavina, and Massimiliano Esposito. "Thermodynamic consistency of quantum master equations". In: *arXiv preprint arXiv:2207.05719* (2022). URL: https://arxiv.org/abs/2207.05719.

[102] Gianluca Stefanucci and Carl-Olof Almbladh. "Time-dependent partition-free approach in resonant tunneling systems". In: *Phys. Rev. B* 69 (19 2004), p. 195318. DOI: 10.1103/PhysRevB.69.195318. URL: https://link.aps.org/doi/10.1103/PhysRevB.69.195318.

[103] Gianluca Stefanucci and Robert Van Leuween. *Nonequilibrium many-body theory of quantum systems: a modern development*. Cambridge University Press, 2013. DOI: https://doi.org/10.1080/00107514.2013.825326.

[104] Philipp Strasberg. "Operational approach to quantum stochastic thermodynamics". In: *Phy. Rev. E* 100.2 (2019), p. 022127. DOI: 10.1103/PhysRevE.100.022127.

[105] Alberto Suárez et al. "Thermodynamic and stochastic theory of nonequilibrium systems: A Lagrangian approach to fluctuations and relation to excess work". In: *The Journal of chemical physics* 102.11 (1995), pp. 4563–4573. DOI: https://aip.scitation.org/doi/10.1063/1.469504.

[106] Andrey V Timofeev et al. "Electronic refrigeration at the quantum limit". In: *Physical Review Letters* 102.20 (2009), p. 200801.

[107] Raam Uzdin, Amikam Levy, and Ronnie Kosloff. "Equivalence of quantum heat machines, and quantum-thermodynamic signatures". In: *Physical Review X* 5.3 (2015), p. 031044. DOI: https://doi.org/10.1103/PhysRevX.5.031044.

[108] Sai Vinjanampathy and Janet Anders. "Quantum thermodynamics". In: *Contemporary Physics* 57.4 (2016), pp. 545–579. DOI: https://doi.org/10.1080/00107514.2016.1201896.

[109] M. Wallquist, V. S. Shumeiko, and G. Wendin. "Selective coupling of superconducting qubits via tunable stripline cavity". In: *Physical Review B* 74.22 (Dec. 15, 2006), p. 224506. ISSN: 1098-0121, 1550-235X. DOI: 10.1103/PhysRevB.74.224506. arXiv: cond-mat/0608209. URL: http://arxiv.org/abs/cond-mat/0608209 (visited on 01/25/2023).

[110] Chen Wang, Jie Ren, and Jianshu Cao. "Nonequilibrium energy transfer at nanoscale: A unified theory from weak to strong coupling". In: *Scientific reports* 5.1 (2015), p. 11787. DOI: https://www.nature.com/articles/srep11787.

[111] Mei-Jiao Wang and Yun-Jie Xia. "Steady-state entanglement and heat current of two coupled qubits in two heat baths". In: *Optik* 182 (2019), pp. 1074–1081. DOI: 10.1088/1674-1056/28/6/060303.

[112] Ulrich Weiss. *Quantum dissipative systems*. World Scientific, 2012. DOI: https://doi.org/10.1142/8334.

[113] Ulrich Weiss. *Quantum dissipative systems*. World Scientific, 2012. DOI: https://doi.org/10.1142/8334.

[114] Herman Weyl. "Quantenmechanik und Gruppentheorie". In: *Z. Physik* 46 (1927), p. 080602. DOI: https://doi.org/10.1007/BF02055756.

[115] Eugene Wigner. "On the Quantum Correction For Thermodynamic Equilibrium". In: *physical review* 40 (1932), p. 080602. DOI: https://journals.aps.org/pr/abstract/10.1103/PhysRev.40.749.

[116] C. M. Wilson et al. "Observation of the dynamical Casimir effect in a superconducting circuit". In: *Nature* 479.7373 (Nov. 2011), pp. 376–379. ISSN: 0028-0836, 1476-4687. DOI: 10.1038/nature10561. URL: http://www.nature.com/articles/nature10561 (visited on 02/02/2023).

[117] Waltraut Wustmann and Vitaly Shumeiko. *Parametric resonance in tunable superconducting cavities*. Feb. 28, 2013. DOI: 10.1103/PhysRevB.87.184501. arXiv: 1302.3484[cond-mat,physics:quant-ph]. URL: http://arxiv.org/abs/1302.3484 (visited on 12/15/2022).

List of Publications

Published papers

- Ref. [61]: S. S. Kadijani, T. L. Schmidt, M. Esposito and N. Freitas "*Heat transport in overdamped quantum systems*"

Papers submitted for publication

- Ref. [20]: V. Cavina S. S. Kadijani, M. Esposito and T. L. Schmidt